Identification and characterisation of MITF-regulated long non-coding RNA candidate regulators of melanoma

Coe, Elizabeth

Award date:
2020

Awarding institution:
University of Bath

Identification and characterisation of MITF-regulated long non-coding RNA candidate regulators of melanoma

Elizabeth Anne Coe

A thesis submitted for the degree of Doctor of Philosophy

University of Bath
Department of Biology & Biochemistry

September 2019

Abstract

Long non-coding RNAs (lncRNAs), that are not translated into protein, comprise a large proportion of transcripts produced by the eukaryotic genome. While many lncRNAs have now been identified, functional characterisation of these transcripts is still limited. However, as more lncRNAs are being studied, they are being recognised as important regulators of key cellular and developmental programmes. With that, dysregulated activity of lncRNAs is also now connected to numerous types of disease, including cancers.

Melanoma is a particularly aggressive form of skin cancer which is associated with a high death rate. With currently limited effective therapeutic options, lncRNAs may represent a new class of therapeutic targets. Two well-characterised proteins in melanocyte and melanoma development are MITF and SOX10. These transcription factors regulate the expression of genes important for melanoma cell proliferation, invasion, and metastasis. While protein-coding genes within the MITF-SOX10 transcriptional programmes are well studied, lncRNAs are not. By understanding the role of lncRNAs in such processes, our knowledge of melanoma development and progression can be enhanced, and possible methods of treatment may be revealed.

For this study, a group of 12 candidate MITF-regulated lncRNAs expressed in melanocytes and/or melanoma cells were initially selected. The nuclear-expressed intergenic lncRNA *Disrupted In Renal Carcinoma* (*DIRC3*) was prioritised for further investigation, as a representative lncRNA involved in the MITF-SOX10 transcriptional response in melanoma. Melanoma patients classified as expressing low levels of *DIRC3* were found to have decreased survival. Knockdown analysis then led to the identification of *DIRC3* as a MITF-SOX10 regulated tumour suppressor in melanoma that inhibits anchorage-independent growth. *DIRC3* appears to perform this function by activating expression of its neighbouring tumour suppressive gene *IGFBP5*. *DIRC3* regulates *IGFBP5* expression through modulating the chromatin structure across its own locus so that it suppresses the ability of SOX10 to bind to putative regulatory

elements. Such regulation of *IGFPB5* also goes on to impact expression of numerous genes involved in cancer-associated processes.

This project highlights the role of *DIRC3* as a tumour suppressive lncRNA in melanoma. Through participating in the regulation of the MITF-SOX10 transcriptional programme, *DIRC3* inhibits anchorage-independent growth, a key hallmark of malignant transformation. This activity demonstrates the potential important roles lncRNAs may play within such regulatory networks as well as implicate them as candidate biomarkers or therapeutic targets.

Acknowledgements

First, I would like to thank my supervisor Keith Vance for giving me the opportunity to take on a PhD project with him. His strong guidance and support have been invaluable throughout the project. In addition, his great enthusiasm and near-constant positivity have made challenging points in the project a lot easier to face.

To my lab mates of 0.53 whom I have had the fortune of developing my research skills alongside. Chris was there when I first started and helped me get to grips with how the department worked but more importantly have provided me with great company throughout. Ioanna, Piotr, and Guissi each started through my PhD and also each added a lot of help and enjoyment through my project.

My partner Harry has played a strong role throughout my PhD. His encouragement when I initially proposed doing a PhD and support throughout helped me get to this point. I am truly grateful for his ability to support me throughout the highs and lows that come with such a project, as well as during my difficulties when writing this thesis.

To those friends who have been just a phone-call away – Sunny, Zeph, Tilly, Sophie, and Diva. You have let me discuss PhD-based ideas and issues – even if you didn't quite understand what I was talking about – as well as been another strong support network throughout my PhD. I have been fortunate to also have support from the friends I have made during my time at the University of Bath. Those who I have shared the PhD experience with and have been another invaluable support network both socially and for the completion of my PhD.

I have also been lucky to have strong support from many members of my family – my parents, siblings, and grandparents. They were always there for me and have had belief in me throughout my academic endeavours.

Table of Contents

List of Figures

Chapter 1

Chapter 2

Chapter 3

Chapter 4

List of Tables

Chapter 2

Chapter 3

Chapter 4

Abbreviations

AIRN	Antisense Igf2r RNA non-coding
ASO	Antisense oligonucleotide
BANCR	BRAF-activated noncoding RNA
BLUSTR	Bivalent locus Sfmbt2
BRG1	Brahma related gene 1
CASC11	Cancer susceptibility candidate 11
CBP	CREB-binding protein
CTCF	CCCTC-binding factor
CHART	Capture hybridisation of RNA targets
ChIP	Chromatin Immunoprecipitation
ChIP-seq	ChIP-sequencing
CRISPR	Clustered regulatory interspaced short palindromic repeats
CRISPRa	CRISPR activation
CRISPRi	CRISPR inhibition
DANCR	Differentiation antagonizing non- protein coding RNA
dCas9	Catalytically inactive Cas9
DINO	Damage induced noncoding
DIRC3	Dysregulated in renal carcinoma
ECM	Extracellular matrix
EMT	Epithelial mesenchymal transition
FFPE	Formaldehyde fixed paraffin embedded
FIRRE	Functional intergenic repeating RNA element
FISH	Fluorescent in situ hybridisation
GAS5	Growth arrest specific 5
GO	Gene Ontology
GSP	Gene specific primers
H3K27ac	Histone 3 lysine 27 acetylation
H3K4me1	Histone 3 lysin 4 monomethylation
H3K4me3	Histone 3 lysin 4 trimethylation
HGP	Horizontal growth phase
HMG	High-mobility group
HMT	Histone methyltransferase
HOTAIR	HOX Transcript Antisense RNA
HOTTIP	HOXA Distal Transcript Antisense RNA
IGFBP5	Insulin like growth factor binding protein 2
IgG	Immunoglobin G
KCNQ1OT1	KCNQ1-overlapping transcript 1
KRAB	Krüppel-associated box
LNA-ASOs	Locked nucleic acid antisense oligonucleotides
LncRNA	Long noncoding RNA
MALAT1	Metastasis associated lung adenocarcinoma transcript 1
MAPK	Mitogen-activated protein kinase
MEG3	Maternally expressed 3

mRNA	Messenger RNA
miRNA	Micro RNA
MITF	Micropthalmia-associated transcription factor
NEAT1	Nuclear Enriched Abundant Transcript 1
NHEK	Normal human epithelial kidney
NORAD	Noncoding RNA activated by DNA damage
ORF	Open reading frame
PANDA	P21 associated ncRNA DNA damage activated
PAX3	Paired box 3
PTENP1	Phosphatase And Tensin Homolog Pseudogene 1
qRT-PCR	Quantitative reverse transcription polymerase chain reaction
RACE	Rapid amplification of cDNA ends
RAP	RNA affinity purification
RIP	RNA immunoprecipitation
RNAPII	RNA polymerase II
RNase H	Ribonuclease H
RNA-seq	RNA sequencing
RT-qPCR	Real-time quantitative PCR
SAMMSON	survival associated mitochondrial melanoma specific oncogenic non-coding RNA
SChLAP1	Second chromosome locus associated with prostate-1
SE	Standard error
siRNA	Small interfering RNA
SLNCR	SRA-like non-coding RNA
sncRNA	Small noncoding RNA
SNP	Single nucleotide polymorphisms
SOX10	Sry-related HMG-box-10
SPRY4-IT1	Sprouty4-Intron 1
TAD	Topologically associated domain
TCGA	The Cancer Genome Atlas
TCLA	The Cancer LncRNome Atlas
TNS1	Tensin 1
TNP1	Transition protein-1
TSS	Transcription start site
UCA1	Urothelial carcinoma-associated 1
UCSC	University of California Santa Cruz
UPH	Upperhand
VGP	Vertical growth phase
Wnt	Wingless-type MMTV integration site family member
WS	Waardenburg syndrome
XCI	X-chromosome inactivation
XIST	X-inactive specific transcript
YY1	Yin-Yang 1

Chapter 1: Introduction

1.1 Non-coding portion of the genome

Traditionally RNA has been viewed as a mediator between genetic information encoded in DNA and functional proteins. However, using deep sequencing methods, the transcriptome has been revealed to be increasingly complex. Roughly 75-90% of the human genome is now estimated to be transcribed, but only 2% is translated into proteins, leaving the majority of transcription occurring in non-protein-coding regions (Djebali *et al.* 2012, Dunham *et al.* 2012). This transcription suggests the transcribed RNAs may have roles beyond being an intermediate between DNA and proteins.

Advances in transcriptome profiling have enabled the identification of a vast repertoire of RNA molecules in the human transcriptome (Djebali *et al.* 2012, Iyer *et al.* 2015, Liao *et al.* 2017). As well as being far more prevalent than protein-coding transcripts, non-protein coding transcripts or non-coding RNAs (ncRNAs) are far more diverse and complex than originally anticipated (Birney *et al.* 2007). Previously, such ncRNAs have been viewed as 'junk' or transcriptional noise from functional DNA elements. However, functional roles for ncRNAs are now being revealed. ncRNAs form a heterogenous group of RNAs, allowing them to encompass a broad range of roles. Some of the most well-known ncRNAs behave as housekeeping genes, such as ribosomal RNAs and transfer RNAs, which are constitutively expressed in cells to help maintain regular cellular activity (Dykes and Emanueli 2017). The remaining regulatory ncRNAs are divided arbitrarily based on their size. Short/small noncoding RNAs (sncRNAs) are less than 200 nucleotides in length and include microRNAs (miRNAs), small interfering RNAs (siRNAs), PIWI-interacting RNAs (piRNAs), and small nucleolar RNAs (snoRNA) (Briggs *et al.* 2015, Deniz and Erman 2016, Jandura and Krause 2017, Richtig *et al.* 2017). Correspondingly, those equal to or greater than 200 nucleotides in length are recognised as long non-coding RNAs (lncRNAs) (Derrien *et*

al. 2012). Whilst most focus has previously been on sncRNAs, lncRNAs are now recognised as a highly heterogenous group of RNAs that regulate key developmental processes via a range of mechanisms and so are receiving increased attention.

1.2 Long non-coding RNAs

1.2.1 LncRNA transcript and genomic features

LncRNAs are generated via pathways similar to protein-coding genes and harbour a number of similar features. The majority of lncRNAs are transcribed by RNA polymerase II (RNAPII). LncRNA transcripts are also spliced, 5'-capped and polyadenylated (Cheetham *et al.* 2013, Bach and Lee 2018, Camacho *et al.* 2018). However, they also have key features that differ from protein-coding genes. One is the lack of functional open reading frame (ORF) leading to their absence of protein-coding potential (Derrien *et al.* 2012). However, it should be noted that short functional ORFs that generate small peptides have been identified within some functional lncRNAs (Choi *et al.* 2018). Compared to mRNAs, lncRNAs are also usually shorter and contain fewer exons (typically 1-3) (Derrien *et al.* 2012, Melé *et al.* 2017). Recent work has also identified differences in chromatin features between lncRNAs and protein-coding genes, including histone marks. Active lncRNA promoters have been found to encompass open chromatin organisation with histone modification profiles distinct from protein-coding genes. Such modifications include increased H3K27me3, H3K9me3, and H3K36me3 marks in lncRNA promoters relative to protein-coding genes expressed to a similar level (Alam *et al.* 2014, Melé *et al.* 2017). Such modifications associated with these actively transcribed lncRNAs typically represent transcriptionally poised or repressed regions, as well as transcriptional elongation respectively (Alam *et al.* 2014). The unexpected increase in H3K9me3 has also been associated with lncRNA with more tissue-specific expression patterns (Melé *et al.* 2017).

Although lncRNAs were originally viewed as transcriptional noise, functional loci have now been identified. However, the overall proportion of functional lncRNAs is still unknown with the majority of lncRNAs currently uncharacterised (Quek *et al.* 2015, Uszczynska-Ratajczak *et al.* 2018). The level of lncRNA conservation between organisms has been key in the debate concerning lncRNA functionality. Overall, lncRNA transcripts are typically less conserved than protein-coding genes across their gene bodies, with 5% of lncRNAs sequenced being under selective constraint in vertebrates (Vance and Ponting 2014); however, their promoters show conservation comparable to protein-coding genes (Derrien *et al.* 2012). Also, lncRNAs experience greater conservation than neutrally evolving ancestral repeat sequences (which are proposed to be under neutral selection) and harbour short stretches of highly conserved sequences (Derrien *et al.* 2012, Guttman and Rinn 2012). Although the majority are typically species-specific (Washietl *et al.* 2014, Hezroni *et al.* 2015), in one study 8,953 lncRNAs were identified in both humans and other species (Sarropoulos *et al.* 2019). Thousands have also been annotated in a range of species and tissues in other studies (Hezroni *et al.* 2015, Melé and Rinn 2016). Conservation in multiple species is currently one of the key indicators for functionality. Consequently, such genomic comparisons between species can be used when identifying putatively functional lncRNAs (Necsulea and Kaessmann 2014). However, conservation of lncRNA sequences not being as constrained as that of protein-coding genes allows them to be more tolerant of mutations, and so more likely to experience quicker evolutionary change. It is also important to consider conservation of lncRNA function through their structure or short regions that interact with binding partners. Such features allow for lncRNA conservation to be held in their folded secondary structures (Johnsson *et al.* 2014). A lack of primary sequence conservation does not hinder the preservation of function. This has been demonstrated by rescue experiments using several human lncRNAs which phenotypically rescued depletion of their homologs in zebrafish (Ulitsky *et al.* 2011). However, forming predictions for which lncRNAs are functional based on structure rather than sequence can currently make identification of candidates more challenging.

Another key feature of lncRNAs is their specificity of expression. RNA-seq analysis has previously found lncRNAs to have more precise expression patterns in several cell and tissue types than protein-coding genes (Fatica and Bozzoni 2014). This specificity of expression may help explain why the level of lncRNA transcript expression is so low (Hezroni *et al.* 2015). Earlier studies looking into the spatial distribution of lncRNA transcription in mouse brains(Mercer *et al.* 2008) and the transcriptional profiles of cells from the developing human neocortex found that while lncRNAs are identified in lower abundance in pooled tissues, they have high levels of expression in specific cell types (Mercer *et al.* 2008, Liu, Nowakowski, *et al.* 2016). Consequently, the process of homogenisation of different tissues combined with precise patterns of expression was proposed to lead to the low level of expression detected (Derrien *et al.* 2012). However, this has been debated with lncRNA abundance being found to not differ greatly from protein-coding genes expressed at a similar level when cell-to-cell variability was explored using fluorescent in situ hybridisation (FISH) (Cabili *et al.* 2015), ultimately arguing against the presence of specific cells expressing particularly high levels of the lncRNAs. Nonetheless, overall, tightly controlled expression patterns make lncRNAs interesting candidates in control of developmental processes. Their functional transcripts are also energetically less costly and quicker to produce than protein regulatory factors which require additional processes, including translation (Marchese *et al.* 2017). Without the need to be translated, lncRNAs may be rapidly up- or down-regulated in response to stimuli so may be useful molecules for rapid regulation of target genes (Geisler and Coller 2013). In addition, such specificity of expression is likely very cost-effective as lncRNAs may interact with generic protein machinery while regulating targets in cell- or tissue-specific manners (Marchese *et al.* 2017). Consequently, fewer protein regulatory factors, which require translation, would be required in addition to the transcription of lncRNAs at precise time points.

1.2.2 LncRNA classification

LncRNAs are primarily categorized based on their genomic location relative to protein-coding genes (Derrien *et al.* 2012). The largest group are intergenic lncRNAs which are present between (and not intersecting) genes. This form differs from the remaining lncRNA classes which typically overlap coding loci. The next most common form are antisense lncRNAs which overlap and are transcribed in the opposite direction relative to their closest gene. Sense-overlapping are transcribed within the exons and introns of genes on the sense strand of the DNA. Sense intronic are present within the introns of protein-coding genes. Bidirectional lncRNAs are located within close proximity to the transcript but on the opposite DNA strand and are often transcribed from a shared promoter (Derrien *et al.* 2012, Bhan *et al.* 2017, Ransohoff *et al.* 2017).

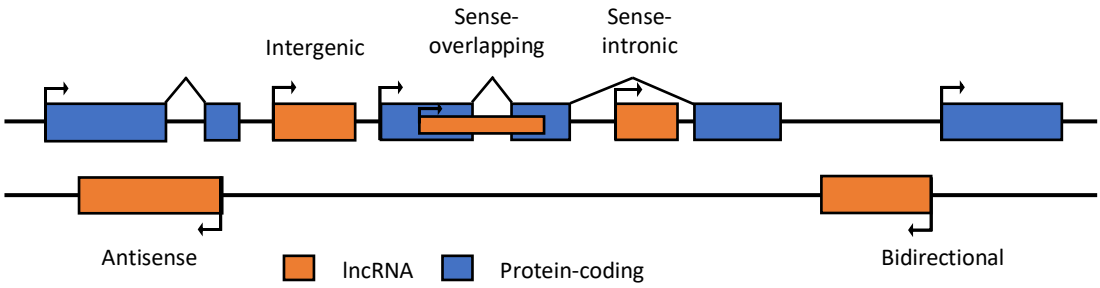

Figure 1.1 Classification of lncRNAs according to their proximity to protein-coding genes. LncRNAs are broadly classified as Antisense, Intergenic, Sense-overlapping, Sense-intronic, and Bidirectional based on the genomic location relative to protein-coding genes. Genes encoding lncRNAs are represented in orange while protein-coding genes are in blue. Figure based on Zhao and Lin 2015.

Such broad classifications have formed due to the discovery and annotation of lncRNAs taking place faster than the understanding of their functions. However, more detailed analyses of lncRNAs has allowed some to also be defined based on structure, and mechanism of action, function, or interaction with protein-coding genes or other known DNA elements as well as their metabolism profiles (St.Laurent *et al.* 2015, Mukherjee *et al.* 2017, Del Vecchio *et al.* 2018).

1.2.3 LncRNAs – a new class of gene expression regulators

LncRNAs have been identified in both the nucleus and cytoplasm where they carry out a diverse range of mechanisms to regulate the activity of their targets. The heterogenous nature of lncRNAs allows them to act at multiple levels of control from epigenetic regulation to mRNA decay (Derrien *et al.* 2012, Cheetham *et al.* 2013). As has been described for protein regulatory factors, lncRNAs may either activate or repress expression of their targets (Kino *et al.* 2010, Goding 2016). They may also regulate broad transcriptional programmes by affecting the activity of key master regulators (Yu *et al.* 2008, Kajino *et al.* 2019). Overall, functional lncRNAs may be broadly categorised based on whether they operate in a transcript-dependent or -independent manner (Kopp and Mendell 2018).

1.2.3.1 Transcript-dependent activity

Functional lncRNA transcripts interact with a range of regulatory factors to execute their function. The tertiary structure of lncRNAs allows the formation of multiple modular recognition domains that specifically interact with different factors including DNA, RNA, and proteins (Chu *et al.* 2011, Briggs *et al.* 2015). This versatility allows lncRNAs to bind a wide plethora of regulatory factors, including transcription and chromatin-modifying factors, as well as mRNAs and miRNAs (Cao *et al.* 2018). These functional lncRNA transcripts may also act local to or distal from their site of synthesis and can be categorised based on their mode of action – scaffolds, guides, decoys, and signals (Wang and Chang 2011). An overview of their functions is described in Figure 1.2.

Scaffold: Using their modular recognition domains lncRNAs can interact with multiple regulatory factors so that they are brought together in a spatiotemporal manner into one functional unit (Briggs *et al.* 2015, Kaikkonen and Adelman 2018). This may occur for protein units which are unable to form direct interactions themselves so rely on lncRNA binding to promote protein complex formation. Such an activity has been

described for *KCNQ1OT1* (KCNQ1-overlapping transcript 1) with PRC2 and G9a, as well as *HOTAIR* (HOX Transcript Antisense RNA) with PRC2 and LSD1 (Rinn *et al.* 2007, Pandey *et al.* 2008). LncRNAs may also interact with enzyme subunits to induce conformational changes that alter their enzymatic activity, such as in the case of *LINK-A* which promotes hyperactivation of AKT by inducing association between its PIP3 and PH domains (Lin *et al.* 2017, Lin and Yang 2018). LncRNAs may also nucleate inter-chromosomal interactions orchestrating chromatin changes so that nuclear structure is regulated (Sun *et al.* 2018).

Guide: LncRNAs may direct targets to specific locations within the cell. In some cases, protein DNA binding domains do not suitably recognise target genes, so they utilise the binding specificity of lncRNAs. Consequently, lncRNAs may modulate protein-DNA binding to regulate the activity of transcription factors or chromatin modifiers (Guttman and Rinn 2012). As a group, the precise activity of lncRNAs would subsequently allow a relatively small number of regulatory proteins to act on a large number of genes (Davidovich *et al.* 2013, Hendrickson *et al.* 2016). This has been suggested to be a reason for the exponential increase in the number of lncRNAs identified in higher eukaryotes as the lncRNAs allow more precise targeting of widely-expressed regulatory proteins (Jandura and Krause 2017). Such activity has previously been described for *HOTTIP* (HOXA Distal Transcript Antisense RNA) which activates, expression of HOXA genes by recruiting the WRD5/MLL histone methyltransferase (HMT) complex (methylation complex) to facilitate H3K4 trimethylation and activation of the HOXA promoter (Wang *et al.* 2011). In the case of *SAMMSON* (survival associated mitochondrial melanoma-specific oncogenic non-coding RNA), the lncRNA re-localises the mitochondria surface protein p32 from the nucleus to the mitochondria to enhance mitochondrial metabolism (Leucci, Vendramin, *et al.* 2016), demonstrating the ability of a lncRNA to regulate cellular activities by relaying communication between the nucleus and mitochondria. The lncRNA *NEAT1* (Nuclear Enriched Abundant Transcript 1) is also able to interact with a range of paraspeckle proteins, including p54nrb, PSPC1, and PSF, for the creation and maintenance of paraspeckles (Clemson *et al.* 2009, Sasaki *et al.* 2009) as well as regulating

paraspeckle positioning so that actively transcribed genes are positioned where they may be easily spliced or near appropriate transcription factors. LncRNAs may also regulate the three-dimensional arrangement of the genome so that sections are in distinct activating or repressive compartments. For example, *FIRRE* (functional intergenic repeating RNA element) promotes chromatin loop formation to organise chromosomal interactions within the nucleus by binding to cohesion and CTCF. This way *FIRRE* guides portions of the X chromosome into distinct repressive compartments during X chromosome inactivation (XCI) (Hacisuleyman *et al.* 2014).

During the process of transcription, nascent transcripts, which have not been released from their locus, may act as tethers, recruiting regulatory factors (transcription and chromatin regulators) to their locus which may encompass regulatory elements such as enhancers (Bach and Lee 2018). Such an interaction has been explored for the transcription factor Yin-Yang 1 (YY1) which interacts with both DNA and RNA in regions proximal to promoters and enhancers (Sigova *et al.* 2015). Sigova et al (2015) hypothesised that by binding to both DNA and RNA, the association of transcription factors with their targets may be reinforced. Using an RNA sequence based on the YY1 target gene promoter increased occupancy and local concentration of YY1 within the enhancer/promoter domain in a positive feedback loop. However, it should be noted this model is limited to YY1 (Sigova *et al.* 2015).

Decoy: LncRNAs may inhibit the activity of other regulatory factors by sequestering them away or competitively binding with their targets. By preventing otherwise inhibitory or stimulatory factors identifying their targets, activities such as post-translational modifications or changes mRNA stability can be prevented (Guttman and Rinn 2012). For example, *GAS5* (Growth arrest specific 5) binds to the DNA binding domain of the glucocorticoid receptor to prevent it interacting with its targets via a DNA recognition sequence and *PANDA* (P21 associated ncRNA DNA damage activated) sequesters NF-YA following DNA damage to limit the expression of pro-apoptotic genes (Kino *et al.* 2010, Hung *et al.* 2011). *MALAT1* (Metastasis associated lung adenocarcinoma transcript 1) is also known to sequester splicing regulatory

factors, including SRSF1 and serine/arginine (SR) and so regulates alternative splicing (Tripathi *et al.* 2010). This mechanism of action may also occur in the cytoplasm. For example, *NORAD* (Noncoding RNA activated by DNA damage) binds to PUM1 and PUM2 to prevent them initiating mRNA decay of their targets (Lee *et al.* 2016). LncRNAs that interact with shared miRNAs are also known as competing endogenous RNAs (ceRNAs) (Wang *et al.* 2016). ceRNAs prevent degradation of their target mRNAs by preventing binding of miRNAs. *H19* binds to mRNA targets of MiR-17-5p to prevent their degradation (Imig *et al.* 2015). Another recognised ceRNA is *PTENP1* (Phosphatase And Tensin Homolog Pseudogene 1) which interacts with miRNAs which would otherwise target the *PTEN*-coding transcript in melanoma cells (Poliseno *et al.* 2010).

Signal: As lncRNAs only require transcription to produce a functional molecule, they can respond quickly to diverse stimuli. Combined with their spatiotemporal specificity of expression in cells and tissues, lncRNAs may act as signals (Guttman and Rinn 2012). Following induction by such a range of unique stimuli, lncRNAs can regulate the activity of a variety of targets. LncRNAs within this group are well associated with key developmental stages or the occurrence of disease (Richtig *et al.* 2017). Some signal-acting lncRNAs regulate allele specificity such as *XIST* (X-inactive specific transcript) which mediates transcriptional silencing of the X chromosome in female cells (reviewed by Pontier and Gribnau, 2011). They may also specify anatomical formation such as positional cell identity and limb patterning, as demonstrated by HOTAIR and HOTTIP which are particularly expressed in posterior cell types (Kumar and Krumlauf 2016). In other cases, lncRNAs may be induced following DNA damage, such as *DINO* (Damage induced noncoding) which binds to and stabilises p53 during the DNA-damage-induced response (Schmitt *et al.* 2016). In these ways, lncRNAs may act as regulators of signalling pathways as well as offer a means of tracking the occurrence of such processes.

LncRNAs frequently use a combination of the mechanisms described to perform their functions. For example, *XIST* is a signal for XCI but in the process acts as a scaffold

and a guide to key regulatory proteins to induce repression (Tian *et al.* 2010, Pontier and Gribnau 2011). In the case of *PANDA* as well as acting as a decoy for NF-YA, its induction by p53 following DNA damage contributes to its role as a signal as well (Hung *et al.* 2011).

For functional lncRNA transcripts, care must be taken when interpreting lncRNA-protein interaction data. In the case of *HOTAIR*, while it was proposed that the lncRNA recruits chromatin modifiers PRC2 and LSD1 to repress activity at the HOXD locus (Rinn *et al.* 2007, Tsai *et al.* 2010), tethering the *HOTAIR* transcript to its target site independent of the chromatin-modifying proteins also repressed activity at the locus. Consequently, it may be the *HOTAIR* transcript that is sufficient to induce transcriptional repression independent of the chromatin-modifying proteins (Chu *et al.* 2011). In line with that, PRC2 has been found to bind non-specifically in a size-dependent manner to lncRNAs (Davidovich *et al.* 2015).

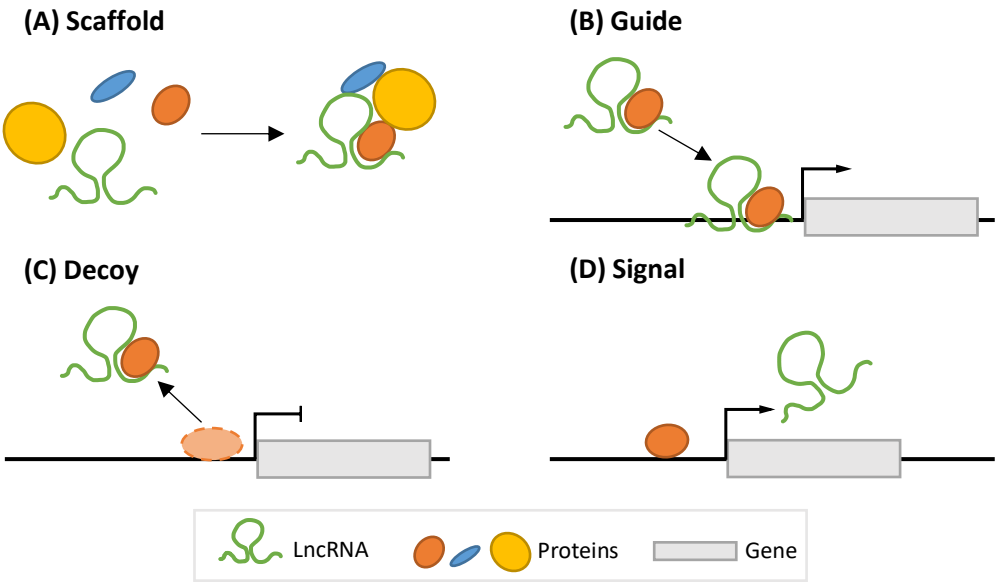

Figure 1.2 Schematic illustration for four mechanisms of transcript-dependent lncRNA regulation. Functional lncRNAs transcripts can interact with DNA, RNA, and/or proteins. (**A**) Scaffolds bring together effector molecules to form a functional unit. As well as interacting with proteins and forming functional ribonucleoprotein complexes, lncRNAs may manipulate nuclear structures. (**B**) Guides bind and direct regulatory factors to precise genomic locations. (**C**) Decoys bind and titrate target proteins or miRNAs away from their targets. (**D**) LncRNAs act as signals due to the specificity of their location and timing of expression. As this is in

response to precise stimuli, expression of such lncRNAs can represent key biological events Figure based on Wang and Chang 2011.

1.2.3.2 Transcript-independent activity

LncRNAs can also function independently of their transcript, making the RNA transcript itself a non-functional by-product (Kopp and Mendell 2018). In some cases, they may utilise machinery used to process the transcript to regulate their targets (Kornienko *et al.* 2013). In this case production of the lncRNA from its locus is important for function and not the mature transcript or sequence. Processes such as splicing may mediate the function of such lncRNAs. In the case of *BLUSTR* (Bivalent locus Sfmbt2), regulation of expression of its neighbouring gene *Sfmbt2* was found to be dependent upon transcription and splicing of the lncRNA (Engreitz *et al.* 2016).

Regulatory elements, such as promoters and enhancers within lncRNA loci may mediate function independently of a functional transcript. For example, *UPH* (Upperhand) positively regulates transcription of neighbouring gene *Hand2* through its own transcription across a super-enhancer for the protein-coding gene (Anderson *et al.* 2016). In the case of *AIRN* (Antisense Igf2r RNA non-coding), the lncRNA is transcribed across the promoter of *Igfr2*, leading to silencing of the gene (Latos *et al.* 2012). In other cases, nucleosome density may be altered due to their disassembly and reformation following transcription elongation – repositioning them so they occlude promoters or binding sites. Or the RNA polymerase II itself may act to displace transcription, or other regulatory factors, bound to DNA (Latos *et al.* 2012, Anderson *et al.* 2016, Kaikkonen and Adelman 2018). In the case of antisense lncRNA transcription, the RNAPII may collide with an RNAPII for its neighbouring gene, resulting in inhibition of the expression of that gene, a process recognised as transcriptional interference (Hobson *et al.* 2012). The process of lncRNA transcription may also enable deposition of active histone modifications such as through histone-modifying enzymes interacting with RNAPII (Ng *et al.* 2003, Lennox and Behlke 2016). Transcription may also promote gene expression by displacing negative regulators (PcG transcriptional repressors) or removing inhibitory nucleosomes making,

regulatory elements such as promoters more accessible (Kaikkonen and Adelman 2018).

A broad range of mechanisms for lncRNAs are being identified that may or may not rely on the presence of a functional transcript. Manipulating expression of functional transcripts has already been explored in detail as similar methods may be used for protein-coding genes – including the use of siRNAs and CRISPR (Gilbert *et al.* 2014, Biswas *et al.* 2018). However, lncRNA loci overlapping regulatory factors can make it difficult to distinguish functional lncRNAs from the DNA elements they encompass (Richard and Eichhorn 2018).

1.2.4 LncRNAs have emerged as important regulators of cancer

Cancer is a complex disease associated with uncontrolled growth and invasion of abnormal cells. Over the multi-step process of tumorigenesis, somatic mutations accumulate, allowing cells to develop so they can eventually metastasise, decreasing the likelihood of patient survival (Hanahan *et al.* 2000, Siegel *et al.* 2019). The causes of cancers are not fully understood, but there are known risk factors that increase an individual's likelihood of developing the disease. Such factors include those which may be modified by the individual (including excess body weight and use of tobacco) as well as those that cannot (including inherited genetic mutations or immune conditions) (Siegel *et al.* 2019). Despite medicinal advances, cancer is a growing global issue as it is now the second leading cause of death worldwide, surpassing infectious disease (Lozano *et al.* 2012).

The hallmarks of cancer are biological activities that enable tumour growth and progression. These include deregulation of energy metabolism, sustained proliferative signalling, avoidance of growth suppressors, replicative immortality, resistance of cell death, evasion of the immune system, induction of angiogenesis, activation of cell invasion, and metastasis (Hanahan and Weinberg 2011). As these hallmarks are acquired, tumours progress towards becoming metastatic and so more

lethal. Tumours may also recruit host cells, secreted proteins and extracellular matrix factors to the tumour microenvironment, forming complex interactions important to tumour development (Hanahan and Weinberg 2011, Ungefroren *et al.* 2011).

At the molecular level, cancer is associated with a broad range of genetic mutations, chromosomal translocations, and epigenetic reprogramming (Suvà *et al.* 2013). Such changes can result in the activation of cancer-causing oncogenes or suppression of tumour suppressors (Bach and Lee 2018). For cancer cells to continue to develop, they can bypass mechanisms typically used to protect the body against such genetic alterations. The chromosomal instability allows cancer cells to continue to evolve by acquiring new mutations and increasing their genetic diversity, enabling them to grow, metastasise, and survive external therapies (Hanahan and Weinberg 2011).

Increasing evidence is pointing towards the non-coding portion of the genome being important in cancer initiation and progression. Recently, reports showed that over 80% of putative cancer-associated single nucleotide polymorphisms (SNPs)(Freedman *et al.* 2011) as well as 122 out of 158 recurrent somatic copy number alterations (SCNAs) (Beroukhim *et al.* 2010), were located outside of protein-coding genes, many of which overlap lncRNA loci (Beroukhim *et al.* 2010, Freedman *et al.* 2011, Iyer *et al.* 2015).

Mutations close to lncRNA loci can influence the expression of lncRNAs. Alterations to promoters or enhancers may lead to dysregulated lncRNA expression (Guo *et al.* 2016, Camacho *et al.* 2018). In addition, epigenetic changes may alter lncRNA expression. It has been recognised that DNA methylation patterns of promoters for lncRNAs are distinct between tumour and healthy samples (Yan *et al.* 2015). In other cases, critical cancer regulatory proteins such as MYC and p53 have been reported to control the expression of cancer-associated lncRNAs (Hart *et al.* 2014, Huarte 2015, Grossi *et al.* 2016). Using comparisons between tumours and normal tissues, highly tumour-specific alterations to lncRNA expression have been identified demonstrating the commonality of lncRNA dysregulation in cancer (Iyer *et al.* 2015, Yan *et al.* 2015).

Mutations may also lead to structural changes which influence lncRNA function. For example, by either disrupting or generating new lncRNA binding sites. This can then influence the ability of lncRNAs to associate with DNA regulatory elements, miRNAs, or regulatory proteins (Wan *et al.* 2014, Zheng *et al.* 2016). LncRNAs may also be unable to form RNA-RNA interactions required for the correct formation of their secondary structure (Wan *et al.* 2014).

Some lncRNAs participate in cancer development and progression as a consequence of their dysregulated activity. As found with protein-coding genes, lncRNAs have been identified that behave both as oncogenes and tumour suppressors. Well-characterised oncogenes include *MALAT1* which regulates proliferation, invasion, and metastasis in non-small cell lung cancer, as well as *SChLAP1* (Second chromosome locus associated with prostate-1) which promotes invasion and metastasis in prostate cancer (Gutschner *et al.* 2013, Prensner *et al.* 2013). Numerous tumour suppressors have also been characterised, including *MEG3* (Maternally expressed 3) in glioma, and Linc-p21 in head and neck squamous cell carcinoma (HNSCC) which both regulate proliferation and cell-cycle arrest (Gong and Huang 2017, Jin *et al.* 2019). Of lncRNAs characterised so far, dozens have been identified that participate in a range of cancers, including *MALAT1*, *H19* and *HOTAIR* (Gupta *et al.* 2010, Luan *et al.* 2016, Xu *et al.* 2017). In some cases, lncRNA candidates have been recognised that regulate resistance to currently available therapies. *HOTAIR* promotes chemoresistance in colorectal cancer by suppressing miR-218 and so activating NF-kB/TS signalling while *GAS5* antagonises chemoresistance in pancreatic cancer by down-regulating miR-181c-5p (Li *et al.* 2017, Gao *et al.* 2018). Consequently, lncRNAs stand as important factors for improving our understanding of how cancers develop and how they may be therapeutically targeted.

1.3 LncRNAs participate in the regulation of melanoma

1.3.1 Melanoma

Numerous lncRNAs have been identified with altered expression and functional roles in melanoma (Hulstaert *et al.* 2017, Sun *et al.* 2019). These could represent novel therapeutic targets as current therapies used to treat metastatic melanoma frequently succumb to the development of resistance or have a low number of patients that effectively respond (Kozar *et al.* 2019). Cutaneous melanoma is the leading cause of skin cancer-related deaths despite accounting for roughly 1% of cases (Yu *et al.* 2018, Siegel *et al.* 2019). The high lethality is a result of melanoma metastasis (Balch *et al.* 2009). The incidence of melanoma is also increasing globally, while it remains typically higher in fair-skinned individuals (Garbe *et al.* 2016, Yu *et al.* 2018). A major risk of melanoma is excessive exposure to ultraviolet (UV) radiation, such as sunlight (Siegel 2019). The risk may also be increased if skin cancer is common in a family, if an individual has a large number (> 50) of moles, a paler complexion, or if they have a weakened immune system (Garbe *et al.* 2016, Siegel *et al.* 2019).

Melanoma is typically known to be derived from the malignant transformation of melanocytes (Mort *et al.* 2015). However, neural crest stem cells or melanoblasts may also play an important role in part due to them being undifferentiated or less differentiated than melanocytes as well as more invasive (White *et al.* 2011, Marie *et al.* 2019). Melanocytes are pigment-producing dendritic cells that originate in the neural crest during embryonic development prior to migration to the skin (Mort *et al.* 2015). The primary function of epidermal melanocytes is to produce melanin through melanogenesis and transfer the melanin pigment in melanosomes to neighbouring keratinocytes via numerous contacts (Mort *et al.* 2015, Shain and Bastian 2016). There, they construct a layer covering the keratinocyte nuclei to protect their DNA from UV radiation damage by scattering and absorbing the UV radiation (Shain and Bastian 2016).

Following increased proliferation, melanocytes form benign naevi (moles). Typically, the cells undergo senescence so that they do not continue to grow uncontrollably (Larue and Beermann 2007). However, cells that bypass senescence continue to proliferate and can pass through a series of phenotypically and transcriptionally distinct phases of growth via the process of melanomagenesis (Larue and Beermann 2007, Braeuer *et al.* 2011) and lead to metastatic melanoma. The key steps are described in Figure 1.3. Following metastasis, secondary melanoma tumours are typically identified in the liver, lung, and brain (Mobley *et al.* 2012).

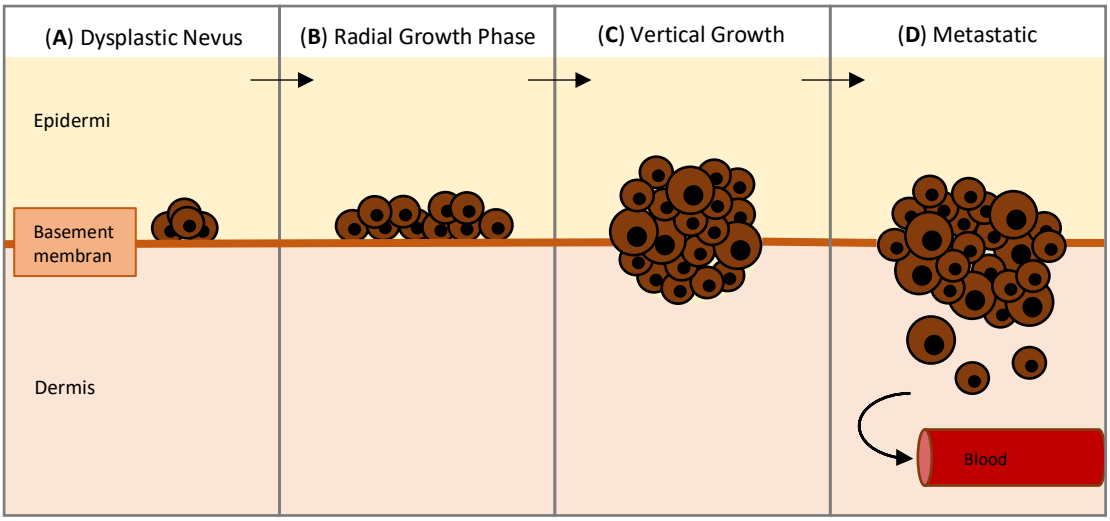

Figure 1.3. Progression of melanocytes to metastatic melanoma. (**A**) Atypical moles are recognised as dysplastic naevi. These irregularly shaped moles have a greater chance of developing into melanoma. Following genetic and epigenetic alterations, melanocytes are transformed into benign naevi. The nevus is formed as melanocytes proliferate at the basal layer of the epidermis and lose contact with keratinocytes. (**B**) Cells that bypass senescence spread horizontally through the epidermis in the pre-malignant radial growth phase (RGP). (**C**) A proportion of cells experience a reduction in adhesive molecules and increased extracellular matrix-degrading enzymes, allowing the cells to cross the basement membrane, invade into through the dermis and into subcutaneous tissue, in the vertical growth phase (VGP) (**D**) Finally cells are able to metastasise as the tumour cells are able to enter the lymphatic and vascular vessels. (Larue and Beermann 2007, Braeuer *et al.* 2011, Mobley *et al.* 2012).

Melanoma primarily occurs following somatic mutations, while a small proportion are the result of inherited mutations. Both lead to aberrant cell proliferation, migration, invasion, and apoptosis (Mort *et al.* 2015, Hulstaert *et al.* 2017). Of

individuals with inherited genetic defects that increase their susceptibility to melanoma, roughly 25-40% inherit the mutated *CDKN2A* (Levy *et al.* 2006, Soura *et al.* 2016). This gene plays an important role in cell cycle control with its mutation being associated with atypical cell proliferation and avoidance of cellular senescence (Potrony *et al.* 2015). Somatic mutations occur through the lifetime of an individual. A range of candidate genes have been identified that are affected by such mutations. Activation of BRAF in the Mitogen-activated protein kinase (MAPK) signalling pathway is the most common mutation in melanoma with it present in 50-60% of cases – 90% of which contain the $BRAF^{V600E}$ protein (Davies *et al.* 2002, Hulstaert *et al.* 2017). Cells containing this mutation typically exhibit increased cell growth and survival (Sullivan and Flaherty 2011). Another member of the MAPK signalling pathway, NRAS, has been identified as mutated in ~25% of melanoma cases, including cells without the BRAF mutation (Tudrej *et al.* 2017). Two other melanoma regulatory factors of interest in melanoma are the transcription factors MITF (Microphthalmia-associated transcription factor) and SOX10 (SRY (sex-determining region Y)-box 10). Both are critical regulators of melanoma cell survival, proliferation, and invasion, as well as have been associated with patient response to therapeutics (Cronin *et al.* 2013, Ploper *et al.* 2015, Tudrej *et al.* 2017). In addition to these oncogenic mutations, IGFBP5 (Insulin-like growth factor binding protein) has been identified as an important tumour suppressor which is repressed in melanoma (Wang *et al.* 2015).

1.3.1.1 IGFBP5

IGFBP5 belongs to a family of six insulin-like growth factor (IGF) binding proteins which act through both IGF-dependent and -independent mechanisms (Baxter 2014, Bach 2018). IGFBPs participate in a range of processes including regulation of DNA damage, transcription, and apoptosis (Grimberg *et al.* 2005, Beattie *et al.* 2006, Azar *et al.* 2014, Baxter 2014).

Dysregulated expression of IGFBP5 has been identified in a variety of human cancers. The protein was found to influence development and progression of cancers as well as resistance to therapies (Su *et al.* 2011, Sureshbabu *et al.* 2012, Baxter 2014, Wang *et al.* 2015, Hwang *et al.* 2016). Numerous preclinical studies in a range of tissues have found IGFBP5 to suppress growth and metastasis of tumours through inhibiting processes including cell adhesion, survival, and angiogenesis (Su *et al.* 2011, Sureshbabu *et al.* 2012, Hwang *et al.* 2016).

The role of IGFBP5 as a tumour suppressor has also been studied in melanoma. It was found to negatively regulate melanoma growth and metastatic properties *in vitro* and *in vivo* (Wang *et al.* 2015). The team found IGFBP5 to function through negatively regulating expression of E-cadherin and stem cell markers including SOX2, NANOG, and OCT4. The protein was also found to inhibit the MEK-ERK and p38-MAPK signalling pathways. It was proposed that through such actions, IGFBP5 is able to regulate a range of cellular activities in melanoma, including suppression of cell proliferation and invasion, as well as EMT, metastasis, and stem cell features (Wang *et al.* 2015).

1.3.1.2 MITF

MITF-M is a key transcription factor involved in the regulation of melanocyte and melanoma development (Hemesath *et al.* 1994, Garraway *et al.* 2005). The MITF protein contains a basic helix-loop-helix leucine zipper (bHLH-Zip) DNA-binding domain that binds to a canonical E-box, as well as two transactivation domains (Levy *et al.* 2006, Seberg *et al.* 2017). Several isoforms of MITF exist, which have either broad or specific expression in different tissue types. These isoforms use alternative promoters and so vary based on their unique 5' ends. MITF-M is the shortest isoform and is expressed almost exclusively in melanocytes and melanomas (Mobley *et al.* 2012, Hartman and Czyz 2015, Kawakami and Fisher 2017).

Known as the 'master regulator of melanocytes', MITF holds a prominent role in the regulation of melanocyte development and differentiation (Hemesath *et al.* 1994, Garraway *et al.* 2005, Kawakami and Fisher 2017). MITF targets genes important for cellular processes including, invasion (GMPR, DIAPH1), pigmentation (TYR, DCT), cell cycle (CDK2), survival (BCL2, BCL2A1) and cell adhesion (CAECAM) (Goding and Arnheiter 2019). The importance of MITF in melanocyte development was first recognised in mice with mutated MITF who experienced defects in pigmentation of the skin, eye, and hair follicles, as well as affected cells in the inner ear. Other affected cells included pigmented epithelial cells, mast cells, and osteoclasts (Hodgkinson *et al.* 1993, Steingrimsson *et al.* 1994). In humans, germline mutation of MITF has been associated with Waardenburg syndrome II (WS2) and Tietz syndrome, which express altered skin and hair pigmentation as well as deafness as a consequence of fewer melanocytes present in the inner ear (Tassabehji *et al.* 1995, Pingault *et al.* 2010).

Expression of MITF is controlled by an interplay of activators and repressors. SOX10, PAX6, as well as ß-catenin of the Wnt signalling pathway, have been found to activate expression of MITF in melanocyte development (Lang *et al.* 2005, Ploper *et al.* 2015). Recognised repressors of MITF include FOXD3 (Forkhead box D) which prevents PAX3 (Paired box 3) binding the MITF promoter, and ATF4 (Activating Transcription Factor 4) which represses expression of MITF mRNA (Thomas and Erickson 2009, Falletta *et al.* 2017). MITF also interacts with a range of co-factors which contribute to its ability to regulate expression of target genes. These include the histone acetyltransferases p300 and CBP (CREB-binding protein), as well as BRG1 (Brahma-related gene 1), a key component of the SWI/SNF complexes BAF and PBAF (Sato *et al.* 1997, Laurette *et al.* 2015).

Aberrant expression of MITF in melanoma is frequently the result of dysregulated expression of key regulatory pathways. The Wnt-ß-catenin (canonical), PI3K-AKT, and MAPK pathways become constitutively activated in melanoma, leading to aberrant activation or repression of target genes (Larue and Delmas 2006, Kwong and Davies 2013, Dantonio *et al.* 2018). An overview of how these pathways can become

dysregulated, leading to increased expression of MITF, is given in Figure 1.4. Genetic and epigenetic mutations lead to activation or suppression of the activity of different components of these pathways resulting in their altered activity. In the case of BRAF, the $BRAF^{V600E}$ point mutation results in constitutive activation of the protein and so increased activity of the MAPK pathway (Pollock *et al.* 2003, Dankort *et al.* 2009). In some cases, dysregulation of individual proteins can impact the activity of multiple pathways. For example, activating point mutations in NRAS lead to activation of both the MAPK and PI3-AKT pathways (Dankort *et al.* 2009, Kwong and Davies 2013). Following increased activity of each of these pathways, there is increased expression of MITF. It should also be noted that in some cases MITF expression is inhibited, such as through activation of Wnt5A in the non-canonical Wnt signalling pathway. In this case, suppression of MITF by Wnt5A activity was found to increase melanoma cell invasion (Weeraratna *et al.* 2002).

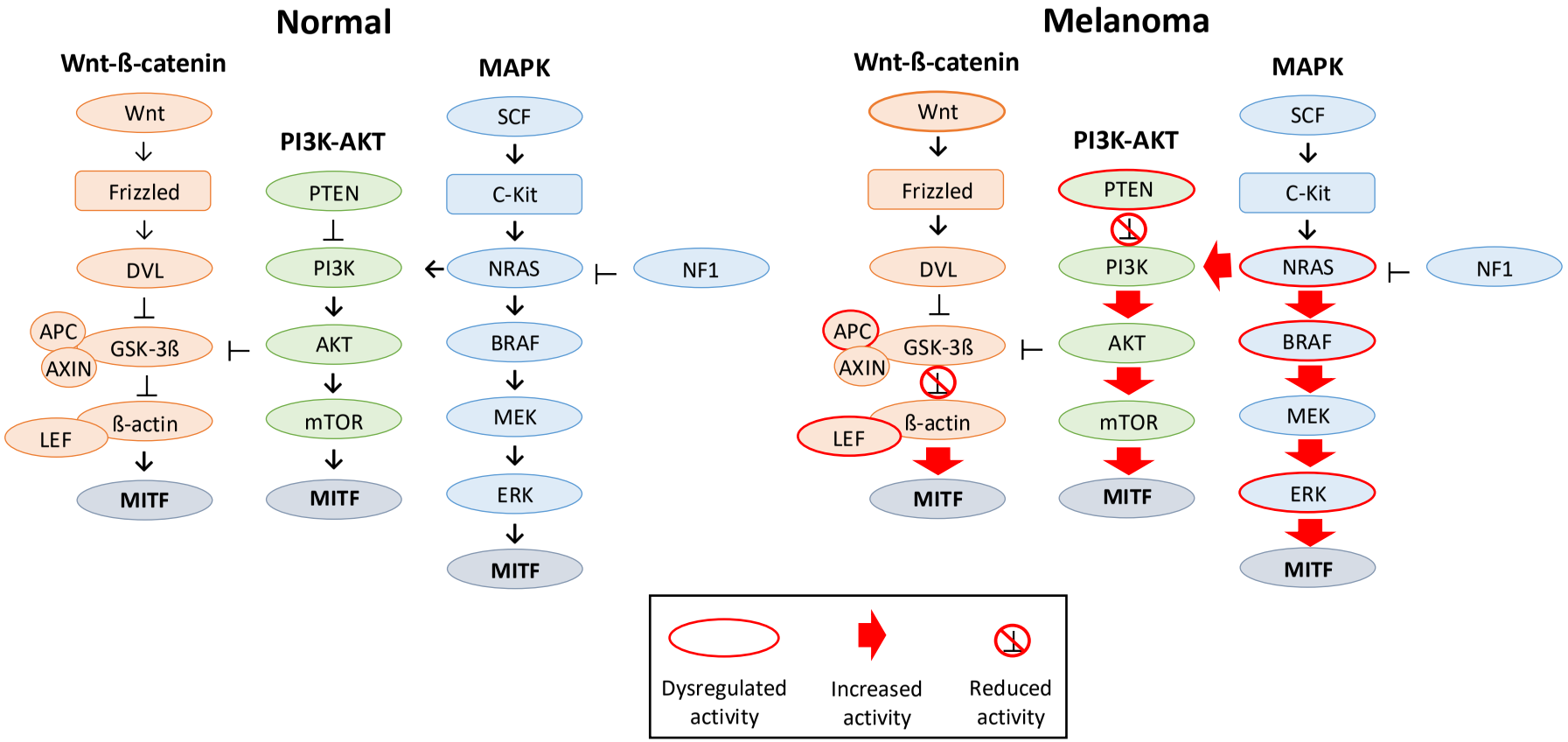

Figure 1.4. The Wnt-ß-catenin, PI3K-AKT, and MAPK are aberrantly activated in melanoma, leading to increased expression of MITF. The activity of the signalling pathways is compared between normal and melanoma cells. Proteins known to have dysregulated activity in melanoma are highlighted with a red band. Wnt-ß-catenin: Increased LEF1 activity and reduced APC activity. PI3K-AKT: Reduced PTEN activity and increased NRAS activity. MAPK: Increased activity of BRAF, NRAS, and ERK. Each of these lead to increased activation of MITF expression (Larue and Delmas 2006, Kwong and Davies 2013, Dantonio et al. 2018).

Evidence of MITF oncogenic behaviour arose following the identification of a gain in copy number at the MITF locus in melanoma cell lines. MITF was then found to be amplified in 10 and 21% of primary cutaneous and metastatic melanomas respectively relative to melanocytic naevi, showing a correlation between MITF activity and cancer aggressiveness (Garraway *et al.* 2005, Hoek and Goding 2010, Verfaillie *et al.* 2015). With its vital role in melanoma cell survival, differentiation, proliferation and migration MITF has been suggested to behave as a 'lineage addiction' oncogene (Garraway *et al.* 2005, Hartman and Czyz 2015). Expression of MITF is also associated with a reduction in 5-year survival rate for melanoma patients, again implicating MITF in progression and lethality of a proportion of melanomas (Garraway *et al.* 2005). Activation of MAPK signalling by $BRAF^{V600E}$ typically represses MITF protein and mRNA expression, however, increased MITF expression is detected in a proportion of $BRAF^{V600E}$ mutated melanoma cells through mechanisms including amplification of MITF gene or activation of Wnt signalling (Garraway *et al.* 2005, Wellbrock *et al.* 2008). It has also been proposed that the mutation across the consensus sequence for SUMOylation of $BRAF^{V600E}$ prevents typical degradation of MITF (Miller *et al.* 2005).

Primary tumours contain distinct subpopulations of cells with MITF-high and -low expression signatures (Ennen *et al.* 2017). Clusters of low MITF expressing cells have been identified at the edge of primary lesions where melanoma invasion is triggered, eventually allowing the cells to metastasise (Caramel *et al.* 2013). High MITF has also been identified at distal sites where proliferating cells have metastasised, demonstrating an ability of the cells to switch their transcriptional state (Verfaillie *et al.* 2015). The level of MITF expression has been proposed to influence cancer phenotype in a dosage-dependent manner. High MITF promoting differentiation, intermediate proliferation, low invasion (and so metastasis), and absence of MITF resulting in senescence (Carreira *et al.* 2006, Hoek *et al.* 2008, Goding 2011, Verfaillie *et al.* 2015), summarised in Figure 1.4. Consequently, active MITF levels determine phenotype switching of melanoma cells in response to environmental triggers or stress responses (Hoek and Goding 2010, Goding 2011, Falletta *et al.* 2017).

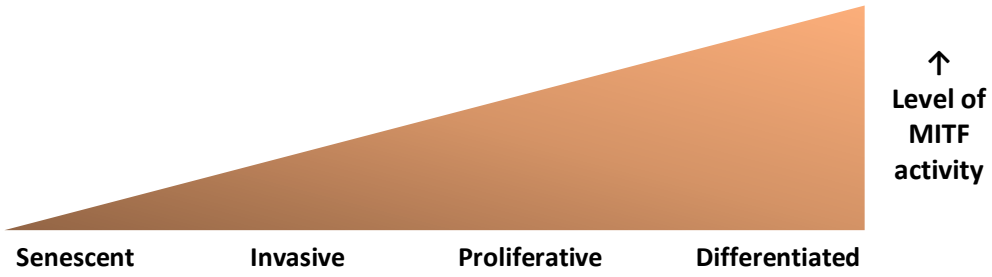

Figure 1.5. Rheostat model for the effect of level of MITF activity on the behaviour of melanoma cells. Melanoma cells with very low levels of MITF activity undergo senescence. If MITF activity is enough that senescence is not induced, cells develop more invasive behaviour. Cells expressing higher MITF activity become more proliferative, while those with the highest levels begin to differentiate. Consequently, this model demonstrates the connection between the level of MITF activity and melanoma cell behaviour, which is associated with the tumour environment. Figure is based on Goding 2011.

1.3.1.3 SOX10

SOX10 plays a vital role in melanocyte and melanoma development (Harris *et al.* 2010, Graf *et al.* 2014). SOX10 belongs to the subgroup SOXE of SOX transcription factors which are characterized by a conserved high-mobility group (HMG) DNA-binding domain that recognises the sequence motif 5'-T/AT/ACAAAG-3' (Haldin and LaBonne 2010). SOX10 participates in regulating neural crest cell proliferation, survival, and multipotency, as well as melanocyte differentiation (Haldin and LaBonne 2010, Harris *et al.* 2010). With that, SOX10 plays a major role throughout melanocyte development (Shakhova *et al.* 2012).

SOX10 regulates melanocyte-specific genes including *MITF*, *MIA*, *DCT*, *TYR*, and *TYRP1* which participate in regulation of cellular processes including proliferation, invasion, differentiation survival and melanogenesis (Harris *et al.* 2010, Fufa *et al.* 2015, Seberg *et al.* 2017, Cronin *et al.* 2018). SOX10 also interacts with coactivators including PAX3 and BRG1 to help facilitate SOX10 regulation of its target genes (Potterf *et al.* 2000, Marathe *et al.* 2017, Cronin *et al.* 2018). The importance of SOX10 in development is demonstrated by embryonic lethality following homozygous deletion of SOX10 in mice (Herbarth *et al.* 1998), while overexpression was found to

induce the formation of giant congenital naevi in mice (Shakhova *et al.* 2012). Humans with SOX10 haploinsufficiency experience pigmentation defects and diseases including Waardenburg syndrome (WS2 and WS4) (Pingault *et al.* 2010).

SOX10 has upregulated expression in both primary and metastatic melanomas (Shakhova *et al.* 2012, Cronin *et al.* 2013, Huang *et al.* 2015). Accordingly, studies have implicated SOX10 in melanoma initiation and maintenance (Shakhova *et al.* 2012), with increased expression being associated with worse prognosis (Civenni *et al.* 2011, Graf *et al.* 2014). SOX10 is not typically mutated in melanoma, and its lack of expression or inhibition lead to cell death in melanoma cells, both of which demonstrate the importance of SOX10 function in melanoma (Shakhova *et al.* 2012, Cronin *et al.* 2013, Graf *et al.* 2014). In addition, when studied in melanoma mouse models, SOX10 haploinsufficiency prevented or significantly delayed malignant tumours developing (Shakhova *et al.* 2012, Cronin *et al.* 2013). Roles for SOX10 have been identified in regulating survival, cell cycle, proliferation, and invasion of melanoma cells (Shakhova *et al.* 2012, Cronin *et al.* 2013, Graf *et al.* 2014). It should also be noted that SOX10 has also been related to positively regulating expression of the oncogenic lncRNA *SAMMSON* which is expressed in 90% of human melanomas (Leucci, Vendramin, *et al.* 2016).

1.3.1.4 MITF-SOX10 pathway

The MITF and SOX10 transcription factors participate together to regulate a wide range of processes in neural crest stem cell, melanocyte, and melanoma development (Seberg *et al.* 2017, Tudrej *et al.* 2017). Studies have identified enrichment of MITF and SOX10 at shared regulatory elements for target genes, suggesting that they co-occupy these regions (Fufa *et al.* 2015, Laurette *et al.* 2015, Verfaillie *et al.* 2015) – these include the genes *DCT*, *TYR,* and *TRP1* (Marathe *et al.* 2017). In addition to jointly regulating melanocyte- and melanoma-specific genes, MITF and SOX10 interact with similar regulatory factors. These include BRG1 and PAX3 which aid in controlling chromatin accessibility (Marathe *et al.* 2017).

As well as SOX10 inducing MITF expression, MITF binding sites have been identified upstream of the SOX10 gene, suggesting direct cross-activation between MITF and SOX10. Accordingly, it has also been proposed that these transcription factors form feed-forward loops, promoting one another's expression (Verfaillie *et al.* 2015). It should also be noted that as well as functioning via regulating MITF activity, SOX10 can function independent of MITF, demonstrated by ectopic expression of MITF in cells not fully rescuing expression of melanocyte-specific SOX10 target genes following SOX10 depletion (Marathe *et al.* 2017). Work in mice also demonstrated that heterozygous loss of both MITF and SOX10 had more severe loss of pigmentation than those with loss of only one (Potterf *et al.* 2000). The cooperative regulation of target genes by MITF and SOX10 demonstrate a higher level of transcriptional organisation.

MITF and SOX10 have also been identified as 'master regulators' of proliferative gene networks in melanoma. Dynamic transcriptional changes in the activity of MITF and SOX10 allow reversible transitions between the proliferative and invasive states (Hoek *et al.* 2008, Verfaillie *et al.* 2015). The proliferative gene expression signature is associated with high levels of MITF and SOX10, while low MITF-SOX10 is identified in cells with an invasive melanoma gene signature (Carreira *et al.* 2006, Hoek *et al.* 2008, Verfaillie *et al.* 2015). These distinct proliferative and invasive transcriptional states also influence the acquisition of resistance to MAPK pathway inhibitors (Konieczkowski *et al.* 2014, Sun *et al.* 2014, Verfaillie *et al.* 2015). For example, reduced SOX10 in melanoma has been reported to lead to activation of TGF-ß signalling and upregulation of epidermal growth factor receptor (EGFR) and platelet-derived growth factor receptor-b (PDGFRB) which promoted resistance to BRAF and MEK inhibitors (Sun *et al.* 2014).

1.4.1 Characterised lncRNAs in melanoma

While protein-coding genes are well-characterised regulators of melanoma, lncRNAs are less well understood. RNA-sequencing projects have identified large numbers of lncRNAs with dysregulated expression in melanoma. For example, the MiTranscriptome compendium identified 339 melanoma-associated lncRNA transcripts whose expression is restricted to melanoma, of which 24 were proposed to have putative functional roles based on their levels of conservation across 46 vertebrate species (Iyer *et al.* 2015).

Both oncogenic and tumour suppressive lncRNAs have been identified that can regulate a range of cellular processes in melanoma. The lncRNA *BANCR* (BRAF-activated noncoding RNA) is connected to the MAPK signalling pathway and is induced by $BRAF^{V600E}$. *BANCR* influences melanoma cell migration and proliferation by activating the ERK1/2 and JNK components of the MAPK pathway (Flockhart *et al.* 2012, Li *et al.* 2014). Another well characterised melanoma-expressed lncRNA is *SLNCR* (SRA-like non-coding RNA). This oncogenic lncRNA promotes proliferation and invasion in melanoma cells by repressing the activity of the tumour suppressor p21Waf1/Cip1 as well as matrix metalloproteinase 9 (MMP9) (Schmidt *et al.* 2016, 2019). *SLNCR* does this by recruiting the androgen receptor (AR) to Early growth response protein 1 (EGR1)-bound genomic loci and switching transcriptional activation by EGR1 to a repressive activity (Schmidt *et al.* 2019). The lncRNA *SPRY4-IT1* (Sprouty4-Intron 1) also acts as a melanoma oncogene by binding to lipin2 and promoting lipid metabolism through avoiding lipotoxicity. This leads to an inhibition of apoptosis as well as increased proliferation and invasion (Mazar *et al.* 2014). As oncogenes, expression of these lncRNAs is associated with worse prognosis and lower survival rate in melanoma patients (Li *et al.* 2014, Liu, Shen, *et al.* 2016, Schmidt *et al.* 2019).

Fewer tumour suppressive lncRNAs in melanoma have so far been characterised. The lncRNA *GAS5* is downregulated in melanoma and suppresses melanoma cell

migration and invasion, at least in part, by inhibiting expression of MMP2 (Chen *et al.* 2016). *PTENP1*, which was found to be deleted in 20.9% of melanoma tissues, has also been recognised as a tumour suppressor in melanoma. *PTENP1* acts as a decoy against miRNAs targeting the melanoma tumour suppressor gene *PTEN*. Deletion of *PTENP1* was also found to be associated with complete or partial deletion of the melanoma-associated *CDKN2A* in human melanoma cell lines, although this was not found in human melanoma tissues (Poliseno *et al.* 2011). *PTENP1* may also act independently of *PTEN*, acting as a decoy for miRNAs that have alternative or additional targets to *PTEN*. Correspondingly, deletion of *PTENP1* led to a reduction in the mRNA levels of tumour suppressive genes including the pro-apoptotic factor BIM (BH3-only protein Bim), the cyclin-dependent kinase (CDK) inhibitor p21, and the BRAF inhibitor Sprouty2 (Yusoff *et al.* 2002, Tarek and Dutta 2009, Gogada *et al.* 2013). It should be noted that each of these genes act as antagonists to the MAPK signalling pathway, leading to the hypothesis that *PTENP1* deletion may promote activation of MAPK signalling (Tsavachidou *et al.* 2004, Akiyama *et al.* 2009, Poliseno *et al.* 2011).

As well as understanding more about causes and development of melanoma, identifying the roles, mechanisms of action, and regulation of expression of oncogenic and tumour suppressive lncRNAs expressed in melanoma will enable the development of novel biomarkers and therapies for treating individuals with the disease.

1.4.2 LncRNAs as biomarkers and therapeutics

For patients diagnosed with melanoma, survival depends greatly on how far the disease has progressed. Individuals with stage I and II melanoma typically have surgery to remove the tumour. This is highly effective with a five-year survival rate of roughly 90% and 70% for stage I and II respectively (Balch *et al.* 2004, Yu *et al.* 2018, Siegel *et al.* 2019). Once the primary tumour thickness passes 2mm the prognosis reduces dramatically as the tumours are more likely to metastasise. Once melanomas

reach the lymph nodes (stage III), the five-year survival drops to 45%, with the prognosis worse if the tumour metastases reach multiple lymph nodes. If metastases have reached distant organs, the five-year survival rate then drastically drops to 10% (Balch *et al.* 2004). For patients with metastatic melanoma, generic cancer treatments such as chemotherapy or radiation therapy are often used (Siegel *et al.* 2019).

The inefficiency of chemotherapy and radiation therapy have led to the development of newer methods to treat metastatic melanoma (Singh and Salama 2016, Pérez-Guijarro *et al.* 2017). Such therapies have begun to focus on the tumours' mutational status, allowing the development of more personalised medicine. This was done in the case of vemurafenib (PLX4032) which targets activity of the $BRAF^{V600E}$, and so reduces MAPK pathway signalling in patients with metastatic melanoma. The BRIM3 clinical trial was the first time a clear clinical response was observed when treating late-stage melanoma, with a response rate of 48% compared to just 5% when using dacarbazine (chemotherapy) (Chapman *et al.* 2011). While vemurafenib is initially effective, resistance to the drug can occur. Consequently, combination therapies are now being increasingly explored, such as targeting $BRAF^{V600E}$ and MEK using a combination of dabrafenib and trametinib to increase efficiency when targeting melanomas (Chapman *et al.* 2014, Brugnara *et al.* 2018). In more recent cases immunotherapies are being explored, including targeting immune checkpoint inhibitors PD-1 and CTLA-41–8 in order to enhance the T-cell-mediated response to tumours. While these have led to great advances in melanoma treatment, they can also cause adverse immune-related effects, leaving only a selection of patients responding positively to the treatment (Grywalska *et al.* 2018, Khair *et al.* 2019).

LncRNAs represent new molecular targets for the diagnosis and treatment of melanoma. Their specificity of expression in tissues and cell types, and at specific points in disease development, makes them ideal candidates for the generation of novel biomarkers and therapeutic molecules (Bolha *et al.* 2017). Using unique signatures based on lncRNA expression, generation of patient diagnosis, prognosis

and identification of the most suitable treatment, as well as monitoring patient progression are all possible (Rapisuwon *et al.* 2016). The specificity of expression is also useful for the generation of novel highly selective therapies to target lncRNA expression to prevent cancer and hopefully minimise off-target effects (Amit and Hochberg 2013). In addition, with lncRNAs greatly outnumbering protein-coding genes, they greatly increase in the number of possible targets. Current methods for targeting lncRNAs is predominantly focused on inhibiting oncogenic lncRNAs using methods such as antisense oligonucleotides (ASOs) and siRNAs (Leucci, Coe, *et al.* 2016).

One lncRNA that demonstrates potential therapeutic targetability in melanoma is *SAMMSON*. This oncogenic lineage-specific lncRNA is detected in greater than 90% of human melanomas and is co-amplified with MITF as well as positively regulated by SOX10. The lncRNA regulates mitochondrial homeostasis and metabolism through promoting the activity of p32, a master regulator of mitochondrial metabolism (Leucci, Vendramin, *et al.* 2016). Invasive melanoma cells which were resistant to MAPK inhibitors (Verfaillie *et al.* 2015) were sensitive to depletion of *SAMMSON*, with the cells experiencing reduced growth. The ability to therapeutically target *SAMMSON* was also assessed *in vivo* using patient-derived xenograft (PDX) melanoma models Mel006 and Mel010. When treated intravenously with GapmeRs targeting *SAMMSON*, tumour growth was inhibited, including a reduction in proliferation and increase in apoptosis. The treatment also showed no adverse effects on the mice used. In addition, although the $BRAF^{V600E}$ inhibitor dabrafenib was able to inhibit tumour growth, when treatment was combined with GapmeR3 the tumour regressed and there was a significant increase in apoptosis. Overall, *SAMMSON* represents a potential lncRNA therapeutic target that may be used in combination with other therapies (Leucci, Vendramin, *et al.* 2016).

By exploring the role of more lncRNAs in melanoma there will be new candidates that may be exploited as biomarkers or therapeutically, be that on their own or in

combination with currently used methods. This way lncRNAs offer a new avenue in the development of agents in the treatment of melanoma.

1.5 Aims of the thesis

The overall objective of this project was to begin to explore the role of novel melanoma-expressed intergenic lncRNAs that participate in the MITF-SOX10 transcriptional pathway. Focus is traditionally placed on the role of protein-coding genes in key regulatory pathways, leaving characterisation of lncRNAs in such processes largely unexplored. *DIRC3* is used as a model intergenic lncRNA to investigate the role of lncRNAs in MITF-SOX10-mediated control of melanoma progression.

The primary objectives for this project were to;

- Identify MITF- and SOX10-regulated lncRNAs expressed in melanocyte and/or melanoma cell lines
- Reveal whether *DIRC3* regulates its neighbouring cancer-associated genes
- Identify *DIRC3* regulation of gene expression programmes important to melanoma development
- Identify whether *DIRC3* expression regulates any of the key hallmarks of cancer using *in vitro* assays
- Begin to explore *DIRC3* mechanism by measuring the levels of SOX10 binding and histone modifications across the *DIRC3* locus upon its knockdown

Chapter 2: Materials and Methods

2.1. Cell manipulation

2.1.1 Cell culture

Human immortalised melanocytes (Hermes) cells were grown in Dulbecco's Modified Eagle Serum (DMEM) (ThermoFisher) which was supplemented with 10% Fetal Bovine Serum (FBS; (ThermoFisher)) human stem cell factor (hSCF)(ThermoFisher) and endothelin-1 (ET-1) (BaChem). They were kept in a humid environment at 37 °C and 5% CO_2 and passaged every two-to-three days when they reached roughly 90% confluency.

Human melanoma (501mel, SKmel28, A375) cell lines were grown in RPMI-1640 (ThermoFisher) with 10% Fetal Bovine Serum (FBS). They were kept in a humid environment at 37 °C and 5% CO_2 and passaged every two-to-three days when they reached roughly 90% confluency.

Table 2.1 Melanoma cell types used and where they were sourced.

Cell Type	Source
Hermes1 – human immortalised melanocyte cell line	Wellcome Trust Functional Genomic Cell Bank
501mel – human immortalised melanoma cell line, $BRAF^{V600E}$ mutant, expresses high level of MITF	Colin Goding, Ludwig Institute, Oxford
Skmel-28 – human immortalised highly invasive melanoma cell line, $BRAF^{V600E}$ mutant, expresses low level of MITF	Colin Goding, Ludwig Institute, Oxford
A375 – human immortalised malignant melanoma cell line, $BRAF^{V600E}$ mutant	ATCC
IGR-37 – human immortalised malignant melanoma cell line, $BRAF^{V600E}$ mutant	Colin Goding, Ludwig Institute, Oxford
IGR-39 – human immortalised primary melanoma cell line, $BRAF^{V600E}$ mutant	Colin Goding, Ludwig Institute, Oxford

2.1.2 Transfection

For siRNA (Sigma-Aldrich) and MISSION® esiRNA (Sigma-Aldrich) knockdown, SKmel28 and 501mel melanoma cells were seeded at a density of $5x10^4$ cell/ml into the wells of a 6-well plate containing 2 mL of medium. After 24 hours the cells were transiently transfected using 4 µl Lipofectamine (ThermoFisher) in 150 µl of OPTI-MEM (ThermoFisher) which was added to 100 pmol of siRNA or 1.5µg of esiRNA in 150 µl of OPTI-MEM medium. Following a 25-minute incubation at room temperature, the mixtures were applied to the prepared cells while gently rocking the plate to allow even distribution. The cells were harvested 72 hours later for analysis.

Table 2.2 siRNA oligos.

Oligo name	Oligo sequence (5'-3')
siMitf1	AGCAGUACCUUUCUACCAC
siMitf1as	GUGGUAGAAAGGUACUGCU
siMitf2	CUCCUGUCCAGCCAACCUU
siMitf2as	AAGGUUGGCUGGACAGGAG
siCtrl	UUCUCCGAACGUGUCACGU
siCtrlas	ACGUGACACGUUCGGAGAA

For ASO LNA GapmeR (Exiqon) knockdown, SKmel28 melanoma cells were seeded at a density of $6x10^4$ cell/ml into the wells of a 6-well plate containing 2 mL of medium. After 24 hours the cells were transiently transfected using 5 µl Lipofectamine in 150 µl of OPTI-MEM which was added to 150 pmol of ASO in 150 µl of OPTI-MEM medium. Following a 25-minute incubation at room temperature, the mixtures were applied to the prepared cells while gently rocking the plate to allow even distribution. The cells were then harvested 72 hours later for analysis.

Table 2.3 Antisense LNA GapmeR oligos.

Oligo name	Oligo sequence (5'-3')
DIRC3 ASO1	ACAAATAAGTAGACGT
DIRC3 ASO2	AACGGAAGGGACGTGT
IGFBP5 ASO1	GGAATGGTGCGAGTAT
NegA	AACACGTCTATACGC

For CRISPRi knockdown, SKmel28 melanoma cells were seeded at a density of $8x10^4$ cell/ml into the wells of a 6-well plate containing 2 mL of medium. After 24 hours the cells were transiently transfected using 4 µl Lipofectamine in 100 µl of OPTI-MEM which was added to 2 µg of vector in 100 µl of OPTI-MEM medium. Following a 25-minute incubation at room temperature, the mixtures were applied to the prepared cells while gently rocking the plate to allow even distribution. After 72 hours, the cells were trypsinised, resuspended in media containing puromycin (0.7 µg/ml), and transferred to a 6-cm dish (ThermoFisher). The cells were harvested as a pool seven days later for analysis.

2.1.3 Establishment of stable clonal cell line

For the generation of CRISPRi knockdown clonal cells, SKmel28, 501mel, and A375 were seeded at a density of $8x10^4$ cell/ml, $1.5x10^4$ cell/ml, and $8x10^4$ cell/ml, respectively, into the wells of a 6-well plate containing 2 mL of medium. After 24 hours the cells were transiently transfected using 4 µl Lipofectamine in 100 µl of OPTI-MEM which was added to 2 µg of vector in 100 µl of OPTI-MEM medium. Following a 25-minute incubation at room temperature, the mixtures were applied to the prepared cells while gently rocking the plate to allow even distribution. After 72 hours, the cells were trypsinised, resuspended in media containing 1 mg/ml (Skmel28), 1.3 mg/ml (501mel), or 1.5 mg/ml (A375) of puromycin, and transferred to a 10-cm dish (ThermoFisher). This was maintained until colonies of resistant cells began to form (roughly two weeks following the beginning of drug selection). The individual colonies were isolated using cloning cylinders (Sigma). The selected clones were expanded in media containing a 0.5 µg/ml of puromycin.

2.1.4 Cell fractionation

Roughly 1 x 10^6 cells were harvested and centrifuged at 1000 rpm for five minutes at 4 °C. The pellet was washed in an equal volume of ice-cold PBS and re-centrifuged.

The pellet was then re-suspended in 200 µl of Lysis Buffer (15 mM HEPES, pH 7.5, 10 mM KCl, 5 mM $MgCl_2$, 0.1 mM EDTA pH 8, 0.5 mM EGTA pH 8, 250 mM Sucrose, 0.4% Igepal, 1 mM DTT, 0.5 mM, protease inhibitor cocktail (Roche), 100 U/ml RNAsin, and incubated at 4 °C for 20 minutes with rotation. The mixture was pipetted up and down 14 times to lyse the cells, and nuclei pelleted at 2000 g for 10 minutes at 4 °C. The supernatant was collected containing the cytoplasmic fraction. RNA was then extracted from the two fractions using the QIAGEN RNeasy Mini Kit (Section 2.3.1).

2.1.5 Proliferation assay

Roughly $1.5x10^4$ SKmel28 clonal CRISPRi knockdown cells were seeded in a 6-well plate. The cells were maintained in media containing 0.5 µg/ml of puromycin and grown in 5% CO_2 at 37°C. The number of cells were counted using a haemocytometer at days 0, 2, and 4.

2.1.6 Invasion assay

SKmel28 cells were serum starved in FBS-free medium for 24 hours prior to setting up the assay. The QCM™ 24-Well Cell Invasion Assay (Millipore) was used. 300 µl of FBS-free media was pipetted into the interior of the inserts (upper chamber). After 15-30 minutes, 250 µl of medium was removed from the inserts and replaced with 250 µl of FBS-free medium containing $8x10^5$ cells. The lower chamber then had 500 µl of media containing 20% FBS added. The cells were incubated in 5% CO2 at 37°C for 52 hours. To detach the cells that had invaded through the membrane, the upper chambers were placed in a well of a clean 24-well plate containing 225 µl pre-warmed Cell Detachment Solution and incubated at 37°C for 30 minutes. The cells were fully dislodged from the underside of the membrane by gently tilting the plate back and forth at several points during the incubation. The inserts were then removed from the wells. The cells were lysed and dyed by adding 75 µl of the kit's dye solution-lysis buffer mix (1:75) to the cell-containing lysis solution. This was covered with tin foil and incubated at room temperature for 15 minutes. Finally, 200 µl of the mix was

transferred to a 96-well plate and fluorescence was measured with a fluorescence plate reader (SoftMax Pro) using a 480/520 nm filter set.

2.1.7 Soft agar colony formation assay

Roughly $5x10^3$ clonal CRISPRi knockdown cells were suspended in 1.5ml growth medium containing 0.3% noble agar, on top of 1.5ml growth medium with 0.5% noble agar in a six-well plate. Cells were grown for 21 days in 5% CO2 at 37°C and supplemented with 100 µl of growth medium every three-to-four days. The cells were then fixed in fixing solution (1% Formaldehyde, 0.01% methanol, PBS) for 20-30 minutes, stained using 0.01% crystal violet for 30-60 minutes, and then washed with distilled water to remove excess stain. Images were taken using a UVP Gel Doc-It^2 Imager. The number of colonies was quantified using ImageJ (Section 2.5.1).

2.1.8 Transformation of competent bacterial cells

DH5α chemically competent cells (ThermoFisher) were used to increase yield of plasmid DNA. The cells were thawed on ice and used in 25 µl aliquots. Typically, 1 µl of plasmid DNA or 2 µl of ligated oligo-vector was added to the cells and incubated on ice for 25 minutes. They were then heat-shocked by incubating at 42 °C for 30 seconds and then on ice for two minutes. Next, 100 µl of room temperature Super Optimal broth with Catabolic repression (SOC) (ThermoFisher) was added to the cells, and they were kept at 37 °C and 220 rpm for one hour. The cells were then spread on Luria-Bertani (LB)-agar plates (Sigma) containing 100 µg/ml of carbenicillin. The plates were kept at 37 °C overnight.

2.1.9 Glycerol stocks

Following growth overnight in LB broth at 37 °C and 220 rpm, 500 µl of transformed DH5α was mixed with 500 µl of 40% Glycerol stock. The cells were flash-frozen and stored at -80°C.

2.2 DNA manipulation

2.2.1 5’ Rapid amplification of cDNA ends (RACE)

LncRNA 5’ and 3’ ends were identified using the GeneRacer™ Core kit (ThermoFisher) in SKmel28 cells according to the manufacturer’s protocol.

In brief, for identification of the 5’ end of the target RNA the 5’ phosphates were removed using calf intestinal phosphatase (CIP) so that the GeneRacer™ RNA oligo could ligate only to full-length transcripts which are capped. The 5’cap structure was then removed from the de-phosphorylated transcripts using tobacco acid pyrophosphatase (TAP), leaving a 5’ phosphate for the GeneRacer™ oligo to anneal to. Using T4 RNA ligase, the GeneRacer™ RNA oligo was then ligated to the 5’ end of the RNA. The prepared mRNA was reverse transcribed using SuperScript™ III RT Module (ThermoFisher) and GeneRacer™ random primers. The resultant first-strand cDNA was amplified using a GeneRacer™ 5’ Primer with a sequence homologous to the GeneRacer™ RNA oligo and reverse Gene Specific Primer. An additional round of PCR could be performed using nested primers.

To identify the 3’ ends, purified mRNA was reverse transcribed using SuperScript™ III RT Module and GeneRace™ Oligo dT primer. The resultant first-strand cDNA was then amplified using a GeneRacer™ 3’ Primer with a sequence homologous to the GeneRacer™ Oligo dT primer. An additional round of PCR could be performed using nested primers.

For both 5’ and 3’ RACE, PCR products were run on a 2 % agarose gel and bands of interest were purified using a QIAGEN PCR purification kit (Section 2.2.3) and cloned into a pGEM-T-Easy vector (Section 2.2.2) before analysis by DNA sequencing (Section 2.2.12).

Table 2.4 RACE oligos.

Oligo name	Oligo sequence (5'-3')
5'RACE (1° PCR)	
Dirc3 5'RACE1	GCACAGCTCAGCACCCAGACTCCTTCCA
5'RACE (2° PCR)	
Dirc3 5'RACE2	CCTCTTGCCTCTCCCTGCCTGTGCTCAT
3'RACE (1° PCR)	
Dirc3 3'RACE1	CCAGATTGTGGGCGCTTCTACTG
3'RACE (2° PCR)	
Dirc3 3'RACE2	ATGTGTTGGGTGTGGAACAGGGTCTCT

2.2.2 pGEM-T-Easy cloning

Fragments of DNA were cloned into the pGEM-T-Easy (ThermoFisher) vector according to the manufacturer's instructions. Features of vector in Appendix Section 8.1. Briefly, the reaction mix was composed of 5 µl Ligation Buffer, 1 µl pGEM-T-Easy vector, 2µl PCR product, and 1 µl T4 DNA ligase, as well as DEPC-treated water, making a total volume of 10 µl. This was left at room temperature for one hour before being used to transform chemically competent DH5α cells, as described in Section 2.2.8.

2.2.3 On column DNA purification

PCR products and digeted vectors were purified using a QIAquick® PCR Purification kit (QIAGEN). The procedure was carried out according to the manufacturer's protocol. In brief, the high salt Buffer PB was added to the sample, which was then passed through a QIAquick™ spin column, binding the DNA to the membrane. The DNA was then washed, to remove impurities. Following a final dry spin, the purified DNA was eluted in 50 µl of Elution buffer. The concentration of the eluted DNA could be determined using a NanoDrop.

2.2.4 CRISPRi plasmid construction

The CRISPRi plasmids pX-dCas9-mod and pX-dCas9-mod-KRAB were donated by Andrew Bassett, Sanger Institute, Cambridge. Both vectors contain a CBh promoter and include resistance to ampicillin and puromycin. Vector map is presented in Appendix Section 8.2. The sgRNAs were designed to target a genomic region -50 and +150 bp of the target transcription start site using the Zhang Lab CRISPR Design Tool (https://zlab.bio/guide-design-resources).

Table 2.5 CRISPRi vectors.

Oligo name	Key Features
pX-dCas9-mod	Contains a CBh promoter and resistance to ampicillin and puromycin.
pX-dCas9-mod-KRAB	Contains a CBh promoter and resistance to ampicillin and puromycin. Has the addition of a Krüppel-associated box (KRAB) protein

Table 2.6 CRISPRi sgRNA oligos.

Oligo name	Oligo sequence (5'-3')
CASC11sg1 F	CACCGCCGAAGAAAGAGGAGTTAC
CASC11sg1 R	AAACGTAACTCCTCTTTCTTCGGC
CASC11sg2 F	CACCGGCAGAAGGTCCGAAGAAAG
CASC11sg2 R	AAACCTTTCTTCGGACCTTCTGCC
DIRC3sg1 F	CACCGTTCGGGAAGCTTTTACTCA
DIRC3sg1 R	AAACTGAGTAAAAGCTTCCCGAAC
DIRC3sg2 F	CACCGTTGGTCCTGCAGGCTGTAC
DIRC3sg2 R	AAACGTACAGCCTGCAGGACCAAC
RefSeq DIRC3sg1 F	CACCGTGCACACGCATATGTGTCC
RefSeq DIRC3sg1 R	AAACGGACACATATGCGTGTGCAC
RefSeq DIRC3sg2 F	CACCGGGCAAGTCGCTCCGTCATG
RefSeq DIRC3sg2 R	AAACCATGACGGAGCGACTTGCCC
NEGsg1 F	CACCGCGCCAAACGTGCCCTGACGG
NEGsg1 R	AAACCCGTCAGGGCACGTTTGGCGC
NEGsg2 F	CACCGTGCGATGGGGGGGTGGGTAGC
NEGsg2 R	AAACGCTACCCACCCCCCCATCGCAC

2.2.5 Oligonucleotide annealing and phosphorylation for the generation of sgRNAs for CRISPRi

5 µl of the 100 µM Forward and Reverse oligonucleotides (Table 2.3) were mixed with 10 µl of 2x Annealing Buffer (20mM Tris, 2mM EDTA, 100 mM NaCl) and incubated at 94 °C for five minutes followed by room temperature for one hour. Samples were then phosphorylated by mixing together 1 µl of the annealed oligo, 1 µl T4 PNK (New England Biolabs), and 1 µl Roche T4 DNA ligase Buffer in a total volume of 10 µl. These were incubated at 37 °C for 30 minutes, and then 65 °C for 20 minutes to inactivate the enzyme. Samples were then diluted 1:10.

2.2.6 Restriction enzyme digestion of CRISPRi vectors

The CRISPRi vectors (pX-dCas9-mod and pX-dCas9-mod-KRAB) were digested using *BpiI* Fast Digest enzyme (ThermoFisher). For this 1 µg of vector was digested using 2 units of enzyme and 1x restriction buffer in a total volume of 20 µl. The mix was kept at 37 °C for 20 minutes and heat inactivated at 65 °C for 10 minutes.

2.2.7 Dephosphorylation of linearised plasmid

Re-ligation of the digested vector was prevented by dephosphorylating the 5' end of the linearised plasmid. This was performed using 1 µl of CIP (Calf Intestinal Alkaline Phosphatase (New England Biolabs) in 20 µl of the digested vector. The mix was kept at 37 °C for one hour and separated on a gel. The plasmid DNA was purified using a QIAGEN QIAquick® Gel Extraction Kit, as described in Section 2.2.8.

2.2.8 DNA gel extraction

Following gel electrophoresis, DNA was purified from the agarose gel using a QIAGEN QIAquick® Gel Extraction Kit (QIAGEN) according to the manufacturer's protocol. In brief, the fragment of interest was excised from the gel and the surrounding gel

dissolved at 50 °C. The DNA was then bound to a membrane, washed, and eluted in 30 µl of Elution Buffer.

2.2.9 DNA ligation

Dephosphorylated linearised plasmids and phosphorylated oligos were annealed together using vector to insert ratios of 1:2, 1:4, or 1:7, using up to 100 ng of vector. In a mixture made up to 10 µl, the vectors and oligos were added to 1 µl T4 DNA ligase (New England Biolabs) and 1 µl T4 DNA ligase buffer. These were incubated overnight at 16 °C.

2.2.10 Colony PCR

Individual colonies were screened for cloned inserts using an AmpliTaq reaction kit (ThermoFisher). Individual colonies were picked and mixed with a reaction mix containing 0.8µl of forward primer targeting the vector, 0.8 µl reverse oligo (Table 2.4), 0.25 µl Taq polymerase (ThermoFisher), 2 µl 10X Taq polymerase buffer, 2 µl Magnesium chloride, and 0.5 µl 10 mM dNTP, made up to 20 µl. The mixes were amplified using PCR and separated using agarose gel electrophoresis (Section 2.2.13) to check the sizes of the bands.

The primers used are given in Table 2.7. For identification of the presence of CRISPRi sgRNAs, the reverse oligos used for generation of the sgRNAs were used as reverse primers.

Table 2.7 Colony PCR oligos.

	Oligo name	Oligo sequence (5'-3')
p-GEM-T-Easy	M13 Forward	GTAAAACGACGGCCAG
	M13 Reverse	CAGGAAACAGCTATGAC
CRISPRi	CRISPRi Fwd	GGCCTATTTCCCATGATTCCT
	CRISPRi Rev	TTTCTTGGGTAGTTTGCAGTTTT

2.2.11 Isolation of plasmid DNA

Single bacterial colonies were isolated from a LB-agar plate. The colonies were individually inoculated in 3-5 ml of LB medium (Sigma) containing 100 µg/ml carbenicillin (ThermoFisher) for small-scale and 50 ml for large-scale purification. These were incubated at 37 °C overnight with shaking (220 rpm). Plasmid DNA was isolated using a QIAprep Spin Miniprep kit (QIAGEN) or QIAprep Spin Midiprep kit (QIAGEN) according to the manufacturer's instructions. In brief, cells are pelleted and then lysed in an alkaline solution. Plasmid DNA was then bound to a silica membrane using a high salt buffer. Unbound material was washed off and the DNA eluted in Elution buffer. The concentration of the eluted plasmid DNA was measured using a NanoPhotometer^{TM} Implen.

2.2.12 DNA sequencing

Sanger Sequencing was performed by Eurofins Scientific. Plasmids were sent at a concentration of 50-100 ng in 17 µl each and 5µl of forward vector primer (10 mM) per sequencing sample.

2.2.13 Agarose gel electrophoresis

Agarose gels (0.5-2%), for horizontal gel electrophoresis, were made by dissolving agarose (Fisher Scientific) in 100 ml of TAE (ThermoFisher) in a microwave. For later visualisation, 1x Gel Red Nucleic Acid Stain (Biotium) was added to the gel. The solidified gels were placed into a gel electrophoresis tank containing 1x TAE buffer. The DNA samples were loaded with 1x loading dye (New England Biolabs) into the wells, alongside a DNA ladder marker (2.2.2.13). The DNA fragments were separated in the electrophoretic tank at 80-120 V (constant voltage). The DNA was visualised using a transilluminator (Gel Doc-It^2 Imager UVP).

2.2.14 DNA ladder marker

A 1kb DNA ladder marker for gel electrophoresis was made by mixing 500 µg/ml of 1 kb DNA ladder (New England Biosciences) with 200 µl of loading buffer (New England Biosciences) and diluted 1:10.

2.2.15 Gel extraction

DNA fragments of interest were visualised using a transilluminator and excised from the agarose gel using a blade. DNA was extracted from the gel using a QIAquick Gel Extraction Kit (QIAGEN) according to the manufacturer's instructions. In brief, the excised region of DNA was dissolved in a solubilising buffer at 50 °C. The solubilised gel was passed through a spin column. DNA was bound to the membrane while unbound material was removed when washed. The DNA was then eluted in Elution buffer and concentration measured using a NanoPhotometer^{TM} Implen.

2.2.16 Chromatin Immunoprecipitation (ChIP)

Roughly 1x10^{7} clonal SKmel28 CRISPRi cells per assay were crosslinked in 1% formaldehyde. Cells were lysed by douncing in hypotonic buffer (10 mM Tris-HCl pH 7.2, 10 mM KCl, 1.5 mM $MgCl_2$, 1% NP40, 1x Protease Inhibitor Cocktail) and then centrifuged to separate the nuclear pellet. The pellet was resuspended in sonication buffer (50 mM Hepes KOH pH 7.9, 10 mM EDTA pH8, 1% SDS, 1x Protease Inhibitor Cocktail) and sonicated to roughly 500 bp in a Bioruptor Pico Diagenode. Debris was separated using centrifugation, and suspended chromatin diluted 1:10 in IP dilution buffer (10 mM Hepes KOH pH 7.9, 1% Triton X-100, 150 mM NaCl, 1mM EDTA pH8, 0.1% SDS, 1x Protease Inhibitor Cocktail). Samples were immunoprecipitated at 4°C overnight using 5 µg of antibody and non-specific Immunoglobin G (IgG) isotype control antibody. Magnetic Pierce™ Protein G Magnetic Beads (ThermoFisher) were also blocked in 1ml of blocking solution (BSA 0.2mg/ml, tRNA 0.1 mg/ml) overnight at 4 °C while rotating. Antibody-bound samples were mixed with Dynabeads

(ThermoFisher) on a rotating wheel at 4°C for four hours. Non-bound proteins were removed by washing beads on a magnetic stand using a series of wash buffers (Wash Buffer I – 0.1% SDS, 1% Triton X-100, 2 mM EDTA, 20 mM Tris-HCl pH 8.1, 150 mM NaCl; Wash Buffer II – 0.1% SDS, 1% Triton X-100, 2 mM EDTA, 20 mM Tris-HCl pH 8.1, 500 mM NaCl; Wash Buffer III – 0.25 M LiCl, 1% NP-40, 1% Sodium Deoxycholate, 1 mM EDTA, 10 mM Tris-HCl pH u8.1). The antibody-bound proteins were then eluted from the beads by suspending the sample in 250 µl Elution Buffer (1% SDS, 0.1 M $NaHCO_3$) and were rotated at room temperature for 15 mins. Beads were isolated using a magnetic stand and supernatant collected. Crosslinking was reversed by adding RNase (0.5mg/ml) and NaCl (0.25M) and incubating at 65°C. The samples were precipitated by adding 2.5 volumes of 100% ethanol and kept at -20°C for 72 hours. The samples were centrifuged to pellet DNA and resuspended in 100 µl of water. The samples were then incubated with Proteinase K buffer (50 mM Tris pH 7.5, 25 mM EDTA, 1.25% SDS, 0.02 mg/ml Proteinase K - ThermoFisher) at 42°C for 1-2 hours to remove the proteins. The DNA fragments were purified using a QIAquick PCR purification kit (Qiagen)(2.2.3) and binding confirmed using RT-qPCR.

Table 2.8 Antibodies used for ChIP-qPCR.

Antibody	Source
Anti-SOX10 (rabbit monoclonal antibody)	Abcam – ab155279
Anti-Histone H3K27ac (rabbit polyclonal)	Active Motif – 39133
Anti-rabbit IgG	Merck – PP64

Table 2.9. qPCR primers used to amplify SOX10-bound genomic sequences.

Oligo Name	Oligo sequence (5'-3')
Control 1 F	CTGCTTTCTCTCCTTGCCCA
Control 1 R	CGGCTGAGCCATATGCTGTA
Control 2F	TCAGATGCATTGTCACGCCT
Control 2R	AGACCCAGTGAGAGAGACCC
Peak 1 F	CCTCTCCCAGGCCATTACAA
Peak 1 R	TAATTCCCCTCAGCTTCCAGC
Peak 2 F	CCCCTCACAGAAGAAAAGCCT
Peak 2 R	GGAGTCTGCATGAAAGGGGC
Peak 3 F	GACAGACAACAGTCATGTGGTT
Peak 3 R	GCTCCTTCCTCTTTTTCCCAGA
Peak 4 F	GAGAGTCCGTGAAGGAGTGG
Peak 4 R	CCTCCGCCAGCAATAGATAA

2.3 RNA manipulation

2.3.1 RNA isolation and removal of DNA contamination

For RNA purification, cells were harvested, washed twice with PBS, and centrifuged at full speed in a microcentrifuge for 10 seconds. RNA was then extracted using a RNeasy Mini Kit (QIAGEN) according to the manufacturer's instructions. In brief, cells were lysed and homogenised by passing them through a QIAshredder (QIAGEN) in a lysis buffer. After adding ethanol to the RNA-containing eluate, the RNA was bound to a spin column membrane. Through a series of washes, contaminants were removed from the RNA. DNA contamination was removed using a RNase-Free DNase kit (as described in Section 2.3.2). Following a final series of washes to remove the DNase, the RNA was eluted using Elution buffer, and concentration measured using a nanodrop.

2.3.2 On column removal of DNA contamination from RNA sample

When RNA was bound to a RNeasy Mini Kit spin column, the contaminant DNA was removed using a RNase-Free DNase Set (QIAGEN). A mixture of 10 µl of DNase and 70 µl of Buffer RDD were added to the RNA and left at room temperature for 15 minutes, after which the enzyme and buffer were washed off in the following steps of the RNeasy Mini Kit protocol.

2.3.3 First strand cDNA synthesis

Extracted RNA was reverse transcribed using a QuantiTect Reverse Transcription Kit (QIAGEN) according to the manufacturer's instructions. In brief, 1 µg of RNA had any remaining genomic DNA removed following the addition of gDNA Wipeout Buffer at 42 °C for three minutes. A mixture containing Quantiscript Reverse Transcriptase, Quantiscript RT buffer, and RT primer mix, making a final volume of 20 µl, was added and incubated at 42 °C for 28 minutes, followed by a three-minute incubation at 95°C

to inactivate the Quantiscript Reverse Transcriptase. The cDNA was then typically diluted 1:4 for RT-qPCR (Section 2.3.4).

2.3.4 Quantitative PCR analysis of RNA expression (RT-qPCR)

Transcripts of interest had primers designed for qPCR analysis using NCBI Primer Blast. Real-time quantitative PCR (RT-qPCR) was performed using Fast SYBR Green™ Master Mix (ThermoFisher) and a StepOne™ Plus Real-Time PCR system (Applied Biosystem). Relative expression levels of the genes were assessed in technical triplicates for each run. Control non-reverse transcribed RNA were included to check for genomic DNA contamination. Expression levels of target transcripts were normalised against housekeeping gene(s) not known to be influenced by altered experimental conditions. Fold changes in target expression were calculated relative to control conditions using the ddCt method.

Table 2.10 LncRNA and transcription factor qPCR oligos.

Oligo name	Oligo sequence (5'-3')
LncRNA	
MelncRNA1 Fwd	ATATCGGCTTGCGGTTCACT
MelncRNA1 Rev	GCCTTGCTGGAGAAGGAACA
MelncRNA4 Fwd	AGGGAATCCTGCCTAAAACCT
MelncRNA4 Rev	GCTGGACCTTTGTGCTGTAG
MelncRNA7 Fwd	AATCTGTTGCCAGGTCCCAC
MelncRNA7 Rev	ACCAAGCCGAAGCCTTAGAG
MelncRNA9 Fwd	TGCCCAGAAACAGCACATTC
MelncRNA9 Rev	TCAAGCTACCAGTCAGCACA
MelncRNA11 Fwd	AGATCCGCAGAGTGGTCTGA
MelncRNA11 Rev	ATGGCCAGGGAAACAGATCC
MelncRNA13 Fwd	ATTCCACTAGCCAAAGCCCC
MelncRNA13 Rev	CAGGCCTTAAGGGCAGTTCA
MelncRNA17 Fwd	ACTCTCGCTATGTGACCCGA
MelncRNA17 Rev	CTTGTCTGCTTTTGGAGCCG
CASC11 Fwd	GCTGCAGAAGGTCCGAAGAA
CASC11 Rev	TGCGGTTGAATAGTCACCTCTG
DANCR Fwd	AATGCAGCTGACCCTTACCC
DANCR Rev	GGCTTCGGTGTAGCAAGTCT
DIRC3 Fwd	CCCACCCCACCACTATTCAC
DIRC3 Rev	CCACTGGGACAACCATCTCC
NEAT1Fwd	CTGGTCATCTGGTAAGCCCG

NEAT1 Rev	ACATTCACTCCCCACCCTCT
STK4AS Fwd	CAGCCATGGGTGTGTAACCT
STK4AS Rev	GGTAGTGGCATTCGGAAGCA
Transcription factor	
MITF1 Fwd	TGGCAAATACGTTGCCTG
MITF1 Rev	ACGCTGTGAGCTCCCTTT
SOX10 Fwd	ACAAGAAAGACCACCCGGAC
SOX10 Rev	AAGTGGGCGCTCTTGTAGTG
Neighbouring Genes	
Igfbp5 Fwd	ACAAGAGAAAGCAGTGCAAACC
Igfbp5 Rev	CGTCAACGTACTCCATGCCT
Tns1 Fwd	GCGTTCCTCCATCCAACCAT
Tns1 Rev	GCTCCTTCTCCCTTGTCCAC
Myc Fwd	GTAGTGGAAAACCAGCAGCC
Myc Rev	AGAAATACGGCTGCACC
Reference Genes	
hPolII Fwd	TTGTGCAGGACACACTCACA
hPolII Rev	CAGGAGGTTCATCACTTCACC

2.4 Protein manipulation

2.4.1 Bradford assay

Roughly 6x10^5 cells were harvested for Western Blot analysis. Cells were pelleted by centrifugation and lysed in 50µl of RIPA (Radioimmunoprecipitation assay) buffer (150 mM NaCl, 1% NP40, 0.5% EDTA, 0.1% SDS, 50 mM Tris pH 8, 0.5 mM protease inhibitor cocktail (Roche)), while rotating in a cold room for 10 minutes.

The concentration of extracted protein was identified using a Bradford assay, so that equal amounts of protein could be loaded onto a gel for Western blotting. The concentration of the extracted proteins were measured using the Pierce™ BCA Protein Assay Kit (ThermoFisher) following the manufacturer's instructions. In brief, Albumin Standard (bovine serum albumin – BSA) was diluted using a diluent supplied in the kit to make up a series of protein standards (0-1.4 mg/ml). The standards and unknown samples were each pipetted into microplate wells in 5 µl volumes, with 250 µl of Working Reagent added. The expression was read on a BioRad iMark microplate reader between 5 and 45 minutes after adding the working reagent.

2.4.2 SDS-PAGE and Western Blotting

SDS-PAGE and Western blotting were performed using a Mini-PROTEAN Tetra cell system (BioRad). Proteins were loaded with 1x sample buffer (Sigma) on a 10 % acrylamide gel and were separated according to size using gel electrophoresis in Running Buffer (2.5 mM Trizma, 2 mM Glycine)(130 V, constant voltage, 50 minutes). The gel, PVDF membrane (GE Healthcare Life Sciences), and sponges were soaked in transfer buffer. The PVDF membrane was activated by soaking in methanol for 10 seconds. The proteins were transferred to the membrane in a wet electroblotting tank for 1-1.5 hours at a constant voltage (150 mA) in Transfer Buffer (20% Propanol, 25 mM Tris, 192 mM Glycine). The membrane was then blocked by rotating for one hour at 4 °C in Blocking Buffer (5% milk, PBS-TWEEN (0.1%)) and then washed three times with Washing Buffer (PBS-TWEEN 0.1%). Specific proteins were targeted by incubating the membrane with blocking buffer containing the primary antibody overnight. The membrane was then washed three times for five minutes each with Washing Buffer. The membrane was incubated with blocking buffer containing the secondary antibody by rocking at 4 °C for one hour, followed by three washes. The bound antibodies were then detected using ECL™ Western Blotting Detection Reagents (Sigma) according to the manufacturer's instructions. The signal was detected using a Vilber Fusion-SL.

Table 2.11 Western blotting antibodies.

Antibody (Primary)	**Source**	**Dilution**
Anti-MITF (Rabbit polyclonal)	MERCK – HPA003259	1:250
Anti-SOX10 (Mouse monoclonal)	Santa Cruz – (A-2) sc-365692	1:1000
ß-actin (Mouse monoclonal)	Santa Cruz – (C4) sc-47778	1:200
Antibody (Secondary)		
Goat anti-rabbit IgG-HRP (Goat polyclonal)	Santa Cruz – (SC-2004)	1:5000
Goat anti-mouse (Goat polyclonal)	Santa Cruz – (SC-2005)	1:2000

2.5 Computational Analysis

2.5.1 Image-J

The number of colonies grown in the soft agar assays were quantified using ImageJ 2.0. Initially, contrast between colonies and background was increased and background removed using GIMP image editor. The file of interest was then imported into ImageJ and converted to 32-Bit. The 'Threshold' was set to the same level for each replicate. Colonies counted were selected based on settings for 'Analyse Particles' at a Size of 3-Infinity, Circularity of 0.80-1.00, and selected to show the Overlay masks so that any debris or background was not counted. Any colonies contacting one another were separated using the clone tool.

2.5.2 RNA-sequencing

Total RNA was prepared in triplicate from *DIRC3* ASO-GapmeR and CRISPRi knockdown, as well as *IGFBP5* ASO-GapmeR knockdown, SKmel28 cells using the GeneJET RNA purification Kit (ThermoFisher Scientific)(Section 2.3.1). The Illumina HiSeq4000 (Novogene) was used to perform PolyA selected 150-bp paired-end RNA sequencing with a minimum depth of 30M mapped reads generated per sample. Computational analysis of gene expression analysis was performed by Michael Shapiro (University of Bath) for ASO-GapmeR knockdown and Yihong Jennifer Tan (University of Lausanne) for CRISPRi knockdown. Using trim_galore version 0.4.4, data was cleaned for adapters and low-quality sequence ends. The cleaned data was then aligned using FLASH v1.2.11 and mapped to the hg19 genome using bowtie version 1.1.2. The human gene annotation file was acquired from Gencode (v19, genome assembly hg19) and data was aligned to these annotations using the Bioconductor package GenomicAlignments version 1.34.0 function. Using the Bioconductor package DESeq2 (R version 3.5.0, DESeq version 1.22.2) data was statistically analysed using default settings. Differential expression of genes was

analysed between the knockdown and control groups. P-values were adjusted by the Benjamini-Hochberg method, controlling for false discovery rate (FDR).

2.5.3 GO analysis

The Bioconductor package GOstats function hyperGtest was used for Gene Ontology analysis of RNA-seq data. A background dataset was generated from a list of all the genes expressed in SKmel28 cells. The resulting p-values were used to generate FDR cut-offs using the brainweaver package function.

2.5.4 Gene expression analysis of TCGA melanoma RNA-seq data

Analysis of RNA-seq data from The Cancer Genome Atlas (TCGA) melanoma (SKCM) data was performed by Pakavarin Louphrasitthiphol (Ludwig Institute Oxford). The data was accessed via the cBioportal for Cancer Genomics (http://www.cbioportal.org) and retrieved using the CGDS-R package (project.org/web/packages/cgdsr/index.html). Gene expression values were recovered as RPKM (reads per kilobase of transcript per million mapped reads) normalised read counts. Samples were ranked based on increasing expression value of the gene of interest, or mean expression for genes from a response signature, (x-axis) and then plotted as a black line representing relative expression. The relative expression of *DIRC3* (y-axis) in each sample was plotted as a bar graph, shown in light grey, with a moving average line based on a sample window of 20. The Spearman correlation coefficient and P-value for the correlation between genes of interact were generated using the R function ‘cor.test’.

Chapter 3: Selection of *DIRC3* as an MITF-SOX10 regulated intergenic lncRNA dysregulated in cutaneous melanoma

3.1 Introduction

Thousands of lncRNAs have dysregulated expression in various cancers, a subset of which have been found to hold functional roles. Using genome-wide approaches, such as RNA-seq and ChIP-seq, it is possible to identify lncRNAs that have altered transcription between healthy and diseased tissues of the same organ (Iyer *et al.* 2015, Yan *et al.* 2015). While the number of annotated lncRNAs has continued to increase, functional annotation is still very limited. It is likely that not all identified lncRNAs are functional and instead are a result of spurious transcription. However, with thousands of novel lncRNAs being identified, there are potentially large numbers which have important roles in regulating cellular processes (Palazzo and Lee 2015). Due to the vast number of lncRNAs present in the human genome, bioinformatic pipelines allow prioritisation of a subset for further study based on specific criteria. By integrating a range of datasets, such as RNA-seq and ChIP-seq, the likelihood of identifying functionally relevant lncRNAs is increased. When at a more manageable number, selected candidates can be functionally validated using experimental techniques.

LncRNAs are often categorised based on their proximity to nearby protein-coding genes. The largest of these categories are intergenic lncRNAs whose loci do not overlap protein-coding genes (Derrien *et al.* 2012). An advantage of studying intergenic lncRNAs is they are easier to specifically knockdown or amplify without the risk of indirectly targeting neighbouring protein-coding genes due to them not overlapping other genes. Of this category, some are known as enhancer- or promoter-associated transcripts based on them overlapping such regulatory elements and having precise patterns of H3 lysine 4 mono- and trimethylation (Ørom *et al.* 2010, Fufa *et al.* 2015, Hon *et al.* 2017). Such lncRNAs function through

controlling the activity of these elements. Enhancer-associated lncRNAs have been identified that function through multiple proposed mechanisms including manipulating chromosomal configuration and bringing regulatory elements together (Lam *et al.* 2014). Aberrant increase or reduction in the expression of lncRNAs due to disrupted regulation (such as by oncogenes), or mutations by copy number alteration or small nucleotide polymorphism, can lead to the occurrence of diseases including cancer (Yan *et al.* 2015, Chaudhary and Lal 2017, Fernando *et al.* 2017). Numerous intergenic lncRNAs have already been studied in different cancers, including melanoma. Such lncRNAs include *BANCR*, *MALAT1*, and *SAMMSON*, each of which have been found to participate in key melanoma functions, including cell migration, survival and metastasis (Flockhart *et al.* 2012, Tian *et al.* 2014, Leucci, Vendramin, *et al.* 2016).

Many cancer-associated lncRNAs expression is regulated by tumour suppressors and oncogenes, such as p53 and MYC (Chaudhary and Lal 2017, Iaccarino 2017). MITF is a key transcription factor involved in the regulation of melanocyte development and melanoma. Acting as a lineage addiction oncogene, MITF is amplified in roughly 10-30% of melanoma cases. This number is larger for individuals with metastatic disease, leading to an association between MITF and worse patient survival (Garraway *et al.* 2005). MITF positively regulates expression of genes important in cell differentiation and proliferation, while repressing those with roles in invasion and motility (Carreira *et al.* 2006, Strub *et al.* 2011, Verfaillie *et al.* 2015). Its expression is also activated by SOX10 which has previously been identified in all primary and the majority of metastatic melanomas (Shakhova *et al.* 2012, Graf *et al.* 2014) where it can regulate genes important in cell survival proliferation and invasion (Cronin *et al.* 2013, Verfaillie *et al.* 2015). Several thousand binding sites are co-occupied by MITF and SOX10, resulting in their joint control of gene programmes involved in melanocyte development and melanoma (Laurette *et al.* 2015). A number of key features for their joint roles in melanoma have already been identified. A rheostat model for MITF function has previously been proposed in which low MITF expression is identified in proliferative cells and elevated MITF in invasive cells, while cells in which MITF is

almost absent undergo senescence (Hoek and Goding 2010). High SOX10 was later identified as another feature of proliferative cells (Verfaillie *et al.* 2015). Consequently, melanoma cells are able to phenotypically switch between these states under the control of MITF and SOX10, likely in response to environmental signals (Verfaillie *et al.* 2015, Kawakami and Fisher 2017). These distinct cell states, characterised by variations in MITF and SOX10 levels of expression, may also influence resistance of melanoma cells to MAPK pathway inhibitors (Konieczkowski *et al.* 2014, Sun *et al.* 2014). Little is currently known about the role of lncRNAs within the MITF-SOX10 transcriptional programmes.

3.1.1 Chapter Summary

This chapter focusses on identifying and beginning to characterise candidate melanoma-expressed intergenic lncRNAs that may have a functional role in melanoma. A key feature for candidate melanocyte- or melanoma-expressed lncRNAs is that they are bound and regulated by the melanoma oncogene MITF. Dysregulated in renal carcinoma 3 (*DIRC3*) was prioritised for further characterisation. Upon exploration of the *DIRC3* locus, the lncRNA was found to be surrounded by two genes, *IGFBP5* and *TNS1*, with known tumour suppressive roles. *DIRC3* was also discovered to be regulated by the melanoma factor SOX10 and its locus was shown to harbour a number of MITF-SOX10 co-occupied binding sites. Using a combination of data from The Cancer Genome Atlas, and analysis of cancer cell lines, *DIRC3* was identified as a potential tumour suppressor in melanoma that is repressed by MITF and SOX10.

3.2 Results

3.2.1 Identification of intergenic lncRNAs bound by MITF and expressed in melanoma and/or melanocyte cell lines

In order to identify novel melanoma-expressed lncRNAs, a pipeline was devised to classify lncRNAs that are located between protein-coding genes (intergenic), expressed in melanoma and/or melanocyte cell lines, and contain binding sites for the oncogene MITF. It was hypothesised that lncRNA holding these features may act as novel drivers or inhibitors of melanoma development and progression.

RNA-sequencing (RNA-seq) analysis was used to identify and catalogue intergenic lncRNAs that are expressed in melanoma and/or melanocyte cell lines. Intergenic lncRNAs were selected solely based on their sequences not overlapping protein coding sequences, independent of distances between them. Two $BRAF^{V600E}$ mutated melanoma cell lines (IGR37 and IGR39) from the same patient and a melanocyte cell line (Hermes) were investigated. IGR37 cells are MITF-high and non-invasive (Luis *et al.* 1989) while IGR39 cells are MITF-low, de-differentiated and invasive (Konieczkowski *et al.* 2014). These cells were used as they represent different stages of the disease. Also, with them being derived from the same individual, any changes in expression observed could be associated with disease stage rather than patient sample. LncRNAs with altered expression in at least one of the melanoma or melanocyte cell lines were selected. Using this method, a catalogue of 11881 intergenic lncRNAs was assembled. A selection of these would later be further characterised in human melanoma cell lines sourced from other patients to confirm broad expression of the lncRNAs in melanoma.

Once lncRNAs expressed in melanoma and melanocyte cells were identified, those that are likely to be regulated by MITF were selected based on the presence of MITF binding sites within their promoters or loci. To do this, the RNA-seq data was combined with ChIP-sequencing (ChIP-seq) data mapping HA-tagged MITF binding

sites genome-wide in the melanoma cell line 501mel (Laurette *et al.* 2015). The ChIP-seq peaks were ranked in order of decreasing strength. Peaks that were less than those identified for experimentally characterised functional MITF binding sites within promoter regions were removed to decrease the likelihood of including false positives for MITF binding. Subsequently, strong binding sites for MITF were identified in 1196 melanoma-expressed lncRNAs. A subset of lncRNAs were prioritised based on the proximity of their loci to key melanoma transcriptional regulators. Such guilt-by-association analyses is based on the prediction that the function of a lncRNA can be proposed based on the function of a local, or co-expressed, known protein-coding gene (Guttman *et al.* 2009, Huarte *et al.* 2010).

Following these selection steps (summarised in Figure 3.1), 12 candidate intergenic lncRNAs were prioritised that were predicted to play an important role in mediating the MITF transcriptional response in melanoma (Table 3.1). These experiments were performed by Keith Vance (University of Bath) and Colin Goding (University of Oxford).

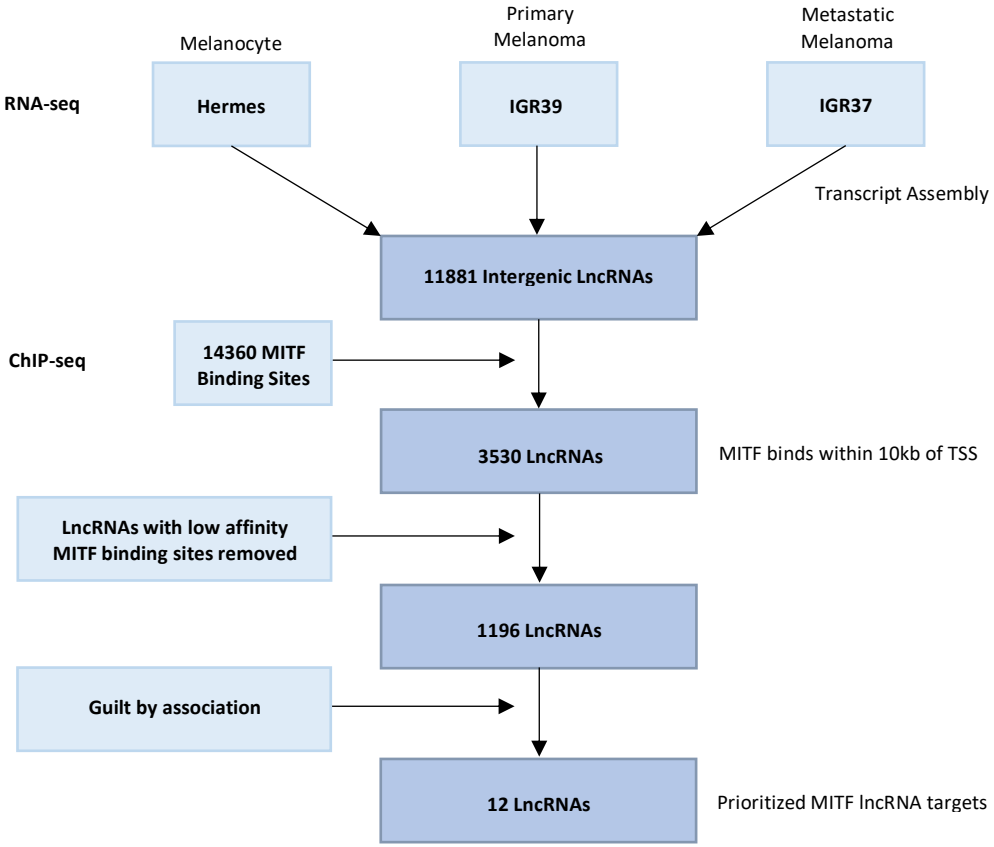

Figure 3.1 Pipeline for identification of candidate intergenic lncRNAs whose genomic loci are bound by MITF in melanoma. RNA-seq of melanoma (IGR39 and IGR37) and melanocyte (Hermes) cell lines were used to identify expressed lncRNAs. Using ChIP-seq, lncRNAs with MITF binding sites across their loci were identified. Final candidates were selected based on their location within cancer susceptibility regions or proximity to oncogenes/tumour suppressors. Analysis performed by Vance and Goding (University of Bath, University of Oxford).

Table 3.1 Prioritised 12 MITF-bound melanoma-expressed lncRNA candidates. A list of intergenic lncRNAs with proposed MITF binding sites, their neighbouring genes and cancer-associated copy number alterations. Identified using The Cancer LncRNome Atlas (http://tcla.fcgportal.org).

Candidate	Closest protein-coding gene		Cancer-associated copy number alteration
	5'	3'	
MelncRNA1	DENND6A	SLMAP	-
MelncRNA4	LRRC37B	SUZ12	-
MelncRNA7	JUNB	HOOK2	19p13.2 amplification (AML)
MelncRNA9	HES1	OPA1	-
MelncRNA11	EN2	INSIG1	-
MelncRNA13	POU2F2	DEDD2	-
MelncRNA17	PTPN1	CEBPB	-
CASC11	MYC	POU5F1B	8q24.21 amplification (SKCM)
DANCR	USP46	ERVMER34-1	-
DIRC3	IGFBP5	TNS1	2q37.1 deletion (COAD, HNSC, LUSC, LUAD)
NEAT1	FRMD8	MALAT1	11p11.2 deletion (SKCM)
STK4AS	STK4	TOMM34	-

3.2.2 MITF represses *CASC11*, *DANCR*, *DIRC3*, and *NEAT1* lncRNAs in 501mel melanoma cells

By using cell lines generated from a single melanoma patient (IGR37, IGR39) to identify expressed lncRNAs, it is not clear whether the proposed candidates are restricted to that individual. Using Real-time quantitative PCR (RT-qPCR), lncRNA expression profiling was performed in additional melanoma (501mel, SKmel28) and melanocyte (Hermes1) cell lines to identify lncRNAs that are more widely expressed in melanoma. The SKmel28 and 501mel immortalised cutaneous melanoma cell lines were derived from metastatic sites (lymph nodes) of a male and female patient respectively and both contain the $BRAF^{V600E}$ mutation. The Hermes1 cell line is a telomerase immortalised melanocyte cell line.

Each of the candidates shows expression in at least one of the cell lines in addition to those used for RNA-seq (Figure 3.2). Their expression varies by seven orders of magnitude, making it possible to group according to low, medium, and high levels of expression. LncRNAs *CASC11*, *DIRC3*, *STK4AS*, MelncRNA7, MelncRNA9, and *DANCR* show increased expression in both melanoma cell lines compared to Hermes1.

Consequently, the pipeline successfully identified lncRNAs that are expressed in multiple cell lines. These lncRNAs may play a general role in the regulation of melanoma initiation and/or progression.

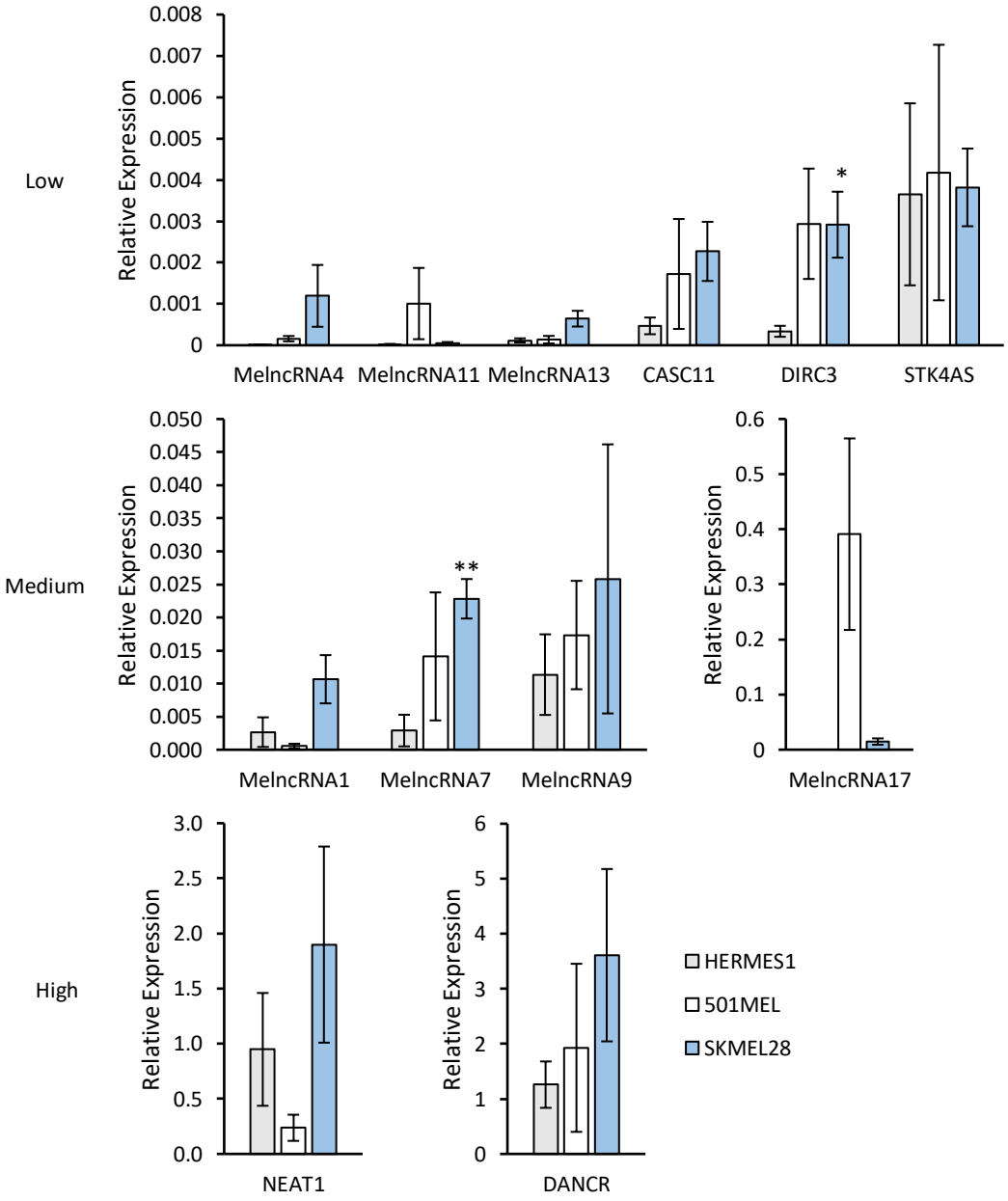

Figure 3.2 Profiling expression of candidate intergenic lncRNAs for melanocyte and melanoma cell lines. RNA was extracted from melanocyte (Hermes1) and melanoma (501mel and SKmel28) cell lines and expression of candidate lncRNAs measured using RT-qPCR. Based on relative expression levels, the lncRNAs are grouped as Low, Medium, or High. Data is presented relative to *POLII* expression. Mean ± SE N=3 Biological Replicates. One-tailed Student's t-test $p<0.05$ = * $p<0.01$ = **

Another key feature of these prioritised candidate lncRNAs is that they are targeted by MITF. While they contain MITF binding sites within the loci, identified using ChIP-seq, this does not mean they are regulated by the transcription factor. It has previously been recognised that transcription factor binding to DNA is frequently insufficient to influence transcription (Zhou and O'Shea 2011). By knocking down *MITF* expression it is possible to identify which of the prioritised lncRNAs are regulated by MITF and so are downstream components of the MITF gene expression network.

To identify direct transcriptional targets of MITF, knockdown of the transcription factor was performed using siRNAs. Western blotting and RT-qPCR were utilised to confirm knockdowns and determine changes in expression of candidate lncRNAs relative to a non-targeting control (siCtrl). Two siRNAs targeting *MITF* (siMitf1, siMitf2) were used to account for off-target effects. In accordance with the ChIP-seq data, 501mel cells were used.

Following siRNA knockdown, expression of MITF mRNA and protein were significantly reduced (Figure 3.3a,b). Greater than a two-fold increase in expression with at least one siRNA was observed for *CASC11*, *DANCR*, *DIRC3*, and *NEAT1* following MITF knockdown (Figure 3.3c). Consequently, these were predicted to be the most strongly regulated by MITF. The different efficiencies at which the siRNAs worked, resulting in a 45% and 58% knockdown in mRNA, also meant dosage responses could be observed. Generally, there is a greater increase in lncRNA expression following the larger knockdown of MITF. It should be noted that lncRNA expression typically only showed a significant change for siMitf1, suggesting changes could be the result of off-target effects. However, the general pattern of expression still suggests MITF negatively regulates expression of the lncRNAs. In addition, expression of linc00152 was measured as a control lncRNA whose expression should not be regulated by MITF. Accordingly, this lncRNA showed little change following MITF depletion.

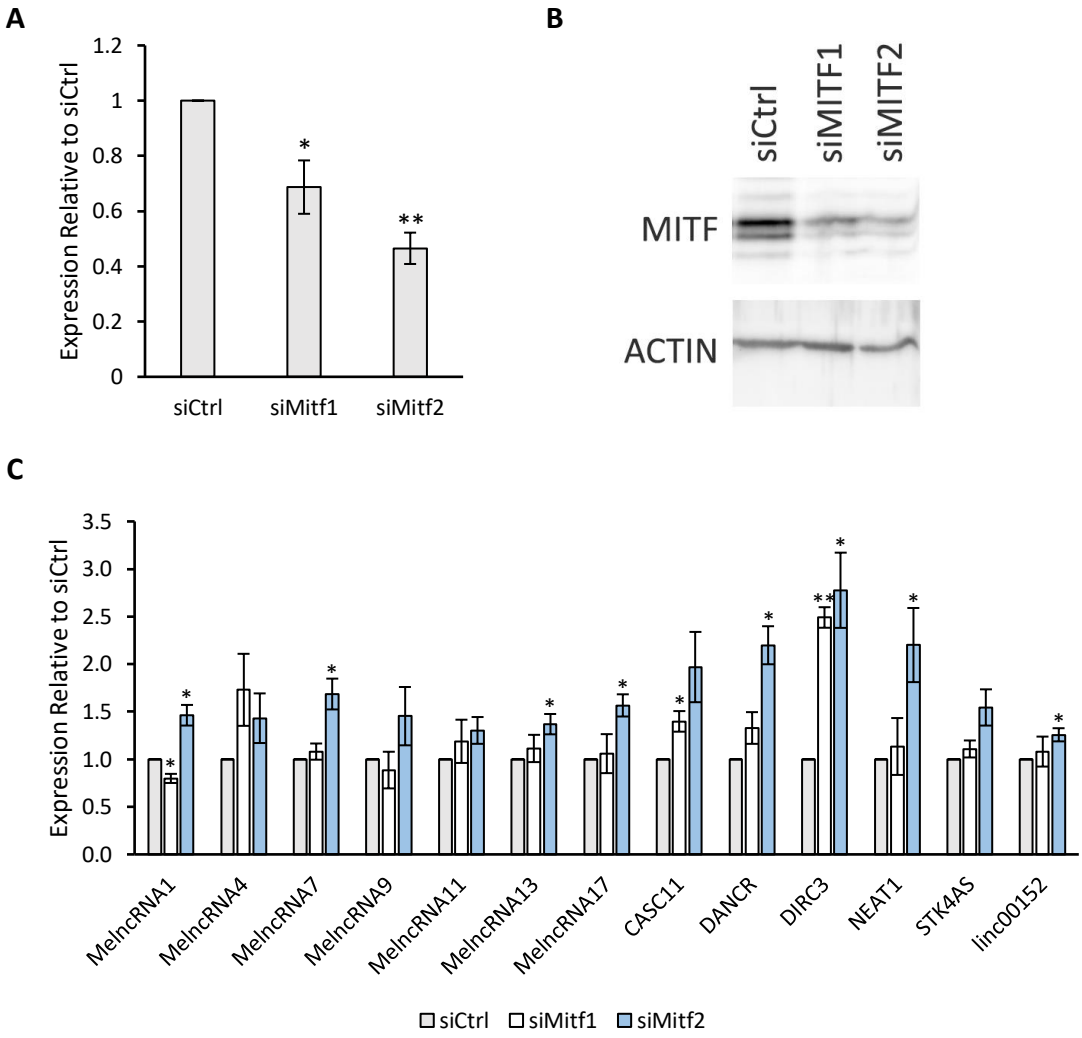

Figure 3.3 MITF negatively regulates the expression of multiple candidate lncRNAs. 501mel cells were transfected with siRNAs targeting *MITF* (siMitf1 or siMitf2) or a non-targeting control (siCtrl). Three days following transfection, the efficiency of MITF knockdown and corresponding changes in lncRNA expression were measured. (**A**) *MITF* mRNA levels were measured using RT-qPCR. (**B**) MITF protein expression was measured using Western Blotting. Equal concentrations of extracted protein were confirmed using ACTIN as a loading control. Representative figure given. (**C**) Intergenic lncRNA expression was measured using RT-qPCR. Results were normalised to *POLII* and presented relative to expression in the siCtrl. Mean ± SE N=3 Biological Replicates. One-tailed Student's t-test $p<0.05$ = * $P<0.01$ = **

While the majority of lncRNAs showed a slight increase following reduced MITF expression, four candidates showed a robust increase suggestive of direct repressive regulation by the oncogene. This confirms that the pipeline is able to identify melanoma-expressed lncRNAs regulated by MITF. Furthermore, those identified

have previously had roles identified in cancer, melanoma, or skin development (Table 3.2).

Table 3.2 Previously identified roles in cancer for candidate intergenic lncRNAs regulated by MITF in 501mel. Of the 12 melanoma-expressed lncRNAs, only those with equal to or greater than two-fold increase in expression following MITF depletion were categorised as experiencing strong repression by MITF.

Candidate	Features
CASC11	Expression positively correlates with MYC and is an identified oncogene in cancers including colorectal and bladder cancer (Zhang 2019; Amir 2019)
DANCR	Oncogenic lncRNA that is overexpressed in a wide range of cancers regulating cell proliferation, invasion and metastasis. (Zar Thin 2018)
DIRC3	Locus is deleted in renal cell cancer (Bodmer 2003).
NEAT1	Is an oncogenic target of p53 and is found to promote skin tumorigenesis (Adriaens et al., 2016)

NEAT1 has previously been identified as a regulator of skin cancer by preventing excessive DNA damage by inducing paraspeckle formation (Adriaens *et al.* 2016). Consequently, the 2.2-fold increase in *NEAT1* expression following reduced MITF, as well as increased expression in SKmel28 compared to Hermes1, validate the use of this pipeline to identify candidate lncRNAs involved in melanoma.

DIRC3 was selected for further study because it is a previously uncharacterised lncRNA whose locus is positioned close to two genes implicated with tumour suppressive roles. *DIRC3* was the most strongly repressed candidate by MITF, experiencing a 2.5-2.7-fold increase in expression upon MITF depletion. The lncRNA also showed high expression in both 501mel and SKmel28 melanoma cell lines compared to the Hermes1 melanocyte cell line.

3.2.3 Initial characterisation of *DIRC3* in melanoma

The *DIRC3* transcript and locus were further characterised to begin to investigate *DIRC3* in melanoma. The eight-exon intergenic lncRNA *DIRC3* (Dysregulated in Renal Carcinoma) (ENSG00000231672) is found on chromosome 2, spanning a region of ~500 Kb. *DIRC3* is also located between genes implicated in tumorigenesis (Figure 3.4). *IGFB5* (insulin-like growth factor-binding protein 5) is located roughly 600 kb

downstream of *DIRC3* and is a melanoma tumour suppressor able to regulate cell migration, invasion, and anchorage-independent growth (Wang *et al.* 2015). Expression of *IGFBP5* has also been associated with increased survival in patients with breast cancer, osteosarcoma (Ahn *et al.* 2010, Su *et al.* 2011). *TNS1* (Tensin1) is located roughly 40 kb upstream of *DIRC3*. The protein is known to localise in and regulate focal adhesions where it participates in the control of cell migration (Chen *et al.* 2002). *TNP1* (Transition protein-1) is also located within close proximity to *DIRC3*. However, this gene is important in sperm development and is only expressed in cells containing a haploid genome resulting in it not being of interest in this study (Luerssen *et al.* 1990).

The *DIRC3* transcript was mapped in SKmel28 using Rapid Amplification of cDNA Ends (RACE) coupled with RT-qPCR. Using this method, the precise 5' and 3' ends and most prevalent isoform of *DIRC3* were identified. The SKmel28-expressed isoform is 3384 nucleotides long and still contains eight exons but is expressed from an alternative transcription start site (TSS) (Figure 3.4a). This TSS is located within the first intron of the previously annotated *DIRC3* (RefSeq gene NR_026597) resulting in a novel shorter isoform of *DIRC3*. The remainder of the transcript is the same. The validation of 5' and 3' ends also confirms *DIRC3* is truly intergenic as it does not overlap with its neighbouring genes.

Located between the *IGFBP5* and *TNS1* protein-coding genes in the mouse genome, there is a positionally equivalent gene for *DIRC3* (Figure 3.4b). The positional conservation of *DIRC3* and its neighbouring genes in mice suggest they may play an important conserved role in development or prevention of disease.

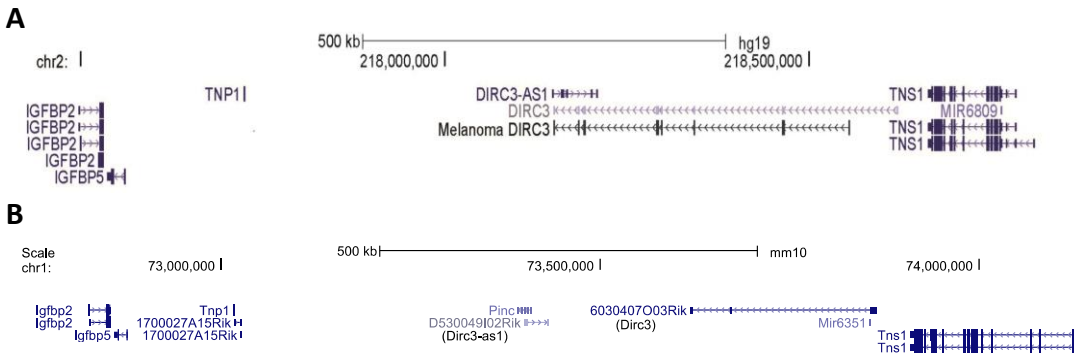

Figure 3.4 Schematic representation of human and mouse *DIRC3* loci and neighbouring genes in human SKmel28 and mice. (**A**) *DIRC3* is located on the reverse strand of chromosome 2 (GRCh37/hg19). The transcript lies between the protein-coding genes *IGFBP5* (600 kb downstream) and *TNS1* (40 kb upstream). Using RACE, the precise 5' and 3' ends of the *DIRC3* sequence were identified. 5'RACE revealed a novel TSS within the first intron of a previously annotated *DIRC3*. 3'RACE remained the same as previously annotated *DIRC3* isoforms. Novel isoform – Black. Previously identified *DIRC3* (RefSeq gene NR_026597) – Purple. (**B**) *DIRC3* is located on the reverse strand of chromosome 1 (GRCm38/mm10). The transcript lies between the protein-coding genes *IGFBP5* and *TNS1*. (https://genome.ucsc.edu).

The importance of the *DIRC3* locus in cancer was initially explored by observing the frequency with which the locus is perturbed in cancer. Alterations to gene expression caused by small changes such as single nucleotide polymorphisms (SNPs) and deletions can result or participate in the occurrence of numerous diseases, including cancer (Yan *et al.* 2015). Using The Cancer LncRNome Atlas (TCLA), the *DIRC3* locus was identified within the cancer susceptibility region (2q37), which is deleted multiple cancer types (Table 3.1) (tcla.fcgportal.org). This region is also a known chromosomal breakpoint for a family prone to renal carcinoma (Bodmer *et al.* 2003). Since tumour suppressive loci are typically lost in cancers, the deletion of *DIRC3* locus suggests that it could act as a putative tumour suppressor in cancer.

Table 3.3 *DIRC3* locus is deleted in multiple cancers. Deletion of the DIRC3 locus was identified using the Cancer LncRNome Atlas (TCLA) (tcla.fcgportal.org)

Cancer Type	*DIRC3* locus
Colon Adenocarcinoma (COAD)	Deleted 2q37.2(chr2:214015746-243199373)
Head and Neck Squamous Cell Carcinoma (HNSC)	Deleted 2q37.2(chr2:214015746-243199373)
Lung Adenocarcinoma (LUAD)	Deleted 2q37.2(chr2:214015746-243199373)
Lung Squamous Cell Carcinoma (LUSC)	Deleted 2q37.1(chr2:213401694-243199373)

The expression correlations of lncRNAs with different classes of protein-coding genes have been used to predict lncRNA function. Analysis of RNA-seq for cutaneous melanoma patient from the Cancer Genome Atlas (TCGA) was performed by Pakavarin Louphrasitthiphol at the Ludwig Institute Oxford, identified the top 10 positively and negatively correlated genes with *DIRC3*. Several of the genes positively correlated with *DIRC3* expression behave as tumour suppressors, including *IGFBP5, PLAGL1,* and *NDRG4* (Valleley *et al.* 2007, Melotte *et al.* 2009, Wang *et al.* 2015). The genes negatively correlated with *DIRC3* expression include the melanoma factor SOX10 as well as the oncogene *VEGFB* (Silvestre *et al.* 2003, Tudrej *et al.* 2017). *DIRC3* is also inversely correlated with *TYR* and *MLPH*, both of which participate in pigment production (Iozumi *et al.* 1993, Matesic *et al.* 2001).

The identification of genes whose expression correlates either positively or negatively with *DIRC3* suggests they may regulate, or be regulated by, *DIRC3*. Of those genes, the presence of regulatory factors involved in melanoma, such as *IGFBP5* and *SOX10* respectively, support the suggestion that *DIRC3* may also participate in regulating melanoma. Finding that *DIRC3* positively correlates with known tumour suppressors and negatively with oncogenes, are consistent with the proposed role of *DIRC3* as a tumour suppressor.

Table 3.4 Top 10 positively and negatively correlated genes with *DIRC3* expression in melanoma. Using data from TCGA based on patients with cutaneous melanoma, expression of most highly positively and negatively correlated genes with *DIRC3* were selected. Analysis performed by Pakavarin Louphrasitthiphol (Ludwig Institute Oxford).

Positively Correlated	Negatively Correlated
CPE	CABLES1
ZNF204P	TFAP2A
TCF4	CLCN7
EDNRA	TMCC2
PLAGL1	SLC3A2
IGFBP5	SOX10
TMC7	ITPKB
NDRG4	TYR
IFT57	VEGFB
FOXP1	MLPH

3.2.4 Increased *DIRC3* expression associates with improved patient survival

Although the *DIRC3* locus is disrupted in multiple cancers and its expression correlates with genes important to melanoma, a direct link between *DIRC3* and melanoma has not yet been discovered. By looking at the relationship between *DIRC3* expression and patient survival it is possible to observe whether changes in expression of the lncRNA can be used to classify how aggressive or advanced the cancer is. Using OncoLnc, melanoma patients were separated based on *DIRC3* expression (using the top 33% showing high *DIRC3* expression versus the bottom 33% showing lowest *DIRC3* expression). The curve was created based on clinical RNA-seq data of human skin cutaneous melanoma patients from TCGA (Anaya 2016). Associated clinical data was then used to generate a survival curve. Melanoma patients expressing higher levels of *DIRC3* showed a significant increase in survival compared to those expressing low *DIRC3* (Figure 3.5). The increased expression of *DIRC3* in longer surviving patients suggests *DIRC3* may have a role as a tumour suppressor. However, it is not possible to tell from this figure whether *DIRC3* plays a functional role in promoting survival or is a bystander effect. If *DIRC3* is found to be functional, there may be future options to promote expression of *DIRC3* in melanoma patients as a new therapy. However, if no functional role is identified for *DIRC3*, the lncRNA could still be used as a biomarker to predict survival of a patient or be used to select the most appropriate therapy.

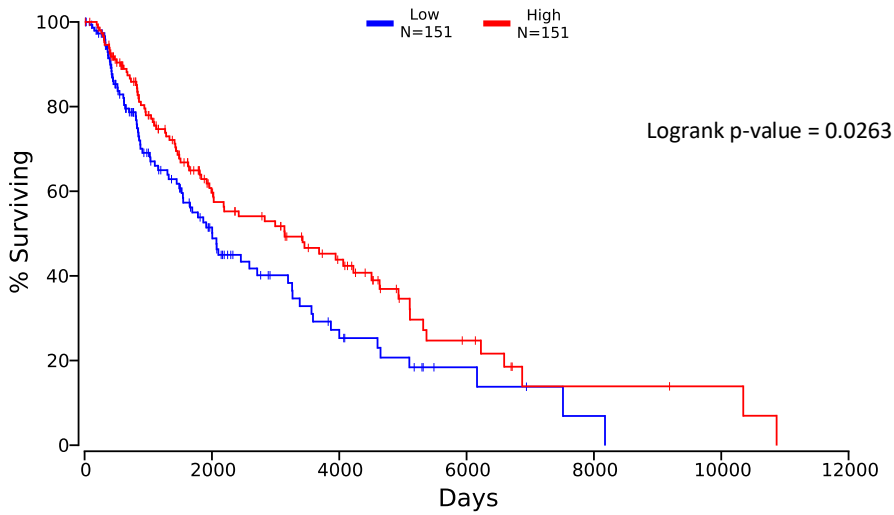

Figure 3.5 Melanoma patients expressing higher *DIRC3* survive longer. OncoLnc generated a Kaplan-Meier plot for SKCM patients. Patients were sorted based on *DIRC3* expression and percent survival compared between *DIRC3* high (Red - top third) and *DIRC3* low (Blue - bottom third) groups. Low *DIRC3* expression was found to correlates with statistically significant decreased survival in melanoma patients based on Cox regression analysis (logrank p-value=0.0263) (Anaya 2016).

3.2.5 *DIRC3* is expressed in additional cancer cells

LncRNAs are known for typically having more restricted expression than protein-coding genes (Fatica and Bozzoni 2014). This is a feature that makes them promising therapeutic targets and biomarkers. To see whether *DIRC3* expression is restricted to melanoma, the presence of this lncRNA in different tumours types, as well as their healthy counterparts, was explored.

Using Gene Expression Profiling Interactive Analysis 2 (GEPIA 2), expression of *DIRC3* was explored. The programme used RNA-seq expression data from 9736 tumours and 8587 normal samples which were collated from TCGA and GTEx projects (Tang *et al.* 2019). The expression profile of *DIRC3* was given as a bar plot for 33 tumour and equivalent healthy tissue samples (Figure 3.6). *DIRC3* expression is detected in the majority of normal and tumour samples, suggesting the lncRNA could have a more general role in regulation of cancers. In addition, the majority of tumours showed a clear reduction in *DIRC3*, suggesting reduced *DIRC3* expression is associated with the

occurrence of cancer, as would be observed for a tumour suppressor. This is observed in the case of skin cutaneous melanoma (SKCM) as well as a range of other cancers including uterine carcinosarcoma (UCS), rectum adenocarcinoma (READ), and adrenocortical carcinoma (ACC).

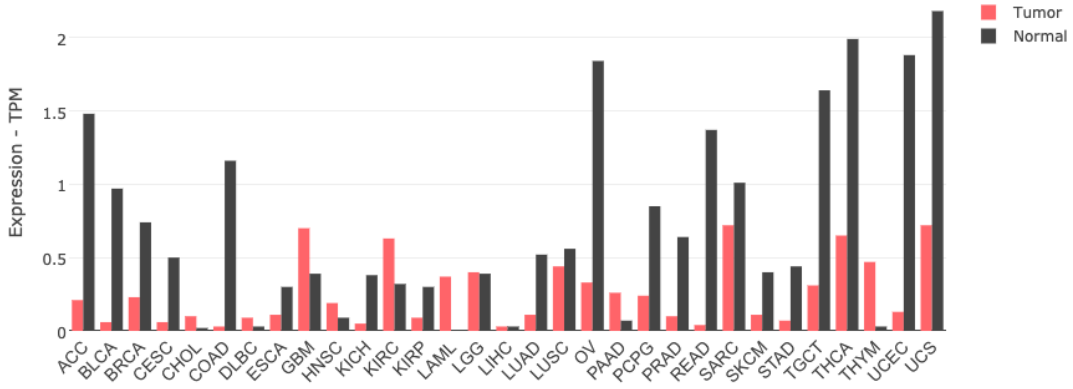

Figure 3.6 *DIRC3* is expressed in a broad range of tissues and is typically reduced in tumours. GEPIA 2-generated bar chart representing RNA-seq data for *DIRC3* expression in tumour and matched normal samples from a range of human tissue types. Expression measured as Transcripts Per Million (TPM) (Tang *et al* 2019).

3.2.6 *DIRC3* is transcriptionally regulated by MITF and SOX10 in melanoma.

The role of lncRNAs within MITF-SOX10 regulated transcriptional programmes is poorly understood. Both MITF and SOX10 play vital roles in regulating transcriptional programmes important in melanoma proliferation, invasion, and metastasis (Garraway *et al.* 2005, Graf *et al.* 2014, Verfaillie *et al.* 2015). While the identification of MITF-targeted lncRNAs was a key component during the initial selection of lncRNAs of interest, binding of *DIRC3* by SOX10 as well as MITF would be a strong indicator of *DIRC3* having a functional role in melanoma. MITF-SOX10 co-occupancy may define active regulatory elements, such as enhancers, important to melanoma (Fufa *et al.* 2015).

By integrating melanoma ChIP-seq data for HA-tagged MITF and SOX10 in 501mel (Laurette *et al.,* 2015), 279 lncRNA, including *DIRC3*, were found to harbour putative co-occupied binding sites of the two transcription factors within their loci. Of these, 34 were promoter bound and 245 identified within the gene bodies. The melanoma-

expressed SKmel28 *DIRC3* isoform contains three sites of MITF-SOX10 co-occupancy (Figure 3.7). One of these sites is present upstream of the promoter and the remaining two are within the gene body. There are also three additional MITF, and one SOX10, individual binding sites.

The presence of SOX10 binding alongside MITF within the promoter region of *DIRC3* suggest that the lncRNA may also be regulated by SOX10. Since only a small proportion of lncRNAs bound by MITF and SOX10 hold sites of co-occupancy, it was proposed that these may more likely possess functional roles. Binding sites across the *DIRC3* locus also suggest the presence of regulatory elements that *DIRC3* may subsequently be able to regulate binding to. Consequently, *DIRC3* may not only be targeted by MITF and SOX10 but may also regulate their transcriptional response through regulating accessibility for their binding to sites across its locus.

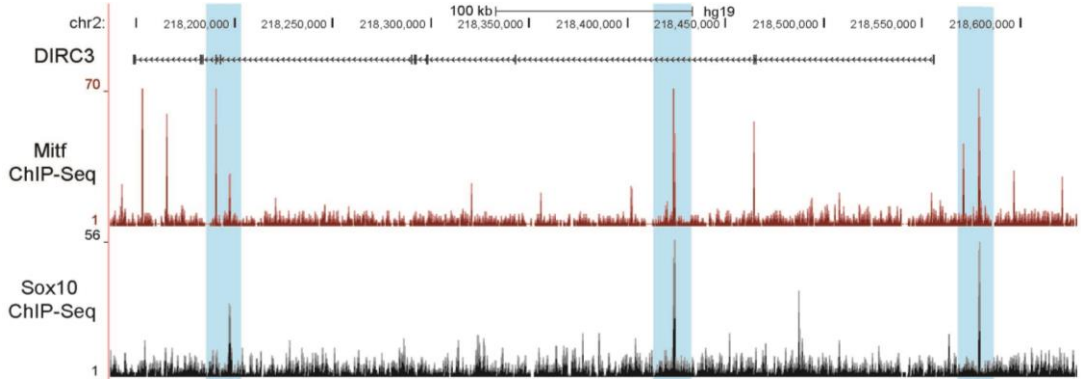

Figure 3.7 Three sites of MITF-SOX10 co-occupancy are located across the *DIRC3* locus. UCSC Genome Browser (GRCh37/hg19) view of ChIP-seq-identified binding sites for MITF and SOX10 across the *DIRC3* locus in 501mel (Laurette, Strub 2015). There are three sites of co-occupancy (highlighted in blue). One binding site is upstream of the TSS, while the other two are within introns of the gene body. MITF and SOX10 also have three and one additional individual binding sites respectively (Laurette *et al.* 2015) (Figure generated from UCSC Genome Browser - https://genome.ucsc.edu).

Although MITF inhibits *DIRC3* expression in 501mel (Figure 3.3), it does not mean this mechanism is shared between melanoma cells. Knockdown of MITF using siRNAs was performed in SKmel28 cells to confirm commonality of the regulatory interaction.

Observation of the behaviour in multiple cancer cell lines or patient samples would suggest that *DIRC3* participates in melanoma as part of the MITF response pathway.

The MITF-*DIRC3* expression correlation was first explored in cutaneous melanoma patients using RNA-seq data from TCGA (data generated by Pakavarin Louphrasitthiphol, Ludwig Institute Oxford). Using this method, it is possible to propose whether the MITF repression of *DIRC3* is observed in melanoma patients. A negative correlation between *MITF* and *DIRC3* is shown (Figure 3.8a), supporting the identified inhibitory effect MITF has on *DIRC3* in 501mel. Knockdown of MITF using siRNAs was also performed in SKmel28. Knockdown of *MITF* in SKmel28 resulted in an 11-18% reduction in mRNA and a clear reduction in protein (Figure 3.8b,c). This reduction in *MITF* was enough to cause a 39-48% increase in *DIRC3* expression (Figure 3.8b) suggesting an inhibitory effect of MITF on *DIRC3*. Together, this data informs that *DIRC3* is transcriptionally repressed by MITF.

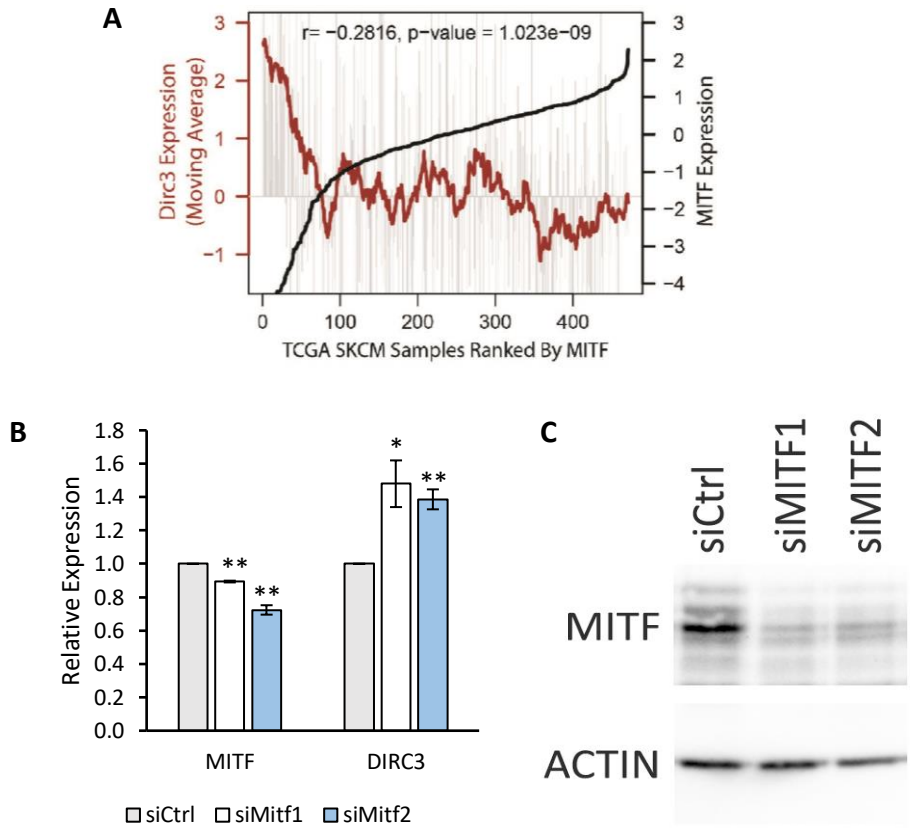

Figure 3.8 MITF represses *DIRC3* expression. (**A**) TCGA RNA-seq data for 471 melanoma patients were ordered based on increasing levels of *MITF* expression. The bold lines represent the moving averages and vertical grey bars show absolute *DIRC3* expression for each melanoma sample. Expression correlation data generated by Pakavarin Louphrasitthiphol, Ludwig Institute Oxford (**B, C**) SKmel28 cells were transfected with siRNAs targeting *MITF* (siMitf1 or siMitf2) or a non-targeting control (siCtrl). Three days following transfection, the efficiency of knockdown and corresponding level of *DIRC3* expression were measured. (**B**) Level of *MITF* and *DIRC3* expression were measured using RT-qPCR. Results were normalised to *POLII* and presented relative to expression in the siCtrl. Mean ± SE N=3 Biological Replicates. One-tailed Student's t-test $p<0.05$ = * $P<0.01$ ** (**C**) Level of MITF protein expression was measured using Western Blotting. Equal concentrations of extracted protein were confirmed using ACTIN as a control. A representative figure is given.

The presence of SOX10 binding sites within the promoter region of *DIRC3* suggest that it may also be regulated by SOX10. Using data from TCGA for cutaneous melanoma patients (data generated by Pakavarin Louphrasitthiphol, Ludwig Institute Oxford), *SOX10* was found to be amongst the top 10 negatively correlated genes with *DIRC3* (Table 3.4). In addition, there is a negative correlation between SOX10 and

DIRC3 expression (Figure 3.9a). Together this data suggests SOX10 may play an important role in negatively regulating expression of *DIRC3*.

To test whether SOX10 directly regulates expression of *DIRC3*, knockdown of SOX10 was performed in the melanoma cell lines 501mel and SKmel28 (as for MITF) using esiRNAs. esiRNAs contain a heterogeneous mixture of siRNAs targeting the same mRNA sequence so only one sample of esiRNAs is required for knockdown as fewer off-target effects occur than when using single siRNAs (Theis and Buchholz 2010). The knockdowns were compared against cells transfected with esiRNA targeting Luciferase (esiLuc) so that any changes that occur due to the transfection of the esiRNAs alone were accounted for. Knockdown of *SOX10* in 501mel resulted in a 71% in mRNA and clear reduction in protein. This also led to a reduction in expression of *DIRC3* by 71% (Figure 3.9b,c). Knockdown of SOX10 in SKmel28 was not as efficient, reaching a 24% reduction for mRNA and slight reduction for protein. In this case, there was a 2.4-fold increase in *DIRC3* expression (Figure 3.9d,e). This supports the inverse relationship identified using TCGA RNA-seq data.

The reduction in *DIRC3* following SOX10 knockdown in 501mel could be the result of the different expression programmes in different cell types resulting in SOX10 activating rather than repressing *DIRC3* expression. Also, the far greater knockdown than observed for SKmel28 could have initiated a compensatory transcriptional response allowing induction of other pathways which would suppress *DIRC3* expression when SOX10 is not present. With the combination of TCGA and SKmel28 knockdown data, there is still strong evidence that *DIRC3* is a direct transcriptional target of both SOX10 in melanoma.

Overall, MITF and SOX10 regulate expression of *DIRC3* in melanoma. This suggests *DIRC3* is more likely to be functional in melanoma.

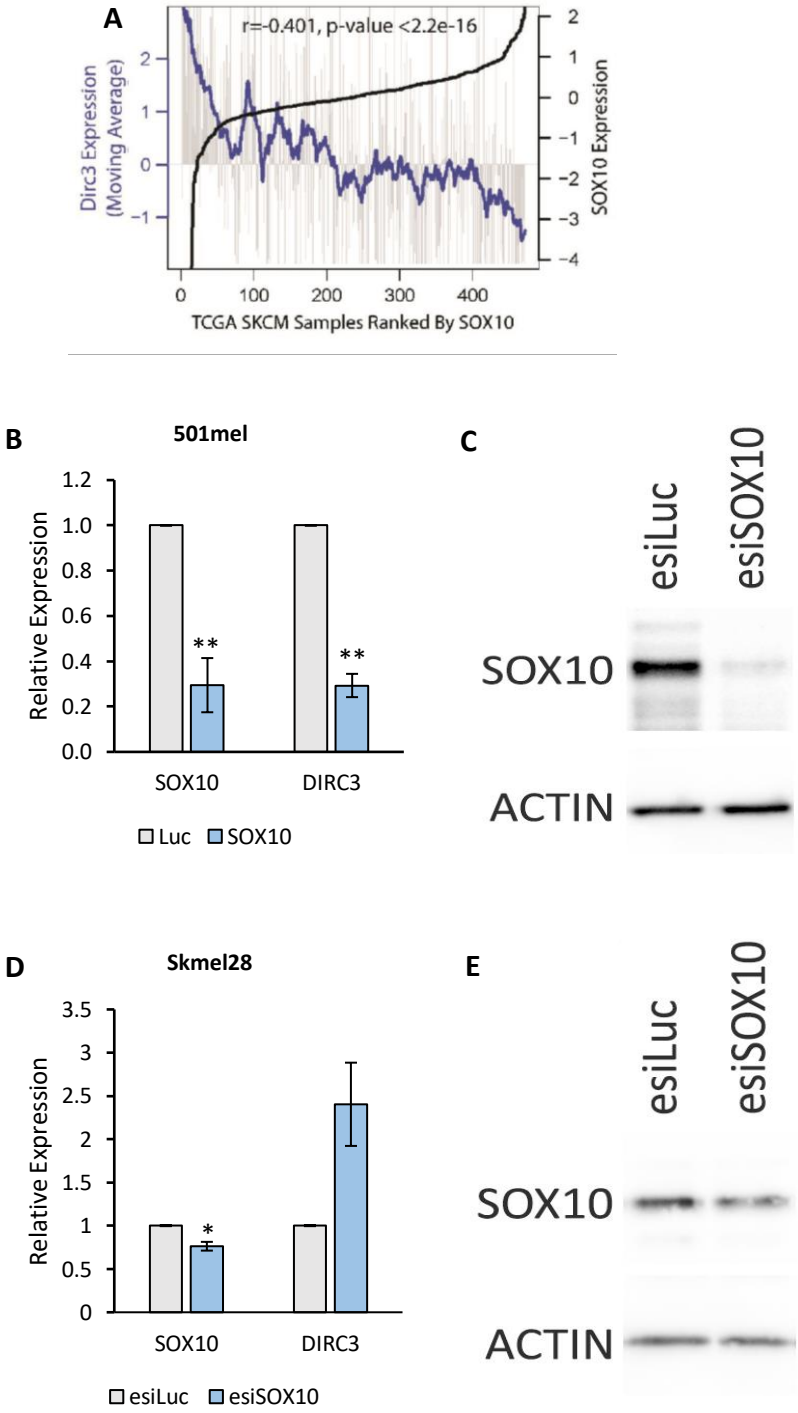

Figure 3.9 SOX10 typically represses *DIRC3* expression in melanoma cells. (**A**) TCGA RNA-seq data for 471 melanoma patients were ordered based on an increasing level of *SOX10* expression against *DIRC3*. The bold lines represent the moving averages and vertical grey bars show absolute expression for each melanoma sample. Expression correlation data generated by Pakavarin Louphrasitthiphol, Ludwig Institute Oxford (**B, C, D, E**) 501mel and SKmel28 cells were transfected with an esiRNA targeting *SOX10* (esiSOX10) or non-targeting control (esiLuc). Three days following transfection, the efficiency of knockdown and corresponding level of *DIRC3* expression were measured. For 501mel levels of RNA (**B**) and protein (**C**) were measured. For skmel28 levels of RNA (**D**) and protein (**E**) were measured.

Level of *SOX10* and *DIRC3* expression were measured using RT-qPCR. Results were normalised to *POLII* and presented relative to esiLuc. Mean ± SE N=3 Biological Replicates. One-tailed Student's t-test $p<0.05$ = * $P<0.01$ **. Level of SOX10 protein expression was measured using Western Blotting. Equal concentrations of extracted protein were confirmed using actin as a control. A representative figure is given.

3.3 Discussion

The transcription factors MITF and SOX10 are important gene expression regulators of melanoma. While their protein-coding targets are well characterised, their non-protein coding targets are not. Understanding the role of lncRNAs in regulating MITF and SOX10 transcriptional responses could reveal new pathways of regulation and so offer new therapeutic avenues for treating individuals with melanoma. Following the completion of a selection process, *DIRC3* was chosen as a likely MITF-regulated intergenic lncRNA involved in melanoma. Further characterisation revealed this lncRNA to be a multi-exonic transcript regulated by both MITF and SOX10 that has features that suggest it may act as a tumour suppressor in melanoma.

Using guilt-by-association, the genes neighbouring *DIRC3* (*IGFBP5* and *TNS1*) suggest its locus may be within a region with tumour suppressive activity. Tensin proteins are known to reside at focal adhesions where they interact with actin filaments and regulate actin polymerisation (Lo *et al.* 1994). Here, they regulate cell adhesion, migration and proliferation (Blangy 2017). TNS1 regulates proliferation and migration of endothelial cells through the TNS1-DLC1-RhoA signalling pathway (Shih *et al.* 2015). It has also been proposed that the tumour suppressive activity of DLC1 is dependent on tensin activity (Blangy 2017). The protein-coding gene *IGFBP5* regulates cell proliferation, differentiation and metabolism via IGF1R-dependent and -independent methods (Tripathi *et al.* 2009, Wang *et al.* 2015, Clemmons 2016). *IGFBP5* also acts as a tumour suppressor in several cancers, including melanoma, osteosarcoma, and breast cancer (Su *et al.* 2011, Ghoussaini *et al.* 2014, Wang *et al.* 2015). Since functionally related genes are known to cluster together, *DIRC3* could be predicted to also behave as a tumour suppressor (Thévenin *et al.* 2014). Furthermore, the identification of a strong positive correlation between *IGFBP5* and *DIRC3* could be the result of *DIRC3* regulating *IGFBP5* expression (or vice versa) or that both are regulated by the same factor, such as MITF or SOX10.

Genetic alteration of lncRNA loci can also indicate the likelihood of involvement in disease. Promoter or enhancer mutations may affect expression of lncRNAs (Camacho *et al.* 2018) whilst mutations within lincRNA exons may affect lncRNA structure and ability to bind with its targets (Sabarinathan *et al.* 2013, Leucci, Coe, *et al.* 2016). Such dysregulation of lncRNA activity can lead to disease-associated responses. The *DIRC3* locus is deleted in a range of cancers (Table 3.3) and Bodmer (2003) also identified a t(2;3)(q35;q21)-associated 2q35 breakpoint that leads to disrupted *DIRC3* expression in renal carcinoma. Depletion of *DIRC3* was also observed in the majority of cancers analysed using GEPIA 2. Loss of function mutations leading to cancer could suggest tumour suppressive behaviour. The frequency with which *DIRC3* is dysregulated could also indicate a more general role in cancer regulation. Although whether *DIRC3* is functional is still to be explored for the majority of the cancers mentioned in Table 3.3, *DIRC3* has already been proposed to behave as a tumour suppressor in renal carcinoma (Bodmer *et al.* 2003).

Linking *DIRC3* expression to clinical outcomes provides a clear positive correlation between *DIRC3* expression and melanoma patient survival. *DIRC3* appears to have a potential tumour suppressive effect due to the reduction in its expression correlating with reduced patient survival. If functional, *DIRC3* could be acting as a tumour suppressor inhibiting melanoma progression. By preventing tumour progression to more lethal stages, such as metastasis, *DIRC3* could increase patient survival. Consequently, *DIRC3* could be a therapeutic target. By up-regulating expression of *DIRC3* it may be possible to stop the disease progressing. If *DIRC3* is not found to be functional, or is not easily targeted therapeutically, the lncRNA could be a biomarker. As a biomarker, *DIRC3* could predict likelihood of survival or inform which therapeutic option is most suitable for a patient.

Increasing numbers of oncogenic and tumour suppressive protein-coding genes are being identified that regulate expression of target lncRNAs. The tumour suppressor p53 can activate expression of hundreds of lncRNAs, including lincRNA-p21 which represses expression of anti-apoptotic genes (Huarte *et al.* 2010, Chaudhary and Lal

2017). The oncogene *Myc* also regulates numerous lncRNAs including H19 which is important in tumour cell transformation (Barsyte-Lovejoy *et al.* 2006, Iaccarino 2017). Accordingly, it could be that MITF and SOX10 regulate expression of *DIRC3* in order to enforce their own oncogenic activity. Their inhibition of *DIRC3* is again suggestive of the lncRNA behaving as a tumour suppressor. The identification of MITF and SOX10 binding sites across the locus of *DIRC3* also implies there may be regulatory elements present which *DIRC3* could regulate MITF and SOX10 accessibility to. MITF and SOX10 also co-occupy binding sites across a subset of the identified intergenic lncRNAs identified in this project. *DIRC3* could consequently represent a mechanism for regulation of MITF and SOX10 activity via binding sites across an intergenic lncRNA locus. *DIRC3,* and other lncRNAs like it, could consequently play an important role in fine-tuning MITF and SOX10 transcriptional responses, and so could participate in the regulation of melanocyte and melanoma cell state.

Although *DIRC3* has features indicative of a tumour suppressor, it is not yet clear whether it is a functional lncRNA or not. If not found to be functional, the significant difference in melanoma patient survival based on *DIRC3* expression suggests *DIRC3* could later be used to inform on melanoma aggressiveness or response to treatment. However, if a functional role is found for *DIRC3*, the lncRNA could be a potential therapeutic target for melanoma treatment. Also, *DIRC3* could add to our expanding understanding of how lncRNA mechanistically work, as well as present an example mechanism for intergenic lncRNAs regulated by MITF and SOX10 but that also harbour MITF and SOX10 binding sites across their loci.

Chapter 4: *DIRC3* is a nuclear lncRNA that regulates its neighbouring gene *IGFBP5* and other genes important in melanoma

4.1 Introduction

4.1.1 LncRNA mechanisms of gene regulation.

LncRNAs have been identified as novel regulators of gene expression. Whether they are localised to the nucleus or cytoplasm gives an initial insight into possible mechanisms a functional lncRNA may execute in gene regulation (Zhang *et al.* 2014). Compared to mRNAs which are predominantly trafficked to the cytoplasm where they undergo translation, lncRNAs show increased enrichment in the nucleus (Derrien *et al.* 2012). Within the nucleus, functional lncRNAs regulate expression of target genes either at sites local to or distant from their site of transcription (Vance *et al.* 2014). Regulation of targets close to a lncRNA's locus may occur either through the act of lncRNA transcription alone or a functional transcript (Kaikkonen and Adelman 2018). LncRNAs may also regulate expression of genes at loci on different chromosomes or alleles. To do so, a functional transcript may be translocated to other sites or manipulations of chromatin structure may bring distal regions close to the lncRNA loci (Hacisuleyman *et al.* 2014, Vance and Ponting 2014). Numerous lncRNAs have also been identified that function in the cytoplasm. Here, functional lncRNA transcripts may participate in regulation of mRNA processing and protein activity (Tian *et al.* 2014, Leucci, Coe, *et al.* 2016).

LncRNA functionality may be attributed to the lncRNA transcript, transcription, splicing and/or DNA elements within the lncRNA locus. (Marchese *et al.* 2017, Kopp and Mendell 2018). Functional transcripts can interact with DNA, RNA or proteins to confer their activity. In other cases, activities such as transcriptional interference and

splicing result in functional transcripts not being required for regulation of target genes, rendering the transcript a by-product of their activity (Latos *et al.* 2012, Engreitz *et al.* 2016). Additionally, when loci harbour regulatory elements, these regions may play a primary role in the regulation of target gene expression rather than expression of the lncRNA (Groff *et al.* 2016). However, lncRNAs are likely to be able to function using combinations of these methods. Some well-characterised examples of melanoma-expressed lncRNAs in the nucleus and cytoplasm, and how they function, are given in Table 4.1.

Table 4.1 Selected examples of well-characterised melanoma-expressed lncRNAs present in the nucleus and cytoplasm.

Nuclear	***SLNCR***	By recruiting the androgen receptor (AR) to EGR1-bound genomic loci, *SLNCR1* switches transcription activation by EGR1 to repression, so that activity of tumour suppressor p21Waf1/Cip1 is repressed (Schmidt *et al.* 2019)
Cytoplasmic	***SAMMSON***	Regulates mitochondrial homeostasis and metabolism through promoting activity of p32, a master regulator of mitochondrial metabolism. When expression was knocked down, cells were less viable were sensitised to MAPK- targeting therapeutics (Leucci, Vendramin, *et al.* 2016).
	UCA1	By targeting miR-507, UCA1 prevents miR-507-mediated inhibition of FOXM1 which is important for promotion of cell proliferation (Tian *et al.* 2014)

4.1.2 Knockout/down methods to identify lncRNA function.

LncRNA function can be studied using a range of methods involving deletion, suppression or overexpression of the target lncRNA. It is important to know whether the transcript is predominantly nuclear or cytoplasmic to assign the most suitable method for analysis of the effect of such lncRNA loss/gain of function. The resulting effect on expression of other genes or the cell's phenotype can then be used to confirm functionality (Stojic *et al.* 2018). If a lncRNA is predominantly cytoplasmic, post-transcriptional knockdown methods such as shRNA knockdown may reduce expression of the target. However, those with expression restricted to the nucleus require methods that utilise cellular machinery within that compartment – such as CRISPRi and antisense oligonucleotides (ASOs).

The use of shRNAs and siRNAs to deplete lncRNA expression is based on their earlier success when knocking down protein-coding genes. Using these oligos, target RNA molecules are degraded using endogenous silencing machinery. Such techniques typically work more efficiently for targets expressed in the cytoplasm. However, in some cases it has been possible to knockdown nuclear-expressed lncRNAs, such as *HOTTIP* (Wang *et al.* 2011). This could be the consequence of some factors required for knockdown, such as Dicer and Argonaute, being identified in nuclei as well as the cytoplasm (Gagnon *et al.* 2014).

Targeting lncRNA transcripts predominantly expressed in the nucleus using siRNAs can be challenging due to the required machinery being limited to the cytoplasm (Lennox and Behlke 2016). However, locked nucleic acid (LNA)-modified antisense oligonucleotides (ASOs) can be used to target nuclear-expressed lncRNAs. The single-stranded DNA oligomers direct RNase H-mediated cleavage of target lncRNAs by forming chimeric RNA-DNA oligonucleotides (Ideue *et al.* 2009). By inducing RNase H activity, LNA-ASOs can target nuclear-expressed lncRNA transcripts for degradation. LNA-ASOs have been successfully used in the knockdown of lncRNAs including *NEAT1* and *LincRNA-p21* (Dimitrova *et al.* 2014, Lennox and Behlke 2016).

When designing experiments to investigate lncRNA function it is important to consider lncRNAs that work through the act of their transcription, as well as the transcript itself. The clustered regularly interspaced short palindromic repeats (CRISPR) system is now commonly used to generate lncRNA knockout models (Gilbert *et al.* 2014). Using a CRISPR-associated protein 9 (Cas9) endonuclease guided by a single-guide RNA (sgRNA), the target DNA region is removed following the creation of a double-strand break in the DNA and repair using endogenous machinery. Utilising the homologous recombination repair pathway, DNA modifications, such as single point mutations or new exogenous sequences, may be inserted (Hsu *et al.* 2014). CRISPR has successfully been used for the knockout of lncRNAs including *CCAT1* (Zare *et al.* 2018). It has also been used to modulate splicing of *XIST* in order

to identify the most active isoform in XCI (Yue and Ogawa 2017). However, deletion of a target site can unintentionally remove or disrupt regulatory elements within that region leading to a misinterpretation of how the targeted gene functions (Liu *et al.* 2017).

Preventing lncRNA activity by removing DNA can make it difficult to distinguish whether any observed effects are the result of the lncRNA or regulatory elements within the DNA sequence from which the lncRNA is transcribed. By preventing transcription of the target lncRNA, the DNA sequence is not affected so any observations are the result of lncRNA transcript-dependent or -independent activity. CRISPR inhibition (CRISPRi) can be used to do this. The catalytically inactive (dead) Cas9 (dCas9) blocks activity of RNAPII through steric hinderance (Gilbert *et al.* 2013, 2014, Qi *et al.* 2013). dCas9 activity may also be enhanced by fusing repressor domains to the protein. Activator domains may also be used to up-regulate the expression of a target gene when performing CRISPR activation (CRISPRa). For gene knockdown, protein repressor domains such as Krüppel-associated box (KRAB) and MAX interactor 1 (Mxi1), fused to dCas9 increases the efficiency of silencing through recruiting chromatin-modifying proteins and inducing local chromatin compaction (Gilbert *et al.* 2013). The combined use of the dCas9 and KRAB proteins is more efficient at knocking down the expression of a target than the use of dCas9 alone (Goyal *et al.* 2017). Gilbert *et al* (2014) also identified a region -50 to +300 bp of the target's TSS as the optimum area for targeting knockdown using the combined dCas9-KRAB repression. This means the precise TSS of a target needs to be known in order to use dCas9-KRAB knockdown efficiently. CRISPRi also holds promise as it is a highly specific and reproducible method which causes undetectable intrinsic toxicity. This version of CRISPR has been tested to deplete expression of a range of lncRNAs, including *GAS5*, *MALAT1*, *NEAT1*, and *XIST* (Gilbert *et al.* 2014).

Knock-in of the polyA cleavage signal is another commonly used method to block lncRNA function by inducing premature termination of lncRNA transcription (Liu and Lim 2018). The transcript upstream to the signal is stabilised as it is protected by the

5’-cap structure, but transcript remaining downstream is rapidly degraded. Accordingly, the addition of polyA sequences is used for gene silencing of sequences downstream to where the signal is inserted. Poly(A) sequences from the bovine growth hormone (bGH) and the simian virus 40 (SV40) are commonly used (Gutschner *et al.* 2011). Sites typically targeted include the promoter, first exon or first intron. However, different portions of a lncRNA transcript can be targeted, allowing identification of the critical region of the lncRNA. CRISPR-Cas9-mediated homologous recombination can be used to insert a PolyA cassette into both alleles of a target gene (Liu and Lim 2018). As well as targeting singular regions, by using multiple sgRNAs an entire gene may be deleted. In the case of *AIRN*, gradual repositioning of the polyA signal across the lncRNA locus showed that the lncRNA regulated expression of *IGF2R* as its locus overlapped the promoter of this neighbouring gene (Latos *et al.* 2012).

4.1.3 Chapter Summary.

Although *DIRC3* expression positively correlates with patient survival, suggesting a tumour suppressive role, this does not mean the lncRNA is functional. The observed changes in *DIRC3* could be a bystander effect representing changes in other genes, rather than its altered expression producing a functional response. To begin to explore possible *DIRC3* functionality, the lncRNA was targeted for knockdown. In order to decide on the most appropriate method, the cellular localisation of *DIRC3* was determined. Due to its predominantly nuclear location, *DIRC3* was targeted using CRISPRi and LNA-ASOs. The effect of *DIRC3* knockdown was first checked by measuring expression of its neighbouring cancer-causing genes *IGFBP5* and *TNS1*. Combining the two knockdown methods revealed the ability of *DIRC3* to regulate *IGFBP5* through a functional transcript. The initial portion of the chapter also focuses on *CASC11*, another MITF-regulated lncRNA. *CASC11* regulates its neighbouring gene *MYC* in colorectal cancer so was used to show that *CASC11* activates *MYC* in melanoma and subsequently optimise the CRISPRi experimental method. The remainder of this chapter focuses on understanding the extent to which *DIRC3*

regulates targets across the genome. RNA-seq analysis of LNA-ASO and CRISPRi *DIRC3* knockdown revealed genes important in the regulation of cancer-associated processes. By including RNA-seq analysis of *IGFBP5* ASO knockdown it also is apparent that *DIRC3* may function through *IGFBP5*-independent and dependent methods. Consequently, *DIRC3* is a functional lncRNA able to regulate expression of genome-wide target genes.

4.2 Results

4.2.1 *DIRC3* transcript is predominantly located in the nucleus

In order to generate initial clues into *DIRC3* and *CASC11* function, as well as decide which method of knockdown was most appropriate, their location within SKmel28 cell was identified.

The cellular localisation of *DIRC3* and *CASC11* was determined in SKmel28 cells. Following separation of the cells into nuclear and cytoplasmic fractions, expression of target lncRNAs were quantified using RT-qPCR. The efficiency of fractionation was confirmed by checking expression of *NEAT1* and *DANCR* in the nucleus and cytoplasm respectively (Lennox and Behlke 2016). *DIRC3* is predominantly localised to the nucleus, with 70-80% of its transcript identified there (Figure 4.1). Expression of *CASC11* is relatively evenly distributed between nucleus and cytoplasm.

The predominantly nuclear localisation of *DIRC3* suggests that it may directly regulate gene expression. *CASC11* identification in both the nuclear and cytoplasmic fraction suggest the lncRNAs more likely acts distally from its locus. CRISPRi and ASOs were selected to generate loss of function models due to the nuclear localisation of both *DIRC3* and *CASC11*.

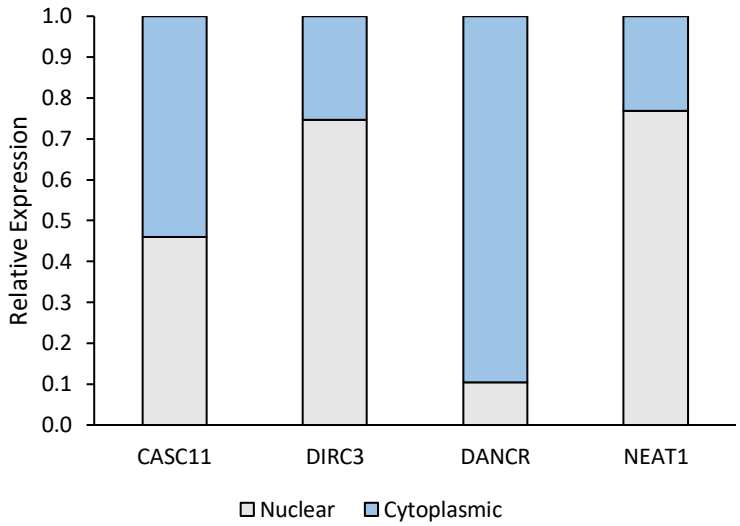

Figure 4.1 *DIRC3* is enriched in the nuclear fraction of SKmel28 cells. Following biochemical nuclear-cytoplasmic fractionation of SKmel28 cells, expression of *DIRC3* and *CASC11* were measured using RT-qPCR. Positive controls *DANCR* (cytoplasmic) and *NEAT1* (nuclear) were used to assess fractionation efficiency. Results are presented relative to expression of transcripts in the nucleus. N=2 Biological Replicates.

4.2.2 *DIRC3* is a functional transcript able to regulate expression of its neighbouring gene

LncRNAs often control the expression of their adjacent protein-coding genes (Vance and Ponting 2014, Engreitz *et al.* 2016), so changes in expression of neighbouring genes with dCas9 alone (steric hindrance) and dCas9-KRAB were measured. Regulation of *IGFBP5* and *TNS1* could also more closely implicate *DIRC3* in regulation of melanoma. *CASC11* was also selected for knockdown because it has recently been found to regulate its upstream neighbouring gene *MYC* in colorectal cancer (Zhang *et al.* 2016) so could be used as a positive control for whether the CRISPRi knockdown method worked.

CRISPRi knockdown of the lncRNAs was performed in SKmel28 cells. A single transfection was performed using a CRISPRi plasmid containing both the sgRNA and dCas9 either with or without KRAB (generated by Andrew Bassett, Sanger Institute, Cambridge). Two different sgRNAs (DIRC3sg1 and DIRC3sg2 / CASC11sg1 and CASC11sg2) were designed to target catalytically inactive dCas9 to the *DIRC3*

promoter to control for off-target effects. CRISPRi knockdown was performed both with and without the presence of the KRAB protein to control for possible chromatin-mediated effects of the transcriptional repressor. Transfected cells were selected using puromycin for seven days. Expression of the lncRNAs and their neighbouring genes were measured using RT-qPCR relative to a scrambled control (NEGsg1).

Knockdown of *CASC11* using dCas9-KRAB resulted in a reproducible 45-52% knockdown of *CASC11* which caused a 45-48% reduction in *MYC* (Figure 4.2a). Use of dCas9 alone to knockdown *CASC11* produced a ~10% knockdown of *CASC11* expression, followed by a 15-30% reduction in *MYC* (Figure 4.2b). This confirmed the reduction of *MYC* observed when including the KRAB domain. The positive regulation of *MYC* by *CASC11* suggests *CASC11* activates *MYC* in melanoma, as was observed in colon cancer (Zhang *et al.* 2016) suggesting *CASC11* regulation of *MYC* may be a more general mechanism.

It is also unlikely that the CRISPRi method itself could have caused the reduction in *MYC* as the gene is present 2 kb downstream from *CASC11*, too far for the CRISPRi method to have caused an effect (Gilbert *et al.* 2013). The comparison between the use of dCas9 alone and in combination with KRAB also demonstrate the increased efficiency of knockdown when using the transcriptional repressor. Such increased efficiency of knockdown has previously been observed by Gilbert *et al* (2013) who observed a five-fold greater knockdown for the dCas9-KRAB fusion compared to the presence of dCas9 alone.

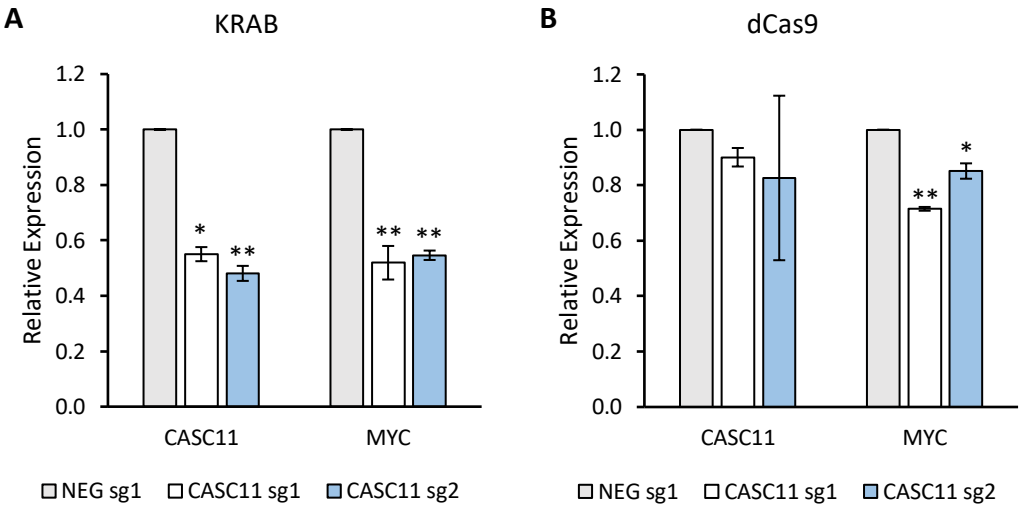

Figure 4.2 *CASC11* activates that adjacent gene *MYC* in SKmel28 melanoma cells. CRISPRi knockdown of *CASC11* was performed in SKmel28 cells using both dCas9-KRAB (**A**) and dCas9 (**B**). Three days after transfection with vectors containing CASC11sg1, CASC11sg2 or NEGsg1, puromycin was added to the cells which were then left under selection for another seven days. RNA was then extracted, and RT-qPCR performed to measure knockdown of *CASC11* and effect on *MYC* expression. Results were normalised to *POLII* and presented relative to expression of NEGsg1. Mean ± SE N=3 Biological Replicates. One-tailed Student's t-test $p<0.05$ = * $P<0.01$ **

Following confirmation of the efficiency of CRISPRi to silence lncRNA expression in melanoma cells when using a single transfection, *DIRC3* knockdown was performed. sgRNAs were initially designed to target both the RefSeg gene NR_026597 and RACE-identified isoforms (Figure 3.4a) to be confident that the most prevalent form is targeted during knockdown. The TSS of both isoforms are not within close enough proximity to that of their neighbouring genes that any changes to their expression could be a consequence of off-target CRISPRi effects. Changes in *DIRC3* neighbouring genes *IGFBP5* and *TNS1* were measured following lncRNA knockdown.

Targeting the TSS of the shorter SKmel28-RACE *DIRC3* isoform using dCas9-KRAB gave more efficient knockdowns (~90%) than targeting the RefSeg gene NR_026597 (~30% max) (Figure 4.3a). This confirmed that the isoform identified using RACE is the more dominant isoform of *DIRC3* in SKmel28. Subsequent CRISPRi knockdowns were performed using sgRNAs targeting this version of *DIRC3*. Inclusion of the KRAB domain (dCas9-KRAB) led to knockdowns of 31% (DIRC3sg1) and 68% (DIRC3sg2). This

resulted in a significant 35% and 37% decrease in *IGFBP5* expression respectively. *TNS1* showed a small but significant increase for DIRC3sg2 but not DIRC3sg1 (Figure 4.3b). Use of dCas9 alone validated this finding as DIRC3sg1 resulted in a significant 30% knockdown of *DIRC3* and 32% reduction in *IGFBP5* expression but no significant change in *TNS1*. DIRC3sg2 showed far greater variation for each gene, resulting in no significant changes in expression (Figure 4.3c).

The initial knockdowns for both of the predicted *DIRC3* isoforms demonstrate the importance of knowing the precise TSS of a target lncRNA when using CRISPRi. The variation in knockdown for DIRC3sg2, unlike DIRC3sg1, when using dCas9 alone was also likely the consequence of the precision required when targeting dCas9 to block RNAPII (steric hindrance). Additionally, the changes in *IGFBP5* and *TNS1* expression were similar both with a without the presence of KRAB, confirming such changes are the consequence of *DIRC3* knockdown and not due to off-target effects induced by KRAB.

No clear regulation of *TNS1* by *DIRC3* is apparent following *DIRC3* knockdown. However, following significant knockdown of *DIRC3*, *IGFBP5* is consistently reduced. Consequently, *DIRC3* appears to positively regulate expression of the tumour suppressor *IGFBP5*. Such activity supports the proposal that *DIRC3* may be a tumour suppressor in melanoma.

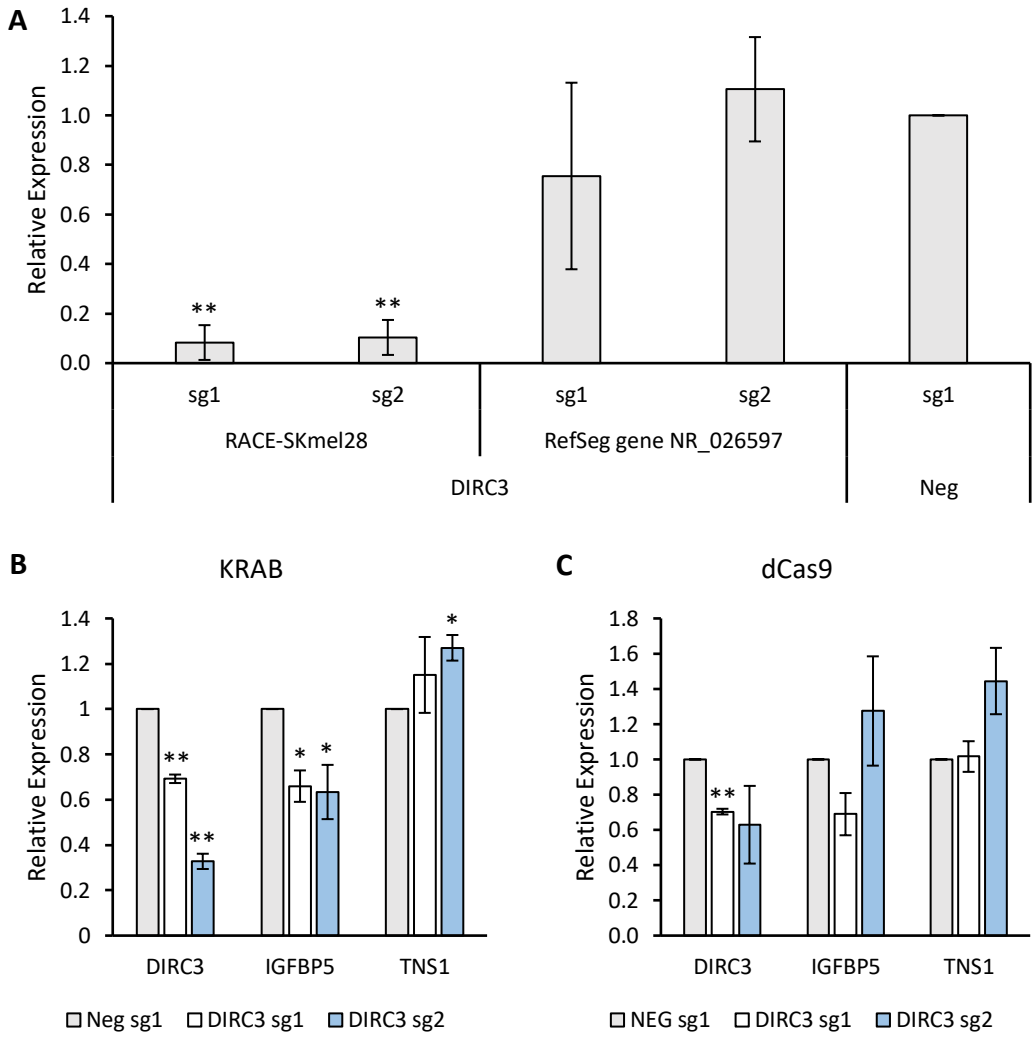

Figure 4.3 CRISPRi knockdown of *DIRC3* causes reduced expression of *IGFBP5*. SKmel28 cells were transfected with CRISPRi vectors targeting *DIRC3*. (**A**) sgRNAs targeting the original (RefSeq gene NR_026597) and novel (RACE-SKmel28) isoforms were designed. CRISPRi vectors dCas9-KRAB (**B**) and dCas9 (**C**) targeted *DIRC3* with the sgRNAs DIRC3sg1 and DIRC3sg2, as well as NEGsg1. Three days after transfection, puromycin was added to the cells which were then left under selection for another seven days. RNA was extracted from the cells and expression of *DIRC3*, *IGFBP5*, and *TNS1* measured using RT-qPCR. Results were normalised to *POLII* and presented relative to expression of NEGsg1. Mean ± SE, N=3 Technical Replicates for (A), N=3 Biological Replicates for (B) and (C). One-tailed Student's t-test $p<0.05$ = * $P<0.01$ **

CRISPRi knockdown of *DIRC3* reveals that it can regulate expression of its neighbouring gene *IGFBP5*. However, it is not clear whether this is the result of a transcript-independent or dependent mechanism. ASOs were therefore used to deplete *DIRC3* transcript in the nucleus to identify transcript-dependent effects

(Ideue *et al.* 2009). Also, if *DIRC3* positive regulation of *IGFBP5* is observed, this would be a way to validate observations following CRISPRi knockdown.

Knockdown of *DIRC3* expression by around 50% using two different ASOs led to a reduction in *IGFBP5* expression levels (44% and 34%), consistent with that identified using CRISPRi-KRAB (Figure 4.4a). However, there were not reproducible changes in *TNS1* using both ASOs. Consistent with these results, *DIRC3*-*IGFBP5* expression was shown to correlate in melanoma patients (Figure 4.4b) observed using RNA-seq data from TCGA for cutaneous melanoma patients (data generated by Pakavarin Louphrasitthiphol, Ludwig Institute Oxford). *IGFBP5* was also amongst the top 10 positively correlated genes with *DIRC3* expression (Table 3.4).

ASO-mediated knockdown of *DIRC3* validates the identification of *DIRC3* positively regulating the tumour suppressor *IGFBP5* using CRISPRi knockdown. By finding the same effect using ASO knockdown, *DIRC3* likely has a functional transcript, thus giving an initial insight into *DIRC3* mode of action. The clear positive regulatory effect *DIRC3* has on *IGFBP5* expression, and strong positive correlation in melanoma patients identified using TCGA, imply that this protein-coding gene is a key mediator of *DIRC3* function in melanoma. By positively regulating expression of *IGFBP5*, *DIRC3* itself likely behaves as a tumour suppressor. *DIRC3* also appears to have directional control of the genes it targets as the lncRNA does not regulate *TNS1*. This is demonstrated as for both CRISPRi and ASO knockdown, only one oligo each resulted in a significant change in *TNS1*, of which both were in opposite directions.

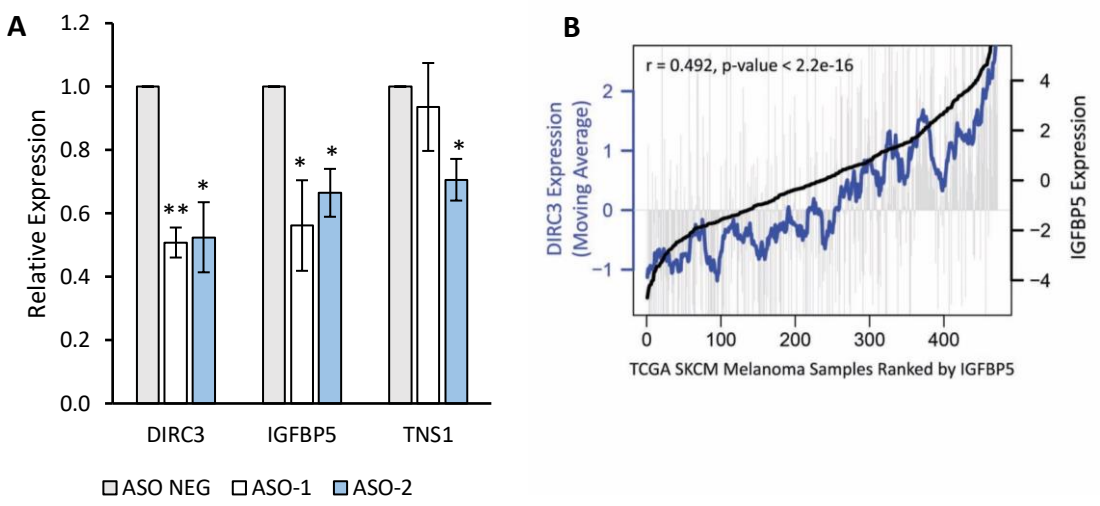

Figure 4.4 *DIRC3* expression positively correlates with *IGFBP5*. (**A**) SKmel28 cells were transfected with antisense oligos (ASOs) targeting *DIRC3*. RNA was extracted three days after transfection. Expression of *DIRC3*, *IGFBP5* and *TNS1* were measured using RT-qPCR. Results were normalised to *POLII* and presented relative to expression of ASO NEG. Mean ± SE, N=3 Biological Replicates. One-tailed Student's t-test p<0.05 = * P<0.01 ** (**B**) TCGA RNA-seq data for 471 melanoma patients was ordered based on an increasing level of *IGFBP5* expression against *DIRC3*. The bold lines represent the moving averages for 20 melanoma samples and vertical grey bars show absolute expression for each melanoma sample. TCGA data analysed by Pakavarin Louphrasitthiphol, Ludwig Institute Oxford.

Taken together, these results provide strong evidence that *DIRC3* is a novel functional nuclear-localised lncRNA able to activate expression of its neighbouring tumour suppressive gene *IGFBP5. DIRC3* is likely to function in a transcript-dependent manner but it cannot yet be ruled out that *DIRC3* could also have some transcript-independent functions.

4.2.3 *DIRC3* regulates expression of genes distal to its locus

LncRNAs have been identified that can function within close proximity to their locus, as well as target genes more distant on their own or other chromosomes (Vance and Ponting 2014). Although *DIRC3* can regulate the melanoma tumour suppressor *IGFBP5* (Wang *et al.* 2015), it may also influence the expression of other genes. The influence a lncRNA has on genes genome-wide can be explored using RNA-seq analysis following lncRNA knockdown. Bioinformatic analysis was performed by

Michael Shapero (University of Bath). As well as seeing which genes are affected, gene grouping by GO analysis allows identification of biological pathways influenced by *DIRC3* expression. The identification of programmes important to cancer could help predict how a lncRNA influences key hallmarks of cancer.

In this study, the influence of *DIRC3* on genes distal to its locus was explored using RNA-seq analysis of *DIRC3* ASO knockdown (DIRC3 ASO-1) in SKmel28 cells compared against a scrambled control (NegA). Since *IGFBP5* is known to play an important role in regulating melanoma cellular processes, the number of genes influenced by both *IGFBP5* (using IGFBP5 ASO-1) and *DIRC3* were identified to see whether *DIRC3* gene regulatory activity is dependent on or independent of *IGFBP5*. For *IGFBP5* knockdown, the gene was again targeted in SKmel28 cells using ASOs.

Knockdown of *DIRC3* resulted in a ~63% reduction and subsequent decrease in *IGFBP5* (Figure 4.5a). This reduced expression led to a significant change in 1886 genes (at a 5% false discovery rate (FDR)) compared to a non-targeting control. Of those, 1015 (54%) showed increased expression while 871 (46%) decreased (Figure 4.6a). For the *IGFBP5* knockdown, a ~79% reduction in expression (Figure 4.5b) resulted in 557 genes (5% FDR) showing altered expression. Of those, 360 were up-regulated and 197 down-regulated (Figure 4.6b). When comparing the *DIRC3* and *IGFBP5* ASO knockdowns, 240 common targets were identified (Figure 4.6c). Compared to random sampling of all expressed genes, there is a significant 22.8-fold enrichment ($p<1e-6$), indicating the overlap is a result of a direct relationship rather than through chance. Also, the majority of shared genes showed changes in expression in the same direction, supporting the discovery that *DIRC3* positively regulates expression of *IGFBP5* (Figure 4.6d).

Of the shared *DIRC3*-*IGFBP5* targets, GO enrichment analysis identified genes involved in cell migration, proliferation, differentiation and metabolism (Figure 4.6e). Such cancer-associated regulatory pathways could participate in controlling melanoma. In addition to acting through *IGFBP5*, *DIRC3* can regulate melanoma-

associated gene categories such as angiogenesis, ERK signalling, and apoptotic signalling, independently of *IGFBP5* (Figure 4.6f).

RNA-seq analysis of the *DIRC3* knockdown using ASOs demonstrates that *DIRC3* has more widespread activity and can regulate gene pathways important in cancer development and progression. However, regulation of these pathways is at least partially dependent upon *IGFBP5*. Consequently, *DIRC3* regulation of *IGFBP5* could be an important determinant of the predicted tumour suppressive activity of *DIRC3* in melanoma. Also, the number of co-regulated genes between *DIRC3* and *IGFBP5* make up almost half (43%) of those identified for *IGFBP5* suggesting *DIRC3* could play an important role in the regulation of *IGFBP5* activity. With two very differently designed oligos (*DIRC3* ASO-1 and *IGFBP5* ASO-1) identifying the same candidates, it is far less likely that these expression changes are the result of off-target effects and so are more likely to play a role as mediators of *DIRC3* functional activity. RNA-seq analysis of *DIRC3* and *IGFBP5* ASO knockdowns demonstrate that the *DIRC3* transcriptional response is via *IGFBP5*-dependent and -independent activities.

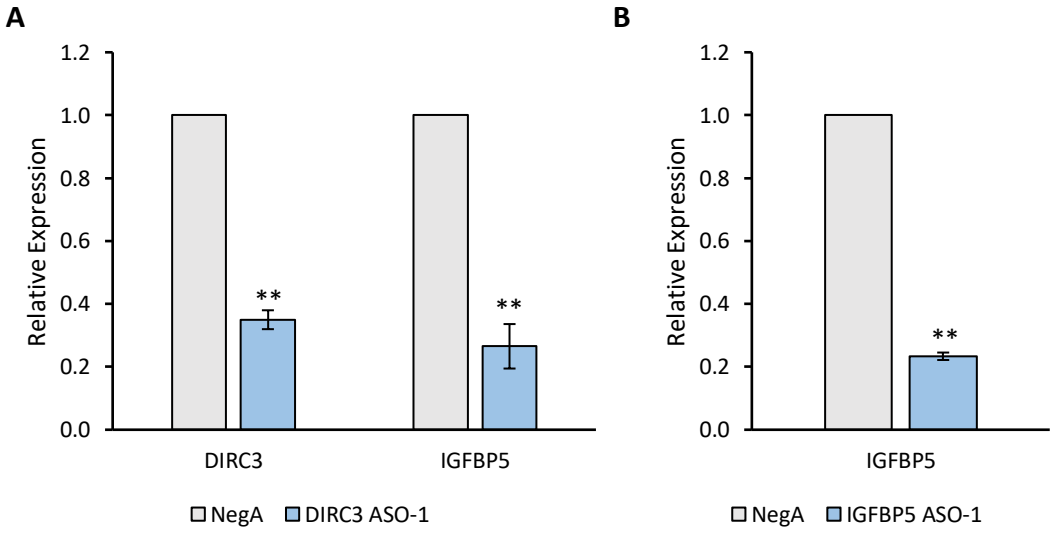

Figure 4.5 Generation of *DIRC3* and *IGFBP5* knockdown for RNA-seq analysis. *DIRC3* (**A**) and (**B**) *IGFBP5* expression were depleted in SKmel28 cells using ASOs. Three days after transfection the level of knockdown was measured using RT-qPCR. Results were normalised to *POLII* and presented relative to expression in the siCtrl. Mean ± SE N=3 Biological Replicates. One-tailed Student's t-test $p<0.05$ = * $P<0.01$ **.

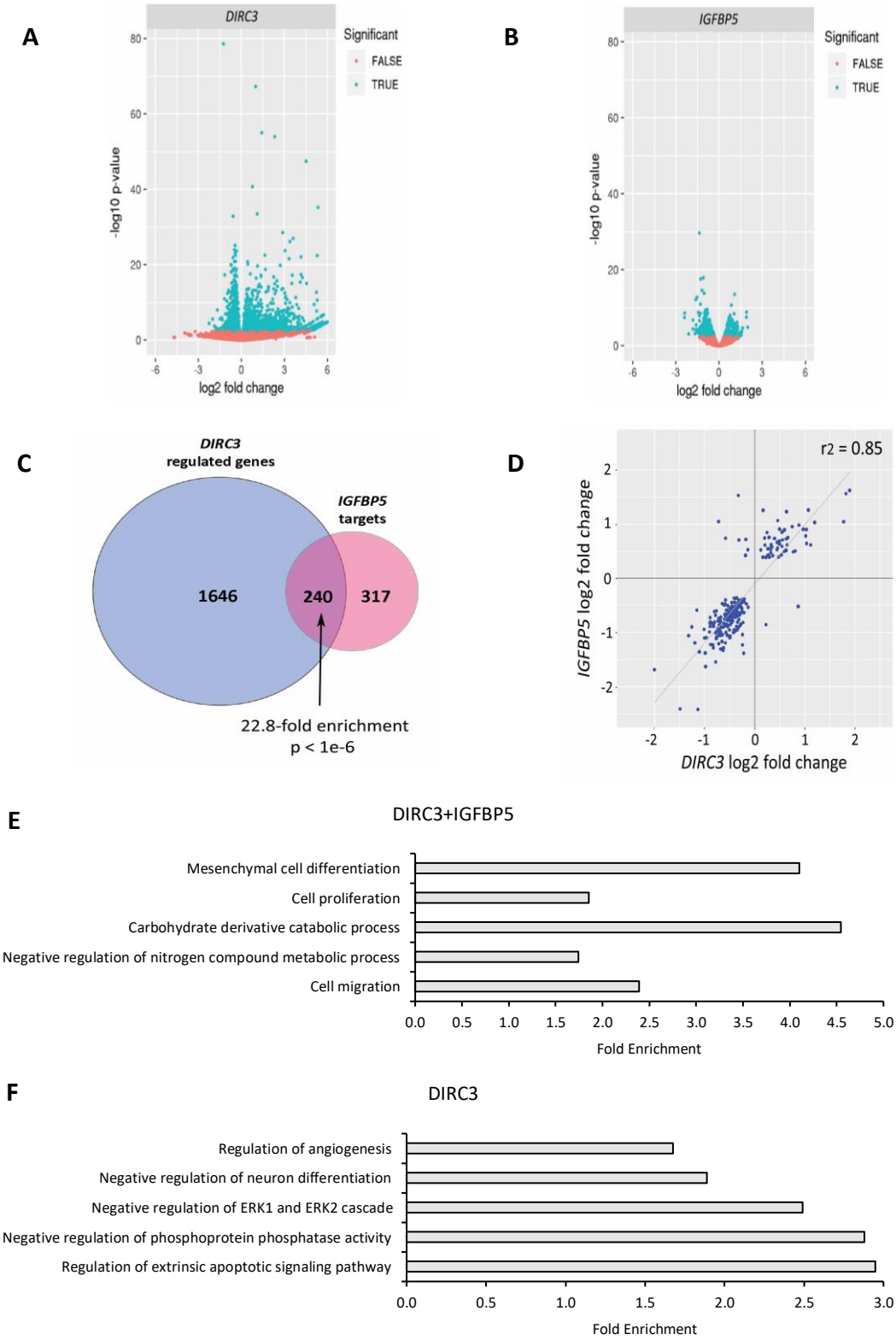

Figure 4.6 RNA-seq analysis of ASO *DIRC3* and *IGFBP5* knockdown show joint and independent gene regulation. Volcano plots show significantly up- and down-regulated genes following *DIRC3* (**A**) and *IGFBP5* (**B**) knockdown. (**C**) Venn diagram presenting the intersection for *DIRC3* and *IGFBP5* independent shared genes (**D**) Plot generated showing an increase or decrease in expression of common targets. Gene Ontology (GO) enrichment

analysis was examined for both *IGFBP5* and *DIRC3* common targets (**E**) and *DIRC3* gene targets alone (**F**). GO enrichment analysis was performed using GOstats and FDR correction was applied. All bioinformatic analyses were generated by Michael Shapiro (University of Bath).

RNA-seq analysis of genes following *DIRC3* depletion was also performed in SKmel28 cells containing *DIRC3* dCas9-KRAB knockdown. Bioinformatic analysis was performed by Yihong Jennifer Tan (University of Lausanne). By using CRISPRi knockdown, genes affected by transcript-independent *DIRC3* function can also be identified. In addition, different knockdown methods have previously been found to identify different genes and gene pathways affected following target gene knockdown (Stojic *et al.* 2016). By combining ASO and CRISPRi knockdowns of *DIRC3* it may be possible to identify which genes or gene pathways consistently overlap. Also, the comparison may help identify which technique is more efficient at generating a list of potential *DIRC3* targets.

The dCas9-KRAB was targeted to *DIRC3* using sgRNA DIRC3sg2 to deplete *DIRC3* levels in SKmel28 cells. After transfection, the cells were selected under puromycin for 10 days. Once the level of *DIRC3* knockdown and corresponding reduction in *IGFBP5* was confirmed using RT-qPCR, the samples were analysed using RNA-seq, and gene expression changes identified compared to cells transfected with a scrambled control (NEGsg1).

Following a 50% reduction in *DIRC3* and 61% reduction in *IGFBP5* expression (Figure 4.7a), 422 genes (5% FDR) significantly changed expression. Of those, 259 were up-regulated and 163 down-regulated (Figure 4.7b). Gene ontology (GO) enrichment analysis found *DIRC3*-regulated genes were particularly enriched in cancer- and melanoma-associated pathways regulating activities including apoptosis, cell cycle control, neural crest cell migration, and mitochondrial activity (Figure 4.7c). When comparing the genes in common following *DIRC3* ASO and CRISPRi knockdown, 35 were found in both (Figure 4.7d). Of those, 21 showed expression changes in the same direction (Table 4.2). These genes include those which participate in the

regulation of melanoma-associated processes including apoptosis (CFLAR), cell adhesion (KAZN), mitochondrial activity (MT-ND4), and activation of MAPK signalling (SEMA4C) (Zeng *et al.* 2011, O'Leary *et al.* 2015).

Analysis of genes affected by *DIRC3* depletion following CRISPRi knockdown confirms *DIRC3* expression can influence the activity of genes across the genome. Identification of 35 genes using both CRISPRi and ASO knockdown techniques suggests they are more likely to be *DIRC3* targets.

ASO knockdown produced a significant change in almost four times more genes than identified using CRISPRi, the genes also showed a greater fold change in expression, suggesting ASO knockdown could be a more effective method for RNA-seq analysis. Of the 35 genes, 21 showed expression changes in the same direction of which several were related to key cancer-associated processes. With the remaining genes changing expression in different directions, they could still be a consequence of off-target effects. Consequently, ASOs could be more effective for detecting gene changes due to differences in their experimental design. One example is the harvesting of the cells three days post-transfection rather than 10, so that the cells have less time to respond to the knockdown and induction of rescue pathways is limited. However, due to the introduction of oligos, ASOs may induce more off-target effects (Stojic 2018).

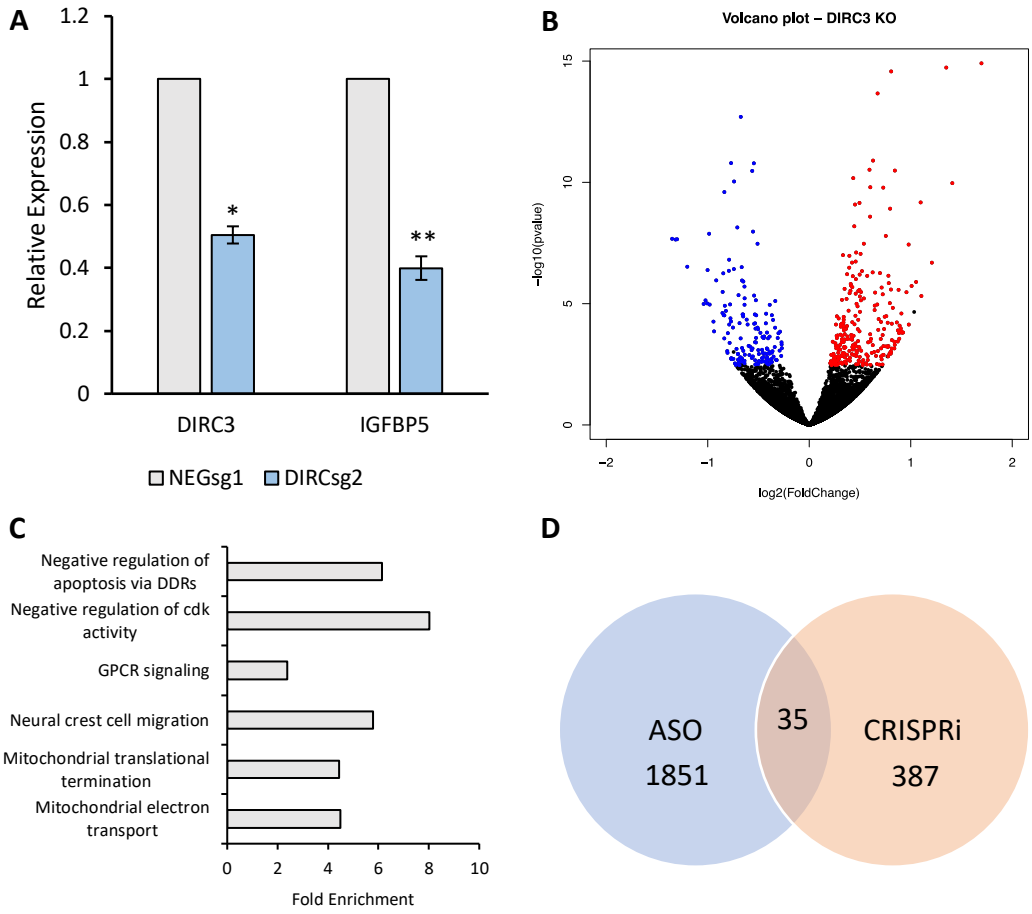

Figure 4.7 *DIRC3* regulates expression of genes in trans. (**A**) *DIRC3* was depleted in SKmel28 cells using CRISPRi-KRAB. The level of knockdown was measured using RT-qPCR 10 days after transfection. Results were normalised to *POLII* and presented relative to expression in the siCtrl. Mean ± SE N=3 Biological Replicates. One-tailed Student's t-test p<0.05 = * P<0.01 ** (**B**) A volcano plot was generated showing significantly upregulated (red) and downregulated (blue) genes following *DIRC3* knockdown (**C**) Gene Ontology (GO) enrichment analysis for genes showing a significant change in expression. (**D**) A Venn diagram demonstrating the overlap of significantly altered genes using either ASOs or CRISPRi. Bioinformatic analysis was performed by Yihong Jennifer Tan (University of Lausanne).

Table 4.2 A list of 35 significantly changed genes identified following RNA-seq analysis of *DIRC3* ASO and CRISPRi knockdown in SKmel28 cells. An increase or decrease in expression following *DIRC3* knockdown are indicated by arrows ↑ and ↓ respectively.

Gene	ASO	CRISPRi
AC004447.2	↑	↑
AC009237.8	↓	↑
ACOT2	↑	↓
ANKRD34A	↑	↑
ARL10	↓	↓
CFLAR	↓	↓
CHL1	↑	↑
CNP	↓	↓
CTC-296K1.3	↓	↓
CTD-2336O2.1	↑	↓
DAK	↑	↓
FARP1	↑	↓
FBXO2	↑	↑
GPR55	↑	↓
KAZN	↑	↑
LYPD1	↓	↓
MALSU1	↑	↓
MT-ND4	↓	↓
NPR2	↑	↑
POM121	↑	↑
PSMC3IP	↓	↓
RP11-203J24.8	↓	↓
RP11-400F19.6	↑	↓
RP11-817O13.8	↑	↑
RP4-751H13.7	↓	↑
SEMA4C	↑	↑
SGPP2	↓	↓
SLC25A26	↓	↑
SLC9A5	↑	↓
SNX32	↓	↓
STK25	↑	↑
TMEM160	↑	↓
TOR3A	↓	↓
ZMIZ1	↑	↓

4.3 DISCUSSION

Regulation of neighbouring genes is common for both non-coding and protein-coding genes. A large proportion of lncRNA loci have been identified that regulate the expression of their neighbouring genes (Ørom *et al.* 2010, Engreitz *et al.* 2016). However, the likelihood of lncRNAs regulating their neighbouring gene decreases with increasing distance apart. Derrien *et al* (2012) found that while 2.95% of identified lncRNA positively correlated with expression of their neighbouring genes when within 20 kb of one another, this dropped to 0.44% when the distance increased to 80-100 kb. However, *DIRC3* positively regulates expression of *IGFBP5* despite it being 600 kb downstream. LncRNAs may regulate their neighbouring genes through actions such as recruiting regulatory complexes, altering RNAPII occupancy, or DNA looping (Wang *et al.* 2011, Kornienko *et al.* 2013, Hacisuleyman *et al.* 2014). If a functional transcript is important for *DIRC3* to regulate *IGFBP5* expression it could be that *DIRC3* guides transcription factors to, or sequesters proteins away from, the *IGFBP5* locus (Deniz and Erman 2016). It should also be noted that while *DIRC3* appears to act using a functional transcript, the presence of potential regulatory elements across the *DIRC3* locus, such as enhancers, could also play a part in *IGFBP5* regulation.

A recent study suggested that ASOs can prevent transcription of a target gene by blocking RNAPII elongation. Greer *et al* (2019) found that when they targeted *Hdac2* with two different ASOs, transcription towards the 3' end of the gene was consistently impeded while transcription at the 5' end was not. Consequently, while initiation of transcription is still possible, elongation is prevented. If this is the case, ASO knockdown of *DIRC3* may not be representative of a functional transcript and instead only act to validate findings using CRISPRi. Presence of the nascent *DIRC3* transcript could be confirmed using nuclear run-on (NRO) (Greer *et al.* 2019). siRNAs have also previously been used to knockdown activity of lncRNA transcripts, such as MALAT1, within the nucleus despite its use of cellular machinery within the

cytoplasm (Tripathi *et al.* 2010). Consequently, if possible to knockdown *DIRC3* using siRNAs, any effects on expression of *IGFBP5* and genes identified using RNA-seq, could indicate whether the *DIRC3* transcript is functional.

As *DIRC3* activation of *IGFBP5* was demonstrated using both CRISPRi and ASO mediated knockdown, this strongly indicates that *DIRC3* is a functional lncRNA. *IGFBP5* itself could, therefore, play an important part in *DIRC3* function in melanoma. *IGFBP5* is expressed in both normal and cancer tissues where it regulates cell adhesion, differentiation, migration, and apoptosis (Su *et al.* 2011, Sureshbabu *et al.* 2012). Dysregulation of *IGFBP5* has been found to drive cancer growth and metastasis in breast cancer, osteosarcoma, and melanoma (Su *et al.* 2011, Sureshbabu *et al.* 2012, Wang *et al.* 2015). In addition, its increased expression is associated with increased patient survival in breast cancer (Ahn *et al.* 2010). *IGFBP5* may also play an important role in inhibiting both tumour growth and metastasis in melanoma as suggested by its lower expression in metastatic tissue compared to primary melanoma samples (Wang *et al.* 2015). Consequently, *IGFBP5* is likely to function as a tumour suppressor in a range of cancer types, including melanoma. As *DIRC3* positively regulates expression of *IGFBP5*, this suggests *DIRC3* may function as a tumour suppressor via its regulation of *IGFBP5*.

The identification that *DIRC3* regulates genes involved in multiple cancer-associated processes, support the hypothesis that *DIRC3* participates in regulating cancer progression. In order to regulate expression of genes distant from the *DIRC3* locus, a range of transcript-dependent and -independent methods may be executed. If there is sufficient quantity of the molecule, the lncRNA transcript may translocate from its site of synthesis to distal genes. This may be achieved through direct RNA-DNA based targeting to genomic sites, or through being guided by proteins. For example, *HOTAIR* can interact with loci genome-wide through directly interacting with the DNA itself (Gupta *et al.* 2010). In the case of *Paupar*, the transcript is guided to distant sites, including those on multiple chromosomes other than its own, by the DNA-binding protein PAX6 which it complexes with (Vance *et al.* 2014). Another proposed

mechanism is that distal regions, either on the same or different chromosomes, may be brought into closer proximity with the lncRNA loci through chromosomal looping such as has been proposed for the lncRNA *Firre* (Hacisuleyman *et al.* 2014).

In some cases, wide-spread expression changes may be observed as a result of downstream effects due to the lncRNA's local activity (Engreitz *et al.* 2016). This was the case for *Linc-p21*. Originally the nuclear-localised lncRNA was thought to directly repress distal genes as part of the p53 response to DNA damage (Huarte *et al.* 2010). However, it has since been recognised that such effects are due to its positive regulation of the protein-coding gene *Cdkn1a* via regulatory elements within the *Linc-p21* locus (Groff *et al.* 2016). The lncRNA ncRNA-a7 has also been recognised for having an enhancer-like function as it positively regulates expression of *Snai1*, through which it affects processes including cell migration. In this case, additional distal genes were also identified that mediate ncRNA-a7 effects independent of *Snai1* (Ørom *et al.* 2010). Due to the overlapping regulated genes identified following *DIRC3* and *IGFBP5* ASO knockdown, a large proportion of genome-wide activity may be through its regulation of *IGFBP5*. Many of those shared genes are involved in cancer-associated processes. However, *DIRC3* also appears to regulate the expression of a range of cancer-causing gene programmes independent of *IGFBP5*.

Using GO analysis of RNA-seq data from ASO and CRISPRi knockdowns of *DIRC3* it was possible to observe similarities in their target gene pathways. Both knockdown techniques highlighted gene expression programmes important to cancer. However, only 35 overlapping genes were identified and ASO knockdown showed almost five-fold more genes with significant changes. Previous studies have also found discrepancies between observed molecular changes when using different methods to knockdown gene expression, including for ASOs and CRISPRi. Some differences can be down to the design of the method used. With CRISPRi preventing transcription of its target, local activities caused by the act of *DIRC3* transcription could influence expression of genes downstream, and so such targets may not be affected by transcript knockdown alone (Stojic *et al.* 2018). It could also be the case that the

CRISPRi method is able to repress expression of regulatory elements, such as enhancers, present locally to the lncRNA TSS, and so effect alternative genes this way (Liu and Lim 2018). Also, although CRISPRi has been found to induce very few off-target effects (Gilbert *et al.* 2014, Stojic *et al.* 2018), the longer period of time between transfection and harvesting the cells (10 days rather than three as for ASOs) could allow transcriptional programmes to be altered within the cell resulting in discrepancies between the methods. Some genes typically altered during *DIRC3* knockdown may have their expression rescued via an alternative method within that time frame. In the case of ASOs, off-target effects are more of a concern as the oligonucleotides may contain sufficient complementarity to transcripts that are not their target, causing these genes to also become repressed (Watts and Corey 2012). Such off-target effects may also be executed by negative controls resulting in it becoming difficult to differentiate which genes changed due to non-specific effects of the negative control oligos (Stojic *et al.* 2018). However, it should be noted that due to the *DIRC3* and *IGFBP5* ASOs targeting such different sequences and still showing overlap, it is highly likely that the 240 overlapping genes are targets of *DIRC3,* likely through its regulation of *IGFBP5* expression. These factors could have contributed to the large discrepancy in the number of *DIRC3* targets identified using by CRISPRi and ASO knockdown in the RNA-seq experiment. Variations in the genes identified following knockdown allow different conclusions to be made about possible functions of the target based on the knockdown method used. However, as genes related to cancer pathways are consistently altered using different *DIRC3* knockdown methods, this suggests *DIRC3* participates in the regulation of cancer initiation and/or progression.

The ability of lncRNAs to translocate from their site of synthesis to distal locations can be investigated using rescue experiments. Following knockdown of *DIRC3* expression, heterologous expression of *DIRC3* from a plasmid can be used to attempt to rescue the lncRNA's activity. If the lncRNA is able to translocate from its locus, functionality should be restored following this ectopic expression. However, care

must be taken to restore expression to physiologic levels in the correct subcellular location (Ransohoff *et al.* 2017, Kopp and Mendell 2018).

Capture hybridisation of RNA targets (CHART)-seq could also be used to map sites of *DIRC3* chromatin occupancy genome-wide and identify genes that are directly bound and regulated by *DIRC3* (Simon *et al.* 2011). *De novo* motif discovery may also be performed to identify possible proteins involved in targeting *DIRC3* to chromatin. In the case of the CNS-expressed lncRNAs *Paupar* and *Dali*, no enrichment in sequence complementarity was identified between the lncRNAs and their identified binding sites. Instead, the proteins PAX6 and Pouf3 were found to be enriched at *Paupar* and *Dali* sites respectively, suggesting that they target the lncRNAs to distant sites in the genome (Vance *et al.* 2014). Consequently, lncRNAs may not only regulate their adjacent protein-coding genes *in cis* but may also bind the proteins that are produced. Tests such as this and RNA immunoprecipitation (RIP) could be performed to identify whether *DIRC3* binds and regulates the *IGFBP5* protein.

Together the data collected show *DIRC3* is a functional nuclear-expressed lncRNA able to regulate its neighbouring gene, *IGFBP5*, in a transcript-dependent manner. *DIRC3* is also able to regulate genes distal from its locus at least partly via its regulation of *IGFBP5*.

Chapter 5: *DIRC3* can negatively regulate anchorage-independent growth

5.1 Introduction

5.1.1 LncRNAs and melanoma

Cancer cells acquire a number of biological characteristics that distinguish them from normal cells, including increased cell survival, proliferation, and invasion. These are known as the hallmarks of cancer (Hanahan and Weinberg 2011, Elia *et al.* 2018). One key hallmark is metastasis. Metastasis enables primary neoplasms to migrate to distant locations in the body and so plays a major role in the lethality of cancer (Steeg 2006, Menyhárt *et al.* 2016). Prior to metastasising, cells lose cell adherence proteins and increase in motility. These cells undergo epithelial-to-mesenchymal-transition (EMT) in which epithelial cells acquire more mesenchymal features so that their migratory and invasive potential increase (Nieto *et al.* 2016). Expression of matrix-degrading proteinases enables them to invade through the extracellular matrix (ECM) and enter blood vessels or the lymphatic system, leading to their dissemination around the body. In order to migrate through the blood to distant sites, the cells must be able to survive in an anchorage-independent manner. The metastatic cells may then extravasate from the vessels and form new colonies (Guadamillas *et al.* 2011, Lambert *et al.* 2017). In the case of melanomas, tumours detected early on that are still benign may be excised surgically and have a high survival rate. However, metastatic melanoma is less treatable and so very lethal. Consequently, while only accounting for a small proportion of skin cancer cases, metastatic melanoma makes up the majority of skin cancer deaths (Siegel *et al.* 2019).

MITF and SOX10 are key factors in regulating the switching of melanoma cells between proliferative and invasive states (Hoek *et al.* 2008, Verfaillie *et al.* 2015).

Proliferative cells in primary tumours have previously been found to express high levels of MITF and SOX10. Subpopulations of cells on the edge of primary lesions express low MITF, allowing acquisition of invasive properties which eventually lead to their metastasis. Metastatic sites have also been found to contain MITF-positive cells, supporting the ability of melanoma cells to switch between proliferative and invasive (Verfaillie *et al.* 2015).

A number of lncRNAs participate in regulating a range of cellular activities in melanoma. *BANCR*, an oncogenic lncRNA upregulated in primary melanomas containing the $BRAF^{V600E}$ mutation, regulates genes involved in melanoma cell proliferation and migration (Li *et al.* 2014). *CASC15* (Cancer susceptibility candidate 15), which is amplified in some metastatic melanoma cases, participates in regulating of cell invasiveness (Lessard *et al.* 2015). *SLNCR1* promotes melanoma cell invasion by promoting *MMP9*, *AR* and *Brn3a* expression (Schmidt *et al.* 2016). These represent a handful of lncRNAs that have been identified with functional roles in melanoma. By accumulating information about the functional roles of lncRNAs in melanoma, it becomes increasingly clear that they are a crucial layer of regulation in cancer prevention or induction. This makes them promising targets in the development of therapeutics that could be used alongside current methods.

5.1.2 Assays for measuring proliferation, invasion, and anchorage-independent growth

Using transcriptomic profiling, changes in lncRNA expression may be associated with genes important to the hallmarks of cancer. Such associations may be used to predict likely cellular activities a lncRNA influences. Cellular assays offer a method to directly identify changes in cellular behaviour following knockdown or activation of a gene of interest.

Dysregulated expression of oncogenes or tumour suppressors can enable uncontrolled proliferation of cancer cells, allowing the formation of tumours

(Hanahan and Weinberg 2011, Borowicz *et al.* 2014). As the cells continue to divide, there are more opportunities for additional mutations to arise. Of these, some may offer a growth selective advantage, enhancing survival and allowing the cancer to progress towards a more metastatic state (Evan and Vousden 2001). The influence *DIRC3* has on proliferation may be assessed by quantifying growth of the cells with reduced *DIRC3* compared to a negative control.

In the early stages, tumours are benign, constrained to a region surrounded by healthy tissue. However, when cells develop more invasive properties, they no longer adhere to their neighbouring cells and penetrate through the barrier of healthy tissue using proteolytic degradation (Steeg 2006, Elia *et al.* 2018). Such behaviour is the beginning of tumours becoming metastatic. Cancer cell invasiveness may be measured using a Matrigel invasion assay. The porous filter of the migration chamber is coated with components reminiscent of the ECM. The presence of a chemoattractant (such as FBS) in the lower well triggers chemotaxis and encourages cells to move through the membrane, degrading the matrix-like components in order to pass through. The number of cells that invade through the matrix may then be quantified (Menyhárt *et al.* 2016, Schmidt *et al.* 2016, Elia *et al.* 2018).

Once cells enter the vascular system, they must survive their journey without being attached to the ECM. Typically, cells undergo anoikis upon detachment (Taddei *et al.* 2012). However, if they are able to avoid this process, cells can travel to sites distant from where they initially formed. A key assay for determining the ability of cells to proliferate in an anchorage-independent manner is the soft-agar assay. Using this assay, cells are grown in a semi-soft agar-based media on top of a slightly denser media, preventing cells from adhering to the plate. The ability of a target gene to influence anchorage-independent growth is revealed by the number and/or size of colonies formed in the absence of an adhesive surface (Borowicz *et al.* 2014). Since cancer cells become more metastatic through EMT, anchorage-independent growth is a hallmark of cellular transformation. Measurement of anchorage-independent growth is also commonly used to assess metastatic potential. When observed *in vitro*,

this phenotype has been found to reflect the metastatic potential of a range of tumour types, including breast, lung, and ovarian cancers (Mori *et al.* 2009). Mori *et al* also found that lung cancer patients with tumours expressing a strong genetic signature for anchorage-independent growth had a worse overall outcome, likely due to the tumours metastasising.

5.1.3 Chapter Summary

DIRC3 regulates *IGFBP5* as well as other cancer-regulating genes through *IGFPB5*-dependent and -independent methods, however, this does not conclusively mean *DIRC3* disruption alters any of the hallmarks of cancer. Clonal cells containing depleted *DIRC3* were used to measure the effect of reduced *DIRC3* expression on proliferation, invasion, and anchorage-independent growth. *DIRC3* does not influence melanoma cell proliferation or invasion under normal growth conditions. However, reduced *DIRC3* induces a strong increase in anchorage-independent growth, which is a central assay used to indicate the ability of cells to metastasise. This is likely to be via its interaction with *IGFBP5* as knockdown of *IGFBP5* also led to an increase in anchorage-independent growth. The proposed *DIRC3* repression of anchorage-independent growth, likely via regulation of *IGFBP5*, supports a tumour suppressive behaviour of *DIRC3*. Consequently, *DIRC3* may also inhibit melanoma metastatic capability by regulating this activity and so represent a good candidate biomarker or therapeutic target.

5.2 Results

5.2.1 *DIRC3* does not regulate proliferation or invasion of SKmel28 cells under normal growth conditions

MITF, SOX10, and *IGFBP5* have each been implicated in regulating melanoma cell proliferation and invasion (Verfaillie *et al.* 2015, Wang *et al.* 2015). By regulating and being regulated by *DIRC3*, respectively, *DIRC3* could also participate in mediating these cellular activities. RNA-seq analysis of the *DIRC3* genome wide transcriptional response (Chapter 4) also suggests a role for *DIRC3* in the regulation of proliferative and invasive phenotypes. Consequently, it was hypothesised that *DIRC3* may have a role in regulating melanoma cell proliferation and invasion.

Initially, expression of *DIRC3* was measured in known proliferative and invasive melanoma cells using RT-qPCR. RNA from short-passage melanoma cultures was donated by Eleonora Leucci (KU Leuven). The MM047 and MM099 cultures have previously been identified as expressing an invasive transcriptional state, while the remainder expressed a more proliferative (Verfaillie *et al.* 2015). *DIRC3* expression was typically higher in the proliferative cells, with four out of six proliferative cell types showing greater *DIRC3* expression. These ranged from six- to 68-fold greater than the invasive cell types (Figure 5.2).

The altered *DIRC3* expression between the proliferative and invasive cell types suggest *DIRC3* expression participates in at least one of these states. It could be the case that changes in cell gene expression which occur during the switch between proliferative and invasive states promote changes in *DIRC3* so that its tumour suppressive effects are initiated or repressed.

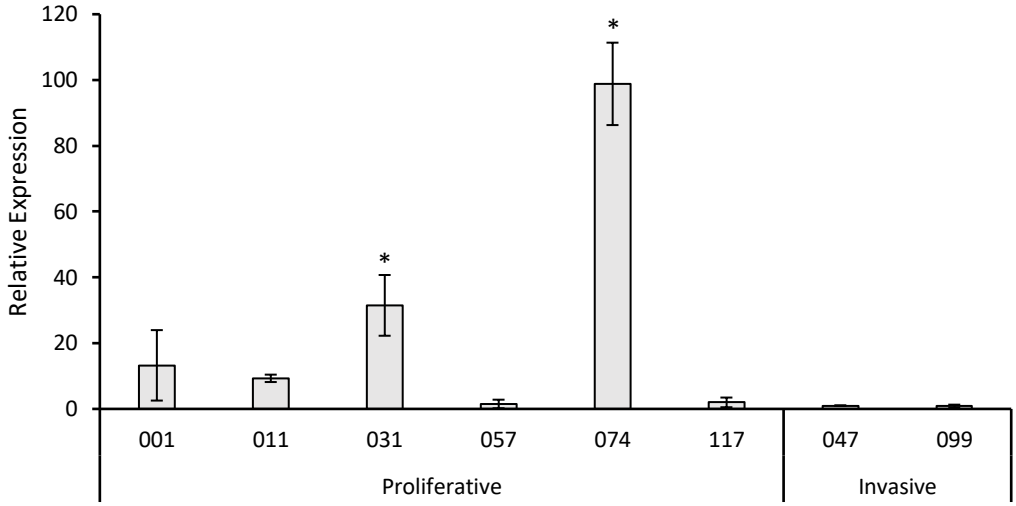

Figure 5.1 *DIRC3* shows increased expression in proliferative melanoma cells. Expression of *DIRC3* was measured in short-term cultures of proliferative and invasive melanoma cells (Verfaillie *et al.* 2015). Expression was analysed using RT-qPCR with results normalised to *POLII*. Mean ± SE N=3 Technical Replicates. One-tailed Student's t-test $p<0.05$ = *

Changes in *DIRC3* expression between cell types recognised for regulating different cellular activities could be indicative of a role for *DIRC3* in such processes. However, they do not give a definitive answer of whether the lncRNA affects cellular activity. By performing cellular proliferation and invasion assays it is possible to investigate whether *DIRC3* has a direct role in these cellular processes.

The effect of *DIRC3* knockdown on melanoma cell proliferation was explored in SKmel28 CRISPRi knockdown cells grown under normal cell culture conditions. Over four days there was no significant difference between proliferation of the control cells (NEGsg1) and *DIRC3* knockdown (DIRC3sg1, sg2) (Figure 5.3a). Consequently, *DIRC3* does not appear to participate in regulating proliferation in melanoma cells under normal growth conditions.

The effect of *DIRC3* knockdown on melanoma cell invasion was also explored in SKmel28 cells containing the CRISPRi *DIRC3* knockdown. Invasion was assessed using a Matrigel invasion chamber. To encourage invasion, cells were starved of FBS 24 hours before being seeded in an FBS-depleted chamber with an FBS-rich chamber below. Invasive capacity was measured by quantifying the number of cells that

invaded through the membrane. There was no significant difference in invasion between *DIRC3* depleted cells (DIRC3sg1, DIRC3sg2) and the controls (NEGsg1) (Figure 5.3b). *DIRC3* consequently appears to not have a role in regulating SKmel28 melanoma invasion in nutrient rich conditions.

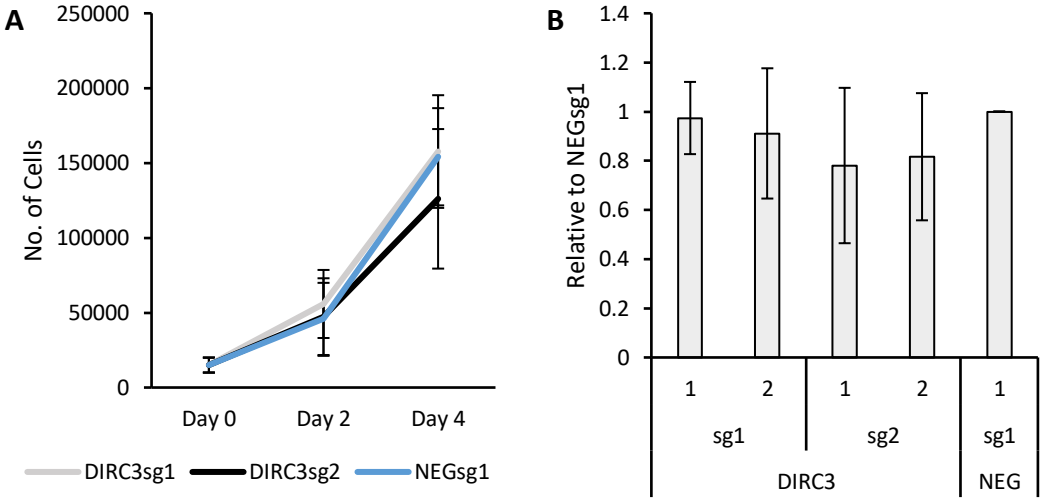

Figure 5.2 *DIRC3* does not regulate SKmel28 cell proliferation or invasion. (**A**) *DIRC3* CRISPRi clonal knockdown SKmel28 were seeded at a density of 1500 cells/well in a 12-well plate. The number of cells were counted at 0, 2, and 4 days. (**B**) Following FBS starvation *DIRC3* clonal knockdown SKmel28 were seeded in Matrigel chambers with 20 % FBS in the lower well. The number of cells that passed through the membrane were quantified after 48 hours. Mean ± SE N=3 Technical Replicates. One-tailed Student's t-test $p<0.05$ = *

Although the proliferation and invasion assays suggest *DIRC3* does not participate in regulating these cellular processes, the conditions that the cells are grown under may have influenced the results. Although the invasion assay included FBS-depletion, neither assay was performed under conditions representative of the tumour microenvironment. Conditions such as glutamine starvation or hypoxia, which are commonly observed in tumours, may trigger expression of other genes (Feige *et al.* 2011, Xue *et al.* 2014). Such changes could then induce or suppress expression of *DIRC3*, meaning involvement of the lncRNA is only initiated in proliferation or invasion when under such stressful conditions. This is consistent with melanoma patient RNA-seq data from TCGA (data generated by Pakavarin Louphrasitthiphol, Ludwig Institute Oxford) which demonstrates a strong positive correlation between expression of *DIRC3* and a glutamine starvation signature (Figure 5.4). Consequently,

it is not yet possible to confidently say whether *DIRC3* regulates proliferation and invasion in melanoma cells. However, it has conclusively shown *DIRC3* does not to participate in regulating proliferation or invasion under normal growth conditions.

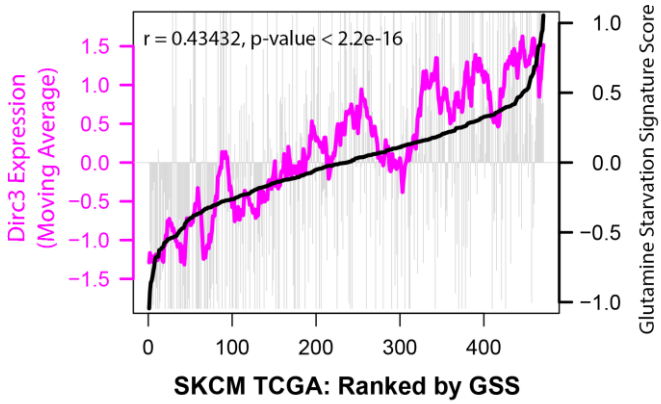

Figure 5.3 *DIRC3* expression correlates with glutamine starvation. TCGA RNA-seq data for 471 melanoma patients was ordered based on increasing levels of expression of the glutamine starvation signature. The bold lines represent the moving averages and vertical grey bars show absolute *DIRC3* expression for each melanoma sample. (Data generated by Pakavarin Louphrasitthiphol, Ludwig Institute Oxford).

5.2.2 Generation of clonal *DIRC3* knockdown SKmel28, 501mel, and A375 melanoma cells

To further investigate the involvement of *DIRC3* in regulating melanoma, its expression was depleted before performing anchorage-independent growth assays. Using the CRISPRi method, clonal cell lines were generated so that a stable *DIRC3* knockdown could be maintained for long periods. This was necessary as the anchorage-independent growth assay require several weeks before results can be obtained.

Clonal cell lines were generated following stable transfection of dCas9-KRAB and sgRNAs (DIRC3sg1, DIRC3sg2, or NEGsg1). Clones were isolated and expanded following puromycin selection. *DIRC3* and *IGFBP5* expression were determined in each cell line using RT-qPCR so that those with the greatest knockdown were selected

for use in the cellular assays. As well as using two sgRNAs to account for off-target effects, two clones were used to control for effects caused by vector integration at different points in the genome. Expression of *IGFPB5* was also measured in case any variations in the cellular assays could be linked to changes in its expression. *DIRC3* loss of function was performed in SKmel28, 501mel and A375 cell lines. By using several melanoma cells lines, general functions of *DIRC3* in melanoma could be identified.

For the SKmel28 clonal loss of function cells, *DIRC3* was significantly knocked down which also led to a significant reduction in *IGFBP5* (Figure 5.1a). *DIRC3* and *IGFBP5* were also significantly reduced following *DIRC3* knockdown in A375 (Figure 5.1c).
In the case of 501mel, significant knockdown of *DIRC3* only led to a significant reduction of *IGFBP5* in DIRC3sg1-targeted cells, with DIRC3sg2 showing no significant change from the NEGsg1 control cells (Figure 5.1b).

As well as measuring and confirming *DIRC3* knockdown in each of the clonal cells, analysis of *IGFBP5* expression supports the positive regulation of *IGFBP5* identified in Chapter 4. The reproducibility of this positive regulation in different cell lines supports the positive regulation being a general feature in melanoma cells. The varied expression of *IGFBP5* in 501mel cells DIRC3sg2, could be a consequence of the prolonged selection allowing amplification of its expression or an off-target effect caused by the sgRNA.

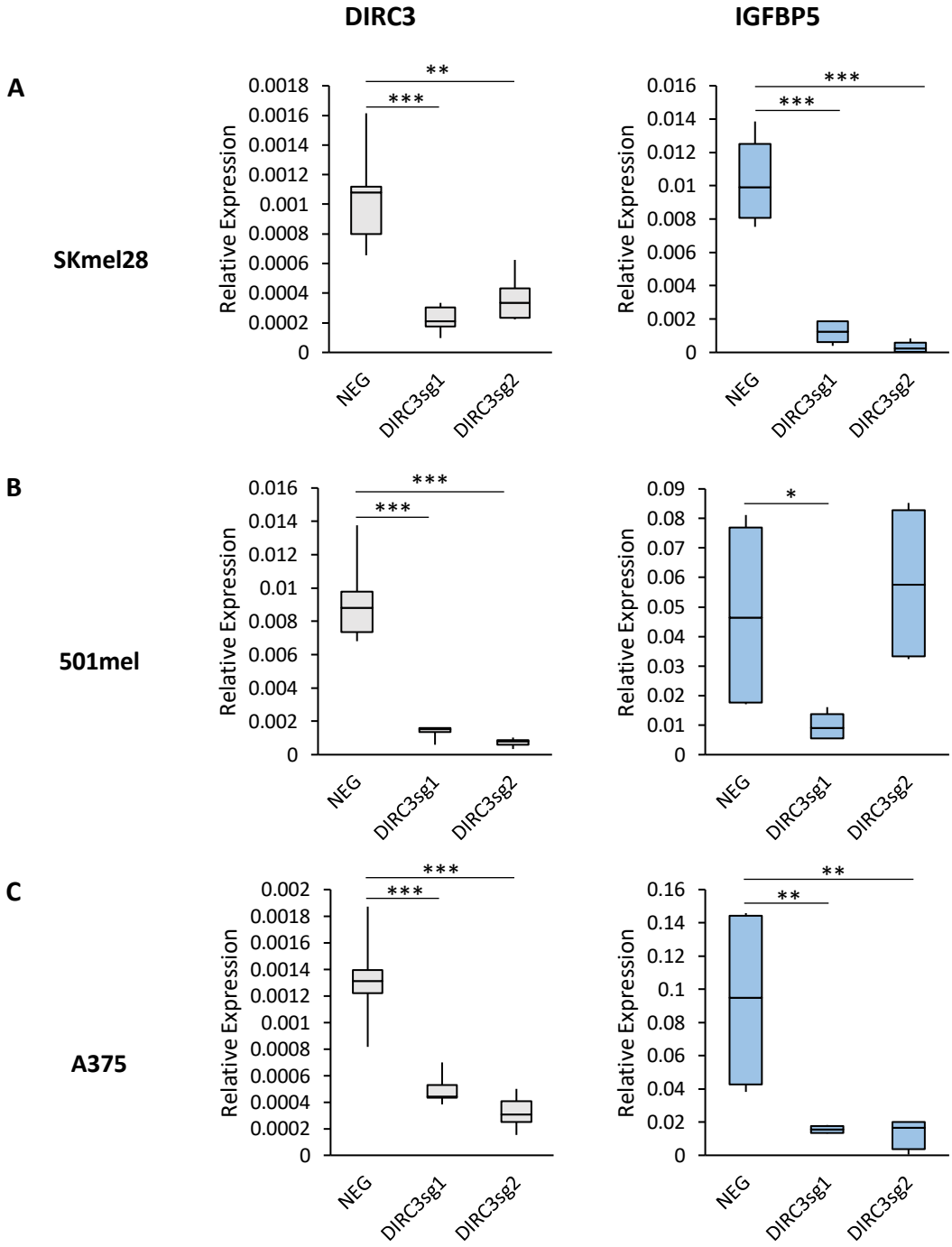

Figure 5.4 *DIRC3* knockdown cells were generated using CRISPRi with dCas9-KRAB. Clonal (**A**) SKmel28 (**B**) 501mel and (**C**) A375 cell lines containing the *DIRC3* CRISPRi knockdown were generated following strong puromycin selection and growth from single cells. The levels of *DIRC3* and *IGFBP5* expression were measured using RT-qPCR. Results were normalised to *POLII*. N=3 Biological Replicates. One-tailed Student's t-test $p<0.05$ = * $p<0.01$ = ** $p<0.001$ = ***

5.2.3 *DIRC3* inhibits anchorage-independent growth of melanoma cells through positive regulation of *IGFBP5*

The anchorage-independent growth assay more accurately represents the tumour phenotype due to cells being assessed in 3D growth conditions rather than 2D monolayers adhered to a plate. By measuring the ability of cancer cells to survive and proliferate without attaching to a substrate the assay can detect malignant transformation of cells and is predictive of the ability of cells to metastasise. The effect of *DIRC3* depletion on anchorage-independent growth was determined in clonal melanoma cell lines SKmel28, 501mel, and A375. The three cell types were used to identify whether any changes are common amongst melanoma cell lines and not restricted to one cell type. The dCas9-KRAB *DIRC3* knockdown cells were suspended in noble agar for three weeks before the number and size of the colonies formed were semi-quantitatively measured using ImageJ.

Anchorage-independent growth was initially studied in *DIRC3* depleted SKmel28 cells. These showed a significant 2.5-7-fold increase in the number of colonies when there was reduced *DIRC3* (Figure 5.5a). There was no consistent change in the size of colonies (Figure 5.5d). For 501mel cells there was a ~2-fold increase in number of colonies for DIRC3sg1, but no great change for DIRC3sg2 (Figure 5.5b) as well as a slight reduction in the size of colonies (Figure 5.5e). The A375 cells also showed a significant ~5-8-fold increase in number of colonies (Figure 5.5c) and no significant change in sizes of colonies following *DIRC3* depletion (Figure 5.5f). Representative figures for the anchorage-independent growth assays are given in Figure 5.5g.

The 501mel DIRC3sg2 knockdown cells that did not show a significant increase in number of colonies following *DIRC3* depletion (Figure 5.5b) express higher *IGFBP5* than the scrambled controls and DIRC3sg1 knockdowns (Figure 5.1b). The reduced anchorage-independent growth only occurring in cells with such high *IGFPB5* suggest the protein-coding gene participates in regulating this process.

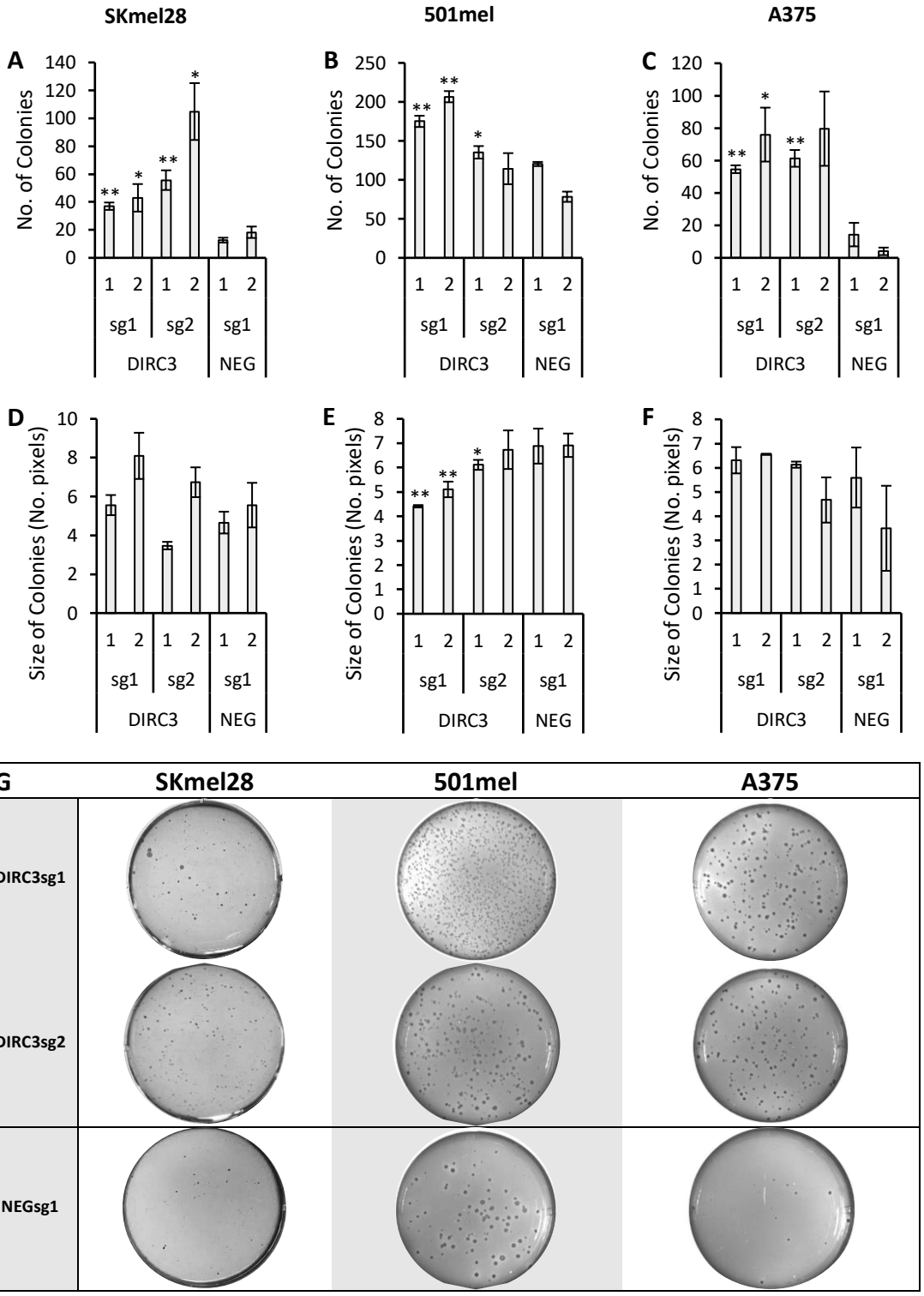

Figure 5.5 *DIRC3* has a tumour suppressive effect on anchorage independent growth. Clonal *DIRC3* loss of function SKmel28 (**i**) 501mel (**ii**) and A375 (**iii**) cells containing the *DIRC3* CRISPRi-KRAB knockdown were grown in soft agar for three weeks. The number (**A**) and size (**B**) of colonies formed were semi-quantified using ImageJ. Representative figures for DIRC3sg1, DIRC3 sg2 and NEGsg1 are given (**C**). Mean ± SE N=3 Biological Replicates. One-tailed Student's t-test $p<0.05$ = *, $p<0.01$ = **

To investigate whether *DIRC3* activation of *IGFBP5* is needed for its tumour suppressive function, the anchorage independent growth assay was repeated in clonal SKmel28 cells containing a CRISPRi knockdown of *IGFBP5* and compared against a scrambled control (NEGsg1). Each knockdown of *IGFBP5* was greater than 90% (Figure 5.6a). Following three weeks of growth, there were significantly more colonies in the *IGFBP5* knockdown cells. In addition, IGFBP5sg1(2) and IGFBP5sg2(2) both showed a significant increase in the average size of colonies that formed (Figure 5.6b,c). Representative figures for the anchorage-independent growth assays are given in Figure 5.6d. The effect of *IGFBP5* knockdown on anchorage-independent growth support the postulation that *DIRC3* regulation of anchorage-independent growth is through its positive regulation of *IGFBP5*.

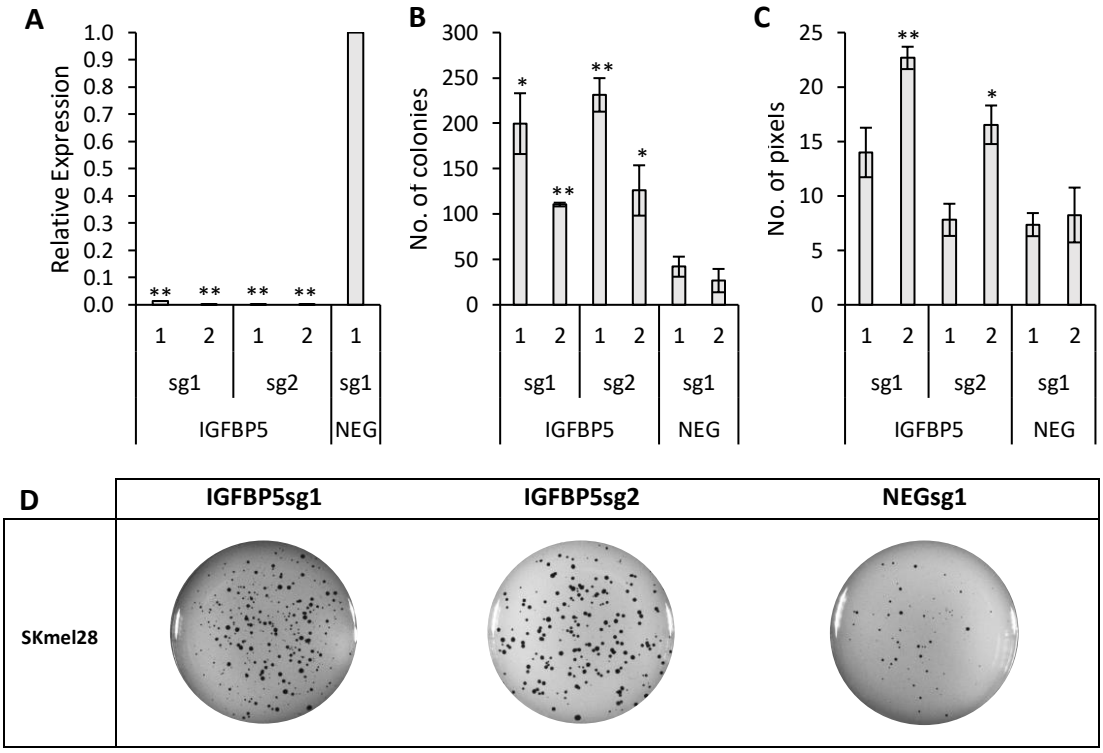

Figure 5.6 *IGFBP5* suppresses anchorage-independent growth in SKmel28 melanoma cells. (**A**) The level of *IGFBP5* in CRISPRi dCas9-KRAB SKmel28 clonal knockdown cells. *IGFBP5* expression was measured using RT-qPCR. Results were normalised to *POLII* and presented relative to expression of an average of NEGsg1. (**B**,**C**,**D**) Clonal SKmel28 cells containing the *IGFBP5* CRISPRi-KRAB knockdown were grown in soft agar for three weeks. The number (**B**) and size (**C**) of colonies formed were semi-quantified using ImageJ. Representative figures for DIRC3sg1, DIRC3 sg2 and NEGsg1 are given (**D**). Mean ± SE N=3 Biological Replicates. One-tailed Student's t-test $p<0.05$ = * $P<0.01$ = **

Overall this data provides strong evidence that *DIRC3* functions as a tumour suppressor by blocking anchorage-independent growth in melanoma cells through its positive regulation of *IGFBP5*. Such an interaction is supported by the identification of numerous cancer-associated genes that are regulated by *DIRC3* in an *IGFBP5*-dependent manner in Chapter 4. As anchorage-independent growth is an indicator of cancer cell ability to metastasise (Mori *et al.* 2009), *DIRC3* may consequently be able to suppress melanoma metastasis. Due to the worse prognosis of patients following cancer metastasis, this would correlate with the earlier finding that melanoma patients expressing higher *DIRC3* typically have longer survival times (Figure 3.5).

5.3 Discussion

DIRC3 suppresses anchorage-independent growth in several melanoma cell lines, suggesting *DIRC3* could play a role in suppressing metastasis of melanoma in patients. *IGFBP5* knockdown phenocopying the suppressed anchorage independent growth seen following *DIRC3* depletion supports the proposal that *DIRC3* positively regulates and works through *IGFBP5* to exert its tumour suppressive function. In addition, it cannot yet be ruled out that *DIRC3* may participate in regulating melanoma cell proliferation and invasion due to the assays used not being representative of the tumour microenvironment.

MITF and SOX10 expression levels regulate the ability of melanoma cells to switch between proliferative and invasive states. Proliferative cells express high levels of MITF and SOX10 while they are reduced in invasive (Hoek and Goding 2010, Verfaillie *et al.* 2015). The negative regulation of *DIRC3* expression by MITF and SOX10 (identified in Chapter 3) means lower expression of *DIRC3* would be expected in proliferative cells and higher in invasive. However, higher *DIRC3* expression was detected in proliferative than invasive cells. In this case, it could be hypothesised that downregulation of *DIRC3* in invasive cells, may allow melanoma progression as cells become metastatic more easily. This would be consistent with the earlier observation that patients expressing lower *DIRC3* have reduced survival compared to those with higher. Individuals expressing higher *DIRC3*, may accordingly find that reduced MITF expression in invasive cells triggers an increase in *DIRC3* leading to reduced ability of cells to metastasise.

The proliferation and invasion assays demonstrated no significant change in SKmel28 following *DIRC3* knockdown under normal cell growth conditions. Despite it being possible to identify alterations in anchorage-independent growth without observing any changes in proliferation and invasion, it is plausible that the assays used do not closely enough represent the tumour environment to elicit an effect by *DIRC3*. Assays that attempt to replicate the *in vivo* environment may alter a cancer cell's

transcriptional state, allowing different genes to be induced or suppressed. LncRNAs may respond to the stressful conditions found in the tumour environment such as hypoxia, immunity evasion, ECM turnover, and angiogenesis. Hypoxia is the result of abnormal vascularisation following growth of tumours (Ackerman and Simon 2014). It has been linked to EMT which allows cells to become more motile before metastasising (Nobre *et al.* 2018). For example, hypoxic conditions stimulate *UCA1* (urothelial carcinoma-associated 1) through inducing hypoxia-inducible factor 1a (HIF-1a) which leads to the promotion of tumour invasion of bladder cancer cell lines *in vitro* (Xue *et al.* 2014). Hypoxia also has an inhibitory effect on *MITF* expression *in vitro* and *in vivo*, leading to growth arrest of the cells (Feige *et al.* 2011). Another feature that may be copied *in vitro* is glutamine starvation. High rates of proliferation mean the nutrient may become depleted in the surrounding tumour environment (Zhang 2017). BRAF inhibitor-resistant melanoma cells can express strong addictions for glutamine (Hernandez-Davies *et al.* 2015). By limiting supplies of glutamine to melanoma cells over prolonged periods, Falletta *et al* (2017) found that *MITF* expression was supressed. This repression of *MITF* was thought to promote cancer cell survival by limiting *MITF*-induced proliferation which would otherwise have a high-nutrient demand on a glutamine supply that was no longer available. The inhibitory effect hypoxia and glutamine starvation have on *MITF* expression could result in *DIRC3* activation. It should be noted that RNA-seq analysis of genes influenced by hypoxic conditions have identified an increase in *DIRC3* expression (Colin Goding, University of Oxford – personal communication). Consequently, adjusting proliferation and invasion assays through methods such as using a hypoxic chamber, generating an oxygen gradient, or inflicting glutamine starvation, could trigger a response in *DIRC3* that would otherwise go unrecognised.

Depletion of *DIRC3* followed by reduced *IGFBP5* in 10 out of the 12 SKmel28, 501mel, and A375 clonal melanoma cells strongly supports the positive regulation of *IGFPB5* by *DIRC3* identified in Chapter 4. The remaining two knockdown cells (501mel) where *IGFBP5* is restored showed the smallest change in anchorage-independent growth compared to scrambled control. Taken together with the finding that *IGFBP5*

knockdown in SKmel28 cells increases anchorage-independent growth, this suggests that *DIRC3* activation of *IGFBP5* mediates its tumour suppressive function. *IGFBP5* has also previously been found to inhibit anchorage-independent growth in A375 melanoma cells (Wang *et al.* 2015) as well as inhibits metastasis in breast cancer and osteosarcoma (Su *et al.* 2011, Sureshbabu *et al.* 2012, Wang *et al.* 2015). It was proposed that *IGFBP5* prevents metastasis by inducing cell adhesion when epithelial cells are exposed to a mesenchymal environment, such as when epithelial–mesenchymal boundaries become compromised during metastasis (Sureshbabu *et al.* 2012). Consequently, *DIRC3* may inhibit melanoma metastasis by promoting expression of *IGFBP5*. In addition, Wang *et al* (2015) found *IGFBP5* expression also inhibits proliferation and invasion in the A375 melanoma cell line, supporting the proposal that *DIRC3* could participate in regulating melanoma cell proliferation and invasion in addition to anchorage-independent growth.

Rescue experiments could also be performed to validate the proposed *DIRC3* tumour suppressive function (Stojic *et al.* 2018). For the soft-agar assays described earlier, re-introduction or overexpression of *DIRC3* should inhibit anchorage-independent growth. CRISPRa can be performed in which a single sgRNA activates transcription of endogenous *DIRC3* through targeting the dCas9 fused to an activating effector domain to the *DIRC3* promoter (Gilbert *et al.* 2014). Also, ectopic expression of *DIRC3* would inform whether the lncRNA is able to execute this function via its transcript targeting locations distal to its locus. However, in either case overexpression requires particular care as low levels of lncRNA expression make it possible to increase expression levels far beyond those biologically possible. Also, intracellular localisation should be preserved (Stojic *et al.* 2018); in this case *DIRC3* expression should predominantly be kept to the nucleus. As well as rescuing *DIRC3* expression, the importance of *DIRC3* regulation of *IGFBP5* for regulation of anchorage-independent growth requires further analysis. To confirm *DIRC3* is working through *IGFBP5*, reintroduction of *IGFBP5* following *DIRC3* knockdown should reduce the level of anchorage-independent growth observed.

Earlier studies have found anchorage-independent growth to indicate cellular transformation *in vitro* as well as predict likelihood of metastasis in patients in a range of cancer types. Mori *et al* (2009) found patients with lung, ovarian, or breast cancer exhibiting anchorage-independent growth signatures displayed worse survival rates. If *DIRC3* is able to repress such metastatic capability by reducing anchorage-independent growth, this could lead to melanoma patients expressing high levels of *DIRC3* displaying significantly increased survival as identified using TCGA clinical data (Figure 3.5). Consequently, *DIRC3* could be a candidate biomarker or therapeutic target. It would also be of interest to determine the level of *DIRC3* expression in patients whose tumours are benign compared to those with highly metastatic in case *DIRC3* is an indicator of tumour stage. Also, its ability to regulate such a key hallmark of cancer means *DIRC3* could potentially be therapeutically targeted so that its expression is activated in the hope this would deter melanoma cells from metastasising.

Chapter 6: *DIRC3* regulates accessibility of SOX10 to potential *IGFBP5* regulatory elements across its locus

6.1 Introduction

Gene expression patterns are precisely regulated through an interplay of transcription- and chromatin modifying- factors at DNA regulatory elements. The act of lncRNA transcription, or lncRNA transcripts, may participate in this process of promoting or repressing expression of target genes (Ernst and Kellis 2010, García-González *et al.* 2016). They can do this by shaping chromosome conformation, regulating ability of regulatory factors to bind to target sites, or allosterically regulating protein functional activity, amongst a range of other activities that may require or be independent of a functional transcript (Briggs *et al.* 2015, Kaikkonen and Adelman 2018, Sun *et al.* 2018).

LncRNAs that have a functional transcript may interact with a multitude of partners to regulate expression of target genes. This includes transcription factors, chromatin-modifying complexes, mRNAs, miRNAs, and DNA (Dykes and Emanueli 2017). LncRNAs can bring proteins together so that they form a functional complex as well as direct them to target genes (Tsai *et al.* 2010, Dykes and Emanueli 2017, Balas and Johnson 2018). In other cases, lncRNAs sequester proteins away from their targets; for example *PANDA* which prevents cell apoptosis by sequestering NF-YA from its targets (Hung *et al.* 2011). A range of lncRNAs have been identified that target modifying complexes to chromatin to either promote or inhibit access to their target sites. This includes *KCNQ1OT1* which represses expression of its targets by recruiting PRC2 and G9a to induce the repressive H3K27me3 and H3K9me3 modifications (Pandey *et al.* 2008). In the case of *SCHLAP1*, the lncRNA impairs function of the SWI/SNF chromatin remodelling complex by preventing SNF5 binding to the genome

(Prensner *et al.* 2013). Another lncRNA, *Evf2*, inhibits ATPase activity and chromatin-remodelling activity of the BRG1 component of the SWI/SNF complex, resulting in reduced chromatin accessibility at target gene enhancers (Cajigas *et al.* 2015). LncRNAs may also participate in regulation of target gene expression by regulating chromatin looping. This activity is commonly induced between promoters and enhancers. LncRNAs may regulate loop formation by associating with the mediator complex, cohesion, or CTCF (CCCTC-binding factor) (Dykes and Emanueli 2017, Kaikkonen and Adelman 2018). In the case of *CCAT1-L* (colon cancer associated transcript 1), the lncRNA interacts with CTCF in order to promote chromatin looping between the *MYC* promoter and its enhancers (Xiang *et al.* 2014).

In other cases, nascent RNA may interact with factors, such as transcription factors and epigenetic regulators, so that they are targeted to actively transcribed regions. Consequently, transcription of the lncRNA can result in increased local concentration of transcription factors as well as encourage activities such as deposition of activating histone marks (Kaneko *et al.* 2014, Kaikkonen and Adelman 2018).

In some instances, the process of lncRNA transcription is sufficient for control of target gene expression without any involvement of the transcript. Numerous lncRNAs harbour DNA regulatory elements within their promoter or gene body, so that the act of lncRNA transcription can be sufficient to regulate target gene expression (Anderson *et al.* 2016, Engreitz *et al.* 2016, Groff *et al.* 2016). In the case of *Uph*, transcription of the lncRNA across an enhancer for its neighbouring gene *Hand2* led to increased *Hand2* expression independent of the lncRNA transcript (Anderson *et al.* 2016). In addition, the presence of RNAPII may prevent or promote transcription factor binding or nucleosome repositioning during transcription and can also make regulatory elements more, or less, accessible (Kornienko *et al.* 2013, Kaikkonen and Adelman 2018, Kopp and Mendell 2018). For *SRG1*, transcription of the lncRNA results in repression of its neighbouring gene *SER3* as it promotes a high density of nucleosomes over its promoter (Hainer *et al.* 2011). Histone modifying enzymes have also been identified that interact with elongating RNAPII (Ng *et al.* 2003, Kaikkonen

and Adelman 2018). Other activities, such as splicing can regulate target gene expression, such as was found for *BLUSTR* which requires lncRNA transcription or splicing, but not transcript, to induce changes in chromatin state and neighbouring gene expression (Engreitz *et al.* 2016).

Information is still limited on how lncRNAs function, so understanding *DIRC3* mechanism of action would build on these general mechanisms currently known for lncRNAs. This would add to the diverse range of activities lncRNAs use in the regulation of gene expression. Understanding the mechanism behind lncRNA functional activity also opens new avenues for more targeted therapeutic intervention to treat disease.

6.1.1 Chapter Summary

DIRC3 is a nuclear lncRNA that activates expression of its adjacent gene *IGFBP5* and induces genome-wide expression programmes involved in cancer. It is not yet clear how *DIRC3* mechanistically regulates expression of *IGFBP5*. Predicted co-occupied binding sites for MITF and SOX10 across the *DIRC3* locus suggest regulatory elements may be present at these locations. Binding of SOX10 is confirmed in SKmel28 cells for three out of its four binding sites previously identified using ChIP-seq in 501mel cells. *DIRC3* depletion leads to increased SOX10 binding and a more open chromatin state (indicated by an increased presence of H3K27ac). This suggests *DIRC3* controls accessibility of SOX10 to binding sites across its locus. Chromosomal looping may also occur between the proposed regulatory elements within the *DIRC3* locus and the *IGFBP5* promoter, and reduced SOX10 and MITF induces an increase in *IGFBP5*, suggesting SOX10 and MITF may participate in regulation of *IGFBP5* expression. If *DIRC3* is able to regulate MITF and SOX10 transcriptional response, it could represent a mechanistic model for the 245 melanoma-expressed lncRNAs identified containing the putative MITF-SOX10 co-bound sites as well as other lncRNAs that overlap regulatory elements for other transcription factors.

6.2 Results

6.2.1 SOX10 binding across the *DIRC3* locus is repressed by *DIRC3* expression.

DIRC3 expression is negatively regulated by MITF and SOX10. However, the presence of MITF-SOX10 co-occupied binding sites across the *DIRC3* locus suggest *DIRC3* may regulate their ability to bind at these sites. The binding sites of MITF and SOX10 were originally identified using ChIP-seq of 501mel melanoma cells (Figure 6.1a)(Laurette *et al.* 2015). To confirm whether SOX10 binds to these sites in SKmel28 cells, ChIP-qPCR using an anti-SOX10 antibody was performed. *DIRC3* regulation of transcription factor binding was focussed on SOX10 as there were no antibodies that could efficiently immunoprecipitate endogenous MITF using ChIP. *DIRC3* was also knocked down using dCas9-KRAB to observe whether a reduction in *DIRC3* transcription and transcript influenced the ability of SOX10 to bind. The level of SOX10 binding in *DIRC3* depleted cells (DIRC3sg1, DIRC3sg2) was compared against those transfected with a scrambled control (NEGsg1). To ensure detected proteins were above background, the level of immunoprecipitation was compared against control regions not known to be targeted by SOX10. Immunoglobin G (IgG) was used as an isotype control to account for non-specific binding of proteins to the antibodies. In addition, clonal populations of SKmel28 containing the *DIRC3* knockdown were used due to the large number of cells required to perform ChIP-qPCR.

The results showed high levels of SOX10 binding at the predicted binding sites 1-3 compared to control regions. *DIRC3* depletion also led to an increase in SOX10 chromatin binding (Figure 6.1b). The presence of SOX10 at binding sites 1-3 in SKmel28 verifies their identification by ChIP-seq in 501mel cells. The reduction in SOX10 binding following depletion of *DIRC3* using CRISPRi could be the result of a functional *DIRC3* transcript targeting SOX10 activity directly. Alternatively, the *DIRC3* transcription and/or transcript could induce a more closed chromatin state which prevents SOX10 binding. Ultimately, the increased binding of SOX10 following

reduced *DIRC3* indicates the ability of *DIRC3* to regulate SOX10 transcriptional activity.

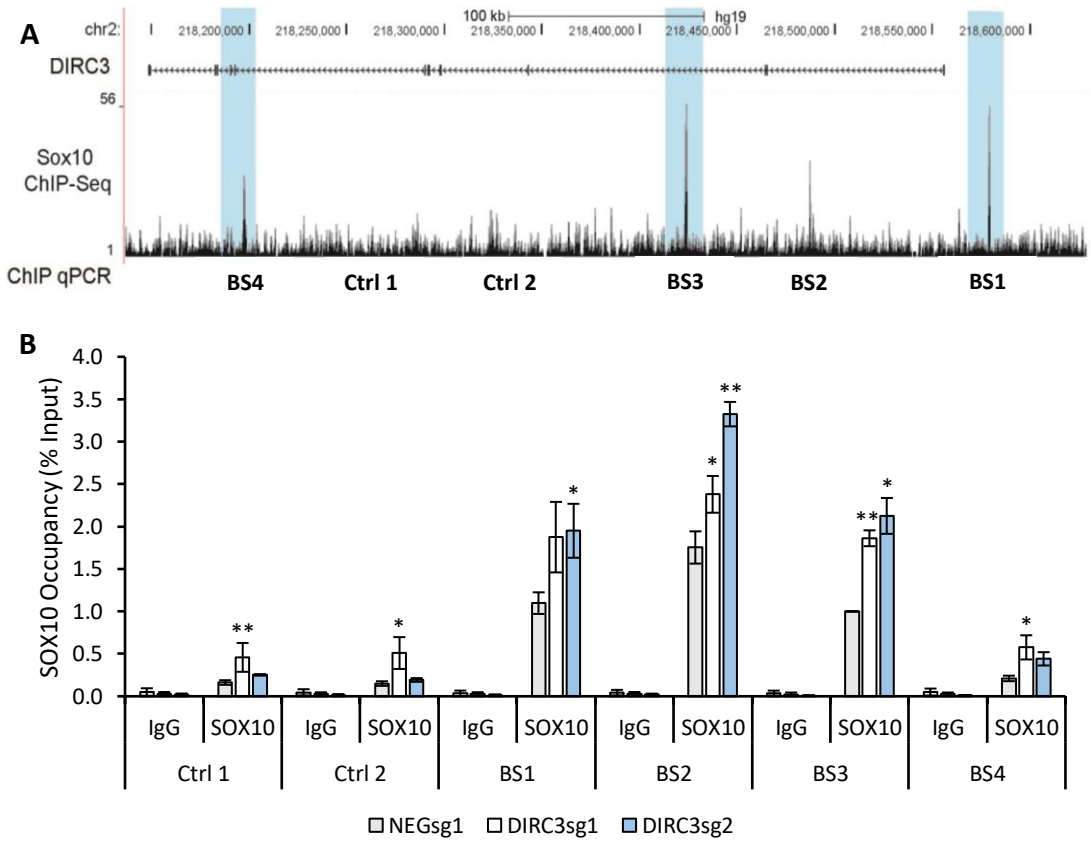

Figure 6.1 *DIRC3* suppresses SOX10 binding across its locus. (**A**) UCSC Genome Browser (GRCh37/hg19) view of predicted binding sites across the *DIRC3* locus in 501mel cells (Laurette *et al.* 2015). BS – binding site. The blue bands indicate regions where there are sites of MITF-SOX10 co-occupancy. (Figure generated from http://genome.ucsc.edu) (**B**) Levels of SOX10 binding in SKmel28 clonal CRISPRi-KRAB DIRC3sg1, DIRC3sg2, and NEGsg1 cells were identified using ChIP-qPCR. An IgG antibody was used as an isotype control for non-specific binding of proteins. The indicated SOX10 binding sites were analysed by qPCR. Percent input was calculated as 100*2^(Ct Input-Ct IP). Data presented relative to NEGsg1 BS3. Mean ± SE N=3 Biological Replicates. One-tailed Student's t-test $p<0.05$ = * $P<0.01$ **

To confirm the changes in SOX10 binding were not a result of changes in expression following *DIRC3* knockdown using dCas9-KRAB, SOX10 protein levels were checked. Following confirmation of *DIRC3* knockdown using RT-qPCR (Figure 6.2a), level of SOX10 expression was measured using Western blotting. Level of SOX10 protein remained consistent between knockdowns and scrambled controls (Figure 6.2b).

Consequently, changes in SOX10 binding observed were the result of *DIRC3* regulating its accessibility to the binding sites.

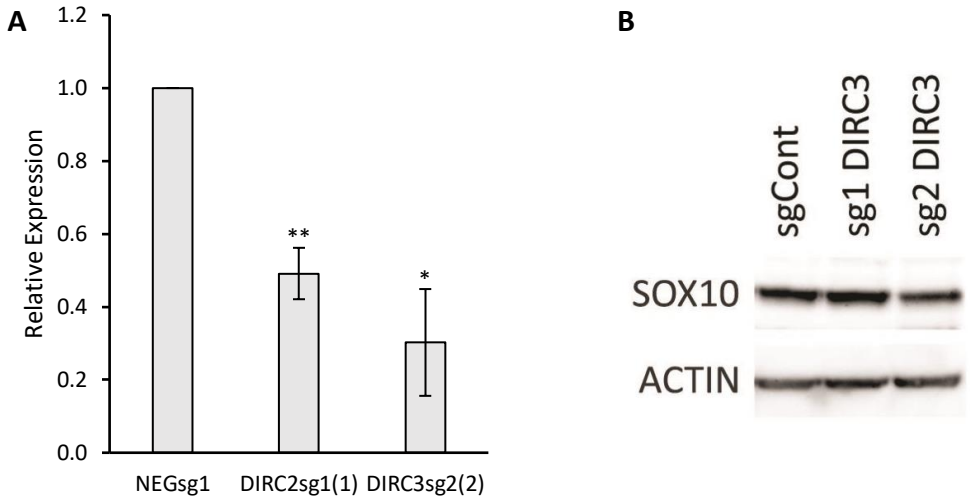

Figure 6.2 SKmel28 clonal CRISPRi knockdown cells contained reduced *DIRC3* but no significant change in SOX10. (**A**) Clonal SKmel28 containing *DIRC3* CRISPRi knockdown had their level of *DIRC3* expression confirmed using RT-qPCR. Results were normalised to *POLII* and presented relative to expression of NEGsg1. Mean ± SE N=3 Biological Replicates. One-tailed Student's t-test p<0.05 = * P<0.01 **. (**B**) Level of SOX10 expression was confirmed using Western blotting. Equal concentrations of extracted protein were confirmed using ACTIN as a control.

6.2.2 Reduced *DIRC3* expression induces a histone modification signature suggestive of an active chromatin state.

The ability of *DIRC3* to block SOX10 binding to sites across its locus suggest *DIRC3* is able to modulate chromatin accessibility. Histone modifications are a key regulator of chromatin accessibility, so can be used to identify transcriptional regulatory regions of DNA. Commonly recognised modifications include histone H3 lysine 27 acetylation (H3K27ac), and histone H3 lysine 27 methylation/trimethylation (H3K4me1/3). These signatures can be used to identify positions of regulatory sequences, such as enhancers, in the genome. Different combinations of acetylation and methylation inform whether sequences are active (H3K27ac and H3K4me1 positive), or poised (H3K27ac negative, H3K4me1 positive). In the case of H3K4me1 to H3K4me3 ratios, high me1:me3 is indicative of enhancers while high me3:me1

suggests the presence of promoters (Creyghton *et al.* 2010, Spicuglia and Vanhille 2012, Fufa *et al.* 2015).

Histone modifications H3K27ac, H3K4me1 and H3K4me3 were explored across the *DIRC3* locus using ChIP-seq data from (Fiziev *et al.* 2017)(Figure 6.3a). The local peaks of increased H3K27ac and H3K4me1, and low H3K4me3 across the locus suggest there are active enhancer-like regions within the *DIRC3* locus. To determine whether *DIRC3* regulates chromatin accessibility within its locus, the H3K27ac signature was measured at SOX10-bound sequences in cells containing a *DIRC3* dCas9-KRAB knockdown compared against a scrambled control. Consistent with the predicted open chromatin signature and binding identified for SOX10 across the *DIRC3* locus, binding sites 1-3 were found to be most enriched for H3K27ac (Figure 6.3b). Following *DIRC3* knockdown there was typically an increase in the presence H3K27ac – this is significant for DIRC3sg2 cells at binding sites 1 and 2. The prediction of chromatin signatures indicate there could be active enhancer-like regulatory elements within the *DIRC3* locus. The confirmation of H3K27ac binding at sites 1-3 is consistent with the pattern for SOX10 binding and reveal a more accessible region to SOX10. The increase in H3K27ac following *DIRC3* depletion also suggest there is a more closed chromatin state when the lncRNA is present. Consequently, *DIRC3* may be able to act locally at its site of expression to modulate chromatin conformation and so control the ability of SOX10 to occupy regulatory elements across its locus.

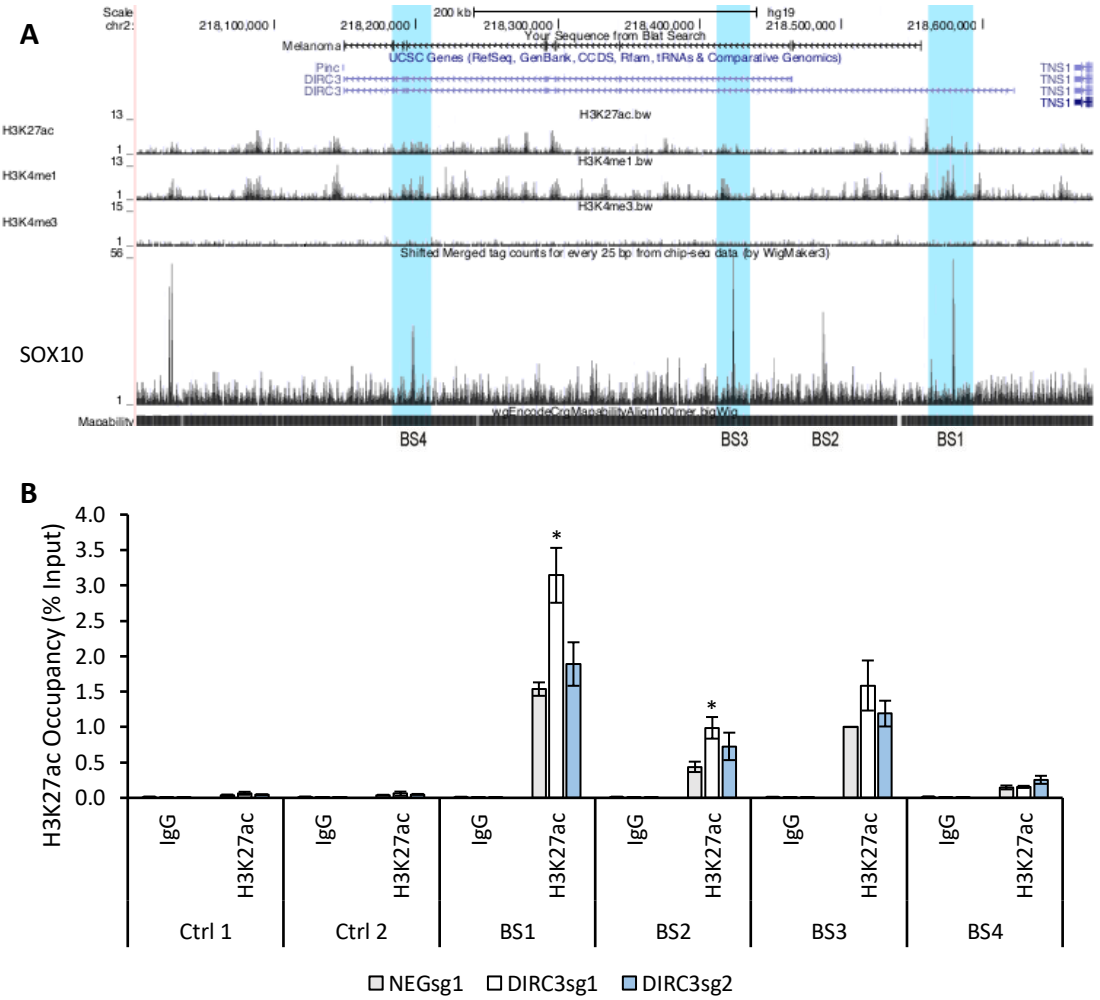

Figure 6.3 Reduced *DIRC3* expression induces an open chromatin state. (**A**) Predicted H3K27 acetylation and H3K4 methylation/trimethylation across the *DIRC3* locus (Fiziev *et al.* 2017). The blue bands indicate regions where there are sites of MITF-SOX10 co-occupancy. (Figure generated from UCSC Genome Browser (GRCh37/hg19) http://genome.ucsc.edu) (**B**) ChIP-qPCR for H3K27ac show the level of binding across SOX10 binding sites at binding sites 1-4. An IgG antibody was used as an isoform control for non-specific binding of proteins. The indicated binding sites were analysed by qPCR. Percent input was calculated as 100*2^(Ct Input-Ct IP). Data presented relative to NEGsg1 Peak 3 Mean ± SE N=3 Biological Replicates. One-tailed Student's t-test p<0.05 = * P<0.01 **

The identification of SOX10 binding and active histone modifications at several sites across the *DIRC3* locus suggest there are regulatory elements, such as enhancers, present that *DIRC3* is able to regulate SOX10 accessibility to. The interplay of *DIRC3* regulating SOX10 binding, and SOX10 repressing *DIRC3* expression in SKmel28 cells (described earlier in Figure 3.7), may allow fine control of the SOX10 binding sites

across the *DIRC3* locus. Consequently, *DIRC3* may participate in the SOX10 transcriptional response.

6.2.3 DNA looping may occur between SOX10 binding sites across the *DIRC3* locus and *IGFBP5*

Due to *DIRC3* being able to act locally to regulate expression of its neighbouring gene, the chromatin structure of the *IGFPB5-DIRC3-TNS1* gene territory was mapped using Hi-C data from normal human epidermal keratinocytes (NHEK) (Rao *et al.*, 2014). A HiC heatmap was generated by Yihong Jennifer Tan (University of Lausanne) using JuiceBox (Durand *et al.* 2016). By revealing the presence of topologically associated domains (TADs) and DNA looping, the mechanism by which *DIRC3* regulates *IGFBP5* may be better understood.

A TAD was identified that contains both *DIRC3* and *IGFBP5*, but not *TNS1* (Figure 6.4). Within this TAD, two potential DNA looping interactions were identified between the promoter of *IGFBP5* and the MITF-SOX10 bound sequences within the *DIRC3* locus. The presence of a TAD region surrounding *DIRC3* and *IGFBP5* but not *TNS1* supports the earlier finding that *DIRC3* does not regulate *TNS1* despite it being closer in the linear sequence. The identification of potential looping interactions between MITF-SOX10 binding sites and the *IGFBP5* promoter region also suggest that the two oncogenes regulate *IGFBP5* expression by interacting with regulatory elements for the tumour suppressor within the *DIRC3* locus. Regulatory elements, such as promoters and enhancers, preferentially form contacts with each other when found within the same TAD (Dixon *et al.* 2012, Hansen *et al.* 2018). Although the TADs and looping regions were identified in NHEK cells, such domains are highly conserved across different cell types, so such sites are likely to be present in the melanoma cells used in this project (Dixon *et al.* 2012).

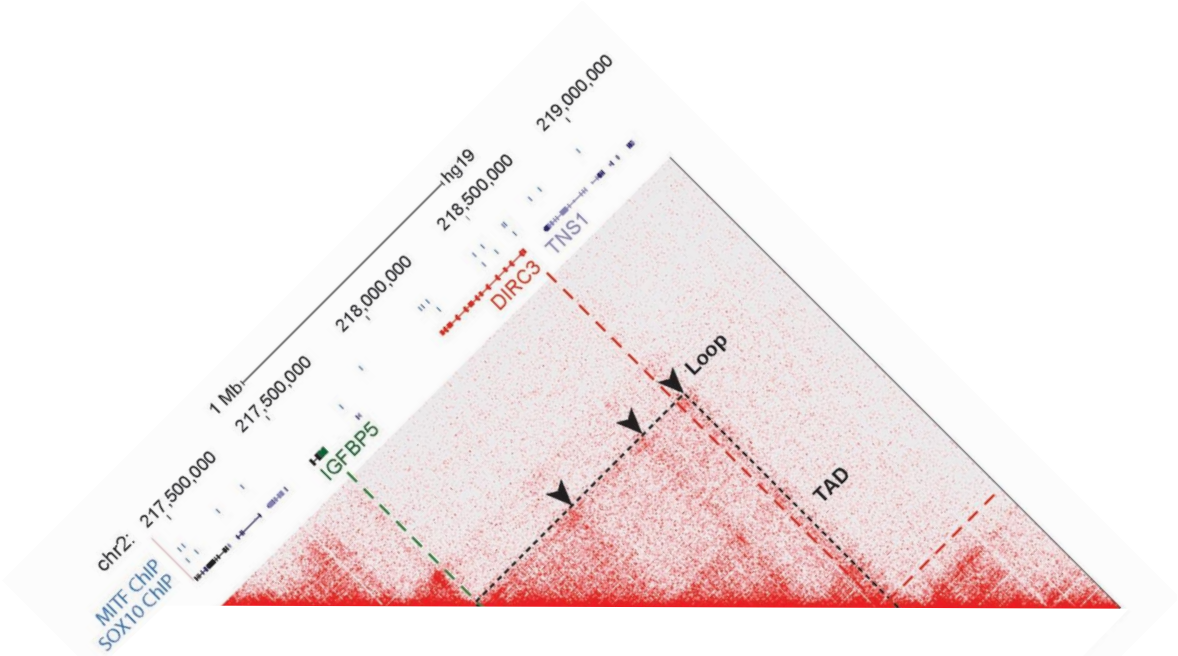

Figure 6.4 *IGFBP5* may directly interact with the *DIRC3* locus via chromosomal looping. Chromosomal interactions identified using Hi-C presented as a heatmap for the regions surrounding *DIRC3* (red), *IGFBP5* (green) and *TSN1* (purple) (Rao *et al.* 2014, Durand *et al.* 2016). Gene browser view given for NHEK (chr2: 217,500,000-219,000,000). The TAD is represented by the dotted black square box and encompasses both *DIRC3* and *IGFBP5*. Chromosomal loops are identified by black arrows. The MITF and SOX10 binding sites are presented as blue boxes. Analysis performed by Yihong Jennifer Tan (University of Lausanne).

6.2.4 SOX10 and MITF negatively regulate expression of *IGFBP5*

The presence of DNA looping between the *IGFPB5* promoter and sequences close to MITF-SOX10 binding sites within the *DIRC3* locus suggest MITF and SOX10 participate in regulation of *IGFBP5* expression. The effect of MITF and SOX10 knockdown on *IGFBP5* expression was tested in melanoma cell lines. *MITF* and *SOX10* siRNA and esiRNA knockdowns, respectively, were performed in SKmel28 cells and changes in *IGFBP5* expression were measured using RT-qPCR.

Following reduced *MITF* expression there was a 41-70% increase in *IGFBP5* expression in (Figure 6.5a). Reduced *SOX10* expression also resulted in an increase in *IGFBP5* (Figure 6.5b). This suggests expression of MITF and SOX10 is important in the regulation of *IGFBP5* expression. However, it does not reveal whether the negative regulation is through MITF and SOX10 interacting with the binding sites across the *DIRC3* locus or is through their negative regulation of *DIRC3*.

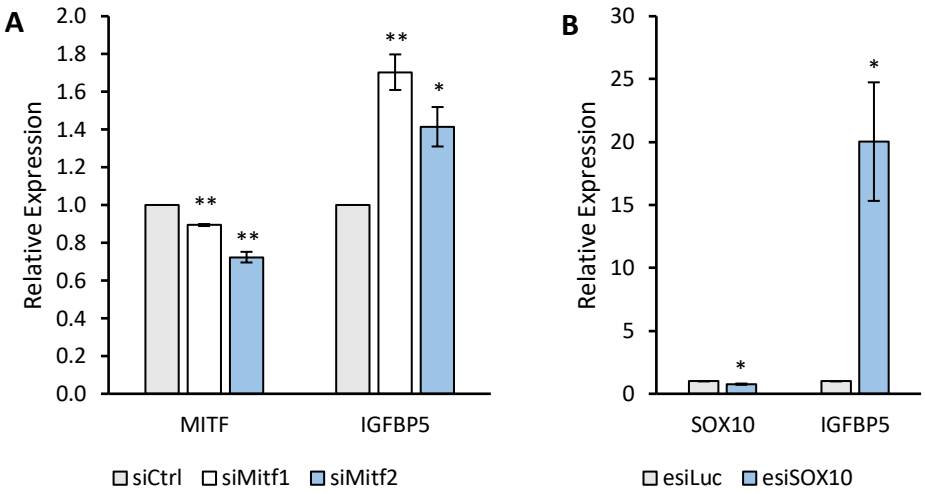

Figure 6.5 Decreased MITF and SOX10 expression leads to an increase in *IGFBP5*. SKmel28 cells were transfected with siRNA/esiRNA targeting *MITF* and *SOX10* respectively and non-targeting controls (siCtrl/esiLuc). Three days following transfection, the efficiency of knockdown for (**A**) *MITF* and (**B**) *SOX10* and corresponding level of *IGFBP5* expression were measured using RT-qPCR. Results were normalised to *POLII* and presented relative to expression in the siCtrl. Mean ± SE N=3 Biological Replicates. One-tailed Student's t-test $p<0.05$ = * $P<0.01$ **

The predicted interaction between MITF-SOX10 and *IGFBP5* suggests the oncogenes bind to *IGFBP5* regulatory elements within the *DIRC3* locus to negatively regulate expression of *IGFBP5*. It could also be that *DIRC3* acts to suppress their inhibition of *IGFBP5* by blocking accessibility to regulatory elements across its locus in a feedback loop allowing fine control of *IGFBP5* expression.

6.3 Discussion

The ability of *DIRC3* to block SOX10 binding across its locus is demonstrated by increased SOX10 binding at sites 1-3 following *DIRC3* depletion in SKmel28 cells. This inhibition may be through *DIRC3* inducing a more closed chromatin state, as suggested by the increased H3K27ac identified in *DIRC3* depleted cells. Inhibition of SOX10 binding may prevent the transcription factor from inhibiting expression of the tumour suppressor *IGFBP5* via regulatory elements within the *DIRC3* locus. Based on the reduced H3K4me3 modification predicted to be present, the regulatory elements may be enhancers for *IGFBP5*. Consequently, *DIRC3* may permit precise control of *IGFBP5* expression via feedback control of SOX10.

Regulation of enhancers by lncRNAs has been described for other lncRNAs. In the case of *Uph*, the lncRNA contains a super-enhancer for *Hand2* within its locus. Transcription of *Uph* promotes the presence of H3K4me1 and H3K27ac epigenetic marks across this enhancer, leading to increased expression of *Hand2*. However, for *Uph*, knockdown using ASOs, and overexpression of the transcript, did not alter expression of *Hand2* mRNA, suggesting the transcript itself is non-functional (Anderson *et al.* 2016). Also, in the case of *DIRC3*, access to the enhancer-like regulatory elements appears to be blocked following the induction of a closed chromatin state.

The prediction that SOX10 binds to regulatory elements within the *DIRC3* locus could be checked by investigating the presence of additional chromatin modifications using ChIP-qPCR. The level of H3 lysine for monomethylation and trimethylation (H3K4me1/3) can be used to assess presence of promoters or enhancers. The signature H3 lysine 27 trimethylation (H3K27me3) is also indicative of the condensed chromatin state so could be used to confirm whether there is a less repressive chromatin state following decreased *DIRC3* expression (García-González *et al.* 2016).

Using CRISPRi for lncRNA knockdown means it is yet to be revealed whether *DIRC3* regulation of SOX10 binding is through a transcript-dependent or -independent method. To see whether the transcript is involved in these local changes, ASO knockdown of *DIRC3* could be performed prior to ChIP analysis. If the same patterns of expression are observed, it is likely the transcript is involved in regulating accessibility of SOX10 to the proposed binding sites across the *DIRC3* locus.

The presence of MITF-SOX10 binding sites, H3K27ac, and predicted chromosomal looping using Hi-C are all suggestive of the presence of DNA elements important for the regulation of *IGFBP5* expression. It could be the case that *DIRC3* transcription across these regulatory elements is what controls *IGFBP5* expression. Using CRISPR, each predicted regulatory element may be removed and the effect on *IGFBP5* expression measured by RT-qPCR (Gilbert *et al.* 2013). Since the majority of the binding sites are within intronic regions of *DIRC3*, it should not perturb activity of the lncRNA transcript. If removal of the sequences alters *IGFBP5* expression, it would also be possible to identify whether they have a typically inhibitory or promoting effect on expression of the tumour suppressor.

The Hi-C data combined with knockdown of MITF and SOX10 suggest these key melanoma regulators may repress *IGFBP5* expression by binding likely regulatory elements for *IGFBP5* within the *DIRC3* locus. During chromosomal looping, target sequences are brought into closer proximity with a high concentration of transcription factors and cofactors important for regulation of transcription (García-González *et al.* 2016). Chromosomal looping is typically restricted to TADs which regulate the spread of interactions between DNA elements (Dixon *et al.* 2012, Rodríguez-Carballo *et al.* 2017), and frequently occurs between enhancers and their target promoters (Hansen *et al.* 2018). Chromosome conformation capture (3C) may be performed to verify whether chromosomal looping occurs between the putative regulatory elements within the *DIRC3* locus and *IGFBP5* (Han *et al.* 2018). Predicted interactions between the DNA regions, as well as lncRNA, may also be confirmed using a combination of RNA- and DNA-fluorescent in situ hybridisation (FISH) to

visualise spatial distributions of the targets. To see whether *DIRC3* is important for looping formation, 3C or FISH could be repeated following *DIRC3* knockdown. Again, using a mixture of transcription- and transcript-targeting knockdown methods, it would be possible to identify whether processes dependent or independent of a functional transcript are required.

Together these data give an insight into how *DIRC3* may act locally to activate *IGFBP5* expression by blocking binding of SOX10 (and possibly MITF) to putative regulatory elements across its locus. Such a mechanism may be representative of MITF-SOX10 bound intergenic lncRNAs ability to control MITF-SOX10 transcriptional response in melanoma by modifying chromatin and blocking their binding at regulatory elements.

Chapter 7: General Discussion

7.1 *DIRC3* is a functional tumour suppressive lncRNA in melanoma

It is now clear that *DIRC3* is a tumour suppressive intergenic lncRNA that blocks anchorage-independent growth in melanoma cells, likely through its positive regulation of *IGFBP5*. *IGFBP5* has already been identified as an important tumour suppressor in a range of cancers including melanoma, regulating proliferation, invasion, and anchorage-independent growth, as well as being indicative of patient survival (Su *et al.* 2011, Sureshbabu *et al.* 2012, Wang *et al.* 2015). *DIRC3* regulation of *IGFBP5* may also play an important role in its manipulation of genes distal to its locus. As well as having its expression regulated by MITF and SOX10, *DIRC3* is able to control SOX10 (and so inferably MITF) binding across its locus through modulating chromatin accessibility. Thus, *DIRC3* has the potential to modify the MITF-SOX10 transcriptional response in melanoma. These findings demonstrate that *DIRC3* is not simply a downstream mediator of MITF-SOX10 activity, but also a feedback regulator. As numerous other intergenic lncRNAs have been identified with MITF-SOX10 co-bound sites, *DIRC3* regulation of SOX10 (and MITF) may be representative of a general activity amongst intergenic lncRNAs which could form part of a new class of melanoma regulator.

7.2 *DIRC3* mechanism of action

By combining knockdown and ChIP-qPCR data a picture of the likely mechanism of action for *DIRC3* has begun to form. With a focus on local activity, expression of *DIRC3* promotes transcription of *IGFBP5* as well as blocks binding of SOX10 to putative regulatory elements across its locus by inducing a repressive chromatin state. The presence of MITF-SOX10 co-occupancy and H3K27ac signature at sites across the *DIRC3* locus suggest these sequences are important in transcriptional regulation, likely behaving as enhancers or silencers of *IGFBP5*. It is also well recognised that

chromatin looping commonly occurs between enhancers and promoters (Mora *et al.* 2015) so the proposed regulatory elements within these regions may also interact with *IGFBP5* through chromosomal looping. In addition, SOX10 (and MITF) inhibition of *DIRC3* expression may allow them to access binding sites across the *DIRC3* locus.

Accordingly, it could be the case that when *DIRC3* is repressed, regulatory elements within its locus are targeted by SOX10 (and MITF), possibly promoting or inhibiting looping between them and the promoter of *IGFBP5*, leading to inhibition of its expression (Figure 7.1a). However, increased *DIRC3* expression reduces acetylation and prevents binding of SOX10 (and MITF) to the regulatory elements so that *IGFBP5* may then be expressed (Figure 7.1b).

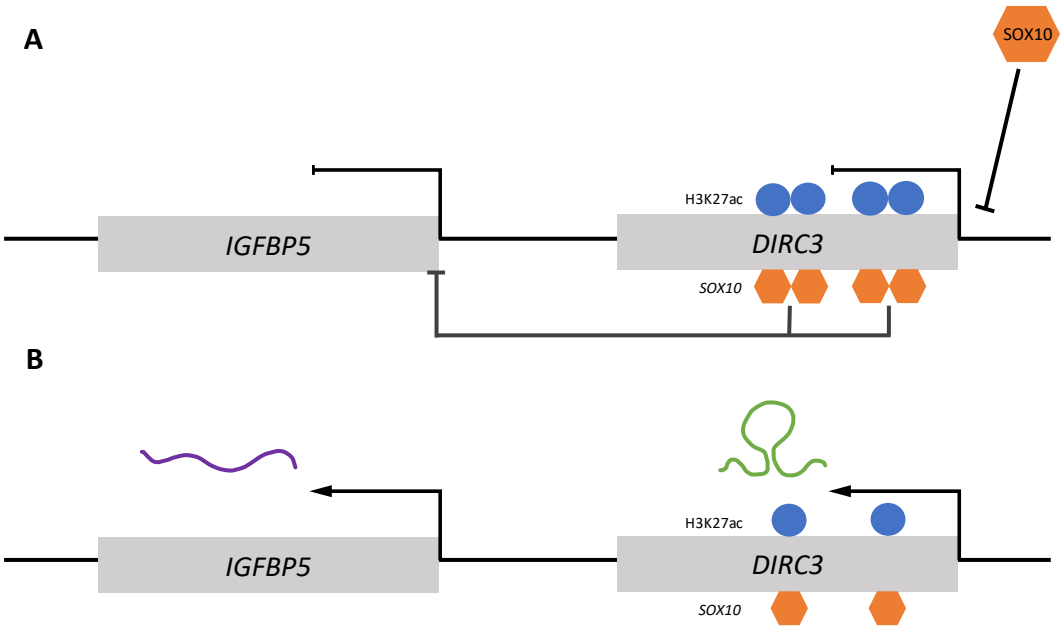

Figure 7.1 Proposed model of *DIRC3* mechanism of action. The model illustrates how *DIRC3* could function at its locus. (**A**) SOX10 suppresses *DIRC3* activity allowing increased SOX10 binding and deposition of H3K27ac. This results in repression of *IGFBP5* expression. (**B**) When *DIRC3* is expressed, there is reduced SOX10 binding and reduced H3K27ac, resulting in *IGFBP5* activation. Orange hexagon – SOX10; Blue circle – H3K27ac mark; Green line – *DIRC3*; Purple line – *IGFBP5*

7.2.1 Proposed activities of a functional *DIRC3* transcript

If confident that the transcript plays a key role mediating *DIRC3's* regulation of MITF-SOX10 and *IGFBP5* activity, the identification of factors it interacts with is key to understanding further its mechanism of action. LncRNA transcripts can interact with proteins or RNAs to modulate their function or binding.

Functional lncRNA transcripts may regulate gene expression by sequestering RNA-binding proteins and transcription factors away from their targets (Morriss and Cooper 2017), such as in the cases of *GAS5* and *PANDA* (Kino *et al.* 2010, Hung *et al.* 2011). Consequently, the reduced SOX10 binding with greater levels of *DIRC3* could suggest that the lncRNA transcript sequesters SOX10 away from the binding sites across the *DIRC3* locus. It could also be the case that *DIRC3* sequesters BRG1, the binding partner of MITF and SOX10 also found at active melanoma regulatory elements (Laurette *et al.* 2015). In the case of *SLNCR* it has been recognised that the lncRNA could switch the activity of a target protein from activating to repressing. *SLNCR* changed EGR1-mediated transcriptional activation of $p21^{Waf1/Cip1}$ to a repressive activity by recruiting AR to chromatin-bound EGR1 (Schmidt *et al.* 2019). This could also be the case for *DIRC3*, with it altering the activity of its associated protein factors, such as SOX10 or BRG1.

A functional *DIRC3* transcript could also guide chromatin modifiers to its locus or sequester them from their sites. Such proteins are typically not able to directly interact with DNA and so require the binding site specificity of factors such as transcription factors and lncRNAs to guide them to desired locations. *DIRC3* could consequently recruit repressive chromatin modifiers to its locus. For example, *PARTICLE,* a shown for functional transcript, interacts with the silencing complexes G9A and PRC2 leading to repression of the tumour suppressors *MAT2A* and *WWOX* through inducing the histone H3K27me3 modification (O'Leary *et al.* 2015, 2017). *DIRC3* could also inhibit the activity of chromatin-modifying factors in a manner similar to *Evf2* which inhibits ATPase activity of the chromatin re-modeller BRG1 so

that it is unable to create a more open (activating) environment for target enhancers (Cajigas *et al.* 2015).

In some cases, lncRNAs can interact with proteins such as Mediator, cohesion and CCCTC-binding factor (CTCF) to promote the looping of DNA sequences (e.g. promoters and enhancers) together. For example, *Wrap53* has been proposed to induce chromatin looping by interacting with CTCF during regulation of p53 expression (Saldaña-Meyer *et al.* 2014). Consequently, chromosomal looping could be regulated by *DIRC3*. If *DIRC3* interacts with one of the aforementioned proteins, it could promote or inhibit chromosomal looping between the regulatory elements present within its locus and the *IGFBP5* promoter.

It is not yet clear which proteins *DIRC3* interacts with, if any. For predicted protein targets such as MITF and SOX10, RIP coupled with RT-qPCR may be performed to confirm whether the lncRNA transcript interacts with them. When identifying unknown interacting protein partners care must be taken if native methods are used. Techniques that do not involve crosslinking frequently pick up false-positive interactions. One chromatin modifier frequently found to bind non-specifically in vitro is PRC2 (Davidovich *et al.* 2015). Consequently, CHART and RNA-antisense purification (RAP) could be used to detect endogenous RNA interactions with proteins (or DNA) in a crosslinked chromatin extract. By combining these RNA-pull down methods with mass-spectrometry, it is possible to identify novel proteins the *DIRC3* transcript interacts with.

Once likely interacting protein targets are identified, confirmation of functional activity could be studied by sterically blocking their interaction with *DIRC3*. This could be performed using LNAs in a manner similar to antagomirs - targeting the *DIRC3* sequence so that they block proteins from interacting (Tsai *et al.* 2011). By measuring features such as expression of *IGFBP5*, binding of SOX10, or the level of anchorage-independent growth, it would be possible to see whether the interaction plays a functional role.

7.2.2 Proposed activities of *DIRC3* function independent of transcript

The results do not rule out the possibility that *DIRC3* is able to function independently of its transcript. Accordingly, activities such as the act of *DIRC3* transcription or splicing could recruit factors key for the regulation of *IGFBP5* expression without the need of a functional transcript.

The process of intergenic lncRNA transcription across a DNA regulatory sequence can regulate target gene expression. Such as in the cases of *Uph*, *Airn*, and *Blustr* (Latos *et al.* 2012, Anderson *et al.* 2016, Engreitz *et al.* 2016). Using CRISPR the predicted regulatory elements could be removed or mutated so that the effects of their absence on *IGFBP5* expression can be observed. The sites that would be targeted do not lie within exons of *DIRC3* so their removal should not influence *DIRC3* transcript-dependent activity.

Splicing has also been found to regulate expression of target genes. In the case of *BLUSTR*, splicing at its 5' splice site is important for activating transcription of *Sfmbt2* through the interaction between the spliceosome and nascent transcript. Splicing can also influence methylation patterns (H3K4me3 and H3K27me3) and RNAPII occupancy (Engreitz *et al.* 2016). Whether *DIRC3* regulates *IGFBP5* through splicing could be identified by knocking out predicted splice sites using CRISPR.

The process of transcription can also alter nucleosome density (Valouev *et al.* 2011). It has been proposed that transcription can induce rearrangement of nucleosomes into positions that either promote or inhibit accessibility to regulatory elements within the lncRNA loci. Re-deposition of nucleosomes can alter their density so that conditions are favourable or unfavourable for transcription factors to bind target regulatory elements (Kornienko *et al.* 2013, Kaikkonen and Adelman 2018). Changes to nucleosome density may be measured using nucleosome density ChIP-seq (ndChIP-seq) and measuring MNase accessibility to open regions of chromatin

(Lorzadeh *et al.* 2016). Nucleosome density could be measured following blocking *DIRC3* transcription using methods such as CRISPRi or insertion of PolyA signals to see whether it increases or decreases following reduced *DIRC3* transcription.

7.3 Understanding the tumour suppressive role of *DIRC3* in melanoma *in vivo*

DIRC3 suppression of anchorage-independent growth *in vitro* combined with the increased survival identified in melanoma patients with greater *DIRC3* expression make this lncRNA a candidate for further study *in vivo*.

Xenografting cultured human cells into immunocompromised mice (*Mus musculus*) is commonly used for testing disease mechanisms and model therapies *in vivo*. The implanted cells can adhere, grow and eventually metastasise. By injecting cells containing stable *DIRC3* knockdown into mice, it would be possible to observe the cellular response within a model organism (Kuzu *et al.* 2015, Aktary *et al.* 2018). Using this model, the effect of *DIRC3* knockdown on primary tumour growth and its ability to metastasise can be observed, although this is limited by the lack of immune response in the mice (Aktary *et al.* 2018). Since anchorage-independent growth *in vitro* has previously been indicative of metastatic ability *in vivo*, it could be predicted that *DIRC3* expression negatively regulates metastasis *in vivo* (Mori *et al.* 2009).

While immortalised cancer cell lines are useful for performing mouse xenograft experiments, there is still the issue that the longer these cells are maintained in culture, the more they will differ from the original tumour. Instead, analysis of *DIRC3* knockdown in patient derived xenografts (PDXs) may be performed. In this case cells directly from human tumours are obtained from patients following surgery or biopsy and transplanted into mice. This can be under the skin, in the same organ as the sample was obtained, or in the renal capsule of immunocompromised mice (Yada *et al.* 2017). To analyse gene depletion, transplanted tumours are removed from the mice and the target gene knocked down before being re-transplanted into mice to see whether tumour growth is affected (Aktary *et al.* 2018). PDXs are proposed to

better model human disease. Morphological cellular and structural characteristics are well preserved in PDXs for numerous cancers (Ben-David *et al.* 2017, Yada *et al.* 2017). PDXs also have greater heterogeneity, so are more representative of tumours than immortalised cell lines. In addition, when PDXs were used from a breast cancer patient, although poorly metastatic, those metastases observed were predominantly the same as those in the patient's original cancer (Derose *et al.* 2011).

A small number of lncRNAs have been studied using PDXs in mouse models. The therapeutic potential of targeting *SAMMSON* using LNA GapmeRs in combination with the $BRAF^{V600E}$ inhibitor dabrafenib was assessed in two PDX melanoma models. The work demonstrated the efficiency of combining treatments and that targeting lncRNAs can enhance response to current therapies (Leucci, Vendramin, *et al.* 2016). Using either xenograft model, it would be possible to explore *DIRC3* participation in primary tumour growth, metastases, as well as possible responses to therapies. This would highlight the clinical importance of *DIRC3* and is necessary for the design of *DIRC3* targeting therapies for melanoma.

An orthologous *DIRC3* gene is present in mice in a syntenic location (Figure 3.4b). Consequently, it would be possible to knockout *DIRC3* expression in the embryo to determine whether its locus directly contributes to a genetic susceptibility to melanoma by observing changes in the animals' susceptibility to and development of cancer. Using such models mean that the effect of knockout on tumour growth can be explored without the need for the organism to be immunocompromised. Knockout mice have previously been used for the study of *NEAT1* in skin cancer. Silencing the lncRNA impaired growth of skin tumours as preneoplastic cell became more sensitised to DNA-damage-induced cell death (Adriaens *et al.* 2016).

By exploring *DIRC3* in mouse models, using xenografts or knockouts, the role of *DIRC3* in development as well as disease can be investigated. If found to be functional in such models, *DIRC3* would be more likely to play an important role in equivalent

human processes due to the genetic and physiological similarities between the two (Köhler *et al.* 2017).

7.3.1 Exploring MITF-SOX10 regulated lncRNA as potential biomarkers and therapeutic targets

7.3.1.1 LncRNAs as biomarkers in cancer

LncRNA expression signatures have potential to be used as biomarkers which utilise changes in expression as an informative tool for a presence or progression of a cancer. Variations in expression of groups, or in some cases individual, genes may be used to define tumour progression, or provide an indication of the likelihood of disease lethality. LncRNAs are particularly promising candidates as biomarkers due to their specificity of expression across specific lineages and tumours, as well as tumour stage (Yan *et al.* 2015, Grimaldi *et al.* 2017). The proportion of lncRNAs with cancer type specific dysregulation has been found to be higher than that for protein coding genes (Yan *et al.* 2015). As well as identifying the presence of cancer, alterations to lncRNA expression have potential to help inform decisions on most suitable treatment options, likelihood of survival, and likelihood of recurrence. Also, with 3-5% of tumours being of unknown primary origin, lncRNA expression signatures could also be used to determine where they originated (Yan *et al.* 2015).

The current method for diagnosing melanoma is assessment of morphology. However, lesions containing overlapping benign and malignant histopathological features can make such diagnosis difficult (Hu *et al.* 2014, Shain and Bastian 2016). Consequently, biomarkers suggestive of malignant behaviour would be useful for identifying patients with the metastatic form of the disease that may go unrecognised or prevent patients with benign cells undergoing unnecessary treatment. In addition, early-stage melanomas have limited starting material, making sub-sampling difficult. Instead, information based on morphology and histology of the tissue sample may be combined with detection of lncRNA localisation and expression levels using

fluorescent in situ hybridisation (FISH). These can then give a prediction of likelihood of tumour metastasis (Leucci, Coe, *et al.* 2016).

Non-invasive methods can be used to profile lncRNA expression in cancers including metastatic melanoma. Free nucleic acids, including lncRNAs, are released from cancer cells and can be detected in body fluid, such as blood, urine, and sputum, allowing non-invasive assessment (Grimaldi *et al.* 2017, Thomas and Marcato 2018). LncRNA secondary structures can also make the transcripts relatively stable, allowing for easier detection (Yan *et al.* 2015). LncRNAs may be detected using techniques such as RT-qPCR, next generation sequencing, and microarrays (Bolha *et al.* 2017). This non-invasive use of biomarkers allows responses to therapies or patient progress to be regularly monitored. In one study, expression of *HOTAIR* in ovarian cancer patients following treatment using carboplatin, indicated likely poor survival, while those who were *HOTAIR*-negative tended to have better responses (Teschendorff *et al.* 2015). A key requirement for lncRNA biomarkers is that they are easily detected during early stages of the disease, as earlier detection significantly increases patient prognosis. One of the most well-known lncRNA biomarkers is *PCA3* (prostate cancer antigen 3). *PCA3* has already been approved for use as a diagnostic marker for prostate cancer through detection in urine samples (Groskopf *et al.* 2006). The lncRNA was found to outperform the prostate-specific antigen (PSA) blood test in sensitivity and specificity (Haese *et al.* 2008, Bolha *et al.* 2017).

The identification of increased *DIRC3* expression in melanoma patients with greater survival (Figure 3.10), and participation in regulating the metastatic activity of anchorage-independent growth (Figure 5.5), suggest that the level of *DIRC3* could be used to predict likelihood of a patient survival, and possibly melanoma metastasis. However, the low expression of *DIRC3* (Figure 3.2) mean it could be challenging to collect enough tissue to detect expression. However, the association of MITF-SOX10 expression with melanoma cell proliferation and invasion, as well as resistance to drugs, (Konieczkowski *et al.* 2014, Sun *et al.* 2014, Verfaillie *et al.* 2015) mean lncRNAs

associated with the transcription factors could be used to generate a signature to predict likelihood of metastasis or survival.

7.3.1.2 Detection of MITF-SOX10 associated lncRNAs, including *DIRC3*, in melanoma patient tumours

Expression of *DIRC3* and other MITF-SOX10-regulated lncRNAs in melanoma has been determined primarily using RNA-seq data from TCGA and data from immortalised melanocyte and melanoma cell lines. By using melanoma samples from patients with benign and metastatic forms of the disease it would be possible to identify levels of lncRNA expression at different stages of melanoma. For example, it may be the case that *DIRC3* is initiated or repressed at certain stages or that patients prone to more aggressive forms of melanoma have reduced *DIRC3* expression overall.

Expression of *DIRC3* and other lncRNAs could be measured using a NanoString nCounter which quantifies RNA using fluorescently tagged probes. Although expensive, such sensitive technology would be favoured over RT-qPCR due to the poor preservation of RNA in patient samples available which are typically formaldehyde fixed paraffin embedded (FFPE). The requirement of only a single cell and no reverse transcription of samples mean less material is needed. This is advantageous due to the typically small size of samples available, particularly for benign tumours (Geiss *et al.* 2008, Mohankumar and Patel 2016). FISH could also be used to determine the level of lncRNA expression in FFPE or fresh tissue samples. The heterogenous nature of tumour cells means FISH can be useful for detecting expression of a target gene in single cells or subpopulations of tumour cells (Hu *et al.* 2014).

Following transformation of melanocytes into benign naevi, cells undergo a number of events which eventually can lead to metastasis. Initially, cells rapidly proliferate and spread horizontally through the epidermis in a premalignant radial growth phase (RGP). As the tumour evolves, it may become metastatic following its transition to a

vertical growth phase (VGP). During VGP, an increase in ECM-degrading enzymes and reduced adhesion allow the tumour to start growing vertically into the dermis, eventually allowing cells to enter into the lymphatic and vascular systems so they may metastasise (Braeuer *et al.* 2011, Mobley *et al.* 2012). The melanoma-expressed lncRNA *SAMMSON* was easily detected in VGP samples while not in normal human melanocyte or RGP samples (Leucci, Vendramin, *et al.* 2016). This demonstrated induction of *SAMMSON* when melanoma cells transition between the growth phases. In the case of *SLNCR*, expression was found to be significantly higher in melanomas that were at least 1 mm thick. When in the VGP, tumours greater than 1 mm thick are more likely to metastasise due to increased likelihood of reaching blood vessels. Consequently, expression of *SLNCR* was also found to correlate with melanoma severity (Schmidt *et al.* 2016). Expression of *DIRC3* and other MITF-SOX10-associated lncRNAs could also be measured to see whether they show any significant changes between RGP and VGP suggestive of tumour development.

If *DIRC3* or other MITF-SOX10-associated lncRNAs show consistent distinct changes between stages of melanoma progression, they could be promising biomarkers predictive of patient prognosis. Also, if sufficient quantities of the lncRNAs can be extracted from patients' blood samples who have metastatic melanoma, monitoring the level of expression against response to therapies could indicate which treatments work most efficiently for patients based on higher or lower levels of the lncRNA detected.

7.3.2 *DIRC3* potential as a therapeutic target

LncRNAs also offer another avenue for developing novel therapeutics for cancer treatment. While melanoma is highly treatable if identified in the very early stages, it is incredibly lethal when they metastasise. Current $BRAF^{V600E}$ inhibitors and immune checkpoint inhibitors are initially very effective for some patients with metastatic melanoma. However, a considerable proportion either do not respond or develop resistance to the therapy (Chapman *et al.* 2011, Villanueva *et al.* 2013). Due to the

rapid evolution of cancers caused by their genetic instability, single-agent therapies for advanced cancers rarely cure patients. Consequently, combination therapies are likely to be advantageous for targeting such diseases by blocking the development of drug resistance.

Two methods currently being explored to target oncogenic lncRNAs are siRNAs and ASOs (Leucci, Coe, *et al.* 2016). ASOs against *MALAT1* have been tested in nude mice intravenously injected with human lung cancer cells. They were able to both reduce tumour growth and metastases (Gutschner *et al.* 2013). In other cases, lncRNA-targeting ASOs combined with current therapies have been explored. For example, knockdown of *NEAT1* sensitised cancer cell lines to chemotherapy and p53 reactivation therapy (Adriaens *et al.* 2016). ASOs targeting *SAMMSON* have also been shown to improve the effectiveness of the BRAF-inhibitor dabrafenib in mice. While use of dabrafenib alone inhibited tumour growth, when combined with *SAMMSON* depletion, both tumour repression and increased apoptosis were observed. The group also identified no adverse effects to the mice undergoing the combination therapy (Leucci, Vendramin, *et al.* 2016).

Another avenue is to exploit the precise expression of lncRNAs to selectively deliver drugs to the cancers and limit off-target effects. The vector DTA-H19 plasmid carrying the gene for the alpha subunit of diphtheria toxin which was regulated by the H19 promoter was successfully used in mice with bladder cancer. The vector was only activated in cells containing the lncRNA H19 and protein-coding gene IGF2-P4 (Amit and Hochberg 2013).

The development of therapeutic strategies targeting tumour suppressor genes has had less focus. However, restoration of tumour suppressor gene function has been explored for a number of protein-coding genes by re-introducing their expression using viral and non-viral vectors (Atkinson and Chalmers 2010). While methods are being explored, there is still limited data on their use for lncRNAs. However, in the case of *GAS5*, LNAs that mimic the lncRNA's hormone response element mimic

(HREM) binding sequence to its target hormone receptors have been found to be capable of restoring cancer cell apoptosis when *GAS5* expression is depleted (Pickard and Williams 2016). Such induction of tumour suppressive function could have future therapeutic potential. Accordingly, by reactivating expression of *DIRC3*, or mimicking its mechanism of action it may be possible to prevent tumours from metastasising.

7.4 Conclusion

The majority of previous cancer research has focused on protein-coding genes and their involvement in cancer development and progression. In the case of melanoma, the function of protein-coding genes within key MITF-SOX10 transcription networks is also well defined. This study reveals that lncRNAs play an important role in regulation of MITF-SOX10 transcriptional responses. These new insights into the roles of lncRNAs in melanoma stimulate ideas for new biomarkers and therapeutics

DIRC3 represents a promising regulator of melanoma progression. *DIRC3* is a tumour suppressive intergenic lncRNA able to inhibit anchorage-independent growth likely through regulation of *IGFBP5* expression in a transcript-dependent manner. *DIRC3* also demonstrates the capability of a lncRNA target of MITF and SOX10 to act as a feedback regulator or regulate the activities of these two key melanoma transcription factors, rather than being purely a downstream mediator of their activity.

While development of therapeutics is an exciting prospect for new candidate lncRNAs, more detailed studies on the mechanism of action of *DIRC3* and its involvement in regulating melanoma progression are still required.

References

Ackerman, D. and Simon, M.C., 2014. Hypoxia, lipids, and cancer: Surviving the harsh tumor microenvironment. *Trends in Cell Biology*, 24 (8), 472–478.

Adriaens, C., Standaert, L., Barra, J., Latil, M., Verfaillie, A., Kalev, P., Boeckx, B., Wijnhoven, P.W.G., Radaelli, E., Vermi, W., Leucci, E., Lapouge, G., Beck, B., Van Den Oord, J., Nakagawa, S., Hirose, T., Sablina, A.A., Lambrechts, D., Aerts, S., Blanpain, C., and Marine, J.C., 2016. P53 induces formation of NEAT1 lncRNA-containing paraspeckles that modulate replication stress response and chemosensitivity. *Nature Medicine*, 22 (8), 861–868.

Ahn, B.Y., Elwi, A.N., Lee, B., Trinh, D.L.N., Klimowicz, A.C., Yau, A., Chan, J.A., Magliocco, A., and Kim, S.W., 2010. Genetic screen identifies insulin-like growth factor binding protein 5 as a modulator of tamoxifen resistance in breast cancer. *Cancer Research*, 70 (8), 3013–3019.

Akiyama, T., Dass, C.R., and Choong, P.F.M., 2009. Bim-targeted cancer therapy: A link between drug action and underlying molecular changes. *Molecular Cancer Therapeutics*, 8 (12), 3173–3180.

Aktary, Z., McMahon, M., and Larue, L., 2018. *Animal Models of Melanoma*. Tumor Models in Cancer Research. Springer New York.

Alam, T., Medvedeva, Y.A., Jia, H., Brown, J.B., Lipovich, L., and Bajic, V.B., 2014. Promoter analysis reveals globally differential regulation of human long non-coding RNA and protein-coding genes. *PLoS ONE*, 9 (10), 1–11.

Amit, D. and Hochberg, A., 2013. Development of targeted therapy for bladder cancer mediated by a double promoter plasmid expressing diphtheria toxin under the control of H19 and IGF2-P4 regulatory sequences. *International Journal of Clinical and Experimental Medicine*, 6 (2), 110–118.

Anaya, J., 2016. OncoLnc: linking TCGA survival data to mRNAs, miRNAs, and lncRNAs. *PeerJ Computer Science*, 2 (6), 67–80.

Anderson, K.M., Anderson, D.M., McAnally, J.R., Shelton, J.M., Bassel-Duby, R., and Olson, E.N., 2016. Transcription of the non-coding RNA upperhand controls Hand2 expression and heart development. *Nature*, 539 (7629), 433–436.

Atkinson, H. and Chalmers, R., 2010. Delivering the goods: Viral and non-viral gene therapy systems and the inherent limits on cargo DNA and internal sequences. *Genetica*, 138 (5), 485–498.

Azar, W.J., Zivkovic, S., Werther, G.A., and Russo, V.C., 2014. IGFBP-2 nuclear translocation is mediated by a functional NLS sequence and is essential for its pro-tumorigenic actions in cancer cells. *Oncogene*, 33 (5), 578–588.

Bach, D.H. and Lee, S.K., 2018. Long noncoding RNAs in cancer cells. *Cancer Letters*, 419 (10), 152–166.

Bach, L.A., 2018. 40 years of IGF1: IGF-binding proteins. *Journal of Molecular Endocrinology*, 61 (1), T11–T28.

Balas, M.M. and Johnson, A.M., 2018. Exploring the mechanisms behind long noncoding RNAs and cancer. *Non-coding RNA Research*, 3 (3), 108–117.

Balch, C.M., Gershenwald, J.E., Soong, S.J., Thompson, J.F., Atkins, M.B., Byrd, D.R., Buzaid, A.C., Cochran, A.J., Coit, D.G., Ding, S., Eggermont, A.M., Flaherty, K.T., Gimotty, P.A., Kirkwood, J.M., McMasters, K.M., Mihm, M.C., Morton, D.L., Ross,

M.I., Sober, A.J., and Sondak, V.K., 2009. Final version of 2009 AJCC melanoma staging and classification. *Journal of Clinical Oncology*, 27 (36), 6199–6206.

Balch, C.M., Soong, S.-J., Atkins, M.B., Buzaid, A.C., Cascinelli, N., Coit, D.G., Fleming, I.D., Gershenwald, J.E., Houghton, A., Kirkwood, J.M., McMasters, K.M., Mihm, M.F., Morton, D.L., Reintgen, D.S., Ross, M.I., Sober, A., Thompson, J.A., and Thompson, J.F., 2004. An Evidence-based Staging System for Cutaneous Melanoma. *CA: A Cancer Journal for Clinicians*, 54 (3), 131–149.

Barsyte-Lovejoy, D., Lau, S.K., Boutros, P.C., Khosravi, F., Jurisica, I., Andrulis, I.L., Tsao, M.S., and Penn, L.Z., 2006. The c-Myc oncogene directly induces the H19 noncoding RNA by allele-specific binding to potentiate tumorigenesis. *Cancer Research*, 66 (10), 5330–5337.

Baxter, R.C., 2014. IGF binding proteins in cancer: Mechanistic and clinical insights. *Nature Reviews Cancer*, 14 (5), 329–341.

Beattie, J., Allan, G.J., Lochrie, J.D., and Flint, D.J., 2006. Insulin-like growth factor-binding protein-5 (IGFBP-5): a critical member of the IGF axis. *Biochemical Journal*, 395 (1), 1–19.

Ben-David, U., Ha, G., Tseng, Y.Y., Greenwald, N.F., Oh, C., Shih, J., McFarland, J.M., Wong, B., Boehm, J.S., Beroukhim, R., and Golub, T.R., 2017. Patient-derived xenografts undergo mouse-specific tumor evolution. *Nature Genetics*, 49 (11), 1567–1575.

Beroukhim, R., Mermel, C.H., Porter, D., Wei, G., Raychaudhuri, S., Donovan, J., Barretina, J., Boehm, J.S., Dobson, J., Urashima, M., Henry, K.T.M., Pinchback, R.M., Ligon, A.H., Cho, Y.-J., Haery, L., Greulich, H., Reich, M., Winckler, W., Lawrence, M.S., Weir, B.A., Tanaka, K.E., Chiang, D.Y., Bass, A.J., Loo, A., Hoffman, C., Prensner, J., Liefeld, T., Gao, Q., Yecies, D., Signoretti, S., Maher, E., Kaye, F.J., Sasaki, H., Tepper, J.E., Fletcher, J.A., Tabernero, J., Baselga, J., Tsao, M.-S., Demichelis, F., Rubin, M.A., Janne, P.A., Daly, M.J., Nucera, C., Levine, R.L., Ebert, B.L., Gabriel, S., Rustgi, A.K., Antonescu, C.R., Ladanyi, M., Letai, A., Garraway, L.A., Loda, M., Beer, D.G., True, L.D., Okamoto, A., Pomeroy, S.L., Singer, S., Golub, T.R., Lander, E.S., Getz, G., Sellers, W.R., and Meyerson, M., 2010. The landscape of somatic copy-number alteration across human cancers. *Nature*, 463 (22), 899–905.

Bhan, A., Soleimani, M., and Mandal, S.S., 2017. Long noncoding RNA and cancer: A new paradigm. *Cancer Research*, 77 (15), 3965–3981.

Birney, E., Stamatoyannopoulos, J.A., Dutta, A., Guigo, R., Gingeras, T.R., Margulies, E.H., Weng, Z., Snyder, M., Dermitzakis, E.T., Holmes, I., Löytynoja, A., Karolchik, D., Frankish, A., Foissac, S., Brent, M., Birney, E., Pardi, F., Gnerre, S., Hartman, S., Thakkapallayil, A., Ruan, Y., Asimenos, G., Yu, M., Newburger, P., Lefebvre, G.C., Lowe, T.M., Navas, P.A., Liefer, L.A., Haussler, D., Tress, M.L., de Bakker, P.I.W., Heintzman, N., Gilbert, J., Guigó, R., Van Calcar, S., Guyer, M.S., Ganesh, M., Yao, F., Weinstock, G.M., Siepel, A., Barrera, L., Nix, D.A., Blakesley, R.W., Flamm, C., Rada-Iglesias, A., Wilson, R.K., Clelland, G.K., Zhu, B., Dorschner, M.O., Ellis, P.D., Ghosh, S., Lopez-Bigas, N., James, K.D., Trinklein, N.D., Humbert, R., Srinivasan, K.G., Ucla, C., Hon, G., Halees, A., Crawford, G.E., Chang, J.L., Ng, P., Yoshinaga, Y., Emanuelsson, O., Lieb, J.D., Mattick, J.S., Lindemeyer, M., Armengol, L., Lagarde, J., Zhang, X., Lee, K., Gibbs, R.A., Haydock, A., Zweig, A.S.,

Squazzo, S., Wyss, C., Brown, J.B., Vega, V.B., Cheng, J., Carter, N.P., Kraus, P., Castelo, R., Woodroffe, A., Singer, M.A., Green, E.D., Ren, B., Komorowski, J., Hinrichs, A.S., Harte, R.A., Richmond, T.A., Noble, W.S., Sodergren, E., de Jong, P.J., Young, A.C., Vetrie, D., Denoeud, F., Stranger, B.E., Swarbreck, D., Clamp, M., Green, R.D., Hubbard, T., Shulha, H.P., Munn, K.J., Huppert, J., Weirauch, M.T., Kern, A.D., Pedersen, J.S., Hansen, N.F., Inman, D., Bird, C.P., Hawrylycz, M., Sandelin, A., Rozowsky, J., Stuart, R., Dimas, A., Barber, G., Choo, C.Y., Massingham, T., Bieda, M.C., Collins, F.S., Sunyaev, S., Good, P.J., Yang, A., Lander, E.S., Weaver, M., Zhu, Z., Lin, J.M., Clark, T.G., Adzhubei, I., Rogers, J., Jaffe, D.B., Shahab, A., Moqtaderi, Z., Haidar, J.N.S., Maduro, V.V.B., Greenbaum, J.A., Aldred, S.F., Hofacker, I.L., Sidow, A., Cao, H., Boyle, P.J., Johnson, B.E., Luna, R., Chrast, J., Hackermüller, J., Dike, S., Zheng, D., Hoon Kim, T., Antonarakis, S.E., Dhami, P., Martin, J.D., Holroyd, N., Church, D., Tullius, T.D., Dermitzakis, E.T., Cooper, G.M., Missal, K., Sandstrom, R., Enroth, S., Dickson, M.C., Kawai, J., Worley, K.C., Zhao, X., Yu, Y., Andrews, R.M., Flicek, P., Seringhaus, M., Estivill, X., Asthana, S., Nagalakshmi, U., Kuehn, M.S., Henrichsen, C.N., Davydov, E., Myers, R.M., Kapranov, P., Wei, C.-L., Karaöz, U., Tanzer, A., Weissman, S., Gerstein, M., Parker, S.C.J., Huang, H., Hillman-Jackson, J., Karnani, N., Wheeler, D.A., Smith, K., Wang, K., Kent, W.J., Whelan, S., Thomas, P.J., Pachter, L., Stadler, P.F., Feingold, E.A., Zhang, Z.D., Thomas, D.J., Iyer, V.R., Sekinger, E.A., Davis, S., Jiang, N., Carninci, P., Stamatoyannopoulos, J.A., Hayashizaki, Y., Trumbower, H., Hertel, J., Urban, A.E., Cheung, E., Zhang, X., Sung, W.-K., Dutta, A., Shafer, A., Margulies, E.H., Neph, S., Lindblad-Toh, K., Thurman, R.E., Manzano, C., Guan, X., Washietl, S., Qu, C., Gingeras, T.R., Ureta-Vidal, A., Taylor, C.M., Ameur, A., Wu, J., Hirsch, H.A., Drenkow, J., Keefe, D., Wetterstrand, K.A., Muzny, D.M., Lian, Z., Jiang, H., Farnham, P.J., Dunham, I., Bickel, P., Rosenzweig, E.R., Langford, C.F., Paten, B., Malhotra, A., Ooi, H.S., Bouffard, G.G., Baertsch, R., Euskirchen, G., Mullikin, J.C., Bruce, A.W., Patel, S., Eyras, E., Koriabine, M., Fiegler, H., Oberley, M.J., Goldy, J., Weng, Z., Alioto, T., Cuff, J., Graves, T., Taylor, R., Johnson, E.M., Koch, C.M., Matthews, N., Kai, C., Glass, C.K., Wadelius, C., Valencia, A., Birney*, E., Neri, F., Abecasis, G.R., Sabo, P.J., Xu, M., Lee, C.W.H., Clawson, H., Osoegawa, K., Rosenbloom, K., Hardison, R.C., Goldman, N., Kuhn, R.M., Couttet, P., Struhl, K., Rosenfeld, M.G., King, D.C., Kim, J., Fried, C., Dekker, J., Miller, W., Dovey, O.M., Korbel, J., Liu, J., Wallerman, O., Hou, M., Cooper, S.J., Abril, J.F., Nefedov, M., Idol, J.R., Wilcox, S., Stone, E.A., Bell, I., McDowell, J.C., Dewey, C.N., Snyder, M., Tammana, H., Fu, Y., Batzoglou, S., Reymond, A., Lian, J., Frum, T.T., Day, N., Nikolaev, S., Harrow, J., Choo, S.W., Fowler, J.C., Montoya-Burgos, J.I., Park, M., Zhang, N.R., Taylor, J., Maskeri, B., Fulton, R., Giresi, P.G., Chiu, K.P., Mardis, E.R., Xu, X., Dillon, S.C., Zody, M.C., Bhinge, A.A., and Hallgrímsdóttir, I.B., 2007. Identification and analysis of functional elements in 1% of the human genome by the ENCODE pilot project. *Nature*, 447 (7146), 799–816.

Biswas, S., Thomas, A.A., Chen, S., Aref-Eshghi, E., Feng, B., Gonder, J., Sadikovic, B., and Chakrabarti, S., 2018. MALAT1: An Epigenetic Regulator of Inflammation in Diabetic Retinopathy. *Scientific Reports*, 8 (1), 1–15.

Blangy, A., 2017. Tensins are versatile regulators of Rho GTPase signalling and cell

adhesion. *Biology of the Cell*, 109 (3), 115–126.

Bodmer, D., Schepens, M., Eleveld, M.J., Schoenmakers, E.F.P.M., and Van Kessel, A.G., 2003. Disruption of a novel gene, DIRC3, and expression of DIRC3-HSPBAPI fusion transcripts in a case of familial renal cell cancer and t(2;3)(q35;q21). *Genes Chromosomes and Cancer*, 38 (2), 107–116.

Bolha, L., Ravnik-Glavač, M., and Glavač, D., 2017. Long Noncoding RNAs as Biomarkers in Cancer. *Disease Markers*, 2017, 1–14.

Borowicz, S., Scoyk, M. Van, Avasarala, S., Kumar, M., Rathinam, K., Tauler, J., Bikkavilli, R.K., and Winn, R.A., 2014. The Soft Agar Colony Formation Assay, 92, 1–6.

Braeuer, R.R., Zigler, M., Villares, G.J., Dobroff, A.S., and Bar-Eli, M., 2011. Transcriptional control of melanoma metastasis: The importance of the tumor microenvironment. *Seminars in Cancer Biology*, 21 (2), 83–88.

Briggs, J.A., Wolvetang, E.J., Mattick, J.S., Rinn, J.L., and Barry, G., 2015. Mechanisms of Long Non-coding RNAs in Mammalian Nervous System Development, Plasticity, Disease, and Evolution. *Neuron*, 88 (5), 861–877.

Brugnara, S., Sicher, M., Bonandini, E.M., Donner, D., Chierichetti, F., Barbareschi, M., Girardelli, C.R., and Caffo, O., 2018. Treatment with combined dabrafenib and trametinib in BRAFV600E-mutated metastatic malignant melanoma: A case of long-term complete response after treatment cessation. *Drugs in Context*, 7 (212515), 5–9.

Cabili, M.N., Dunagin, M.C., McClanahan, P.D., Biaesch, A., Padovan-Merhar, O., Regev, A., Rinn, J.L., and Raj, A., 2015. Localization and abundance analysis of human lncRNAs at single-cell and single-molecule resolution. *Genome Biology*, 16 (1), 1–16.

Cajigas, I., Leib, D.E., Cochrane, J., Luo, H., Swyter, K.R., Chen, S., Clark, B.S., Thompson, J., Yates, J.R., Kingston, R.E., and Kohtz, J.D., 2015. Evf2 lncRNA/BRG1/DLX1 interactions reveal RNA-dependent inhibition of chromatin remodeling . *Development*, 142 (15), 2641–2652.

Camacho, C. V., Choudhari, R., and Gadad, S.S., 2018. Long noncoding RNAs and cancer, an overview. *Steroids*, 133, 93–95.

Cao, H., Wahlestedt, C., and Kapranov, P., 2018. Strategies to Annotate and Characterize Long Noncoding RNAs: Advantages and Pitfalls. *Trends in Genetics*, 34 (9), 704–721.

Caramel, J., Papadogeorgakis, E., Hill, L., Browne, G.J., Richard, G., Wierinckx, A., Saldanha, G., sborne, J., Hutchinson, P., Tse, G., Lachuer, J., Puisieux, A., Pringle, J.H., Ansieau, S., and Tulchinsky, E., 2013. A Switch in the Expression of Embryonic EMT-Inducers Drives the Development of Malignant Melanoma. *Cancer Cell*, 24 (4), 466–480.

Carreira, S., Goodall, J., Denat, L., Rodriguez, M., Nuciforo, P., Hoek, K.S., Testori, A., Larue, L., and Goding, C.R., 2006. Mitf regulation of Dia1 controls melanoma proliferation and invasiveness. *Genes & Development*, 20, 3426–3439.

Chapman, P.B., Hauschild, A., Robert, C., Haanen, J.B., Ascierto, P., Larkin, J., Dummer, R., Garbe, C., Testori, A., Maio, M., Hogg, D., Lorigan, P., Lebbe, C., Jouary, T., Schadendorf, D., Ribas, A., O'Day, S.J., Sosman, J.A., Kirkwood, J.M., Eggermont, A.M.M., Dreno, B., Nolop, K., Li, J., Nelson, B., Hou, J., Lee, R.J.,

Flaherty, K.T., and McArthur, G.A., 2011. Improved Survival with Vemurafenib in Melanoma with BRAF V600E Mutation. *New England Journal of Medicine*, 364 (26), 2507–2516.

Chapman, P.B., Solit, D.B., and Rosen, N., 2014. Combination of RAF and MEK Inhibition for the Treatment of BRAF-Mutated Melanoma: Feedback Is Not Encouraged. *Cancer Cell*, 26 (5), 603–604.

Chaudhary, R. and Lal, A., 2017. Long noncoding RNAs in the p53 network. *Wiley Interdisciplinary Reviews: RNA*, 8 (3), 1–17.

Cheetham, S.W., Gruhl, F., Mattick, J.S., and Dinger, M.E., 2013. Long noncoding RNAs and the genetics of cancer. *British Journal of Cancer*, 108 (12), 2419–2425.

Chen, H., Duncan, I.C., Bozorgchami, H., and Lo, S.H., 2002. Tensin1 and a previously undocumented family member, tensin2, positively regulate cell migration. *Proceedings of the National Academy of Sciences*, 99 (2), 733–738.

Chen, L., Yang, H., Xiao, Y., Tang, X., Li, Y., Han, Q., Fu, J., Yang, Y., and Zhu, Y., 2016. Lentiviral-mediated overexpression of long non-coding RNA GAS5 reduces invasion by mediating MMP2 expression and activity in human melanoma cells. *International Journal of Oncology*, 48 (4), 1509–1518.

Choi, S.-W., Kim, H.-W., and Nam, J.-W., 2018. The small peptide world in long noncoding RNAs. *Briefings in Bioinformatics*, bby055, 1–12.

Chu, C., Qu, K., Zhong, F.L., Artandi, S.E., and Chang, H.Y., 2011. Genomic Maps of Long Noncoding RNA Occupancy Reveal Principles of RNA-Chromatin Interactions. *Molecular Cell*, 44 (4), 667–678.

Civenni, G., Walter, A., Kobert, N., Mihic-Probst, D., Zipser, M., Belloni, B., Seifert, B., Moch, H., Dummer, R., Van Den Broek, M., and Sommer, L., 2011. Human CD271-positive melanoma stem cells associated with metastasis establish tumor heterogeneity and long-term growth. *Cancer Research*, 71 (8), 3098–3109.

Clemmons, D.R., 2016. Role of IGF Binding Proteins in Regulating Metabolism. *Trends in Endocrinology and Metabolism*, 27 (6), 375–391.

Clemson, C.M., Hutchinson, J.N., Sara, S.A., Ensminger, A.W., Fox, A.H., Chess, A., and Lawrence, J.B., 2009. An Architectural Role for a Nuclear Noncoding RNA: NEAT1 RNA Is Essential for the Structure of Paraspeckles. *Molecular Cell*, 33 (6), 717–726.

Creyghton, M.P., Cheng, A.W., Welstead, G.G., Kooistra, T., Carey, B.W., Steine, E.J., Hanna, J., Lodato, M.A., Frampton, G.M., Sharp, P.A., Boyer, L.A., Young, R.A., and Jaenisch, R., 2010. Histone H3K27ac separates active from poised enhancers and predicts developmental state. *Proceedings of the National Academy of Sciences*, 107 (50), 21931–21936.

Cronin, J.C., Loftus, S.K., Baxter, L.L., Swatkoski, S., Gucek, M., and Pavan, W.J., 2018. Identification and functional analysis of SOX10 phosphorylation sites in melanoma. *PLoS ONE*, 13 (1), 1–18.

Cronin, J.C., Watkins-Chow, D.E., Incao, A., Hasskamp, J.H., Schönewolf, N., Aoude, L.G., Hayward, N.K., Bastian, B.C., Dummer, R., Loftus, S.K., and Pavan, W.J., 2013. SOX10 ablation arrests the cell cycle, induces senescence and suppresses melanomagenesis. *Cancer Research*, 73 (18), 5709–5718.

Dankort, D., Curley, D.P., Cartlidge, R.A., Nelson, B., Karnezis, A.N., Damsky, W.E., You, M.J., DePinho, R.A., McMahon, M., and Bosenberg, M., 2009. BrafV 600E

cooperates with Pten loss to induce metastatic melanoma. *Nature Genetics*, 41 (5), 544–552.

Dantonio, P.M., Klein, M.O., Freire, M.R.V.B., Araujo, C.N., Chiacetti, A.C., and Correa, R.G., 2018. Exploring major signaling cascades in melanomagenesis: A rationale route for targetted skin cancer therapy. *Bioscience Reports*, 38 (5), 1–34.

Davidovich, C., Wang, X., Cifuentes-Rojas, C., Goodrich, K.J., Gooding, A.R., Lee, J.T., and Cech, T.R., 2015. Toward a consensus on the binding specificity and promiscuity of PRC2 for RNA. *Molecular Cell*, 57 (3), 552–558.

Davidovich, C., Zheng, L., Goodrich, K.J., and Cech, T.R., 2013. Promiscuous RNA binding by Polycomb repressive complex 2. *Nature Structural and Molecular Biology*, 20 (11), 1250–1257.

Davies, H., Bignell, G.R., Cox, C., Stephens, P., Edkins, S., Clegg, S., Teague, J., Woffendin, H., Garnett, M.J., Bottomley, W., Davis, N., Dicks, E., Ewing, R., Floyd, Y., Gray, K., Hall, S., Hawes, R., Hughes, J., Kosmidou, V., Menzies, A., Mould, C., Parker, A., Stevens, C., Watt, S., Hooper, S., Jayatilake, H., Gusterson, B.A., Cooper, C., Shipley, J., Hargrave, D., Pritchard-Jones, K., Maitland, N., Chenevix-Trench, G., Riggins, G.J., Bigner, D.D., Palmieri, G., Cossu, A., Flanagan, A., Nicholson, A., Ho, J.W.C., Leung, S.Y., Yuen, S.T., Weber, B.L., Seigler, H.F., Darrow, T.L., Paterson, H., Wooster, R., Wooster, R., Stratton, M.R., and Futreal, P.A., 2002. Mutations of the BRAF gene in human cancer. *Nature*, 417 (6892), 949–954.

Deniz, E. and Erman, B., 2016. Long noncoding RNA (lincRNA), a new paradigm in gene expression control. *Functional and Integrative Genomics*, 17 (2–3), 135–143.

Derose, Y.S., Wang, G., Lin, Y.C., Bernard, P.S., Buys, S.S., Ebbert, M.T.W., Factor, R., Matsen, C., Milash, B.A., Nelson, E., Neumayer, L., Randall, R.L., Stijleman, I.J., Welm, B.E., and Welm, A.L., 2011. Tumor grafts derived from women with breast cancer authentically reflect tumor pathology, growth, metastasis and disease outcomes. *Nature Medicine*, 17 (11), 1514–1520.

Derrien, T., Johnson, R., Bussotti, G., Tanzer, A., Djebali, S., Tilgner, H., Guernec, G., Martin, D., Merkel, A., Knowles, D.G., Lagarde, J., Veeravalli, L., Ruan, X., Ruan, Y., Lassmann, T., Carninci, P., Brown, J.B., Lipovich, L., Gonzalez, J.M., Thomas, M., Davis, C.A., Shiekhattar, R., Gingeras, T.R., Hubbard, T.J., Notredame, C., Harrow, J., and Guigo, R., 2012. The GENCODE v7 catalog of human long noncoding RNAs. *Genome Research*, 22, 1775–1789.

Dimitrova, N., Zamudio, J.R., Jong, R.M., Soukup, D., Resnick, R., Sarma, K., Ward, A.J., Raj, A., Lee, J.T., Sharp, P.A., and Jacks, T., 2014. LincRNA-p21 Activates p21 In cis to Promote Polycomb Target Gene Expression and to Enforce the G1/S Checkpoint. *Molecular Cell*, 54 (5), 777–790.

Dixon, J.R., Selvaraj, S., Yue, F., Kim, A., Li, Y., Shen, Y., Hu, M., Liu, J.S., and Ren, B., 2012. Topological domains in mammalian genomes identified by analysis of chromatin interactions. *Nature*, 485 (7398), 376–380.

Djebali, S., Davis, C.A., Merkel, A., Dobin, A., Lassmann, T., Mortazavi, A., Tanzer, A., Lagarde, J., Lin, W., Schlesinger, F., Xue, C., Marinov, G.K., Khatun, J., Williams, B.A., Zaleski, C., Rozowsky, J., Röder, M., Kokocinski, F., Abdelhamid, R.F., Alioto, T., Antoshechkin, I., Baer, M.T., Bar, N.S., Batut, P., Bell, K., Bell, I., Chakrabortty,

S., Chen, X., Chrast, J., Curado, J., Derrien, T., Drenkow, J., Dumais, E., Dumais, J., Duttagupta, R., Falconnet, E., Fastuca, M., Fejes-Toth, K., Ferreira, P., Foissac, S., Fullwood, M.J., Gao, H., Gonzalez, D., Gordon, A., Gunawardena, H., Howald, C., Jha, S., Johnson, R., Kapranov, P., King, B., Kingswood, C., Luo, O.J., Park, E., Persaud, K., Preall, J.B., Ribeca, P., Risk, B., Robyr, D., Sammeth, M., Schaffer, L., See, L.H., Shahab, A., Skancke, J., Suzuki, A.M., Takahashi, H., Tilgner, H., Trout, D., Walters, N., Wang, H., Wrobel, J., Yu, Y., Ruan, X., Hayashizaki, Y., Harrow, J., Gerstein, M., Hubbard, T., Reymond, A., Antonarakis, S.E., Hannon, G., Giddings, M.C., Ruan, Y., Wold, B., Carninci, P., Guig, R., and Gingeras, T.R., 2012. Landscape of transcription in human cells. *Nature*, 489 (7414), 101–108.

Dunham, I., Kundaje, A., Aldred, S.F., Collins, P.J., Davis, C.A., Doyle, F., Epstein, C.B., Frietze, S., Harrow, J., Kaul, R., Khatun, J., Lajoie, B.R., Landt, S.G., Lee, B.K., Pauli, F., Rosenbloom, K.R., Sabo, P., Safi, A., Sanyal, A., Shoresh, N., Simon, J.M., Song, L., Trinklein, N.D., Altshuler, R.C., Birney, E., Brown, J.B., Cheng, C., Djebali, S., Dong, X., Ernst, J., Furey, T.S., Gerstein, M., Giardine, B., Greven, M., Hardison, R.C., Harris, R.S., Herrero, J., Hoffman, M.M., Iyer, S., Kellis, M., Kheradpour, P., Lassmann, T., Li, Q., Lin, X., Marinov, G.K., Merkel, A., Mortazavi, A., Parker, S.C.J., Reddy, T.E., Rozowsky, J., Schlesinger, F., Thurman, R.E., Wang, J., Ward, L.D., Whitfield, T.W., Wilder, S.P., Wu, W., Xi, H.S., Yip, K.Y., Zhuang, J., Bernstein, B.E., Green, E.D., Gunter, C., Snyder, M., Pazin, M.J., Lowdon, R.F., Dillon, L.A.L., Adams, L.B., Kelly, C.J., Zhang, J., Wexler, J.R., Good, P.J., Feingold, E.A., Crawford, G.E., Dekker, J., Elnitski, L., Farnham, P.J., Giddings, M.C., Gingeras, T.R., Guigó, R., Hubbard, T.J., Kent, W.J., Lieb, J.D., Margulies, E.H., Myers, R.M., Stamatoyannopoulos, J.A., Tenenbaum, S.A., Weng, Z., White, K.P., Wold, B., Yu, Y., Wrobel, J., Risk, B.A., Gunawardena, H.P., Kuiper, H.C., Maier, C.W., Xie, L., Chen, X., Mikkelsen, T.S., Gillespie, S., Goren, A., Ram, O., Zhang, X., Wang, L., Issner, R., Coyne, M.J., Durham, T., Ku, M., Truong, T., Eaton, M.L., Dobin, A., Tanzer, A., Lagarde, J., Lin, W., Xue, C., Williams, B.A., Zaleski, C., Röder, M., Kokocinski, F., Abdelhamid, R.F., Alioto, T., Antoshechkin, I., Baer, M.T., Batut, P., Bell, I., Bell, K., Chakrabortty, S., Chrast, J., Curado, J., Derrien, T., Drenkow, J., Dumais, E., Dumais, J., Duttagupta, R., Fastuca, M., Fejes-Toth, K., Ferreira, P., Foissac, S., Fullwood, M.J., Gao, H., Gonzalez, D., Gordon, A., Howald, C., Jha, S., Johnson, R., Kapranov, P., King, B., Kingswood, C., Li, G., Luo, O.J., Park, E., Preall, J.B., Presaud, K., Ribeca, P., Robyr, D., Ruan, X., Sammeth, M., Sandhu, K.S., Schaeffer, L., See, L.H., Shahab, A., Skancke, J., Suzuki, A.M., Takahashi, H., Tilgner, H., Trout, D., Walters, N., Wang, H., Hayashizaki, Y., Reymond, A., Antonarakis, S.E., Hannon, G.J., Ruan, Y., Carninci, P., Sloan, C.A., Learned, K., Malladi, V.S., Wong, M.C., Barber, G.P., Cline, M.S., Dreszer, T.R., Heitner, S.G., Karolchik, D., Kirkup, V.M., Meyer, L.R., Long, J.C., Maddren, M., Raney, B.J., Grasfeder, L.L., Giresi, P.G., Battenhouse, A., Sheffield, N.C., Showers, K.A., London, D., Bhinge, A.A., Shestak, C., Schaner, M.R., Kim, S.K., Zhang, Z.Z., Mieczkowski, P.A., Mieczkowska, J.O., Liu, Z., McDaniell, R.M., Ni, Y., Rashid, N.U., Kim, M.J., Adar, S., Zhang, Z., Wang, T., Winter, D., Keefe, D., Iyer, V.R., Zheng, M., Wang, P., Gertz, J., Vielmetter, J., Partridge, E.C., Varley, K.E., Gasper, C., Bansal, A., Pepke, S., Jain, P., Amrhein, H., Bowling, K.M., Anaya, M., Cross, M.K., Muratet, M.A., Newberry, K.M., McCue, K., Nesmith, A.S., Fisher-Aylor,

K.I., Pusey, B., DeSalvo, G., Parker, S.L., Balasubramanian, S., Davis, N.S., Meadows, S.K., Eggleston, T., Newberry, J.S., Levy, S.E., Absher, D.M., Wong, W.H., Blow, M.J., Visel, A., Pennachio, L.A., Petrykowska, H.M., Abyzov, A., Aken, B., Barrell, D., Barson, G., Berry, A., Bignell, A., Boychenko, V., Bussotti, G., Davidson, C., Despacio-Reyes, G., Diekhans, M., Ezkurdia, I., Frankish, A., Gilbert, J., Gonzalez, J.M., Griffiths, E., Harte, R., Hendrix, D.A., Hunt, T., Jungreis, I., Kay, M., Khurana, E., Leng, J., Lin, M.F., Loveland, J., Lu, Z., Manthravadi, D., Mariotti, M., Mudge, J., Mukherjee, G., Notredame, C., Pei, B., Rodriguez, J.M., Saunders, G., Sboner, A., Searle, S., Sisu, C., Snow, C., Steward, C., Tapanari, E., Tress, M.L., Van Baren, M.J., Washietl, S., Wilming, L., Zadissa, A., Zhang, Z., Brent, M., Haussler, D., Valencia, A., Addleman, N., Alexander, R.P., Auerbach, R.K., Balasubramanian, S., Bettinger, K., Bhardwaj, N., Boyle, A.P., Cao, A.R., Cayting, P., Charos, A., Cheng, Y., Eastman, C., Euskirchen, G., Fleming, J.D., Grubert, F., Habegger, L., Hariharan, M., Harmanci, A., Iyengar, S., Jin, V.X., Karczewski, K.J., Kasowski, M., Lacroute, P., Lam, H., Lamarre-Vincent, N., Lian, J., Lindahl-Allen, M., Min, R., Miotto, B., Monahan, H., Moqtaderi, Z., Mu, X.J., O'Geen, H., Ouyang, Z., Patacsil, D., Raha, D., Ramirez, L., Reed, B., Shi, M., Slifer, T., Witt, H., Wu, L., Xu, X., Yan, K.K., Yang, X., Struhl, K., Weissman, S.M., Penalva, L.O., Karmakar, S., Bhanvadia, R.R., Choudhury, A., Domanus, M., Ma, L., Moran, J., Victorsen, A., Auer, T., Centanin, L., Eichenlaub, M., Gruhl, F., Heermann, S., Hoeckendorf, B., Inoue, D., Kellner, T., Kirchmaier, S., Mueller, C., Reinhardt, R., Schertel, L., Schneider, S., Sinn, R., Wittbrodt, B., Wittbrodt, J., Jain, G., Balasundaram, G., Bates, D.L., Byron, R., Canfield, T.K., Diegel, M.J., Dunn, D., Ebersol, A.K., Frum, T., Garg, K., Gist, E., Hansen, R.S., Boatman, L., Haugen, E., Humbert, R., Johnson, A.K., Johnson, E.M., Kutyavin, T. V., Lee, K., Lotakis, D., Maurano, M.T., Neph, S.J., Neri, F. V., Nguyen, E.D., Qu, H., Reynolds, A.P., Roach, V., Rynes, E., Sanchez, M.E., Sandstrom, R.S., Shafer, A.O., Stergachis, A.B., Thomas, S., Vernot, B., Vierstra, J., Vong, S., Wang, H., Weaver, M.A., Yan, Y., Zhang, M., Akey, J.M., Bender, M., Dorschner, M.O., Groudine, M., MacCoss, M.J., Navas, P., Stamatoyannopoulos, G., Beal, K., Brazma, A., Flicek, P., Johnson, N., Lukk, M., Luscombe, N.M., Sobral, D., Vaquerizas, J.M., Batzoglou, S., Sidow, A., Hussami, N., Kyriazopoulou-Panagiotopoulou, S., Libbrecht, M.W., Schaub, M.A., Miller, W., Bickel, P.J., Banfai, B., Boley, N.P., Huang, H., Li, J.J., Noble, W.S., Bilmes, J.A., Buske, O.J., Sahu, A.D., Kharchenko, P. V., Park, P.J., Baker, D., Taylor, J., and Lochovsky, L., 2012. An integrated encyclopedia of DNA elements in the human genome. *Nature*, 489 (7414), 57–74.

Durand, N.C., Robinson, J.T., Shamim, M.S., Machol, I., Mesirov, J.P., Lander, E.S., and Aiden, E.L., 2016. Juicebox Provides a Visualization System for Hi-C Contact Maps with Unlimited Zoom. *Cell Systems*, 3 (1), 99–101.

Dykes, I.M. and Emanueli, C., 2017. Transcriptional and Post-transcriptional Gene Regulation by Long Non-coding RNA. *Genomics, Proteomics and Bioinformatics*, 15 (3), 177–186.

Elia, I., Doglioni, G., and Fendt, S.M., 2018. Metabolic Hallmarks of Metastasis Formation. *Trends in Cell Biology*, 28 (8), 673–684.

Engreitz, J.M., Haines, J.E., Perez, E.M., Munson, G., Chen, J., Kane, M., McDonel, P.E., Guttman, M., and Lander, E.S., 2016. Local regulation of gene expression by

lncRNA promoters, transcription and splicing. *Nature*, 539 (7629), 452–455.

Ennen, M., Keime, C., Gambi, G., Kieny, A., Coassolo, S., Thibault-Carpentier, C., Margerin-Schaller, F., Davidson, G., Vagne, C., Lipsker, D., and Davidson, I., 2017. MITF -High and MITF -Low Cells and a Novel Subpopulation Expressing Genes of Both Cell States Contribute to Intra- and Intertumoral Heterogeneity of Primary Melanoma. *Clinical Cancer Research*, 23 (22), 7097–7107.

Ernst, J. and Kellis, M., 2010. Discovery and Characterization of Chromatin States for Systematic Annotation of the Human Genome. *Computational Biology*, 28 (8), 817–825.

Evan, G. and Vousden, K., 2001. Proliferation, cell cycle and apoptosis in cancer. *Nature*, 411, 342–348.

Falletta, P., Sanchez-del-Campo, L., Chauhan, J., Effern, M., Kenyon, A., Kershaw, C.J., Siddaway, R., Lisle, R., Freter, R., Daniels, M.J., Lu, X., Tüting, T., Middleton, M., Buffa, F.M., Willis, A.E., Pavitt, G., Ronai, Z.A., Sauka-Spengler, T., Hölzel, M., and Goding, C.R., 2017. Translation reprogramming is an evolutionarily conserved driver of phenotypic plasticity and therapeutic resistance in melanoma. *Genes and Development*, 31 (1), 18–33.

Fatica, A. and Bozzoni, I., 2014. Long non-coding RNAs: New players in cell differentiation and development. *Nature Reviews Genetics*, 15 (1), 7–21.

Feige, E., Yokoyama, S., Levy, C., Khaled, M., Igras, V., Lin, R.J., Lee, S., Widlund, H.R., Granterd, S.R., Kun, A.L., Fisher, D.E., and ADepartment, 2011. Hypoxia-induced transcriptional repression of the melanoma-associated oncogene MITF. *PNAS*, 108 (43), 924–933.

Fernando, T.R., Contreras, J.R., Zampini, M., Rodriguez-Malave, N.I., Alberti, M.O., Anguiano, J., Tran, T.M., Palanichamy, J.K., Gajeton, J., Ung, N.M., Aros, C.J., Waters, E. V., Casero, D., Basso, G., Pigazzi, M., and Rao, D.S., 2017. The lncRNA CASC15 regulates SOX4 expression in RUNX1-rearranged acute leukemia. *Molecular Cancer*, 16 (1), 1–15.

Fiziev, P., Akdemir, K.C., Miller, J.P., Keung, E.Z., Samant, N.S., Sharma, S., Natale, C.A., Terranova, C.J., Maitituoheti, M., Amin, S.B., Martinez-Ledesma, E., Dhamdhere, M., Axelrad, J.B., Shah, A., Cheng, C.S., Mahadeshwar, H., Seth, S., Barton, M.C., Protopopov, A., Tsai, K.Y., Davies, M.A., Garcia, B.A., Amit, I., Chin, L., Ernst, J., and Rai, K., 2017. Systematic Epigenomic Analysis Reveals Chromatin States Associated with Melanoma Progression. *Cell Reports*, 19 (4), 875–889.

Flockhart, R.J., Webster, D.E., Qu, K., Mascarenhas, N., Kovalski, J., Kretz, M., and Khavari, P.A., 2012. BRAFV600E remodels the melanocyte transcriptome and induces BANCR to regulate melanoma cell migration. *Genome Research*, 22 (6), 1006–1014.

Freedman, M.L., Monteiro, A.N.A., Gayther, S.A., Coetzee, G.A., Risch, A., Plass, C., Casey, G., De Biasi, M., Carlson, C., Duggan, D., James, M., Liu, P., Tichelaar, J.W., Vikis, H.G., You, M., and Mills, I.G., 2011. Principles for the post-GWAS functional characterization of cancer risk loci. *Nature Genetics*, 43 (6), 513–518.

Fufa, T.D., Harris, M.L., Watkins-Chow, D.E., Levy, D., Gorkin, D.U., Gildea, D.E., Song, L., Safi, A., Crawford, G.E., Sviderskaya, E. V., Bennett, D.C., Mccallion, A.S., Loftus, S.K., and Pavan, W.J., 2015. Genomic analysis reveals distinct mechanisms and functional classes of SOX10-regulated genes in melanocytes.

Human Molecular Genetics, 24 (19), 5433–5450.
Gagnon, K.T., Li, L., Chu, Y., Janowski, B.A., and Corey, D.R., 2014. RNAi factors are present and active in human cell nuclei. *Cell Reports*, 6 (1), 211–221.
Gao, Z.Q., Wang, J. feng, Chen, D.H., Ma, X.S., Yang, W., Zhe, T., and Dang, X.W., 2018. Long non-coding RNA GAS5 antagonizes the chemoresistance of pancreatic cancer cells through down-regulation of miR-181c-5p. *Biomedicine and Pharmacotherapy*, 97 (1), 809–817.
Garbe, C., Peris, K., Hauschild, A., Saiag, P., Middleton, M., Bastholt, L., Grob, J.J., Malvehy, J., Newton-Bishop, J., Stratigos, A.J., Pehamberger, H., and Eggermont, A.M., 2016. Diagnosis and treatment of melanoma. European consensus-based interdisciplinary guideline - Update 2016. *European Journal of Cancer*, 63, 201–217.
García-González, E., Escamilla-Del-Arenal, M., Arzate-Mejía, R., and Recillas-Targa, F., 2016. Chromatin remodeling effects on enhancer activity. *Cellular and Molecular Life Sciences*, 73 (15), 2897–2910.
Garraway, L.A., Widlund, H.R., Rubin, M.A., Getz, G., Berger, A.J., Ramaswamy, S., Beroukhim, R., Milner, D.A., Granter, S.R., Du, J., Lee, C., Wagner, S.N., Li, C., Golub, T.R., Rimm, D.L., Meyerson, M.L., Fisher, D.E., and Sellers, W.R., 2005. Integrative genomic analyses identify MITF as a lineage survival oncogene amplified in malignant melanoma. *Nature*, 436 (7047), 117–122.
Geisler, S. and Coller, J., 2013. RNA in unexpected places: long non-coding RNA functions in diverse cellular contents. *Molecular Cell Biology*, 14 (11), 699–712.
Geiss, G.K., Bumgarner, R.E., Birditt, B., Dahl, T., Dowidar, N., Dunaway, D.L., Fell, H.P., Ferree, S., George, R.D., Grogan, T., James, J.J., Maysuria, M., Mitton, J.D., Oliveri, P., Osborn, J.L., Peng, T., Ratcliffe, A.L., Webster, P.J., Davidson, E.H., Hood, L., and Dimitrov, K., 2008. Direct multiplexed measurement of gene expression with color-coded probe pairs. *Nature biotechnology*, 26 (3), 317–25.
Ghoussaini, M., Edwards, S.L., Michailidou, K., Nord, S., Cowper-Sal-lari, R., Desai, K., Kar, S., Hillman, K.M., Kaufmann, S., Glubb, D.M., Beesley, J., Dennis, J., Bolla, M.K., Wang, Q., Dicks, E., Guo, Q., Schmidt, M.K., Shah, M., Luben, R., Brown, J., Czene, K., Darabi, H., Eriksson, M., Klevebring, D., Bojesen, S.E., Nordestgaard, B.G., Nielsen, S.F., Flyger, H., Lambrechts, D., Thienpont, B., Neven, P., Wildiers, H., Broeks, A., Vant Veer, L.J., Rutgers, E.J.T., Couch, F.J., Olson, J.E., Hallberg, E., Vachon, C., Chang-Claude, J., Rudolph, A., Seibold, P., Flesch-Janys, D., Peto, J., Dos-Santos-Silva, I., Gibson, L., Nevanlinna, H., Muranen, T.A., Aittomäki, K., Blomqvist, C., Hall, P., Li, J., Liu, J., Humphreys, K., Kang, D., Choi, J.Y., Park, S.K., Noh, D.Y., Matsuo, K., Ito, H., Iwata, H., Yatabe, Y., Guénel, P., Truong, T., Menegaux, F., Sanchez, M., Burwinkel, B., Marme, F., Schneeweiss, A., Sohn, C., Wu, A.H., Tseng, C.C., Van Den Berg, D., Stram, D.O., Benitez, J., Zamora, M.P., Perez, J.I.A., Menéndez, P., Shu, X.O., Lu, W., Gao, Y.T., Cai, Q., Cox, A., Cross, S.S., Reed, M.W.R., Andrulis, I.L., Knight, J.A., Glendon, G., Tchatchou, S., Sawyer, E.J., Tomlinson, I., Kerin, M.J., Miller, N., Haiman, C.A., Henderson, B.E., Schumacher, F., Marchand, L. Le, Lindblom, A., Margolin, S., Teo, S.H., Yip, C.H., Lee, D.S.C., Wong, T.Y., Hooning, M.J., Martens, J.W.M., Collée, J.M., Van Deurzen, C.H.M., Hopper, J.L., Southey, M.C., Tsimiklis, H., Kapuscinski, M.K., Shen, C.Y., Wu, P.E., Yu, J.C., Chen, S.T., Alnæs, G.G., Borresen-Dale, A.L., Giles,

G.G., Milne, R.L., McLean, C., Muir, K., Lophatananon, A., Stewart-Brown, S., Siriwanarangsan, P., Hartman, M., Miao, H., Buhari, S.A.B.S., Teo, Y.Y., Fasching, P.A., Haeberle, L., Ekici, A.B., Beckmann, M.W., Brenner, H., Dieffenbach, A.K., Arndt, V., Stegmaier, C., Swerdlow, A., Ashworth, A., Orr, N., Schoemaker, M.J., García-Closas, M., Figueroa, J., Chanock, S.J., Lissowska, J., Simard, J., Goldberg, M.S., Labrèche, F., Dumont, M., Winqvist, R., Pylkäs, K., Jukkola-Vuorinen, A., Brauch, H., Brüning, T., Koto, Y.D., Radice, P., Peterlongo, P., Bonanni, B., Volorio, S., Dörk, T., Bogdanova, N. V., Helbig, S., Mannermaa, A., Kataja, V., Kosma, V.M., Hartikainen, J.M., Devilee, P., Tollenaar, R.A.E.M., Seynaeve, C., Van Asperen, C.J., Jakubowska, A., Lubinski, J., Jaworska-Bieniek, K., Durda, K., Slager, S., Toland, A.E., Ambrosone, C.B., Yannoukakos, D., Sangrajrang, S., Gaborieau, V., Brennan, P., McKay, J., Hamann, U., Torres, D., Zheng, W., Long, J., Anton-Culver, H., Neuhausen, S.L., Luccarini, C., Baynes, C., Ahmed, S., Maranian, M., Healey, C.S., González-Neira, A., Pita, G., Alonso, M.R., Álvarez, N., Herrero, D., Tessier, D.C., Vincent, D., Bacot, F., De Santiago, I., Carroll, J., Caldas, C., Brown, M.A., Lupien, M., Kristensen, V.N., Pharoah, P.D.P., Chenevix-Trench, G., French, J.D., Easton, D.F., Dunning, A.M., Webb, P., and De Fazio, A., 2014. Evidence that breast cancer risk at the 2q35 locus is mediated through IGFBP5 regulation. *Nature Communications*, 4, 1–12.

Gilbert, L.A., Horlbeck, M.A., Adamson, B., Villalta, J.E., Chen, Y., Whitehead, E.H., Guimaraes, C., Panning, B., Ploegh, H.L., Bassik, M.C., Qi, L.S., Kampmann, M., and Weissman, J.S., 2014. Genome-Scale CRISPR-Mediated Control of Gene Repression and Activation. *Cell*, 159 (3), 647–661.

Gilbert, L.A., Larson, M.H., Morsut, L., Liu, Z., Brar, G.A., Torres, S.E., Stern-Ginossar, N., Brandman, O., Whitehead, E.H., Doudna, J.A., Lim, W.A., Weissman, J.S., and Qi, L.S., 2013. CRISPR-mediated modular RNA-guided regulation of transcription in eukaryotes. *Cell*, 154 (2), 442–451.

Goding, C.R., 2011. A picture of Mitf in melanoma immortality. *Oncogene*, 30 (20), 2304–2306.

Goding, C.R., 2016. Targeting the lncRNA SAMMSON Reveals Metabolic Vulnerability in Melanoma. *Cancer Cell*, 29 (5), 619–621.

Goding, C.R. and Arnheiter, H., 2019. MITF — the first 25 years. *Genes and Development*, 33, 1–25.

Gogada, R., Yadav, N., Liu, J., Tang, S., Zhang, D., Schneider, A., Seshadri, A., Sun, L., Aldaz, C.M., Tang, D.G., and Chandra, D., 2013. Bim, a proapoptotic protein, up-regulated via transcription factor E2F1-dependent mechanism, functions as a prosurvival molecule in cancer. *Journal of Biological Chemistry*, 288 (1), 368–381.

Gong, X. and Huang, M., 2017. Long non-coding RNA MEG3 promotes the proliferation of glioma cells through targeting Wnt/β-catenin signal pathway. *Cancer Gene Therapy*, 24, 381–385.

Goyal, A., Myacheva, K., Groß, M., Klingenberg, M., Duran Arqué, B., and Diederichs, S., 2017. Challenges of CRISPR/Cas9 applications for long non-coding RNA genes. *Nucleic acids research*, 45 (3), 1–13.

Graf, S.A., Busch, C., Bosserhoff, A.K., Besch, R., and Berking, C., 2014. SOX10 promotes melanoma cell invasion by regulating melanoma inhibitory activity.

Journal of Investigative Dermatology, 134 (8), 2212–2220.

Greer, C., Poplawski, S., Garbett, K., McMahan, R., Kordasiewicz, H., Zhao, H., Kennedy, A., Goleva, S., Sanders, T., Motley, T., Swayze, E., Ecker, D., Michael, T., and Sweatt, D., 2019. An antisense oligonucleotide leads to suppressed transcriptional elongation of Hdac2 and long- term memory enhancement. *bioRxiv*.

Grimaldi, A., Zarone, M.R., Irace, C., Zappavigna, S., Lombardi, A., Kawasaki, H., Caraglia, M., and Misso, G., 2017. Non-coding RNAs as a new dawn in tumor diagnosis. *Seminars in Cell and Developmental Biology*, 78, 37–50.

Grimberg, A., Coleman, C.M., Burns, T.F., Himelstein, B.P., Koch, C.J., Cohen, P., and El-Deiry, W.S., 2005. P53-Dependent and P53-Independent Induction of Insulin-Like Growth Factor Binding Protein-3 By Deoxyribonucleic Acid Damage and Hypoxia. *Journal of Clinical Endocrinology and Metabolism*, 90 (6), 3568–3574.

Groff, A.F., Sanchez-Gomez, D.B., Soruco, M.M.L., Gerhardinger, C., Barutcu, A.R., Li, E., Elcavage, L., Plana, O., Sanchez, L. V., Lee, J.C., Sauvageau, M., and Rinn, J.L., 2016. In Vivo Characterization of Linc-p21 Reveals Functional cis-Regulatory DNA Elements. *Cell Reports*, 16 (8), 2178–2186.

Groskopf, J., Aubin, S.M.J., Deras, I.L., Blase, A., Bodrug, S., Clark, C., Brentano, S., Mathis, J., Pham, J., Meyer, T., Cass, M., Hodge, P., Macairan, M.L., Marks, L.S., and Rittenhouse, H., 2006. APTIMA PCA3 molecular urine test: Development of a method to aid in the diagnosis of prostate cancer. *Clinical Chemistry*, 52 (6), 1089–1095.

Grossi, E., Sánchez, Y., and Huarte, M., 2016. Expanding the p53 regulatory network: LncRNAs take up the challenge. *Biochimica et Biophysica Acta - Gene Regulatory Mechanisms*, 1859 (1), 200–208.

Grywalska, E., Pasiarski, M., Góźdź, S., and Roliński, J., 2018. Immune-checkpoint inhibitors for combating T-cell dysfunction in cancer. *OncoTargets and Therapy*, 11, 6505–6524.

Guadamillas, M.C., Cerezo, A., and del Pozo, M.A., 2011. Overcoming anoikis - pathways to anchorage-independent growth in cancer. *Journal of Cell Science*, 124 (19), 3189–3197.

Guo, H., Ahmed, M., Zhang, F., Yao, C.Q., Li, S., Liang, Y., Hua, J., Soares, F., Sun, Y., Langstein, J., Li, Y., Poon, C., Bailey, S.D., Desai, K., Fei, T., Li, Q., Sendorek, D.H., Fraser, M., Prensner, J.R., Pugh, T.J., Pomerantz, M., Bristow, R.G., Lupien, M., Feng, F.Y., Boutros, P.C., Freedman, M.L., Walsh, M.J., and He, H.H., 2016. Modulation of long noncoding RNAs by risk SNPs underlying genetic predispositions to prostate cancer. *Nature Genetics*, 48 (10), 1142–1150.

Gupta, R.A., Shah, N., Wang, K.C., Kim, J., Horlings, H.M., Wong, D.J., Tsai, M.C., Hung, T., Argani, P., Rinn, J.L., Wang, Y., Brzoska, P., Kong, B., Li, R., West, R.B., Van De Vijver, M.J., Sukumar, S., and Chang, H.Y., 2010. Long non-coding RNA HOTAIR reprograms chromatin state to promote cancer metastasis. *Nature*, 464 (7291), 1071–1076.

Gutschner, T., Baas, M., and Diederichs, S., 2011. Noncoding RNA gene silencing through genomic integration of RNA destabilizing elements using zinc finger nucleases. *Genome Research*, 21 (11), 1944–1954.

Gutschner, T., Hämmerle, M., Eißmann, M., Hsu, J., Kim, Y., Hung, G., Revenko, A.,

Arun, G., Stentrup, M., Groß, M., Zörnig, M., MacLeod, A.R., Spector, D.L., and Diederichs, S., 2013. The noncoding RNA MALAT1 is a critical regulator of the metastasis phenotype of lung cancer cells. *Cancer Research*, 73 (3), 1180–1189.

Guttman, M., Amit, I., Garber, M., French, C., Lin, M.F., Feldser, D., Huarte, M., Zuk, O., Carey, B.W., Cassady, J.P., Cabili, M.N., Jaenisch, R., Mikkelsen, T.S., Jacks, T., Hacohen, N., Bernstein, B.E., Kellis, M., Regev, A., Rinn, J.L., and Land, E.S., 2009. Chromatin signature reveals over a thousand highly conserved large non-coding RNAs in mammals. *Nature*, 458 (7235), 223–227.

Guttman, M. and Rinn, J.L., 2012. Modular regulatory principles of large non-coding RNAs. *Nature*, 482 (7385), 339–346.

Hacisuleyman, E., Goff, L.A., Trapnell, C., Williams, A., Henao-Mejia, J., Sun, L., McClanahan, P., Hendrickson, D.G., Sauvageau, M., Kelley, D.R., Morse, M., Engreitz, J., Lander, E.S., Guttman, M., Lodish, H.F., Flavell, R., Raj, A., and Rinn, J.L., 2014. Topological organization of multichromosomal regions by the long intergenic noncoding RNA Firre. *Nature Structural and Molecular Biology*, 21 (2), 198–206.

Haese, A., de la Taille, A., van Poppel, H., Marberger, M., Stenzl, A., Mulders, P.F.A., Huland, H., Abbou, C.C., Remzi, M., Tinzl, M., Feyerabend, S., Stillebroer, A.B., van Gils, M.P.M.Q., and Schalken, J.A., 2008. Clinical Utility of the PCA3 Urine Assay in European Men Scheduled for Repeat Biopsy. *European Urology*, 54 (5), 1081–1088.

Hainer, S.J., Pruneski, J.A., Mitchell, R.D., Monteverde, R.M., and Martens, J.A., 2011. Intergenic transcription causes repression by directing nucleosome assembly. *Genes and Development*, 25 (1), 29–40.

Haldin, C.E. and LaBonne, C., 2010. SoxE factors as multifunctional Neural Crest Regulatory Factors. *Int J Biochem Cell Biol*, 42 (3), 441–444.

Han, J., Zhang, Z., and Wang, K., 2018. 3C and 3C-based techniques: The powerful tools for spatial genome organization deciphering. *Molecular Cytogenetics*, 11 (1), 1–10.

Hanahan, D. and Weinberg, R.A., 2011. Review Hallmarks of Cancer : The Next Generation. *Cell*, 144 (5), 646–674.

Hanahan, D., Weinberg, R.A., and Francisco, S., 2000. The Hallmarks of Cancer Review University of California at San Francisco, 100, 57–70.

Hansen, A.S., Cattoglio, C., Darzacq, X., and Tjian, R., 2018. Recent evidence that TADs and chromatin loops are dynamic structures. *Nucleus*, 9 (1), 20–32.

Harris, M.L., Baxter, L.L., Loftus, S.K., and Pavan, W.J., 2010. Sox proteins in melanocyte development and melanoma. *Pigment Cell Melanoma*, 1 (23), 496–513.

Hart, J.R., Roberts, T.C., Weinberg, M.S., Morris, K. V., and Vogt, P.K., 2014. MYC regulates the non-coding transcriptome. *Oncotarget*, 5 (24), 12543–12554.

Hartman, M.L. and Czyz, M., 2015. MITF in melanoma: Mechanisms behind its expression and activity. *Cellular and Molecular Life Sciences*, 72 (7), 1249–1260.

Hemesath, T.J., Steingrímsson, E., McGill, G., Hansen, M.J., Vaught, J., Hodgkinson, C.A., Arnheiter, H., Copeland, N.G., Jenkins, N.A., and Fisher, D.E., 1994. microphthalmia, A critical factor in melanocyte development, defines a discrete transcription factor family. *Genes and Development*, 8 (22), 2770–2780.

Hendrickson, D., Kelley, D.R., Tenen, D., Bernstein, B., and Rinn, J.L., 2016. Widespread RNA binding by chromatin-associated proteins. *Genome Biology*, 17 (1), 1–18.

Herbarth, B., Pingault, V., Bondurand, N., Kuhlbrodt, K., Hermans-Borgmeyer, I., Puliti, A., Lemort, N., Goossens, M., and Wegner, M., 1998. Mutation of the Sry-related Sox10 gene in Dominant megacolon, a mouse model for human Hirschsprung disease. *Proceedings of the National Academy of Sciences of the United States of America*, 95 (9), 5161–5165.

Hernandez-Davies, J.E., Tran, T.Q., Reid, M.A., Rosales, K.R., Lowman, X.H., Pan, M., Moriceau, G., Yang, Y., Wu, J., Lo, R.S., and Kong, M., 2015. Vemurafenib resistance reprograms melanoma cells towards glutamine dependence. *Journal of Translational Medicine*, 13 (1), 1–11.

Hezroni, H., Koppstein, D., Schwartz, M.G., Avrutin, A., Bartel, D.P., and Ulitsky, I., 2015. Principles of Long Noncoding RNA Evolution Derived from Direct Comparison of Transcriptomes in 17 Species. *Cell Reports*, 11 (7), 1110–1122.

Hobson, D.J., Wei, W., Steinmetz, L.M., and Svejstrup, J.Q., 2012. RNA Polymerase II Collision Interrupts Convergent Transcription. *Molecular Cell*, 48 (3), 365–374.

Hodgkinson, C.A., Moore, K.J., Nakayama, A., Steingrímsson, E., Copeland, N.G., Jenkins, N.A., and Arnheiter, H., 1993. Mutations at the mouse microphthalmia locus are associated with defects in a gene encoding a novel basic-helix-loop-helix-zipper protein. *Cell*, 74 (2), 395–404.

Hoek, K.S., Eichhoff, O.M., Schlegel, N.C., Döbbeling, U., Kobert, N., Schaerer, L., Hemmi, S., and Dummer, R., 2008. In vivo switching of human melanoma cells between proliferative and invasive states. *Cancer Research*, 68 (3), 650–656.

Hoek, K.S. and Goding, C.R., 2010. Cancer stem cells versus phenotype-switching in melanoma. *Pigment Cell and Melanoma Research*, 23 (6), 746–759.

Hon, C.C., Ramilowski, J.A., Harshbarger, J., Bertin, N., Rackham, O.J.L., Gough, J., Denisenko, E., Schmeier, S., Poulsen, T.M., Severin, J., Lizio, M., Kawaji, H., Kasukawa, T., Itoh, M., Burroughs, A.M., Noma, S., Djebali, S., Alam, T., Medvedeva, Y.A., Testa, A.C., Lipovich, L., Yip, C.W., Abugessaisa, I., Mendez, M., Hasegawa, A., Tang, D., Lassmann, T., Heutink, P., Babina, M., Wells, C.A., Kojima, S., Nakamura, Y., Suzuki, H., Daub, C.O., De Hoon, M.J.L., Arner, E., Hayashizaki, Y., Carninci, P., and Forrest, A.R.R., 2017. An atlas of human long non-coding RNAs with accurate 5′ ends. *Nature*, 543 (7644), 199–204.

Hsu, P.D., Lander, E.S., and Zhang, F., 2014. Development and applications of CRISPR-Cas9 for genome engineering. *Cell*, 157 (6), 1262–1278.

Hu, L., Ru, K., Zhang, L., Huang, Y., Zhu, X., Liu, H., Zetterberg, A., Cheng, T., and Mia, W., 2014. Fluorescence in situ hybridization (FISH): An increasingly demanded tool for biomarker research and personalized medicine. *Biomarker Research*, 2 (1), 1–13.

Huang, Y., Jankowski, A., Cheah, K.S.E., and Prabhakar, S., 2015. SOXE transcription factors form selective dimers on non-compact DNA motifs through multifaceted interactions between dimerization and high-mobility group domains. *Nature Publishing Group*, 5, 1–12.

Huarte, M., 2015. The emerging role of lncRNAs in cancer. *Nature Medicine*, 21 (11), 1253–1261.

Huarte, M., Guttman, M., Feldser, D., Garber, M., Koziol, M.J., Kenzelmann-Broz, D., Khalil, A.M., Zuk, O., Amit, I., Rabani, M., Attardi, L.D., Regev, A., Lander, E.S., Jacks, T., and Rinn, J.L., 2010. A large intergenic noncoding RNA induced by p53 mediates global gene repression in the p53 response. *Cell*, 142 (3), 409–419.

Hulstaert, E., Brochez, L., Volders, P.-J., Vandesompele, J., and Mestdagh, P., 2017. Long non-coding RNAs in cutaneous melanoma: clinical perspectives. *Oncotarget*, 8 (26).

Hung, T., Wang, Y., Lin, M.F., Koegel, A.K., Kotake, Y., Grant, G.D., Horlings, H.M., Shah, N., Umbricht, C., Wang, P., Wang, Y., Kong, B., Langerød, A., Børresen-Dale, A.L., Kim, S.K., Van De Vijver, M., Sukumar, S., Whitfield, M.L., Kellis, M., Xiong, Y., Wong, D.J., and Chang, H.Y., 2011. Extensive and coordinated transcription of noncoding RNAs within cell-cycle promoters. *Nature Genetics*, 43 (7), 621–629.

Hwang, J.R., Cho, Y.J., Lee, Y., Park, Y., Han, H.D., Ahn, H.J., Lee, J.H., and Lee, J.W., 2016. The C-terminus of IGFBP-5 suppresses tumor growth by inhibiting angiogenesis. *Scientific Reports*, 6 (August), 1–12.

Iaccarino, I., 2017. LncRNAs and MYC: An intricate relationship. *International Journal of Molecular Sciences*, 18 (7), 1–14.

Ideue, T., Hino, K., Kitao, S., Yokoi, T., and Hirose, T., 2009. Efficient oligonucleotide-mediated degradation of nuclear noncoding RNAs in mammalian cultured cells. *RNA*, 15 (8), 1578–1587.

Imig, J., Brunschweiger, A., Brümmer, A., Guennewig, B., Mittal, N., Kishore, S., Tsikrika, P., Gerber, A.P., Zavolan, M., and Hall, J., 2015. MiR-CLIP capture of a miRNA targetome uncovers a lincRNA H19-miR-106a interaction. *Nature Chemical Biology*, 11 (2), 107–114.

Iozumi, K., Hoganson, G.E., Pennella, R., Everett, M.A., and Fuller, B.B., 1993. Role of tyrosinase as the determinant of pigmentation in cultured human melanocytes. *Journal of Investigative Dermatology*, 100 (6), 806–811.

Iyer, M.K., Niknafs, Y.S., Malik, R., Singhal, U., Sahu, A., Hosono, Y., Barrette, T.R., Prensner, J.R., Evans, J.R., Zhao, S., Poliakov, A., Cao, X., Dhanasekaran, S.M., Wu, Y.M., Robinson, D.R., Beer, D.G., Feng, F.Y., Iyer, H.K., and Chinnaiyan, A.M., 2015. The landscape of long noncoding RNAs in the human transcriptome. *Nature Genetics*, 47 (3), 199–208.

Jandura, A. and Krause, H.M., 2017. The New RNA World: Growing Evidence for Long Noncoding RNA Functionality. *Trends in Genetics*, 33 (10), 665–676.

Jin, S., Yang, X., Li, J., Yang, W., Ma, H., and Zhang, Z., 2019. P53-targeted lincRNA-p21 acts as a tumor suppressor by inhibiting JAK2/STAT3 signaling pathways in head and neck squamous cell carcinoma. *Molecular Cancer*, 18 (1), 1–18.

Johnsson, P., Lipovich, L., Grandér, D., and Morris, K. V., 2014. Evolutionary conservation of long noncoding RNAs; sequence, structure, function. *Biochem and Biophys Acta*, 23 (3), 1–7.

Kaikkonen, M.U. and Adelman, K., 2018. Emerging Roles of Non-Coding RNA Transcription. *Trends in Biochemical Sciences*, 43 (9), 654–667.

Kajino, T., Shimamura, T., Gong, S., Yanagisawa, K., Ida, L., Nakatochi, M., Griesing, S., Shimada, Y., Kano, K., Suzuki, M., Miyano, S., and Takahashi, T., 2019. Divergent lnc RNA MYMLR regulates MYC by eliciting DNA looping and promoter-enhancer

interaction . *The EMBO Journal*, 38 (17), 1–13.
Kaneko, S., Son, J., Bonasio, R., Shen, S.S., and Reinberg, D., 2014. Nascent RNA interaction keeps PRC2 activity poised and in check. *Genes and Development*, 28 (18), 1983–1988.
Kawakami, A. and Fisher, D.E., 2017. The master role of microphthalmia-associated transcription factor in melanocyte and melanoma biology. *Laboratory Investigation*, 97 (6), 649–656.
Khair, D.O., Bax, H.J., Mele, S., Crescioli, S., Pellizzari, G., Khiabany, A., Nakamura, M., Harris, R.J., French, E., Hoffmann, R.M., Williams, I.P., Cheung, A., Thair, B., Beales, C.T., Touizer, E., Signell, A.W., Tasnova, N.L., Spicer, J.F., Josephs, D.H., Geh, J.L., Ross, A.M.K., Healy, C., Papa, S., Lacy, K.E., and Karagiannis, S.N., 2019. Combining immune checkpoint inhibitors: Established and emerging targets and strategies to improve outcomes in melanoma. *Frontiers in Immunology*, 10 (MAR), 1–20.
Kino, T., Hurt, D.E., Ichijo, T., Nader, N., and Chrousos, G.P., 2010. Noncoding RNA Gas5 Is a Growth Arrest and Starvation-Associated Repressor of the Glucocorticoid Receptor, 3 (107).
Köhler, C., Nittner, D., Rambow, F., Radaelli, E., Stanchi, F., Vandamme, N., Baggiolini, A., Sommer, L., Berx, G., van den Oord, J.J., Gerhardt, H., Blanpain, C., and Marine, J.C., 2017. Mouse Cutaneous Melanoma Induced by Mutant BRaf Arises from Expansion and Dedifferentiation of Mature Pigmented Melanocytes. *Cell Stem Cell*, 21 (5), 679–693.
Konieczkowski, D.J., Johannessen, C.M., Abudayyeh, O., Kim, J.W., Cooper, Z.A., Piris, A., Frederick, D.T., Barzily-Rokni, M., Straussman, R., Haq, R., Fisher, D.E., Mesirov, J.P., Hahn, W.C., Flaherty, K.T., Wargo, J.A., Tamayo, P., and Garraway, L.A., 2014. A melanoma cell state distinction influences sensitivity to MAPK pathway inhibitors. *Cancer Discovery*, 4 (7), 816–827.
Kopp, F. and Mendell, J.T., 2018. Functional Classification and Experimental Dissection of Long Noncoding RNAs. *Cell*, 172 (3), 393–407.
Kornienko, A.E., Guenzl, P.M., Barlow, D.P., and Pauler, F.M., 2013. Gene regulation by the act of long non-coding RNA transcription. *BMC Biology*, 11 (59), 1–14.
Kozar, I., Margue, C., Rothengatter, S., Haan, C., and Kreis, S., 2019. Many ways to resistance: How melanoma cells evade targeted therapies. *Biochimica et Biophysica Acta - Reviews on Cancer*, 1871 (2), 313–322.
Kumar, B. De and Krumlauf, R., 2016. Molecular Biology: HOXs and lincRNAs: Two sides of the same coin. *Science Advances*, 2 (1), 1–8.
Kuzu, O.F., Nguyen, F.D., Noory, M.A., and Sharma, A., 2015. Current State of Animal (Mouse) Modeling in Melanoma Research. *Cancer Growth and Metastasis*, 8, 81–94.
Kwong, L.N. and Davies, M.A., 2013. Navigating the Therapeutic Complexity of PI3K Pathway Inhibition in Melanoma Lawrence. *Clinical Cancer Research*, 19 (19), 1–17.
Lam, M.T.Y., Li, W., Rosenfeld, M.G., and Glass, C.K., 2014. Enhancer RNAs and regulated transcriptional programs. *Trends in Biochemical Sciences*, 39 (4), 170–182.
Lambert, A.W., Pattabiraman, D.R., and Weinberg, R.A., 2017. Emerging Biological

Principles of Metastasis. *Cell*, 168 (4), 670–691.

Lang, D., Lu, M.M., Huang, L., Engleka, K.A., Zhang, M., Chu, E.Y., Lipner, S., Skoultchi, A., Millar, S.E., and Epstein, J.A., 2005. Pax3 functions at a nodal point in melanocyte stem cell differentiation. *Nature*, 433 (7028), 884–887.

Larue, L. and Beermann, F., 2007. Cutaneous melanoma in genetically modified animals. *Pigment Cell Research*, 20 (6), 485–497.

Larue, L. and Delmas, V., 2006. The WNT/beta-catenin pathway in melanoma. *Frontiers in Bioscience*, 11 (1 P.447-888), 733–742.

Latos, P.A., Pauler, F.M., Koerner, M. V., Şenergin, H.B., Hudson, Q.J., Stocsits, R.R., Allhoff, W., Stricker, S.H., Klement, R.M., Warczok, K.E., Aumayr, K., Pasierbek, P., and Barlow, D.P., 2012. Airn Transcriptional Overlap, But Not Its lncRNA Products, Induces Imprinted Igf2r Silencing. *Science*, 338 (6113), 1469–1472.

Laurette, P., Strub, T., Koludrovic, D., Keime, C., Le Gras, S., Seberg, H., Van Otterloo, E., Imrichova, H., Siddaway, R., Aerts, S., Cornell, R.A., Mengus, G., and Davidson, I., 2015. Transcription factor MITF and remodeller BRG1 define chromatin organisation at regulatory elements in melanoma cells. *eLife*, 4, 1–40.

Lee, S., Kopp, F., Chang, T.C., Sataluri, A., Chen, B., Sivakumar, S., Yu, H., Xie, Y., and Mendell, J.T., 2016. Noncoding RNA NORAD Regulates Genomic Stability by Sequestering PUMILIO Proteins. *Cell*, 164 (1–2), 69–80.

Lennox, K.A. and Behlke, M.A., 2016. Cellular localization of long non-coding RNAs affects silencing by RNAi more than by antisense oligonucleotides. *Nucleic Acids Research*, 44 (2), 863–877.

Lessard, L., Liu, M., Marzese, D.M., Wang, H., Chong, K., Kawas, N., Donovan, N.C., Kiyohara, E., Hsu, S., Nelson, N., Izraely, S., Sagi-Assif, O., Witz, I.P., Ma, X.J., Luo, Y., and Hoon, D.S.B., 2015. The CASC15 Long Intergenic Noncoding RNA Locus Is Involved in Melanoma Progression and Phenotype Switching. *Journal of Investigative Dermatology*, 135 (10), 2464–2474.

Leucci, E., Coe, E.A., Marine, J.C., and Vance, K.W., 2016. The emerging role of long non-coding RNAs in cutaneous melanoma. *Pigment Cell and Melanoma Research*, 29 (6), 619–626.

Leucci, E., Vendramin, R., Spinazzi, M., Laurette, P., Fiers, M., Wouters, J., Radaelli, E., Eyckerman, S., Leonelli, C., Vanderheyden, K., Rogiers, A., Hermans, E., Baatsen, P., Aerts, S., Amant, F., Van Aelst, S., Van Den Oord, J., De Strooper, B., Davidson, I., Lafontaine, D.L.J., Gevaert, K., Vandesompele, J., Mestdagh, P., and Marine, J.C., 2016. Melanoma addiction to the long non-coding RNA SAMMSON. *Nature*, 531 (7595), 518–522.

Levy, C., Khaled, M., and Fisher, D.E., 2006. MITF: master regulator of melanocyte development and melanoma oncogene. *Trends in Molecular Medicine*, 12 (9), 406–414.

Li, P., Zhang, X., Wang, L., Du, L., Yang, Y., Liu, T., Li, C., and Wang, C., 2017. lncRNA HOTAIR Contributes to 5FU Resistance through Suppressing miR-218 and Activating NF-κB/TS Signaling in Colorectal Cancer. *Molecular Therapy - Nucleic Acids*, 8 (247), 356–369.

Li, R., Zhang, L., Jia, L., Duan, Y., Li, Y., Bao, L., and Sha, N., 2014. Long non-coding RNA BANCR promotes proliferation in malignant melanoma by regulating MAPK pathway activation. *PLoS ONE*, 9 (6), 1–9.

Liao, J.Y., Wu, J., Wang, Y.J., He, J.H., Deng, W.X., Hu, K.S., Zhang, Y.C., Zhang, Y., Yan, H., Wang, D.L., Liu, Q., Zeng, M.S., Phillip Koeffler, H., Song, E., and Yin, D., 2017. Deep sequencing reveals a global reprogramming of lncRNA transcriptome during EMT. *Biochimica et Biophysica Acta - Molecular Cell Research*, 1864 (10), 1703–1713.

Lin, A., Hu, Q., Li, C., Xing, Z., Ma, G., Wang, C., Li, J., Ye, Y., Yao, J., Liang, K., Wang, S., Park, P.K., Marks, J.R., Zhou, Y., Zhou, J., Hung, M.C., Liang, H., Hu, Z., Shen, H., Hawke, D.H., Han, L., Zhou, Y., Lin, C., and Yang, L., 2017. The LINK-A lncRNA interacts with PtdIns(3,4,5)P 3 to hyperactivate AKT and confer resistance to AKT inhibitors. *Nature Cell Biology*, 19 (3), 238–251.

Lin, C. and Yang, L., 2018. Long Noncoding RNA in Cancer: Wiring Signaling Circuitry. *Trends in Cell Biology*, 28 (4), 287–301.

Liu, S.J. and Lim, D.A., 2018. Modulating the expression of long non-coding RNAs for functional studies. *EMBO Reports*, 1–11.

Liu, S.J., Nowakowski, T.J., Pollen, A.A., Lui, J.H., Horlbeck, M.A., Attenello, F.J., He, D., Weissman, J.S., Kriegstein, A.R., Diaz, A.A., and Lim, D.A., 2016. Single-cell analysis of long non-coding RNAs in the developing human neocortex. *Genome Biology*, 17 (1), 1–17.

Liu, T., Shen, S.K., Xiong, J.G., Xu, Y., Zhang, H.Q., Liu, H.J., and Lu, Z.G., 2016. Clinical significance of long noncoding RNA SPRY4-IT1 in melanoma patients. *FEBS Open Bio*, 6 (2), 147–154.

Liu, Y., Han, X., Yuan, J., Geng, T., Chen, S., Hu, X., Cui, I.H., and Cui, H., 2017. Biallelic insertion of a transcriptional terminator via the CRISPR/Cas9 system efficiently silences expression of protein-coding and non-coding RNA genes. *Journal of Biological Chemistry*, 292 (14), 5624–5633.

Lo, S.H., Janmey, P.A., Hartwig, J.H., and Chen, L.B., 1994. Interactions of tensin with actin and identification of its three distinct actin-binding domains. *Journal of Cell Biology*, 125 (5), 1067–1075.

Lorzadeh, A., Bilenky, M., Hammond, C., Knapp, D.J.H.F., Li, L., Miller, P.H., Carles, A., Heravi-Moussavi, A., Gakkhar, S., Moksa, M., Eaves, C.J., and Hirst, M., 2016. Nucleosome Density ChIP-Seq Identifies Distinct Chromatin Modification Signatures Associated with MNase Accessibility. *Cell Reports*, 17 (8), 2112–2124.

Lozano, R., Naghavi, M., Foreman, K., Lim, S., Shibuya, K., Aboyans, V., Abraham, J., Adair, T., Aggarwal, R., Ahn, S.Y., AlMazroa, M.A., Alvarado, M., Anderson, H.R., Anderson, L.M., Andrews, K.G., Atkinson, C., Baddour, L.M., Barker-Collo, S., Bartels, D.H., Bell, M.L., Benjamin, E.J., Bennett, D., Bhalla, K., Bikbov, B., Abdulhak, A. Bin, Birbeck, G., Blyth, F., Bolliger, I., Boufous, S., Bucello, C., Burch, M., Burney, P., Carapetis, J., Chen, H., Chou, D., Chugh, S.S., Coffeng, L.E., Colan, S.D., Colquhoun, S., Colson, K.E., Condon, J., Connor, M.D., Cooper, L.T., Corriere, M., Cortinovis, M., de Vaccaro, K.C., Couser, W., Cowie, B.C., Criqui, M.H., Cross, M., Dabhadkar, K.C., Dahodwala, N., De Leo, D., Degenhardt, L., Delossantos, A., Denenberg, J., Des Jarlais, D.C., Dharmaratne, S.D., Dorsey, E.R., Driscoll, T., Duber, H., Ebel, B., Erwin, P.J., Espindola, P., Ezzati, M., Feigin, V., Flaxman, A.D., Forouzanfar, M.H., Fowkes, F.G.R., Franklin, R., Fransen, M., Freeman, M.K., Gabriel, S.E., Gakidou, E., Gaspari, F., Gillum, R.F., Gonzalez-Medina, D., Halasa, Y.A., Haring, D., Harrison, J.E., Havmoeller, R., Hay, R.J.,

Hoen, B., Hotez, P.J., Hoy, D., Jacobsen, K.H., James, S.L., Jasrasaria, R., Jayaraman, S., Johns, N., Karthikeyan, G., Kassebaum, N., Keren, A., Khoo, J.-P., Knowlton, L.M., Kobusingye, O., Koranteng, A., Krishnamurthi, R., Lipnick, M., Lipshultz, S.E., Ohno, S.L., Mabweijano, J., MacIntyre, M.F., Mallinger, L., March, L., Marks, G.B., Marks, R., Matsumori, A., Matzopoulos, R., Mayosi, B.M., McAnulty, J.H., McDermott, M.M., McGrath, J., Memish, Z.A., Mensah, G.A., Merriman, T.R., Michaud, C., Miller, M., Miller, T.R., Mock, C., Mocumbi, A.O., Mokdad, A.A., Moran, A., Mulholland, K., Nair, M.N., Naldi, L., Narayan, K.M.V., Nasseri, K., Norman, P., O'Donnell, M., Omer, S.B., Ortblad, K., Osborne, R., Ozgediz, D., Pahari, B., Pandian, J.D., Rivero, A.P., Padilla, R.P., Perez-Ruiz, F., Perico, N., Phillips, D., Pierce, K., Pope III, C.A., Porrini, E., Pourmalek, F., Raju, M., Ranganathan, D., Rehm, J.T., Rein, D.B., Remuzzi, G., Rivara, F.P., Roberts, T., De León, F.R., Rosenfeld, L.C., Rushton, L., Sacco, R.L., Salomon, J.A., Sampson, U., Sanman, E., Schwebel, D.C., Segui-Gomez, M., Shepard, D.S., Singh, D., Singleton, J., Sliwa, K., Smith, E., Steer, A., Taylor, J.A., Thomas, B., Tleyjeh, I.M., Towbin, J.A., Truelsen, T., Undurraga, E.A., Venketasubramanian, N., Vijayakumar, L., Vos, T., Wagner, G.R., Wang, M., Wang, W., Watt, K., Weinstock, M.A., Weintraub, R., Wilkinson, J.D., Woolf, A.D., Wulf, S., Yeh, P.-H., Yip, P., Zabetian, A., Zheng, Z.-J., Lopez, A.D., and Murray, C.J.L., 2012. Global and regional mortality from 235 causes of death for 20 age groups in 1990 and 2010: a systematic analysis for the Global Burden of Disease Study 2010. *The Lancet*, 380 (9859), 2095–2128.

Luan, W., Li, L., Shi, Y., Bu, X., Xia, Y., Wang, J., Djangmah, H.S., Liu, X., You, Y., and Xu, B., 2016. Long non-coding RNA MALAT1 acts as a competing endogenous RNA to promote malignant melanoma growth and metastasis by sponging miR-22. *Oncotarget*, 7 (39), 63901–63912.

Luerssen, H., Mattei, M.G., Schröter, M., Grzeschik, K.H., Adham, I.M., and Engel, W., 1990. Nucleotide sequence of the gene for human transition protein 1 and its chromosomal localization on chromosome 2. *Genomics*, 8 (2), 324–330.

Luis, J., Martin, J. -M, El Battari, A., Reynier, M., Marvaldi, J., and Pichon, J., 1989. A human melanoma-derived cell line (IGR39) with a very high number of vasoactive-intestinal-peptide (VIP) receptors: 1. Molecular characterization of the binding site. *European Journal of Biochemistry*, 180 (2), 429–433.

Marathe, H.G., Watkins-chow, D.E., Weider, M., Hoffmann, A., Mehta, G., Trivedi, A., Aras, S., Basuroy, T., Mehrotra, A., Bennett, C., Wegner, M., Pavan, W.J., and Serna, I.L. De, 2017. BRG1 interacts with SOX10 to establish the melanocyte lineage and to promote differentiation. *Nucleic acids research*, 45 (11), 6442–6458.

Marchese, F.P., Raimondi, I., and Huarte, M., 2017. The multidimensional mechanisms of long noncoding RNA function. *Genome Biology*, 18 (1), 1–13.

Marie, K.L., Sassano, A., Yang, H.H., Michalowski, A.M., Michael, T., Guo, T., Tsai, Y.C., Weissman, A.M., Lee, M.P., Lisa, M., Zaidi, M.R., Pérez-guijarro, E., Day, C., Arnheiter, H., and Davis, S., 2019. Melanoblast transcriptome analysis reveals novel pathways promoting melanoma metastasis. *bioRxiv doi10.1101/721712*.

Matesic, L.E., Yip, R., Reuss, A.E., Swing, D.A., O'Sullivan, T.N., Fletcher, C.F., Copeland, N.G., and Jenkins, N.A., 2001. Mutations in Mlph, encoding a member

of the Rab effector family, cause the melanosome transport defects observed in leaden mice. *Proceedings of the National Academy of Sciences*, 98 (18), 10238–10243.

Mazar, J., Zhao, W., Khalil, A.M., Lee, B., Shelley, J., Govindarajan, S.S., Yamamoto, F., Ratnam, M., Aftab, M.N., Collins, S., Finck, B.N., Han, X., Mattick, J.S., Dinger, M.E., and Perera, R.J., 2014. The Functional Characterization of Long Noncoding RNA SPRY4- IT1 in Human Melanoma Cells. *Oncotarget*, 5 (19), 8959–8969.

Melé, M., Mattioli, K., Mallard, W., and Shechner, D.M., 2017. Chromatin environment, transcriptional regulation, and splicing distinguish lincRNAs and mRNAs. *Genome Research*, 27, 27–37.

Melé, M. and Rinn, J.L., 2016. 'Cat's Cradling' the 3D Genome by the Act of LncRNA Transcription. *Molecular Cell*, 62 (5), 657–664.

Melotte, V., Lentjes, M.H.F.M., Van Den Bosch, S.M., Hellebrekers, D.M.E.I., De Hoon, J.P.J., Wouters, K.A.D., Daenen, K.L.J., Partouns-Hendriks, I.E.J.M., Stessels, F., Louwagie, J., Smits, K.M., Weijenberg, M.P., Sanduleanu, S., Khalid-De Bakker, C.A.J., Oort, F.A., Meijer, G.A., Jonkers, D.M.A.E., Herman, J.G., De Bruïne, A.P., and Van Engeland, M., 2009. N-Myc Downstream-Regulated Gene 4 (NDRG4): A Candidate Tumor Suppressor Gene and Potential Biomarker for Colorectal Cancer. *Journal of the National Cancer Institute*, 101 (13), 916–927.

Menyhárt, O., Harami-papp, H., Sukumar, S., Schäfer, R., Magnani, L., Barrios, O. De, and Gy, B., 2016. Guidelines for the selection offunctional assays to evaluate the hallmarks of cancer, 1866, 300–319.

Mercer, T.R., Dinger, M.E., Sunkin, S.M., Mehler, M.F., and Mattick, J.S., 2008. Specific expression of long noncoding RNAs in the mouse brain. *Proceedings of the National Academy of Sciences of the United States of America*, 105 (2), 716–721.

Miller, A.J., Levy, C., Davis, I.J., Razin, E., and Fisher, D.E., 2005. Sumoylation of MITF and its related family members TFE3 and TFEB. *Journal of Biological Chemistry*, 280 (1), 146–155.

Mobley, A.K., Braeuer, R.R., Kamiya, T., Shoshan, E., and Bar-Eli, M., 2012. Driving transcriptional regulators in melanoma metastasis. *Cancer and Metastasis Reviews*, 31 (3–4), 621–632.

Mohankumar, S. and Patel, T., 2016. Extracellular vesicle long noncoding RNA as potential biomarkers of liver cancer. *Briefings in Functional Genomics*, 15 (3), 249–256.

Mora, A., Sandve, G.K., Gabrielsen, O.S., and Eskeland, R., 2015. In the loop: promoter–enhancer interactions and bioinformatics. *Briefings in Bioinformatics*, 17 (6), 980–995.

Mori, S., Chang, J.T., Andrechek, E.R., Matsumura, N., Yao, G., Kim, J.W., Gatza, M., Murphy, S., and Nevins, R., 2009. An Anchorage-Independent Cell Growth Signature Identifies Tumors with Metastatic Potential. *Oncogene*, 28 (31), 2796–2805.

Morriss, G.R. and Cooper, T.A., 2017. Protein sequestration as a normal function of long noncoding RNAs and a pathogenic mechanism of RNAs containing nucleotide repeat expansions. *Human Genetics*, 136 (9), 1247–1263.

Mort, R.L., Jackson, I.J., and Elizabeth Patton, E., 2015. The melanocyte lineage in development and disease. *Development (Cambridge)*, 142 (4), 620–632.

Mukherjee, N., Calviello, L., Hirsekorn, A., De Pretis, S., Pelizzola, M., and Ohler, U., 2017. Integrative classification of human coding and noncoding genes through RNA metabolism profiles. *Nature Structural and Molecular Biology*, 24 (1), 86–96.

Necsulea, A. and Kaessmann, H., 2014. Evolutionary dynamics of coding and non-coding transcriptomes. *Nature Reviews Genetics*, 15 (11), 734–748.

Ng, H.H., Young, R.A., and Struhl, K., 2003. Targeted Recruitment of Set1 Histone Methylase by Elongating Pol II Provides a Localized Mark and Memory of Recent Transcriptional Activity, 11, 709–719.

Nieto, M.A., Huang, R.Y.Y.J., Jackson, R.A.A., and Thiery, J.P.P., 2016. Emt: 2016. *Cell*, 166 (1), 21–45.

Nobre, A.R., Entenberg, D., Wang, Y., Condeelis, J., and Aguirre-Ghiso, J.A., 2018. The Different Routes to Metastasis via Hypoxia-Regulated Programs. *Trends in Cell Biology*, 28 (11), 941–956.

O'Leary, V.B., Hain, S., Maugg, D., Smida, J., Azimzadeh, O., Tapio, S., Ovsepian, S.V., and Atkinson, M.J., 2017. Long non-coding RNA PARTICLE bridges histone and DNA methylation. *Scientific Reports*, 7 (1), 1–12.

O'Leary, V.B., Ovsepian, S.V., Carrascosa, L.G., Buske, F.A., Radulovic, V., Niyazi, M., Moertl, S., Trau, M., Atkinson, M.J., and Anastasov, N., 2015. PARTICLE, a triplex-forming long ncRNA, regulates locus-specific methylation in response to low-dose irradiation. *Cell Reports*, 11 (3), 474–485.

Ørom, U.A., Derrien, T., Beringer, M., Gumireddy, K., Gardini, A., Bussotti, G., Lai, F., Zytnicki, M., Notredame, C., Huang, Q., Guigo, R., and Shiekhattar, R., 2010. Long noncoding RNAs with enhancer-like function in human cells. *Cell*, 143 (1), 46–58.

Palazzo, A.F. and Lee, E.S., 2015. Non-coding RNA: What is functional and what is junk? *Frontiers in Genetics*, 5, 1–11.

Pandey, R.R., Mondal, T., Mohammad, F., Enroth, S., Redrup, L., Komorowski, J., Nagano, T., Mancini-DiNardo, D., and Kanduri, C., 2008. Kcnq1ot1 Antisense Noncoding RNA Mediates Lineage-Specific Transcriptional Silencing through Chromatin-Level Regulation. *Molecular Cell*, 32 (2), 232–246.

Pérez-Guijarro, E., Day, C.P., Merlino, G., and Zaidi, M.R., 2017. Genetically engineered mouse models of melanoma. *Cancer*, 123, 2089–2103.

Pickard, M.R. and Williams, G.T., 2016. The hormone response element mimic sequence of GAS5 lncRNA is sufficient to induce apoptosis in breast cancer cells. *Oncotarget*, 7 (9).

Pingault, V., Ente, D., Dastot-Le Moal, F., Goossens, M., Marlin, S., and Bondurand, N., 2010. Review and update of mutations causing Waardenburg syndrome. *Human Mutation*, 31 (4), 391–406.

Ploper, D., Taelman, V.F., Robert, L., Perez, B.S., Titz, B., Chen, H.-W., Graeber, T.G., Euw, E. von, Ribas, A., and Robertis, E.M. De, 2015. MITF drives endolysosomal biogenesis and potentiates Wnt signaling in melanoma cells. *Proceedings of the National Academy of Sciences*, 112 (5), 420–429.

Poliseno, L., Haimovic, A., Christos, P.J., Vega y Saenz de Miera, E.C., Shapiro, R., Pavlick, A., Berman, R.S., Darvishian, F., and Osman, I., 2011. Deletion of PTENP1 Pseudogene in Human Melanoma. *Journal of Investigative Dermatology*, 131

(12), 2497–2500.
Poliseno, L., Salmena, L., Zhang, J., Carver, B., Haveman, W.J., and Pandolfi, P.P., 2010. A coding-independent function of gene and pseudogene mRNAs regulates tumour biology. *Nature*, 465 (7301), 1033–1038.
Pollock, P.M., Harper, U.L., Hansen, K.S., Yudt, L.M., Stark, M., Robbins, C.M., Moses, T.Y., Hostetter, G., Wagner, U., Kakareka, J., Salem, G., Pohida, T., Heenan, P., Duray, P., Kallioniemi, O., Hayward, N.K., Trent, J.M., and Meltzer, P.S., 2003. High frequency of BRAF mutations in nevi. *Nature Genetics*, 33 (1), 19–20.
Pontier, D.B. and Gribnau, J., 2011. Xist regulation and function eXplored. *Human Genetics*, 130 (2), 223–236.
Potrony, M., Aguilera, P., Carrera, C., Malvehy, J., Puig, S., Badenas, C., and Puig-Butille, J.A., 2015. Update in genetic susceptibility in melanoma. *Annals of Translational Medicine*, 3 (15), 1–12.
Potterf, S.B., Furumura, M., Dunn, K.J., Arnheiter, H., and Pavan, W.J., 2000. Transcription factor hierarchy in Waardenburg syndrome: Regulation of MITF expression by SOX10 and PAX3. *Human Genetics*, 107 (1), 1–6.
Prensner, J.R., Iyer, M.K., Sahu, A., Asangani, I.A., Cao, Q., Patel, L., Vergara, I.A., Davicioni, E., Erho, N., Ghadessi, M., Jenkins, R.B., Triche, T.J., Malik, R., Bedenis, R., McGregor, N., Ma, T., Chen, W., Han, S., Jing, X., Cao, X., Wang, X., Chandler, B., Yan, W., Siddiqui, J., Kunju, L.P., Dhanasekaran, S.M., Pienta, K.J., Feng, F.Y., and Chinnaiyan, A.M., 2013. The long noncoding RNA SChLAP1 promotes aggressive prostate cancer and antagonizes the SWI/SNF complex. *Nature Genetics*, 45 (11), 1392–1403.
Qi, L.S., Larson, M.H., Gilbert, L.A., Doudna, J.A., Weissman, J.S., Arkin, A.P., and Lim, W.A., 2013. Repurposing CRISPR as an RNA-γuided platform for sequence-specific control of gene expression. *Cell*, 152 (5), 1173–1183.
Quek, X.C., Thomson, D.W., Maag, J.L. V, Bartonicek, N., Signal, B., Clark, M.B., Gloss, B.S., and Dinger, M.E., 2015. lncRNAdb v2.0: Expanding the reference database for functional long noncoding RNAs. *Nucleic Acids Research*, 43 (D1), D168–D173.
Ransohoff, J.D., Wei, Y., and Khavari, P.A., 2017. The functions and unique features of long intergenic non-coding RNA. *Nature Reviews Molecular Cell Biology*, 19 (3), 143–157.
Rao, S.S.P., Huntley, M.H., Durand, N.C., Stamenova, E.K., Bochkov, I.D., Robinson, J.T., Sanborn, A.L., Machol, I., Omer, A.D., Lander, E.S., and Aiden, E.L., 2014. Article A 3D Map of the Human Genome at Kilobase Resolution Reveals Principles of Chromatin Looping. *Cell*, 159 (7), 1665–1680.
Rapisuwon, S., Vietsch, E.E., and Wellstein, A., 2016. Circulating biomarkers to monitor cancer progression and treatment. *Computational and Structural Biotechnology Journal*, 14, 211–222.
Richard, J.L. and Eichhorn, P.J.A., 2018. Platforms for Investigating LncRNA Functions. *SLAS Technology*, 23 (6), 493–506.
Richtig, G., Ehall, B., Richtig, E., Aigelsreiter, A., Gutschner, T., and Pichler, M., 2017. Function and clinical implications of long non-coding RNAs in melanoma. *International Journal of Molecular Sciences*, 18 (4).
Rinn, J.L., Kertesz, M., Wang, J.K., Squazzo, S.L., Xu, X., Brugmann, S.A., Goodnough,

L.H., Helms, J.A., Farnham, P.J., Segal, E., and Chang, H.Y., 2007. Functional Demarcation of Active and Silent Chromatin Domains in Human HOX Loci by Noncoding RNAs. *Cell*, 129 (7), 1311–1323.

Rodríguez-Carballo, E., Lopez-Delisle, L., Zhan, Y., Fabre, P.J., Beccari, L., El-Idrissi, I., Nguyen Huynh, T.H., Ozadam, H., Dekker, J., and Duboule, D., 2017. The HoxD cluster is a dynamic and resilient TAD boundary controlling the segregation of antagonistic regulatory landscapes. *Genes and Development*, 31 (22), 2264–2281.

Sabarinathan, R., Tafer, H., Seemann, S.E., Hofacker, I.L., Stadler, P.F., and Gorodkin, J., 2013. The RNAsnp web server: predicting SNP effects on local RNA secondary structure. *Nucleic acids research*, 41, 475–479.

Saldaña-Meyer, R., González-Buendía, E., Guerrero, G., Narendra, V., Bonasio, R., Recillas-Targa, F., and Reinberg, D., 2014. CTCF regulates the human p53 gene through direct interaction with its natural antisense transcript, Wrap53. *Genes and Development*, 28 (7), 723–734.

Sarropoulos, I., Marin, R., Cardoso-moreira, M., and Kaessmann, H., 2019. Developmental dynamics of lncRNAs across mammalian organs and species. *Nature*, 571, 1–23.

Sasaki, Y.T.F., Ideue, T., Sano, M., Mituyama, T., and Hirose, T., 2009. MENε/β noncoding RNAs are essential for structural integrity of nuclear paraspeckles. *Proceedings of the National Academy of Sciences of the United States of America*, 106 (8), 2525–2530.

Sato, S., Roberts, K., Gambino, G., Cook, A., Kouzarides, T., and Goding, C.R., 1997. CBP/p300 as a co-factor for the Microphthalmia transcription factor. *Oncogene*, 14 (25), 3083–3092.

Schmidt, K., Carroll, J.S., Yee, E., Thomas, D.D., Wert-Lamas, L., Neier, S.C., Sheynkman, G., Ritz, J., and Novina, C.D., 2019. The lncRNA SLNCR Recruits the Androgen Receptor to EGR1-Bound Genes in Melanoma and Inhibits Expression of Tumor Suppressor p21. *Cell Reports*, 27 (8), 2493–2507.

Schmidt, K., Joyce, C.E., Buquicchio, F., Brown, A., Ritz, J., Distel, R.J., Yoon, C.H., and Novina, C.D., 2016. The lncRNA SLNCR1 Mediates Melanoma Invasion through a Conserved SRA1-like Region. *Cell Reports*, 15 (9), 2025–2037.

Schmitt, A.M., Garcia, J.T., Hung, T., Flynn, R.A., Shen, Y., Qu, K., Payumo, A.Y., Peres-Da-Silva, A., Broz, D.K., Baum, R., Guo, S., Chen, J.K., Attardi, L.D., and Chang, H.Y., 2016. An inducible long noncoding RNA amplifies DNA damage signaling. *Nature Genetics*, 48 (11), 1370–1376.

Seberg, H.E., Otterloo, E. Van, and Cornell, R.A., 2017. Beyond MITF: Multiple transcription factors directly regulate the cellular phenotype in melanocytes and melanoma, 30 (5), 454–466.

Shain, A.H. and Bastian, B.C., 2016. From melanocytes to melanomas. *Nature Reviews Cancer*, 16 (6), 345–358.

Shakhova, O., Zingg, D., Schaefer, S.M., Hari, L., Civenni, G., Blunschi, J., Claudinot, S., Okoniewski, M., Beermann, F., Mihic-Probst, D., Moch, H., Wegner, M., Dummer, R., Barrandon, Y., Cinelli, P., and Sommer, L., 2012. Sox10 promotes the formation and maintenance of giant congenital naevi and melanoma. *Nature Cell Biology*, 14 (8), 882–889.

Shih, Y.P., Sun, P., Wang, A., and Lo, S.H., 2015. Tensin1 positively regulates RhoA activity through its interaction with DLC1. *Biochimica et Biophysica Acta - Molecular Cell Research*, 1853 (12), 3258–3265.

Siegel, R.L., Miller, K.D., and Jemal, A., 2019. Cancer Facts & Figures, 2019. *CA: A Cancer Journal for Clinicians*, 69 (1), 7–34.

Sigova, A.A., Abraham, B.J., Ji, X., Molinie, B., Hannett, N.M., Guo, Y.E., Jangi, M., Giallourakis, C.C., Sharp, P.A., and Young, R.A., 2015. Transcription factor trapping by RNA in gene regulatory elements, 350 (6263), 978–982.

Silvestre, J.S., Tamarat, R., Ebrahimian, T.G., Le-Roux, A., Clergue, M., Emmanuel, F., Duriez, M., Schwartz, B., Branellec, D., and Lévy, B.I., 2003. Vascular endothelial growth factor-B promotes in vivo angiogenesis. *Circulation Research*, 93 (2), 114–123.

Simon, M.D., Wang, C.I., Kharchenko, P. V., West, J.A., Chapman, B.A., Alekseyeno, A.A., Borowsky, M.L., Kuroda, M.I., and Kingston, R.E., 2011. The genomic binding sites of a noncoding RNA. *PNAS*, 108 (51), 20497–20502.

Singh, B.P. and Salama, A.K.S., 2016. Updates in therapy for advanced melanoma. *Cancers*, 8 (1), 1–15.

Soura, E., Eliades, P., Shannon, K., Stratigos, A., and Tsao, H., 2016. Hereditary Melanoma: Update on Syndromes and Management - Genetics of familial atypical multiple mole melanoma syndrome. *J Am Acad Dermatol.*, 74 (3), 395–407.

Spicuglia, S. and Vanhille, L., 2012. Chromatin signatures of active enhancers. *Nucleus*, 3 (2), 126–131.

St.Laurent, G., Wahlestedt, C., and Kapranov, P., 2015. The Landscape of long noncoding RNA classification. *Trends in Genetics*, 31 (5), 239–251.

Steeg, P.S., 2006. Tumor metastasis : mechanistic insights and clinical challenges, 12 (8), 895–904.

Steingrimsson, E., Moore, K.J., Lamoreux, M.L., Amare, A.R.F., Burlef, S.K., Sanders, D.C., Loren, Z., Colin, C.S., Arnheiter, H., Copeland, N.G., and Jenkins, N.A., 1994. Molecular basis of mouse microphthalmia (mi) mutations helps explain their developmental and phenotypic consequences. *Nature Publishing Group*, 8 (10), 256–263.

Stojic, L., Lun, A.T.L., Mangei, J., Mascalchi, P., Quarantotti, V., Barr, A.R., Bakal, C., Marioni, J.C., Gergely, F., and Odom, D.T., 2018. Specificity of RNAi, LNA and CRISPRi as loss-of-function methods in transcriptional analysis. *Nucleic Acids Research*, 46 (12), 5950–5966.

Stojic, L., Niemczyk, M., Orjalo, A., Ito, Y., Ruijter, A.E.M., Uribe-Lewis, S., Joseph, N., Weston, S., Menon, S., Odom, D.T., Rinn, J., Gergely, F., and Murrell, A., 2016. Transcriptional silencing of long noncoding RNA GNG12-AS1 uncouples its transcriptional and product-related functions. *Nature Communications*, 7, 1–14.

Strub, T., Giuliano, S., Ye, T., Bonet, C., Keime, C., Kobi, D., Le Gras, S., Cormont, M., Ballotti, R., Bertolotto, C., and Davidson, I., 2011. Essential role of microphthalmia transcription factor for DNA replication, mitosis and genomic stability in melanoma. *Oncogene*, 30 (20), 2319–2332.

Su, Y., Wagner, E.R., Luo, Q., Huang, J., Chen, L., He, B.C., Zuo, G.W., Shi, Q., Zhang, B.Q., Zhu, G., Bi, Y., Luo, J., Luo, X., Kim, S.H., Shen, J., Rastegar, F., Huang, E.,

Gao, Y., Gao, J.L., Yang, K., Wietholt, C., Li, M., Qin, J., Haydon, R.C., He, T.C., and Luu, H.H., 2011. Insulin-like growth factor binding protein 5 suppresses tumor growth and metastasis of human osteosarcoma. *Oncogene*, 30 (37), 3907–3917.

Sullivan, R.J. and Flaherty, K.T., 2011. BRAF in Melanoma: Pathogenesis, Diagnosis, Inhibition, and Resistance. *Journal of Skin Cancer*, 2011, 1–8.

Sun, C., Wang, L., Huang, S., Heynen, G.J.J.E., Prahallad, A., Robert, C., Haanen, J., Blank, C., Wesseling, J., M.Willems, S., Zecchin, D., Hobor, S., Bajpe, P.K., Lieftink, C., Mateus, C., Vagner, S., Grernrum, W., Hofland, I., Schlicker, A., Wessels, L.F.A., Beijersbergen, R.L., Bardelli, A., Nicolantonio, F. Di, Eggermont, A.M.M., Bernards, R., and Treatment, 2014. Reversible and adaptive resistance to BRAF(V600E) inhibition in melanoma. *Nature*, 508, 118–122.

Sun, L., Guan, Z., Wei, S., Tan, R., Li, P., and Yan, L., 2019. Identification of long non-coding and messenger RNAs differentially expressed between primary and metastatic melanoma. *Frontiers in Genetics*, 10 (APR), 1–14.

Sun, Q., Hao, Q., and Prasanth, K. V., 2018. Nuclear Long Noncoding RNAs: Key Regulators of Gene Expression. *Trends in Genetics*, 34 (2), 142–157.

Sureshbabu, A., Okajima, H., Yamanaka, D., Tonner, E., Shastri, S., Maycock, J., Szymanowska, M., Shand, J., Takahashi, S.-I., Beattie, J., Allan, G., and Flint, D., 2012. IGFBP5 induces cell adhesion, increases cell survival and inhibits cell migration in MCF-7 human breast cancer cells. *Journal of Cell Science*, 125 (7), 1693–1705.

Suvà, M.L., Riggi, N., and Bernstein, B.E., 2013. Epigenetic reprogramming in cancer Transcription factors and chromatin regulators: partners in specification of. *Science*, 339 (6127).

Taddei, M.L., Giannoni, E., Fiaschi, T., and Chiarugi, P., 2012. Anoikis: An emerging hallmark in health and diseases. *Journal of Pathology*, 226 (2), 380–393.

Tang, Z., Kang, B., Li, C., Chen, T., and Zhang, Z., 2019. GEPIA2: an enhanced web server for large-scale expression profiling and interactive analysis. *Nucleic acids research*, 47 (W1), W556–W560.

Tarek, A. and Dutta, A., 2009. P21 in Cancer. *Nature reviews Cancer*, 9 (6), 400–414.

Tassabehji, M., Newton, V.E., Liu, X.Z., Brady, A., Donnai, D., Krajewska-walasek, M., Murday, V., Norman, A., Obersztyn, E., Reardon, W., Rice, J.C., Trembath, R., Wieacker, P., Whiteford, M., Winter, R., and Read, A.P., 1995. The mutational spectrum in waardenburg syndrome. *Human Molecular Genetics*, 4 (11), 2131–2137.

Teschendorff, A.E., Lee, S.H., Jones, A., Fiegl, H., Kalwa, M., Wagner, W., Chindera, K., Evans, I., Dubeau, L., Orjalo, A., Horlings, H.M., Niederreiter, L., Kaser, A., Yang, W., Goode, E.L., Fridley, B.L., Jenner, R.G., Berns, E.M.J.J., Wik, E., Salvesen, H.B., Wisman, G.B.A., van der Zee, A.G.J., Davidson, B., Trope, C.G., Lambrechts, S., Vergote, I., Calvert, H., Jacobs, I.J., and Widschwendter, M., 2015. HOTAIR and its surrogate DNA methylation signature indicate carboplatin resistance in ovarian cancer. *Genome Medicine*, 7 (1), 1–12.

Theis, M. and Buchholz, F., 2010. MISSION esiRNA for RNAi Screening in Mammalian Cells. *Journal of Visualized Experiments*, (39), 3–5.

Thévenin, A., Ein-Dor, L., Ozery-Flato, M., and Shamir, R., 2014. Functional gene groups are concentrated within chromosomes, among chromosomes and in the

nuclear space of the human genome. *Nucleic Acids Research*, 42 (15), 9854–9861.

Thomas, A.J. and Erickson, C.A., 2009. FOXD3 regulates the lineage switch between neural crest-derived glial cells and pigment cells by repressing MITF through a non-canonical mechanism. *Development*, 136 (11), 1849–1858.

Thomas, M.L. and Marcato, P., 2018. Epigenetic modifications as biomarkers of tumor development, therapy response, and recurrence across the cancer care continuum. *Cancers*, 10 (4), 1–21.

Tian, D., Sun, S., and Lee, J.T., 2010. The long noncoding RNA, Jpx, is a molecular switch for X- chromosome inactivation. *Cell*, 143 (3), 390–403.

Tian, Y., Zhang, X., Hao, Y., Fang, Z., and He, Y., 2014. Potential roles of abnormally expressed long noncoding RNA UCA1 and Malat-1 in metastasis of melanoma. *Melanoma Research*, 24 (4), 335–341.

Tripathi, G., Salih, D.A.M., Drozd, A.C., Cosgrove, R.A., Cobb, L.J., and Pell, J.M., 2009. IGF-independent effects of insulin-like growth factor binding protein-5 (Igfbp5) in vivo. *FASEB Journal*, 23 (8), 2616–2626.

Tripathi, V., Ellis, J.D., Shen, Z., Song, D.Y., Pan, Q., Watt, A.T., Freier, S.M., Bennett, C.F., Sharma, A., Bubulya, P.A., Blencowe, B.J., Prasanth, S.G., and Prasanth, K. V., 2010. The nuclear-retained noncoding RNA MALAT1 regulates alternative splicing by modulating SR splicing factor phosphorylation. *Molecular Cell*, 39 (6), 925–938.

Tsai, M.-C., Spitale, R., and Chang, H., 2011. Long intergenic noncoding RNAs - new links in cancer progression. *Cancer Research*, 71, 3–7.

Tsai, M., Manor, O., Wan, Y., Mosammaparast, N., Wang, J.K., Lan, F., Shi, Y., Segal, E., and Chang, H.Y., 2010. Modification Complexes. *Science*, 329, 689–694.

Tsavachidou, D., Coleman, M.L., Athanasiadis, G., Li, S., Licht, J.D., Olson, M.F., and Weber, B.L., 2004. SPRY2 is an inhibitor of the Ras/extracellular signal-regulated kinase pathway in melanocytes and melanoma cells with wild-type BRAF but not with the V599E mutant. *Cancer Research*, 64 (16), 5556–5559.

Tudrej, K.B., Czepielewska, E., and Kozlowska-Wojciechowska, M., 2017. SOX10-MITF pathway activity in melanoma cells. *Archives of Medical Science*, 13 (6), 1493–1503.

Ulitsky, I., Shkumatava, A., Jan, C.H., Sive, H., and Bartel, D.P., 2011. Conserved function of lincRNAs in vertebrate embryonic development despite rapid sequence evolution. *Cell*, 147 (7), 1537–1550.

Ungefroren, H., Sebens, S., Seidl, D., Lehnert, H., and Hass, R., 2011. Interaction of tumor cells with the microenvironment. *Cell Communication and Signaling*, 9, 1–8.

Uszczynska-Ratajczak, B., Lagarde, J., Frankish, A., Guigó, R., and Johnson, R., 2018. Towards a complete map of the human long non-coding RNA transcriptome. *Nature Reviews Genetics*, 19 (9), 535–548.

Valleley, E.M., Cordery, S.F., and Bonthron, D.T., 2007. Tissue-specific imprinting of the ZAC/PLAGL1 tumour suppressor gene results from variable utilization of monoallelic and biallelic promoters. *Human Molecular Genetics*, 16 (8), 972–981.

Valouev, A., Johnson, S.M., Boyd, S.D., Smith, C.L., Fire, A.Z., and Sidow, A., 2011.

Determinants of nucleosome organization in primary human cells. *Nature*, 474 (7352), 516–522.

Vance, K.W. and Ponting, C.P., 2014. Transcriptional regulatory functions of nuclear long noncoding RNAs. *Trends in Genetics*, 30 (8), 348–355.

Vance, K.W., Sansom, S.N., Lee, S., Chalei, V., Kong, L., Cooper, S.E., Oliver, P.L., and Ponting, C.P., 2014. The long non-coding RNA paupar regulates the expression of both local and distal genes. *EMBO Journal*, 33 (4), 296–311.

Del Vecchio, F., Lee, G.H., Hawezi, J., Bhome, R., Pugh, S., Sayan, E., Thomas, G., Packham, G., Primrose, J., Pichler, M., Mirnezami, A., Calin, G., and Bullock, M., 2018. Long non-coding RNAs within the tumour microenvironment and their role in tumour-stroma cross-talk. *Cancer Letters*, 421, 94–102.

Verfaillie, A., Imrichova, H., Atak, Z.K., Dewaele, M., Rambow, F., Hulselmans, G., Christiaens, V., Svetlichnyy, D., Luciani, F., Van Den Mooter, L., Claerhout, S., Fiers, M., Journe, F., Ghanem, G.E., Herrmann, C., Halder, G., Marine, J.C., and Aerts, S., 2015. Decoding the regulatory landscape of melanoma reveals TEADS as regulators of the invasive cell state. *Nature Communications*, 6, 1–16.

Villanueva, J., Vultur, A., and Herlyn, M., 2013. Future Treatment Options. *Cancer Research*, 71 (23), 7137–7140.

Wan, Y., Qu, K., Zhang, Q.C., Flynn, R.A., Manor, O., Ouyang, Z., Zhang, J., Spitale, R.C., Snyder, M.P., Segal, E., and Chang, H.Y., 2014. Landscape and variation of RNA secondary structure across the human transcriptome. *Nature*, 505 (7485), 706–709.

Wang, J., Ding, N., Li, Y., Cheng, H., Wang, D., Yang, Q., Deng, Y., Yang, Y., Li, Y., Ruan, X., Xie, F., Zhao, H., and Fang, X., 2015. Insulin-like growth factor binding protein 5 (IGFBP5) functions as a tumor suppressor in human melanoma cells. *Oncotarget*, 6 (24).

Wang, K.C. and Chang, H.Y., 2011. Molecular Mechanisms of Long Noncoding RNAs. *Molecular Cell*, 43 (6), 904–914.

Wang, K.C., Yang, Y.W., Liu, B., Sanyal, A., Corces-Zimmerman, R., Chen, Y., Lajoie, B.R., Protacio, A., Flynn, R.A., Gupta, R.A., Wysocka, J., Lei, M., Dekker, J., Helms, J.A., and Chang, H.Y., 2011. A long noncoding RNA maintains active chromatin to coordinate homeotic gene expression. *Nature*, 472 (7341), 120–126.

Wang, Y., Hou, J., He, D., Sun, M., Zhang, P., Yu, Y., and Chen, Y., 2016. The Emerging Function and Mechanism of ceRNAs in Cancer. *Trends in Genetics*, 32 (4), 211–224.

Washietl, S., Kellis, M., and Garber, M., 2014. Evolutionary dynamics and tissue specificity of human long noncoding RNAs in six mammals. *Genome Research*, 24 (4), 616–628.

Watts, J. and Corey, D., 2012. Gene silencing by siRNAs and antisense oligonucleotides in the laboratory and the clinic. *The Journal of pathology*, 226 (2), 365–379.

Weeraratna, A.T., Jiang, Y., Hostetter, G., Rosenblatt, K., Duray, P., Bittner, M., and Trent, J.M., 2002. Wnt5a signaling directly affects cell motility and invasion of metastatic melanoma. *Cancer Cell*, 1 (3), 279–288.

Wellbrock, C., Rana, S., Paterson, H., Pickersgill, H., Brummelkamp, T., and Marais, R., 2008. Oncogenic BRAF regulates melanoma proliferation through the lineage

specific factor MITF. *PLoS ONE*, 3 (7).
White, R.M., Cech, J., Ratanasirintrawoot, S., Lin, C.Y., Rahl, P.B., Burke, C.J., Langdon, E., Tomlinson, M.L., Mosher, J., Kaufman, C., Chen, F., Long, H.K., Kramer, M., Datta, S., Neuberg, D., Granter, S., Young, R.A., Morrison, S., Wheeler, G.N., and Zon, L.I., 2011. DHODH modulates transcriptional elongation in the neural crest and melanoma. *Nature*, 471 (7339), 518–522.
Xiang, J.F., Yin, Q.F., Chen, T., Zhang, Y., Zhang, X.O., Wu, Z., Zhang, S., Wang, H. Bin, Ge, J., Lu, X., Yang, L., and Chen, L.L., 2014. Human colorectal cancer-specific CCAT1-L lncRNA regulates long-range chromatin interactions at the MYC locus. *Cell Research*, 24 (5), 513–531.
Xu, Y., Wang, Z., Jiang, X., and Cui, Y., 2017. Overexpression of long noncoding RNA H19 indicates a poor prognosis for cholangiocarcinoma and promotes cell migration and invasion by affecting epithelial-mesenchymal transition. *Biomedicine and Pharmacotherapy*, 92, 17–23.
Xue, M., Li, X., Li, Z., and Chen, W., 2014. Urothelial carcinoma associated 1 is a hypoxia-inducible factor-1α-targeted long noncoding RNA that enhances hypoxic bladder cancer cell proliferation, migration, and invasion. *Tumor Biology*, 35 (7), 6901–6912.
Yada, E., Wada, S., Yoshida, S., and Sasada, T., 2017. Use of patient-derived xenograft mouse models in cancer research and treatment. *Future Science OA*, 4 (3), 1–4.
Yan, X., Hu, Z., Feng, Y., Hu, X., Yuan, J., Zhao, S.D., Zhang, Y., Yang, L., Shan, W., He, Q., Fan, L., Kandalaft, L.E., Tanyi, J.L., Li, C., Yuan, C.X., Zhang, D., Yuan, H., Hua, K., Lu, Y., Katsaros, D., Huang, Q., Montone, K., Fan, Y., Coukos, G., Boyd, J., Sood, A.K., Rebbeck, T., Mills, G.B., Dang, C. V., and Zhang, L., 2015. Comprehensive Genomic Characterization of Long Non-coding RNAs across Human Cancers. *Cancer Cell*, 28 (4), 529–540.
Yu, W., Gius, D., Onyango, P., Muldoon-Jacobs, K., Karp, J., Feinberg, A.P., and Cui, H., 2008. Epigenetic silencing of tumour suppressor gene p15 by its antisense RNA. *Nature*, 451 (7175), 202–206.
Yu, X., Zheng, H., Tse, G., Chan, M.T., and Wu, W.K., 2018. Long non-coding RNAs in melanoma. *Cell Proliferation*, 51 (4), 1–6.
Yue, M. and Ogawa, Y., 2017. CRISPR/Cas9-mediated modulation of splicing efficiency reveals short splicing isoform of Xist RNA is sufficient to induce X-chromosome inactivation. *Nucleic Acids Research*, 46 (5), 1–11.
Yusoff, P., Lao, D.H., Ong, S.H., Miin Wong, E.S., Lim, J., Lo, T.L., Leong, H.F., Fong, C.W., and Guy, G.R., 2002. Sprouty2 inhibits the Ras/MAP kinase pathway by inhibiting the activation of Raf. *Journal of Biological Chemistry*, 277 (5), 3195–3201.
Zare, K., Shademan, M., Ghahramani Seno, M.M., and Dehghani, H., 2018. CRISPR/Cas9 Knockout Strategies to Ablate CCAT1 lncRNA Gene in Cancer Cells. *Biological Procedures Online*, 20 (1), 1–12.
Zeng, R., Han, M., Luo, Y., Li, C., Pei, G., Liao, W., Bai, S., Ge, S., Liu, X., and Xu, G., 2011. Role of Sema4C in TGF-β1-induced mitogen-activated protein kinase activation and epithelialmesenchymal transition in renal tubular epithelial cells. *Nephrology Dialysis Transplantation*, 26 (4), 1149–1156.
Zhang, K., Shi, Z.M., Chang, Y.N., Hu, Z.M., Qi, H.X., and Hong, W., 2014. The ways of

action of long non-coding RNAs in cytoplasm and nucleus. *Gene*, 547 (1), 1–9.
Zhang, Q., 2017. Long Non-Coding RNAs as Regulators of Angiogenesis : A Mini-Review. *Cellular and Molecular Medical Research*, 1 (1), 7–10.
Zhang, Z., Zhou, C., Chang, Y., Zhang, Z., Hu, Y., Zhang, F., Lu, Y., Zheng, L., Zhang, W., Li, X., and Li, X., 2016. Long non-coding RNA CASC11 interacts with hnRNP-K and activates the WNT/β-catenin pathway to promote growth and metastasis in colorectal cancer. *Cancer Letters*, 376 (1), 62–73.
Zhao, X.Y. and Lin, J.D., 2015. Long Noncoding RNAs: A New Regulatory Code in Metabolic Control. *Trends in Biochemical Sciences*, 40 (10), 586–596.
Zheng, J., Huang, X., Tan, W., Yu, D., Du, Z., Chang, J., Wei, L., Han, Y., Wang, C., Che, X., Zhou, Y., Miao, X., Jiang, G., Yu, X., Yang, X., Cao, G., Zuo, C., Li, Z., Wang, C., Cheung, S.T., Jia, Y., Zheng, X., Shen, H., Wu, C., and Lin, D., 2016. Pancreatic cancer risk variant in LINC00673 creates a miR-1231 binding site and interferes with PTPN11 degradation. *Nature Genetics*, 48 (7), 747–757.
Zhou, X. and O'Shea, E.K., 2011. Integrated Approaches Reveal Determinants of Genome-wide Binding and Function of the Transcription Factor Pho4. *Molecular Cell*, 42 (6), 826–836.

Appendix

8.1 pGEM-T-Easy vector (Promega)

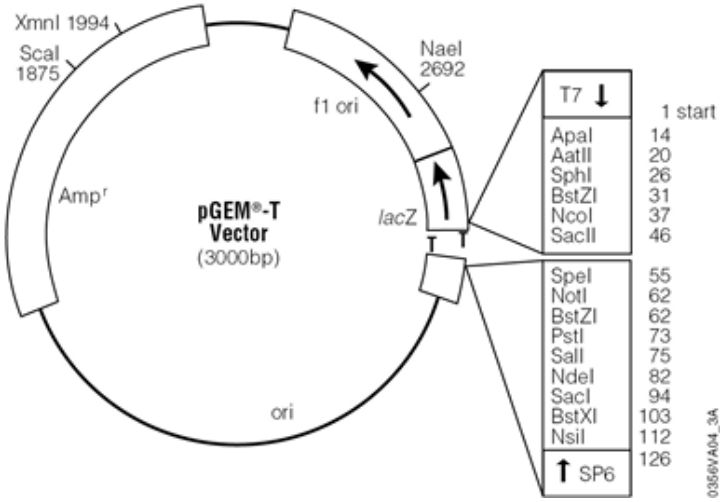

8.2 pX-dCas9-mod-KRAB

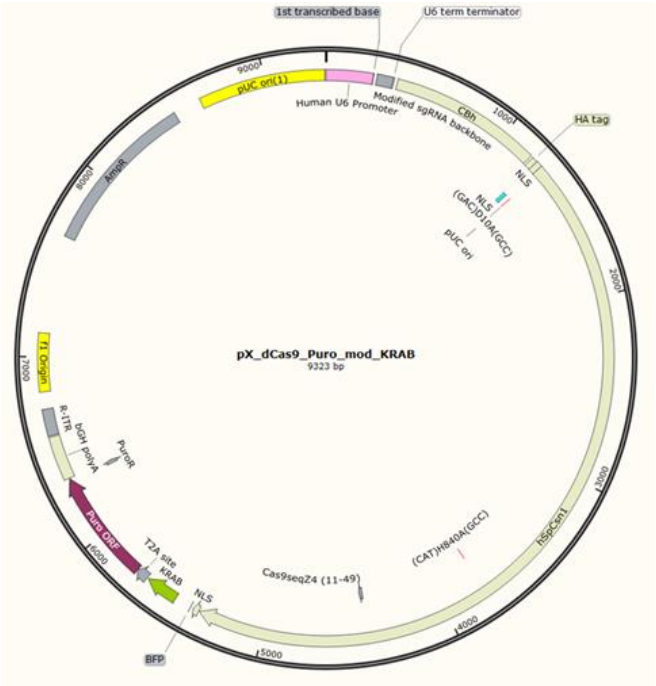

Figure 8.1 Circular map of pxdCas9Krab plasmid. The vector contains both the sgRNA and dCas9-KRAB fusion. The plasmid is driven by a CBh promoter. Increased binding to a dCas9 is allowed following small modifications to the sgRNA backbone. Presence of ampicillin and puromycin resistance allow for selection following transformation and transfection respectively. The px5gRNAsCas9Puro vector has the same structure and features but lacks the KRAB protein.